EVALUATION OF PREFERENTIAL ENERGY ABSORPTION IN EARLYWOOD AND LATEWOOD FIBERS OF LOBLOLLY PINE IN CYCLIC COMPRESSION

A Thesis Submitted by

Cheryl B. Rueckert

B.S. 1985,1987 University of Wisconsin – Oshkosh

M.S. 1993, Institute of Paper Science and Technology

in partial fulfillment of the requirements
of the Insititue of Paper Science and Technology
for the degree of Doctor of Philosophy,
Atlanta, Georgia

December, 1998

EVALUATION OF PREFERENTIAL ENERGY ABSORPTION IN EARLYWOOD AND LATEWOOD FIBERS OF LOBLOLLY PINE IN CYCLIC COMPRESSION

A Thesis Submitted by

Cheryl B. Rueckert

B.S. 1985,1987 University of Wisconsin – Oshkosh

M.S. 1993, Institute of Paper Science and Technology

in partial fulfillment of the requirements
of the Insititue of Paper Science and Technology
for the degree of Doctor of Philosophy,
Atlanta, Georgia

December, 1998

ABSTRACT

Mechanical pulping is a process that uses mechanical energy to grind logs or refine wood chips into papermaking fibers. Although the refining process has been around for many years, the exact mechanism of how wood breaks down into fiber is unknown. It is thought that during the refining process two mechanical processes are occurring, shear and cyclic compression.

Some species of pulpwood have relatively uniform fiber morphology throughout the tree. In the Southern United States, the majority of wood used for mechanical pulping are the southern yellow pines. These pines are known for their abrupt transition between earlywood and latewood within an annual growth ring. Therefore, the wood source has fibers with very different fiber morphology subjected to the same refining conditions. Knowledge of how earlywood and latewood are affected by refining should enable the production of better fibers for papermaking. Earlier studies at the Institute of Paper Science and Technology (IPST) have shown that there is a difference in energy absorption between the two types of fibers while in the wood chip level of fiber organization. By understanding the role of cyclic compression throughout the refining process, it should be possible to identify morphological traits that can be used to select southern pine variants with the potential to produce stronger mechanical pulps with lower energy requirements.

The working hypothesis for this dissertation is that earlywood fibers selectively absorb energy applied by cyclic compression. The experimentation simulated fiber compression in a disk refiner, and determined whether there was differential energy absorption by the earlywood fibers. This was accomplished by separating earlywood and latewood chips of a loblolly pine, refining them separately and fractionating for whole fibers. Selected fibers were stained, and the stained and unstained fibers were recombined into an aggregate with the same earlywood and latewood proportions as the tree. Using an electromagnetic shaker, the aggregates were subjected to cyclic compression at frequencies ranging from 10 to 200 Hz. High-speed video and infrared imaging were used to record fiber deformation and temperature variations, respectively.

The images were then analyzed to determine if the earlywood fibers selectively absorbed the applied energy.

This research has shown that at higher frequencies and at the fiber aggregate level of pulp organization, there is little impact of fiber morphology on energy absorption between the earlywood and latewood fibers. There were few instances of the earlywood and latewood data exhibiting differential energy absorption, especially as the frequency of the applied compressions increased. This is theorized to be from the viscoelastic nature of the fibers. As the fibers are compressed, time is required for the fibers to relax and return to their uncompressed state. As frequency increases, the time between compressions becomes smaller, the fibers experience the next compression from an already stressed state, and less energy is absorbed. The frequency becomes high enough that the mechanical differences between the two fiber types is nullified.

To summarize the results of all of the experiments, at the fiber aggregate level there is no evidence of a preferential strain, with the possible exception of the lowest frequencies and first cycle of compression. The mechanical deformation analysis has the same outcome as the thermal image analysis. The change in temperature shows no differences between the earlywood and latewood fibers. At frequencies above 30 Hz, the fiber aggregates showed no difference in their energy absorption behavior, as seen by the change in curl index within cycles or the change in temperature. This is mechanical behavior is hypothesized to be due to the viscoelastic nature of the fibers and at the higher frequencies there is not enough time for the fibers to recover from one stress before the next is applied.

EVALUATION OF PREFERENTIAL ENERGY ABSORPTION IN EARLYWOOD AND LATEWOOD FIBERS OF LOBLOLLY PINE IN CYCLIC COMPRESSION

A Thesis Submitted by

Cheryl B. Rueckert

B.S. 1985,1987 University of Wisconsin – Oshkosh

M.S. 1993, Institute of Paper Science and Technology

in partial fulfillment of the requirements
of the Insititue of Paper Science and Technology
for the degree of Doctor of Philosophy,
Atlanta, Georgia

December, 1998

ABSTRACT

Mechanical pulping is a process that uses mechanical energy to grind logs or refine wood chips into papermaking fibers. Although the refining process has been around for many years, the exact mechanism of how wood breaks down into fiber is unknown. It is thought that during the refining process two mechanical processes are occurring, shear and cyclic compression.

Some species of pulpwood have relatively uniform fiber morphology throughout the tree. In the Southern United States, the majority of wood used for mechanical pulping are the southern yellow pines. These pines are known for their abrupt transition between earlywood and latewood within an annual growth ring. Therefore, the wood source has fibers with very different fiber morphology subjected to the same refining conditions. Knowledge of how earlywood and latewood are affected by refining should enable the production of better fibers for papermaking. Earlier studies at the Institute of Paper Science and Technology (IPST) have shown that there is a difference in energy absorption between the two types of fibers while in the wood chip level of fiber organization. By understanding the role of cyclic compression throughout the refining process, it should be possible to identify morphological traits that can be used to select southern pine variants with the potential to produce stronger mechanical pulps with lower energy requirements.

The working hypothesis for this dissertation is that earlywood fibers selectively absorb energy applied by cyclic compression. The experimentation simulated fiber compression in a disk refiner, and determined whether there was differential energy absorption by the earlywood fibers. This was accomplished by separating earlywood and latewood chips of a loblolly pine, refining them separately and fractionating for whole fibers. Selected fibers were stained, and the stained and unstained fibers were recombined into an aggregate with the same earlywood and latewood proportions as the tree. Using an electromagnetic shaker, the aggregates were subjected to cyclic compression at frequencies ranging from 10 to 200 Hz. High-speed video and infrared imaging were used to record fiber deformation and temperature variations, respectively.

The images were then analyzed to determine if the earlywood fibers selectively absorbed the applied energy.

This research has shown that at higher frequencies and at the fiber aggregate level of pulp organization, there is little impact of fiber morphology on energy absorption between the earlywood and latewood fibers. There were few instances of the earlywood and latewood data exhibiting differential energy absorption, especially as the frequency of the applied compressions increased. This is theorized to be from the viscoelastic nature of the fibers. As the fibers are compressed, time is required for the fibers to relax and return to their uncompressed state. As frequency increases, the time between compressions becomes smaller, the fibers experience the next compression from an already stressed state, and less energy is absorbed. The frequency becomes high enough that the mechanical differences between the two fiber types is nullified.

To summarize the results of all of the experiments, at the fiber aggregate level there is no evidence of a preferential strain, with the possible exception of the lowest frequencies and first cycle of compression. The mechanical deformation analysis has the same outcome as the thermal image analysis. The change in temperature shows no differences between the earlywood and latewood fibers. At frequencies above 30 Hz, the fiber aggregates showed no difference in their energy absorption behavior, as seen by the change in curl index within cycles or the change in temperature. This is mechanical behavior is hypothesized to be due to the viscoelastic nature of the fibers and at the higher frequencies there is not enough time for the fibers to recover from one stress before the next is applied.

TABLE OF CONTENTS

LIST OF FIGURES

LIST OF TABLES

INTRODUCTION

This thesis concerns the development of a method to discern what is happening to the wood fibers due to cyclic compressive forces in a refiner. It was hypothesized that the earlywood fibers were preferentially absorbing the energy applied during refining. If the earlywood fibers are preferentially absorbing energy compared to latewood fibers they may become over refined, leading to a loss of pulp quality (3). The southern yellow pines are probably where this problem would be most self-evident; therefore, loblolly pine was chosen as a fiber source for this thesis.

One of the questions raised by the high-energy requirements of the southern yellow pines is whether the fibers in the wood are absorbing the applied energy uniformly. There is a possibility that the earlywood fibers are being over-refined and broken into fine particles. In this case, the latewood fibers would then be under-refined and thereby left coarse, inflexible, and uncollapsed. If this were happening, the resulting paper would not be as smooth or strong.

Previous research has shown that earlywood fibers do show preferential energy absorption within a model wood chip. Simulated wood chips were cyclically compressed and the thickness and temperatures of the different growth zones within the annual growth recorded (26). The earlywood growth zones were compressed by 37% and latewood by only 3% of their original width. The temperature experiments recorded that temperature increased immediately after the initiation of the compression cycles for earlywood, but the latewood lagged. Temperature for both fiber types eventually reached a plateau, but the earlywood had a higher temperature plateau and it took longer to reach the plateau than the latewood fibers. The mechanical deformation and the temperature change are evidence that the earlywood fibers are preferentially absorbing energy at the wood chip stage.

The time that a fiber is present as a wood chip within a refiner is short. The wood chip is already splitting and breaking in the line feeding the refiner (73). Cinematography has given researchers a window into a refiner, and this window shows few wood particles, mostly fiber aggregates (14,39). Therefore, a study needs to be completed to understand whether uneven or

preferential energy absorption occurs among of fiber aggregates within refiners. The fiber aggregate stage brings the study to a microscopic level, with its concomitant problems. Individual fibers are approximately two millimeters long and thirty microns wide. Because the fibers are no longer glued to each other and voids exist within the aggregates, individual fiber mechanical deformation within an aggregate cannot be measured by the change in fiber width during cyclic compression. By the same reasoning, individual fiber temperature cannot be measured by inserting a thermocouple into the aggregates. Another problem to overcome is how to identify individual fibers as earlywood or latewood. This thesis documents a study performed to explore energy absorption in fiber aggregates subjected to cyclic compression and how the accompanying problems were handled.

In the literature review for this thesis, wood and fiber structure, chemistry, and seasonal variations are covered. Some of the relevant theories to date on the process of how wood chips are separated and fibrillated into a pulp are reviewed. This will cover the two proposed mechanisms that occur within the refiner, shear and cyclic compression. A section on wood mechanics is included. Current ideas are examined on how wood morphology could impact refining, followed lastly by a review of another investigation into the hypothesis of preferential energy absorption by the earlywood fiber due to cyclic compression.

The experiments necessary to analyze whether there is preferential energy absorption by earlywood fibers in fiber aggregates have measured: 1) the change in the absolute value of curl index (showing a deformation of shape) and 2) the change in temperature during cyclic compression. The experiments included video recording at both regular and high speed, and high-speed infrared imaging systems.

The thesis objective states the hypothesis that the earlywood fibers of a fiber aggregate will show preferential energy absorption due to cyclic compression. Therefore, the goal of this study is to investigate the distribution of mechanical deformation and temperature change between earlywood and latewood fibers in aggregates placed under cyclic loads. This research expands on the previous research in the use of fiber aggregates and higher frequencies.

The methods used to test the hypothesis are defined and clarified. The separation of fibers and preparation of the fiber aggregates, apparatus design, the fiber aggregate holder during the various types of imaging, the imaging devices, and how the testing was done for both mechanical deformation and thermal studies.

The results present the changes observed in the absolute value of curl index and change in temperature experiment by experiment. Each experiment has the data presented and discussed. For the majority of the experiments within this thesis, the data shows that earlywood does not preferentially absorb energy at the frequencies of cyclic compression approaching the bar cross frequency of disk refiners.

To summarize the results of all of the experiments, at the fiber aggregate level there is no evidence of a preferential strain, with the possible exception of the lowest frequencies and first cycle of compression. The mechanical deformation analysis has the same outcome as the thermal image analysis. The change in temperature shows no differences between the earlywood and latewood fibers. At frequencies above 30 Hz, the fiber aggregates showed no difference in their energy absorption behavior, as seen by the change in curl index within cycles or the change in temperature. This is mechanical behavior is hypothesized to be due to the viscoelastic nature of the fibers and at the higher frequencies there is not enough time for the fibers to recover from one stress before the next is applied.

The lack of preferential energy absorption by the earlywood fibers, at the fiber aggregate stage, is good and bad news for the people who are presently using mechanical pulping. The good news is that the present equipment/process is not causing one type of fiber to be over refined and the latewood fibers to be under-refined. Unfortunately, this research has not shown a possible method of reducing the amount of energy required to produce mechanical pulps or a means to improve the quality of mechanical pulps.

REVIEW OF THE LITERATURE

WOOD AND FIBER STRUCTURE AND MORPHOLOGY

The Layered Structure of Wood and Fibers

The loblolly pine fiber (tracheid) was at one time a living cell in the tree. The fiber is shaped similarly to a straw but with tapered ends and an elliptical cross section. The fiber has a hollow center, the fiber lumen. In loblolly pine, fibers average 4 mm in length and 30-45 microns in diameter, with an average cell wall thickness of 5.2 microns (1). The fiber wall (or cell) is a layered structure (Figure 1). It is composed of three main layers: the middle lamella, the primary cell wall, and the secondary cell wall. The middle lamella and the primary cell wall are often called a combined structure - the compound middle lamella, due to the thinness of the primary cell wall that makes it difficult to separate the regions. The secondary cell wall is itself composed of three layers: the S1, S2, and S3. The S2 is the layer that dominates the bulk of the mechanical tissue of the cell wall. In the tree used for this study, the earlywood cell wall thickness was on average 60% of that of the latewood cell wall (Appendix 1).

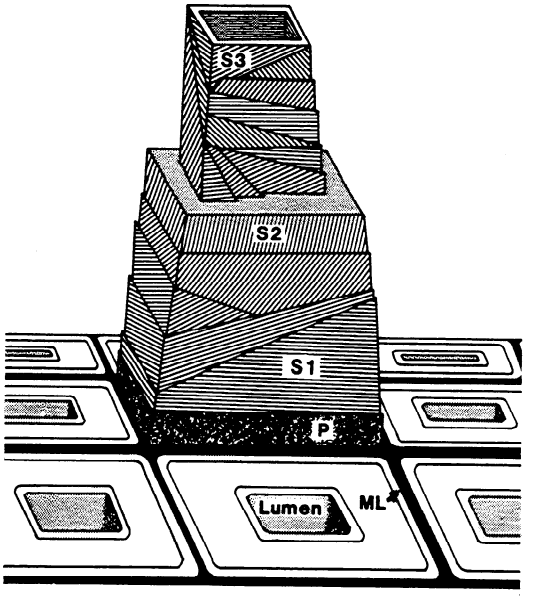

Figure 1. The layered structure of the woody cell (2).

Each layer of the cell wall has its typical chemical constituents and physical organization of these constituents. The principal chemical constituents in trees are cellulose, hemicellulose, and lignin. Cellulose comprises roughly half of the dry weight of wood and has the largest effect on the mechanical characteristics of wood due to its concentration in the large S2 layer (Figure 2) (3). The basic repeating unit of cellulose is cellobiose, which consists of two glucose molecules bonded together with a β 1-4 linkage. The cellobiose unit can repeat up to 10,000 times, determined by the species. These chains of cellulose are grouped in well-ordered crystalline regions, or unordered amorphous regions.

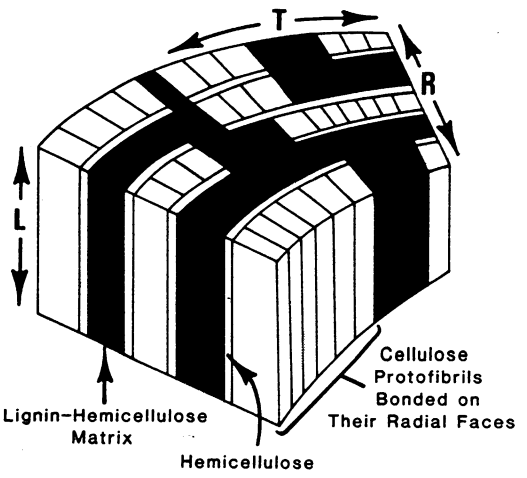

Figure 2. Distribution of the principal chemicals within the layers of the cell wall in conifers (2).

Hemicelluloses are less well defined than cellulose. They are the part of the total carbohydrate that is soluble in dilute alkali and hydrolyzes readily in dilute acid to form sugars and sugar acids. The hemicelluloses are of two general classes: xylans and galactoglucomannans. The hemicellulose and cellulose fractions of wood combined are called holocellulose, which makes between 60 and 85% of the dry weight of wood. Hemicelluloses are generally thought to chemically join the cellulose to the lignin, and have an amorphous chemical structure that is very hygroscopic (3). The amorphous chemical structure of hemicellulose makes it very sensitive to temperature changes when considering its effect upon mechanical behavior.

Lignin is a large, amorphous, three-dimensional polymer. It is believed to be present in living plants for rigidity and the increased stiffness it gives to the cell walls. Lignin is less hygroscopic than cellulose and thereby retards dimensional changes in the cell with moisture changes. This is due to the effect of cross-linking and lignin's basic structure of a phenylpropane 'backbone' not attracting and hydrogen bonding polar liquids such as water. Lignin is also thermoplastic, changing from glassy to elastic mechanical behavior with increasing temperature. Lignin comprises 15 to 35% of the dry weight of wood and is found in the greatest concentration in the compound middle lamella (Figure 2).

The cellulose and hemicelluloses are combined into long strands known as microfibrils (3). The microfibrils are essentially a core of crystalline cellulose encased in a shell of hemicellulose. Microfibrils are present in both the primary and secondary cell walls. The orientation of the microfibrils varies with each layer in the cell wall. The primary cell wall has a random pattern of orientation. The S1 is made of many sub-layers that alternate their orientations with each sub-layer, the outer layers have angles of ±50 to 70° from the cell axis. This angle decreases from layer to layer with the inner layer fibrils being almost parallel to this axis. The high angles of the S1 cell wall help the cells resist transverse forces. The S2 cell wall layer is the thickest in the cell and its microfibrils are only 10 to 30° from the cell axis. Because of the thickness of the S2 cell wall, it dominates the physical behavior of the papermaker's fiber especially in the axial direction. The S3 layer is the thinnest and least studied of the layers of the secondary cell wall. The orientation of microfibrils in this layer is close to perpendicular to the cell axis, with some major deviations. Lignin is deposited in the cell after the microfibrils are formed, and encases and binds them into a rigid structure.

Variation within the Annual Growth Ring

Cell dimensions vary due to environmental conditions present during growth and maturity. There are regular changes in growing conditions during the spring and summer seasons. These changes lead to the tree forming fibers of very different morphology (1). Fibers (cells) grown during the early, fast-growing period in the spring are called earlywood or springwood. These fibers have shorter fiber length, larger cross-sectional area, higher microfibrillar angle, lower wall thickness, less alpha cellulose, and slightly more lignin than fibers grown later in the slower growing period of the summer (1,3-9). The cells formed in the summer are called latewood or summerwood. Due to the larger cross-sectional area and thinner fiber walls, earlywood has a much larger lumen or central void and consequently, lower wood specific gravity than latewood. In wood, the strength, work to maximum load, elongation and

modulus of elasticity differ greatly between the two growth regions, with earlywood having the smaller values (4-9). Tensile testing of microspecimens shows a difference in the mode of fracture. Earlywood has a tendency to break across the cell walls while latewood fibers fail between the cells in the middle lamella (10). Single fiber strength of the latewood tracheid is superior (7).

Compared to the northern softwoods, the southern pines have a much larger proportion of latewood in the annual ring. The latewood fibers have an average wall thickness approximately double the earlywood fibers. A histogram of the cell wall thickness in loblolly pine shows distinct bimodal distribution because of the two fiber types (Figure 3). This difference will lead to differing mechanical properties. The latewood fiber will be more rigid than the earlywood fiber.

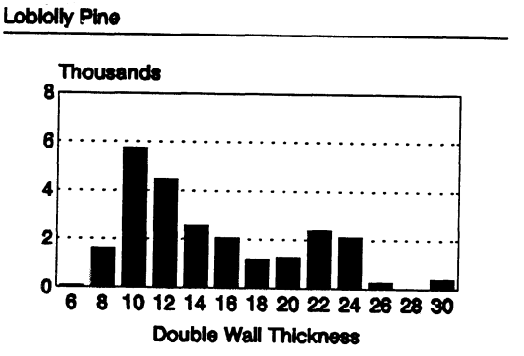

Figure 3. Bimodal distribution of loblolly pine wall thickness (11).

Other differences in mechanical properties are also present at the single fiber level. Defects such as kinks and curl lower the elastic modulus of a fiber and its capability of

transmitting stress along the fiber length (12). Fibril angle, degree of crystallinity and composition of the cell wall also influence fiber mechanical properties (13).

The angle of the microfibrils in the S2 layer has a large impact on tensile strength and compression strength of the fiber. A latewood fiber generally has a low microfibril angle (closer to parallel to the fiber axis) which results in a larger single fiber axial tensile strength (12).

The degree of crystallinity also has a considerable effect upon fiber mechanical behavior. There are three factors why cellulose found within the cell wall of fibers is in a crystalline form (3). One, the cellulose molecule is a uniform ribbon-shaped structure. Two, carbon-to-carbon bonding gives the chain great rigidity and solidarity. Three, there are abundant hydroxyl groups accessible along the length of the molecule for bonding to other cellulose chains. Because the hydroxyl groups are bonded to other hydroxyl groups, and thereby inaccessible, cellulose polymers are not as hygroscopic and exhibit lower dimensional and mechanical changes as the moisture content of the fiber changes. There is more cellulose present within a latewood fiber and this cellulose has a larger crystalline percentage (3).

The difference in chemical composition within the fibers of a growth ring is not huge, but is significant. Fibers rich in cellulose generally are much more rigid and have higher tensile strengths. A higher percentage of hemicellulose will generally cause the fiber to be more hygroscopic, less dimensionally and thermally stable, and show increased strain for the same force (3). Lignin enrichment will give mechanical values between the two forms of carbohydrate but will have less moisture sensitivity (3). Latewood fibers generally have more alpha cellulose and less lignin than the earlywood fibers with the accompanying mechanical, thermal, and hygroscopic responses (3).

THEORIES ON REFINING

History of Mechanical Refining

The history of the use of refiners to produce pulp suitable for paper starts in 1929 with the invention of the defibrator process by Arne Asplund (14). It was initially used to grind wood chips to produce particle board for the board industry. Later this process was adapted to produce a type of groundwood pulp – refiner-mechanical pulp (RMP). The earliest commercial refining operations started up in 1970 (15). At the time the RMP process was maturing, environmental concern with the discharge from chemical pulping mills increased, along with the pressure for the best roundwood to go to the lumber industry instead of the stone-groundwood mills (SGW) (15). These concerns forced the pulp and paper industry (especially newsprint) to look for other processes to produce a pulp with greater strength than groundwood to replace the expensive chemical pulp in their printing papers. By using RMP instead of the SGW process, pulp mills did achieve a much stronger pulp with little loss in opacity. The other benefits of this new process are the ability to use scraps of the lumber business and a much higher yield, less effluent, and lower cost than the chemical pulps. RMP is not the energy saving process it was once hoped to be. Depending upon the wood species, SGW averages approximately 1400 kWh and refiner pulps need 1800+ kWh to produce an oven-dried ton of pulp (2). Since the 1970s, most new mechanical pulp capacity has been added as a version of refiner pulping, usually thermomechanical pulping (TMP). The major difference between TMP and RMP is that the TMP refiner is pressurized and operates at temperatures above the boiling point of water.

Refiner pulps are very different from SGW. SGW fibers are very short and have a large quantity of fine material (Figure 4). At high magnification, the surface of the SGW fiber is rather smooth. A TMP pulp has many more long fibers, and at higher magnification, the fiber has a fibrillated surface (Figure 5).

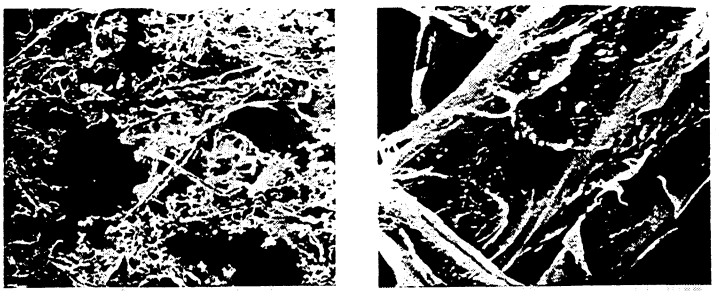

Figure 4. Groundwood pulp at 117X and 2350X magnification (2).

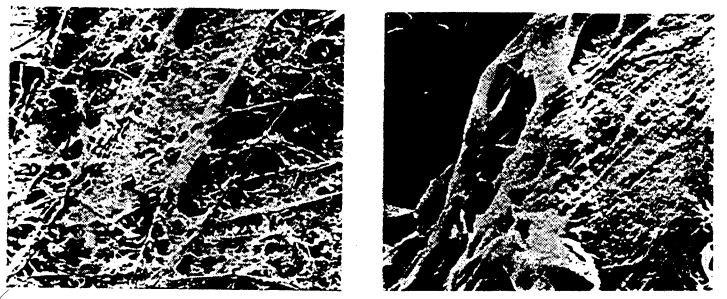

Figure 5. Thermomechanical pulp at 116X and 2350X magnification (2).

Mechanical Pulping of Wood Chips

A typical flow diagram for TMP is easily described. Chips feed into the system with a screw conveyor from a pre-steaming bin and pass through a plug screw feeder, which seals the system, and the steam then pressurizes the system. The chips preheat in another screw conveyer. A screw or ribbon feeder then transports the chips into the eye of the refiner. From the center of the refiner, the chips move outward between the plates of the refiner. Exposure to various compressive and shear forces occurs between the refiner plates. These forces change the wood chips into pulp. Larger chips break into smaller chips by the breaker bars on the refiner plates. Due to centrifugal forces and more chips being fed to the system, the smaller chips enter the intermediate and fine bar refining zones. The pulp leaves the refiner and then enters various

chests, cleaners, and reject refiners before going to the paper machine (16). The opposing movement of the bars on the plates leads to a crossing frequency in the range of 10^4 hertz.

When a pulping system has its refiners in series, each refiner is a numbered stage, and the number depends upon whether it is the first, second, or third refiner in the series. It is common to have a two-stage TMP system in which the second stage has an atmospheric discharge in older mills; newer mills may have a pressurized second stage. It is also possible to have pressurized refining without preheating the chips; this is called pressurized RMP (2).

Mechanisms of Refining

The mechanics of fiber separation within a refiner is not fully understood. It has been observed that wood chips broke down into "matchstick-like" fragments with evidence of internal breakdown in cross section (16) even before entering the eye of the refiner. These fragments enter the refining region in random orientation. A substantial amount of fibrous material is already produced by halfway through the refiner. Pearson (18) suggests that the chips or fibers may be rolling between the plates, and this rolling could be a method of fiber separation or fibrillation. Work by Atack (16) casts serious doubt on this theory. Using cinematography through transparent portions of a refiner plate, Atack found that there is no evidence of particle rolling within the refiner. He states that in order for fiber rolling to occur the fiber axis must be oriented radially within the plates, and that all pictures of fibers and fiber clumps (rafts) depict a major axis tangential to the refiner bars (16). He further states that the bars on the refiner plates provide an environment in which fibers are exposed to varying shear and compressive forces. An idealized wood chip exposed to the various stresses within a refiner is shown in Figure 6.

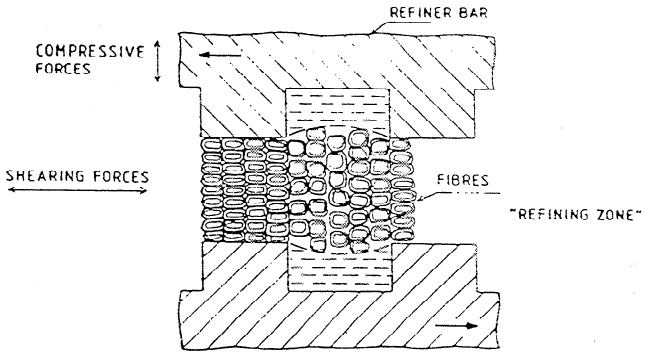

Figure 6. Shear and compressive forces present within the different parts of the refiner clearance (19).

Shear

Shear is essential to fiber separation. This mechanism physically "peels" the fibers from the chip. It is caused by the refiner bars rubbing along the length of the wood chip, which then tears fibers from the surface (16). Without shear, fibers do not separate, and the chips would char (20). Shear forces are also applied to fiber aggregates after fiber liberation. This is accomplished by the moving bars working along the length of fibers, which are trapped momentarily on an opposing bar (21).

Studies performed on the significance of fiber morphology in shear found that earlywood fibers behave differently than latewood fibers. After varying sulfite chemical pretreatments, Lai and Iwamida (22) sheared wood blocks using an Instron tensile tester. They found that with no chemical pretreatment the earlywood fibers showed extensive fragmentation from fiber splitting along the cell axis and trans-wall cutting of the fiber. Latewood fibers separated at the S1 and were uniformly fibrillated. Chemical pretreatment was shown to move the earlywood fracture from trans-wall to the primary cell wall and the middle lamella, similar to that of the latewood fibers.

Compression, Fatigue, and Wood Mechanics

Compressive force is applied to wood chips or fibers by impacts between opposing bars on the refiner plates. These compressive forces are repetitively applied throughout the chip/fiber passage through the refiner. Due to the regularity of the compressive pulse, this is referred to as cyclic compression. Cyclic compression is thought to initiated by a fatigue-type process within the refiner that aid in fiber separation and flexibility (23,24). Studies show good correspondence between fatigue measurements and refining results (25).

When a stress is applied to a material, a strain is produced. A linear elastic material responds to increasing stress with larger strains, and when the stress is removed, the strain immediately returns to zero (26). In a viscoelastic substance, such as wet wood, application of stress also produces strains. Up to a given stress, the material will behave the same as the linear elastic material. After that point, a larger strain is produced for the same increase in stress (27). After the stress is removed, there is some immediate strain recovery followed by a slower strain recovery. If the applied stress is large enough, a plastic deformation will occur, and the deformation will not completely recover after removal of the stress (28).

Viscoelastic materials absorb energy in the cycle of stress application and removal. When the stress is removed, there is a lagging of the strain response before the strain returns to the unstressed state (Figure 7). Hysteresis is defined as a lagging of an effect behind its cause (29). Due to this lagging, there is a different amount of strain at the same stress level depending on whether one is applying or removing the stress. The area within the stress strain curve represents the amount of energy absorbed per cycle of stress (30). At some frequency there is not enough time before the application of the next stress for the strain to have returned to zero. In this case, the material will start the next stress cycle from a pre-strained state. The second cycle of stress can follow the same curve as the first, or it may have greater or less strain depending upon the material (30).

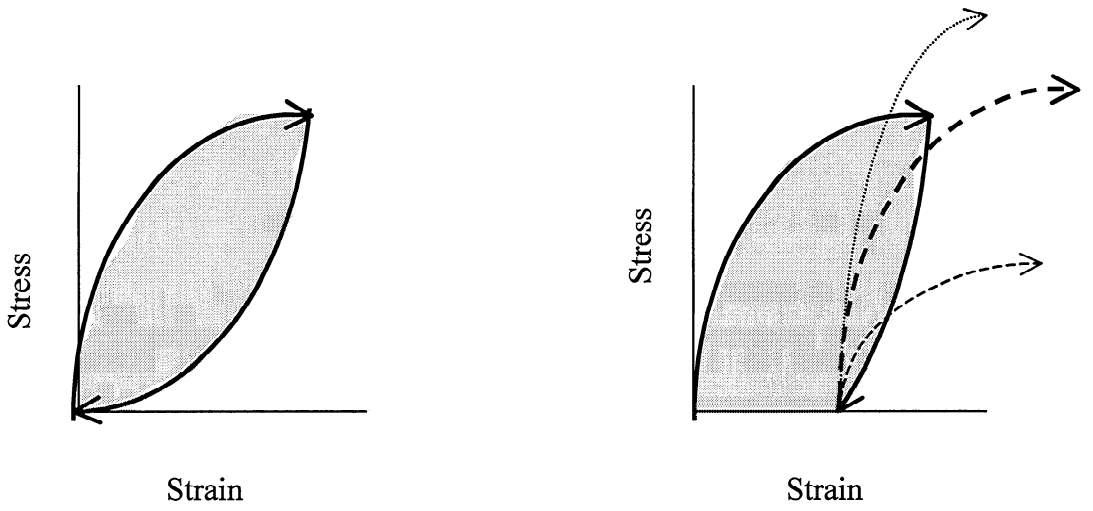

Figure 7. Stress strain curves showing hysteresis and energy absorption per cycle.

The relationship between the stress and strain of a material is defined as a modulus (31). The modulus of a material varies depending upon temperature, time, and moisture content. As the temperature increases, the moduli will decrease and the material properties change from glassy to rubbery. The effect of time is demonstrated during testing. The length of the duration of a stress is reflected in a decrease in the moduli. If stressed for a long period of time, most materials would appear to have a low modulus.

Wet wood is a viscoelastic substance, and as the moisture content increases, the modulus of elasticity decreases. This is due to the water molecules acting as a plasticizer (31-33). The polar water molecules disrupt the hydrogen bonding between the polar components of the materials within the fiber allowing greater chain mobility. Thereby, when a stress is applied to a fiber, the fiber is more capable of relieving that stress. This effect of water is also seen in the decrease of the glass transition temperature with the addition of water (31).

When wood is mechanically deformed, energy is consumed in the process (34). It has been estimated, using the amount of energy required to create new surface area, that the amount of energy required to separate wood into fiber is 0.01 to 300 kWh/ton, depending upon the method of calculation (35-40). In contrast, the industry requires approximately 1400 to 2000 kWh/ton to produce TMP (41). The extra energy is due to the energy absorbed in cyclic

deformation of a viscoelastic material. Generation of small cracks or fractures within the fiber wall may require a cyclic loading/fatigue failure process (34,41-43).

Fatigue is defined as a weakening caused by long-continued use or strain (29). In a refiner the term fatigue is usually applied to cases of intermittent or repetitive stressing but can also be used for a one-time stress, as in the case of creep rupture (30). The wood chips or fibers are subjected to compressive forces that can be greater or less than enough stress to cause plastic failure (17). This stress is applied repetitively to the fibers throughout the interval within the refiner. When a material is subjected to an applied stress, many chemical and rheological events may occur. The effect depends on several competing factors: molecular properties and composition of the material, temperature, time scale, and the environment (30).

Fatigue failure can occur due to hysteretic heating. The largest cause of thermal failure is believed to involve the accumulation of hysteretic energy generated during each loading cycle (29). Because this energy is largely dissipated in the form of heat (30), the temperature of a material increases with every loading cycle when isothermal conditions are not met. The temperature rise can be great enough to cause the material to melt, thereby preventing it from carrying a load. The failure is presumed to occur by viscous flow with some bond breakage (30).

Three forms of fatigue testing occur in laboratories: stress controlled, deflection controlled, and strain controlled. They are different in their response to each loading cycle and their rate of heat generation and temperature increase. For stress controlled testing, the rate of heat generation, as proposed by Schmidt and Marlies (30), is proportional to

$$H_F \propto DF^2/E_d. \qquad (1)$$

where H_F is the rate of heat generation under stress (or force) control, D is the damping capacity of the material, F is the force, and E_d is the dynamic modulus. In this testing case, as the sample heats, the dynamic modulus will decrease and the damping capacity will increase, thereby increasing the rate of heat generation (30). This relationship does not take into account the transfer of heat to the surroundings, controlling the rate of heat generation and limiting thermal failure.

Deflection and strain controlled testing and their rates of generation are closely related (30). The equation developed by Schmidt and Marlies (30) to explain the rate of heat generation in these cases is

$$H_X \propto DE_d x^2. \qquad (2)$$

where H_X is the rate of heat generation due to fixed displacement, D is the damping capacity, E_d is the dynamic modulus, and x is the displacement amplitude. This relationship shows that thermal failure cannot take place in either deflection or strain controlled testing. As heating occurs, the dynamic modulus will decrease, thereby lowering the heat generation rate. An equilibrium temperature is quickly reached. This equation also does not include a term for the transfer of heat to the surroundings. Studies show that the stress applied in a constant deflection test decays with repeated cycling (30). This decay is due to plastic deformation and hysteretic-heating induced softening of the material. It has been argued that stresses should not be calculated from deflection controlled testing because dynamic modulus changes during the initial portion of the test, changing the relationship between sample deflection and applied stress level (30).

Cyclic Compression Studies of Wood Blocks

Salmen et al. (42) have found, with cyclic compression of wet wood, that structural breakdown is favored by higher temperatures and lower frequencies. Higher temperatures lead to a greater change in the wood's elastic modulus. Within fibrous materials, the structural breakdown is generally in the form of generating new surface areas or fractures. The higher the temperature during refining, the further the fracture moves into the middle lamella from the S2 layer of the wood (25,41,43). Lower frequencies of cyclic compression show a larger decrease in elastic modulus thought to be from increased fracture. This fracture is probably from the greater amount of energy applied to the wet wood at low frequencies, due to the long interval between stresses leading to a greater time for stress relaxation between cycles. One problem with

Salmen's work is that it was performed at frequencies well below those found in refiners, 1 to 20 Hz, compared to 1000 and 10,000 Hz in the fine bar section of a refiner.

Atack and May (20), in their study with the steel wheel (a laboratory model of a grinder capable of varying the amount of compression and shear, while holding the force constant), demonstrate that cyclic compression produces increased temperatures in wood blocks. Localized cyclic viscoelastic deformations lead to subsurface charring in the wood blocks, which is an indication of energy dissipation as heat in the wood. The surface fibers do not char because they were cooled with water showers. These results are consistent with the idea of energy being dissipated as heat in a localized, highly strained zone near the wood surface.

Hickey et al. (23) also demonstrated that cyclic loading of water-saturated wood blocks does cause the temperature of the specimen to increase, and the temperature increase is higher in the earlywood than latewood zones within an annual growth ring (Figure 8). The temperature of the blocks compressed at 15 and 30 Hz rose dramatically during these experiments. These results suggest that the majority of the energy applied in the early stages of disk refining absorbed by the earlywood (23). The temperature versus time chart (Figure 8) demonstrates the characteristic shape of a deflection-controlled experiment. The temperature quickly reaches equilibrium.

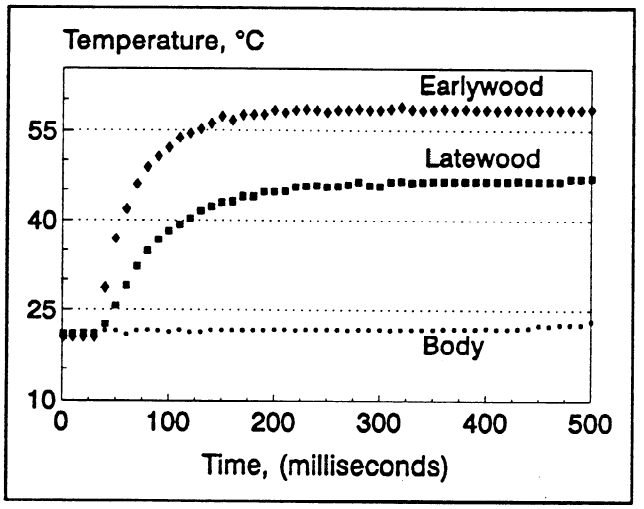

Figure 8. Temperature record of the sample tested at room temperature and 15 Hz (23).

Cyclic Compression Studies of Wood Fibers

Studies have been performed on a type of single fiber cyclic loading (44). Instead of transverse cyclic compression, the fibers are bent cyclically until failure. These studies indicate that it is possible to weaken the structure of fibers by subjecting them to either a small number of loading cycles at high stresses, or to a large number of loading cycles at lower stresses (44). This result is similar to Salmen's work with wood blocks, showing that mechanical characteristics of wood blocks can possibly be applied to those of fibers. The problem with this work is that the fibers selected for stressing are those that are free from physical defects such as kinks. In a real-world refiner, there are probably very few fibers without some type of defect.

Temperature

Temperature impacts mechanical pulping and wood properties due to the glass transition of wood's major components. Glass transition is defined as the temperature at which the transition from a glassy state to a rubbery state occurs when measured using a slow process (60).

Under water-saturated conditions, hemicellulose has a glass transition of about 50-60 °C; lignin has a transition temperature of 90-100 °C, followed by cellulose around 235 °C (45).

The influence of temperature and glass transition on mechanical behavior can be seen in a study of wood using a torsional pendulum. By twisting the sample, releasing it, and recording the oscillations as it moves back to equilibrium, one can measure the dynamic elastic behavior of the sample (46). Torsional modulus and internal friction are both measured with a torsional pendulum apparatus. The frequency at which the sample oscillates while returning to equilibrium correlates to the torsional modulus of the sample. The rate of decay in the amplitude of the oscillations shows the internal friction (or damping capacity). Figure 9 shows how torsional modulus and internal friction are impacted by temperature at two test frequencies (graphed by displacing the x-axis so the curves overlap) (46). Torsional modulus drops with increased temperature at both frequencies as the materials within the wood change from glassy (stiff) to rubbery behavior.

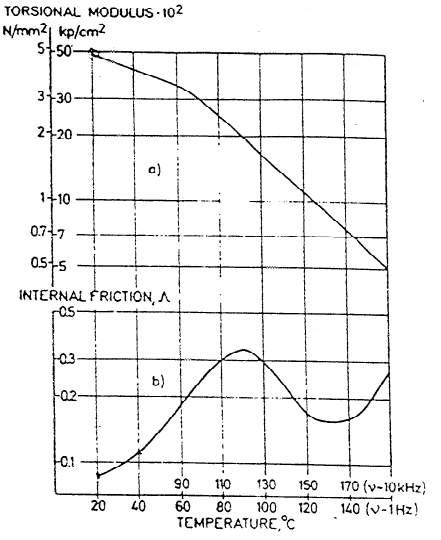

Figure 9. Torsional modulus and internal friction of spruce wood vs. temperature at two different test frequencies (46).

Internal friction increases up to a particular temperature, decreases almost to where it started, and then rises again. The temperatures of the peaks and valley are different for both test frequencies, but they follow the same pattern. The first rise and fall is attributable to the glass transition of the lignin and hemicellulose within the wood. These two major components of wood have low transition temperatures from glassy to rubbery behavior. The glass transition temperature for cellulose, the other major component of wood that comprises approximately 45% of the dry mass, is much higher than lignin or hemicellulose. As the wood heats into the lignin and hemicellulose transition zone, the behavior of the lignin and hemicellulose dominates the mechanical behavior of the wood. At this temperature range for the glass transition, the segments within the lignin and hemicellulose begin to be rotated, translated, and have short-range diffusional motions (31). It is these motions that cause the internal friction to rise. After the glass transition region for lignin and hemicellulose is passed, the internal friction falls due to their rubbery state. At this point, the cellulose is the major contributor to the internal friction behavior. When the cellulose begins to reach its glass transition, the internal friction again rises.

Impact of Wood Morphology on Refining

Wood properties can impact mechanical pulping. The property that most studies have focused on is wood density (11,16,23,47-51). This property shows a strong correlation to energy required for production of a useful pulp.

A fiber with a thick cell wall causes overall higher wood density, and generally has high tensile strength and a lower fibril angle. Looking at Figure 10, one can see the relationship between paper strength and density, at a given input of energy. Spruce and loblolly pine are examples of low and high-density softwood, respectively. Higher density wood species seem to require a larger input of energy to reach the same strength as the lower density wood species.

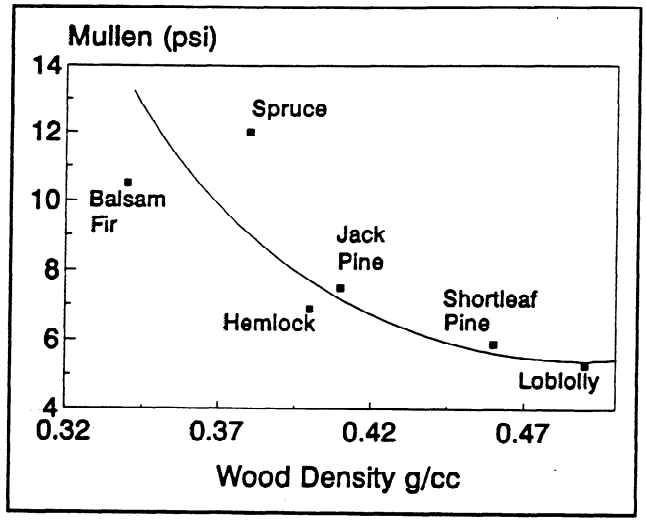

Figure 10. Relationship between burst strength (Mullen) and wood density at a specific power consumption level (11).

This can also be seen in Corson's work with Radiata pine (48). The butt log samples (mature wood with high density) require more energy to reach target freeness than did logs of lower density (Figure 11). Freeness is highly correlated to the hydrodynamic surface area of fibers (50) and is a simple test of whether the pulp is refined and ready for papermaking. Corson also compared the effects of mature wood versus corewood on refining energy (49). The hypothesis tested was that the lower density corewood should use less energy to refine to a specific freeness. However, this was not observed in this case.

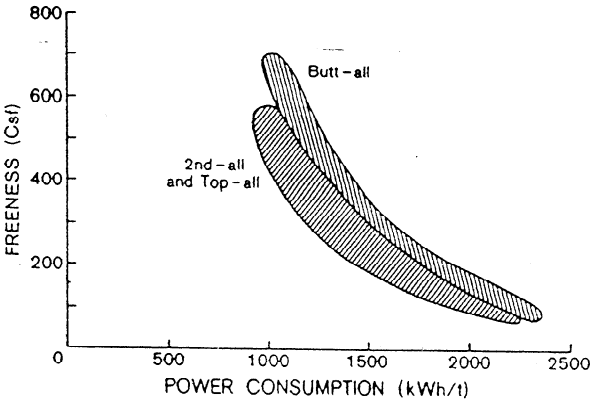

Figure 11. Freeness versus power consumption in Radiata pine (48).

Fiber Morphology and Energy Absorption

Various studies with cyclic compression of wood samples reveal that earlywood behaves differently than does latewood (23,24,52). Hickey's experimentation videotaped wood blocks during a compression sequence and the width of the earlywood and latewood growth zones were measured before compression and then after a predetermined number of compressions. Earlywood consistently showed greater mechanical deformation of the thickness of the growth ring. Latewood showed very little change during the cyclic compression tests (Figure 12). On average, the earlywood portion compressed by 37% of the initial width, but the latewood zone only compressed by 3% of its initial width. Temperature and frequency had little effect on this response. By placing thermocouples within the growth rings, Hickey (23) measured the temperature change that occurred during the compression test (Figure 8). This figure reveals how earlywood began absorbing energy immediately, as evidenced by the temperature rising as soon as the compression sequence began. The latewood temperature began to rise a short time later, but never reached the temperature level of the earlywood.

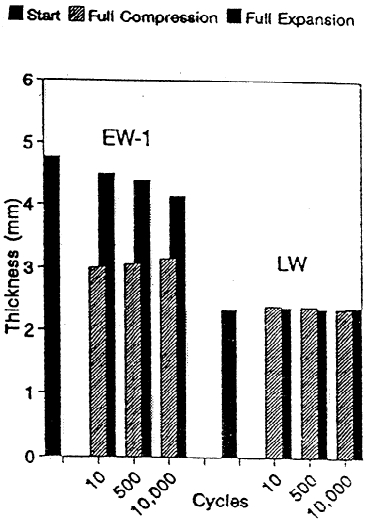

Figure 12. Response of earlywood and latewood to cyclic compression. Compressed width after 10,000 cycles (23).

The temperature difference at equilibrium and the time lag both appear to be dependent on the latewood bandwidth (Figure 13), indicating that the latewood heating may be due to the thermal conductivity of the wood. Interestingly, the temperature rise is not as large at 30 Hz as at 15 Hz. This is probably due to the sample not having time to recover from the previous compression stroke before the next is applied. That is, the next stroke is starting with a pre-compressed piece of wood; so less work is done on the sample, resulting in a smaller temperature increase. This study would seem to reinforce what Salmen et al. have stated, that lower frequencies will allow conservation of energy with the production of more flexible fiber (25). Hickey's study leads to the hypothesis that the earlywood is preferentially absorbing energy during cyclic compression at low frequencies, and, possibly, at the higher frequencies of refining. However, this study does not reveal whether fibers once liberated from wood demonstrate preferential energy absorption.

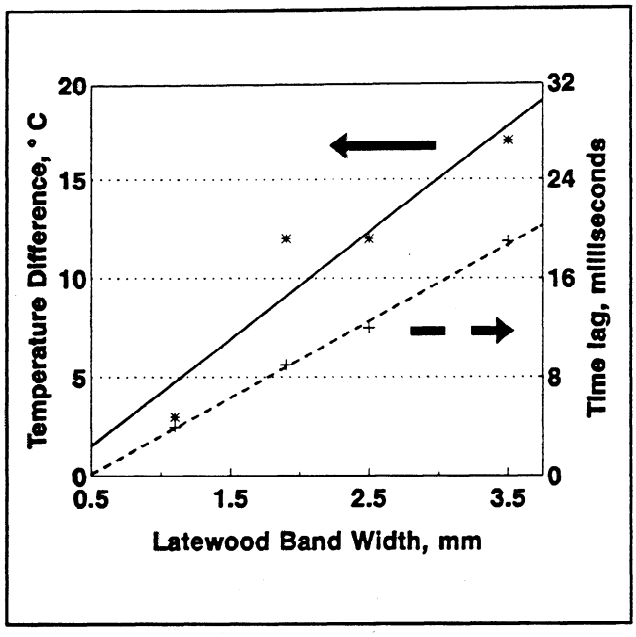

Figure 13. Equilibrium temperature difference between earlywood and latewood (23).

Thiruvengadaswamy and Ouellet have also seen differences between the earlywood and latewood portions of a wood block (24). Cycling at low frequencies promoted widespread damage (fractures) within the earlywood zones of the annual growth rings. Higher frequencies led to localized damage in the earlywood growth zones.

STATEMENT OF THE PROBLEM

One of the questions raised by the high-energy requirements of the southern yellow pines to produce mechanical pulp is whether the fibers in the wood are absorbing the applied energy equally. If the fibers are not responding to the applied energy equally, there is the possibility that one of the fiber types (probably earlywood by virtue of its thinner cell wall and more flexible attributes) is over-refined and broken into fine particles. If this is the case, the latewood fibers would then be under-refined and thereby left coarse, inflexible, and uncollapsed. The resulting paper would not be as smooth or strong as desired and would require additional energy to flexibilize the latewood fibers. Studies have been carried out with wood blocks demonstrating evidence of preferential energy absorption by the earlywood fibers (23,24,52), but no studies have been reported on energy absorption in fiber aggregates. The relative time the fiber spends in the refiner as part of a wood block is small. The single fiber is then continuously in the process of joining, leaving, and rejoining fiber aggregates during the rest of the refining process. This makes it important to understand whether preferential energy absorption exists within fiber aggregates.

THESIS OBJECTIVES

The work of Hickey et al. (23) shows that earlywood absorbs an unequal amount of the energy absorption in the early stages of TMP pulping. With the addition of small amounts of refining energy, the wood chips are broken down into small clusters of fibers and individual fibers. In the refining process, these fibers form large aggregates and the aggregates continue to be subjected to cyclic compression as they pass between the bars and grooves of the refiner plates.

The goal of this research is to investigate the distribution of energy absorption between earlywood and latewood in fiber aggregates of a southern yellow pine subjected to cyclic loads, simulating a disk refiner. The hypothesis is that earlywood fibers within the aggregates preferentially absorb energy. If differential mechanical deformation is occurring in fiber aggregates, it will be demonstrated by greater changes in curl index (a shape factor) per cycle by the earlywood fibers. The more energy absorbed, the more the curl index will change within a cycle. A direct measure of preferential energy absorption can be obtained by observing a larger temperature increase by the earlywood fibers than the latewood fibers during the experimentation. This study will also bring cyclic compression studies a step closer to frequencies predicted within mill refiners by a factor of 10 (200 hertz versus 20 or 30 hertz).

EXPERIMENTAL APPROACH

Two factors were studied to evaluate the hypothesis of preferential energy absorption by earlywood fibers within fiber aggregates: mechanical deformation and temperature change. These two factors were chosen as a way to understand the energy balance for the experiments. By cyclically compressing a fiber aggregate, work was done on the system. In this case the system was the fiber aggregate. Work has been defined as energy that flows in response to a driving force other than a temperature difference (53). The piston was applying a force and moving and deforming the fibers within the aggregate. The fibers were deformed (changed their shape) by the moving piston due to their entanglement with the other fibers within the aggregate.

$$\text{Work} = \text{Force} \times \text{Distance} \qquad (3)$$

Assuming that the force is equally distributed to both the earlywood and latewood fibers, the fibers that have a larger change in shape (move) should have absorbed more energy. By measuring the fiber deformation, an indirect comparison was made between the energy absorption of the earlywood and latewood fibers.

The second factor measured, temperature change, is a direct measure of energy absorption. Energy was applied to the fiber aggregates through the force from the piston in the experimental setup. The force caused the fibers and the aggregates to move (distance); therefore, work was performed on the fiber aggregates. Because work was done, the fiber aggregates are not in their lowest energy state (53). To regain equilibrium, heat must be given off by the aggregates, therefore, a temperature change.

The factor selected to measure deformation was curl index. The experimental approach included fiber separation into earlywood and latewood, aggregate preparation, apparatus design, imaging devices, and cyclic compression testing procedures.

The experiments were carried out in four sequential blocks:

1. Development of an apparatus to induce and record high frequency cyclic compression, up to 200 hertz.

2. Perform the necessary experiments to measure the mechanical deformation distribution between mixed earlywood and latewood fiber aggregates subjected to cyclic compression. Experiments were performed at 10, 30, 50, 100, and 200 hertz. The change in fiber curl index per cycle, recorded by regular and high-speed video, was determined. These experiments were performed at room temperature at an initial 30% fiber consistency.
3. Perform experiments to measure temperature changes by infrared imaging in mixed and pure earlywood and latewood fiber aggregates. The experiments were performed at room temperature and an initial 45% fiber consistency.
4. Statistical analysis for significant differences between earlywood and latewood fibers within the aggregate for both changes in curl index (mechanical deformation) and temperature used t-tests to compare the average values.

This plan would have been more like a model refiner if frequencies could have been even higher than those tested here. Testing was performed at room temperature because the infrared and video images would be obscured by the steam and condensate within a pressurized enclosure needed to raise the temperature.

FIBER SEPARATION AND PREPARATION

The wood fiber used for these experiments was from one loblolly pine tree (*Pinus taeda*), a representative species of the family of southern yellow pines commonly used as a pulp fiber source. A 12"-diameter, four-foot long section of the tree was obtained from Bowater, Inc., in Calhoun, Tennessee. The log was cut into one-inch thick disks, and the disks into wedges. Then the earlywood and latewood within the growth rings were separated into chips using a hand press. All wood chipped was between the 12th and 33rd annual rings. This was done so the sample would be from mature wood and also because these rings were wide and easy to separate into earlywood and latewood. Each growth ring was separated into three chips: earlywood,

transition wood, and latewood. The earlywood and latewood were set aside for refining, and the transition chips were discarded. The total mass chipped was 400 g of latewood and 200 g earlywood chips, on an oven-dry basis.

The two sets of chips were refined separately with an Asplund Defibrator D using five minutes of atmospheric presteaming. Approximately 20 kWh/t of energy went into the chips so that excessive fiber cutting/delamination did not occur after fiber separation. The amount of energy was estimated from previous work with the defibrator, where chips were blown straight through the refiner.

After refining, the fibers were classified in a Bauer-McNett classifier using the 4, 14, 28, and 48 mesh sized screens. The pass 14 and retained on 28 mesh screen fraction was preserved for these experiments. This fraction was expected to contain mostly whole fibers (54).

To preserve the fibers from rotting due to fungal or bacterial contamination until needed for testing, a known quantity of fibers was placed in a small heat-sealable bag. Nitrogen gas was blown into the bags removing any oxygen and then the bag was sealed. The fiber containing bags were pasteurized at 65°C for 75 minutes, and then refrigerated without regard to moisture content. Studies have shown that wood subjected to temperatures up to 65°C for relatively short periods of time shows no loss of strength or change in elastic properties (3).

AGGREGATE PREPARATION

The pasteurized fibers were removed from the refrigerator prior to testing to bring them to room temperature. The fibers were removed from the bag, mixed in water, and filtered. The fiber consistency was then determined. A mass of fibers (either earlywood or latewood) was then stained, depending upon the test. The fiber types (after knowing the consistencies) were mixed and brought to either a 30% consistency or 45% consistency, depending upon the experiment. After a day for the entire mass of fibers to come to consistency equilibrium, the

fibers were weighed out into smaller aggregates for testing. These aggregates were placed in small bottles with waterproof lids to keep the fiber moisture constant until testing.

Some of the separated fibers were stained to ease identification of fiber type during the cyclic compression experiments. Two stains were used: Congo Red for high-speed video testing and a fluorescent dye, Leucophor B-302 (obtained from Sandoz Chemicals), for infrared testing and low-speed video testing. Stained fibers of either earlywood or latewood were added to the fiber aggregate, depending upon the test. There was no evidence of dye transfer fiber to fiber during any of the experiments with either of the stains.

Fiber Aggregate Fiber Type Distribution Determination

The fibers collected on the pass 14, retained 28 mesh screen were used for all experiments. These were mostly separate fibers with few broken ends. The fibers were analyzed for fiber length and diameter (Appendix 1) to see if a reasonable separation of the fiber types occurred. The earlywood and latewood fibers were then recombined into the approximate proportions found within the tree: 50 percent earlywood and 50 percent latewood by mass (Table 1). This was determined by experimentation. A narrow (5 mm) wood slice was taken through the center of the log used for the fiber source, and each ring present was divided into either earlywood or latewood. The small chips were oven dried and weighed and the percentages calculated.

Table 1. Mass percentages for earlywood and latewood fiber source.

SAMPLE		MASS (g)	PERCENTAGE
Juvenile	EW	0.828	52.9
	LW	0.737	47.1
Mature Middle	EW	1.354	51.1
	LW	1.296	48.9
Mature Outer	EW	0.451	45.1
	LW	0.548	54.9

Fiber Aggregate Mass Determination

The mass of fibers used in these experiments mimics the expanded density of a fiber aggregate present on the bars within a refiner. This mass was determined by a small study using a 12" Sprout Waldron atmospheric refiner, available at IPST. Loblolly pine chips were fed into the refiner, and when good loading occurred, the refiner was stopped and opened. Fiber aggregates were removed from the bars on the refiner plates, and measured for length, width, and depth to get volume. The bundles were then air dried, and the density calculated (Table 2). This was tested for both the first and second passes of the pulp through the refiner. The density will actually be less than calculated, due to the mass measured on air-dried, not oven-dried, samples. The average density of the second pass fiber bundles was used for most of this experimentation. A recent study has imaged fibers within a refiner and these aggregates are visually of similar densities to the aggregates used in these experiments (55). Actual fiber aggregate density is still not known because a fiber aggregate can not be removed from the refiner while pressurized.

Table 2. Density determinations of fiber bundles.

Sample number	Mass (g)	Volume (cm^3)	Density (g/cm^3)	Average Density
First Pass - 0.045 inch plate gap				
1	0.678	4.73	0.144	0.129
2	0.168	0.88	0.190	
3	0.436	6.00	0.073	Std. dev.
4	0.219	1.35	0.162	0.045
5	0.157	1.41	0.111	
6	0.082	0.90	0.091	
Second Pass - 0.030 inch plate gap				
7	0.083	1.00	0.083	Average
8	0.132	1.00	0.132	0.082
9	0.037	0.38	0.097	
10	0.092	1.88	0.049	Std. dev.
11	0.119	2.25	0.053	0.031
12	0.113	1.41	0.080	

APPARATUS DESIGN

The cyclic compression device developed for the majority of the testing was adapted from components of other systems. The major components are a model FG2A Circuitmate function generator, a model Pro-1500 Hafler amplifier, a model V-203 electromagnetic vibration generator (shaker or exciter), a model 1208-4C2-0 Danly die set, plane sapphire window, and an IPST manufactured piston and an acrylic block (Figure 14) (Appendix 2). The function generator, amplifier, and the shaker were purchased as a system from Ling Dynamic Systems, Yalesville, Connecticut.

The function generator was set to produce a sine wave pattern. The frequency and amplitude of the compressions were established and the output of the function generator was connected into the mono input of the amplifier. The amplifier was wired to the shaker with polarized speaker wire. The pulse output of the function generator was monitored by an IPST manufactured counting device. This device counted each cycle and, at a specific number of compression cycles, triggered the imaging device to record the fiber aggregate undergoing compression.

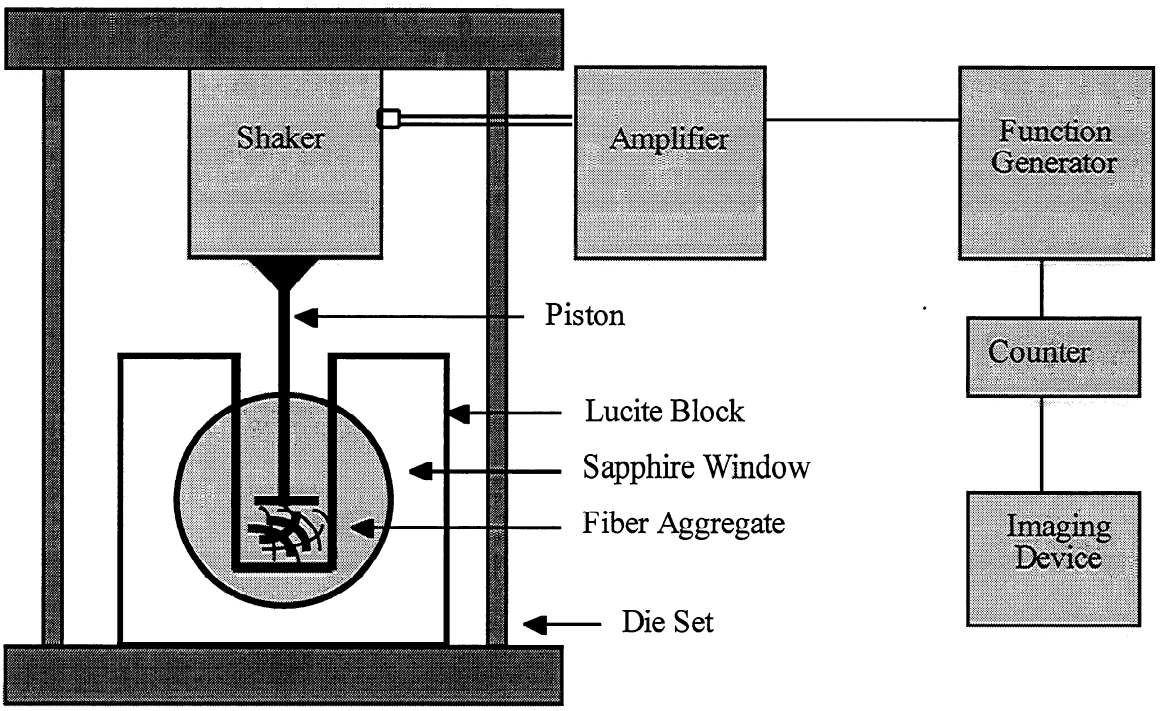

Figure 14. Schematic for cyclic compression device (not to scale).

Electrodynamic shakers generate force by the interaction of a current flow in a DC magnetic field. The DC magnetic field is typically generated by an energized field coil embedded within a massive iron structure (the shaker body). A power amplifier supplies the current and voltage to the shaker. The shaker selected for this study is capable of oscillating at frequencies between 10 and 200 Hz, while moving the piston in a sine wave with peak-to-peak amplitude of one millimeter.

Maximum frequency with a one millimeter peak to peak amplitude was determined using the equations for sinusoidal motion (Table 3). The calibration of the amplitude was done using a Keyence laser triangulation device and oscilloscope. The Keyence unit has a light-emitting element and a position-sensitive detector. The light emitting element focuses on the target and the emitted light reflects into the detector. As the target moves, the beam spot also moves. The displacement of the target can be determined by detecting the movement of the beam spot, which is displayed as a millivolt reading on the oscilloscope. The millivolt readings of the total

possible peak-to-peak displacement of the piston were read. Knowing the maximum possible stroke of the shaker was 5mm, the number of millivolts for a 1mm peak-to-peak amplitude was calculated. Limit lines were then set on the oscilloscope, and the amplitude button on the function generator was adjusted so the sine wave from the function generator would fill the limit lines. This was done for each test frequency and the function generator was marked where the amplitude button was to be placed for each frequency. Amplitudes were checked three times during the testing period with little variation between calibrations.

Table 3. Sinusoidal motion equations (56).

$g\ (peak) = 0.0511\ f^2 D$	(4)
$D = (19.56 / f^2)\ g\ (peak)$	(5)

where: f = frequency (Hz or cycles per sec)
g = acceleration due to gravity (9.8 m/sec^2)
D = displacement (peak-to-peak amplitude)

The sample cell was fabricated at IPST. It was constructed from a block of acrylic with a rectangular groove of one square centimeter by 25 centimeters tall machined from the long face of the acrylic block. The groove was covered with a sapphire window for viewing the fiber aggregate during the compression sequence. Sapphire was chosen for the window due to its high transmittance of visible and infrared light, its strength, and its imperviousness to water. The sapphire window was purchased from Infrared Optical Products and had a diameter of one inch and a thickness of one millimeter. The shaker and acrylic block were bolted to the die set. The die set was chosen for both its mass and parallel plates. The shaker had a piston attached to the moving coil, thereby moving the piston up and down within the acrylic block. The piston was made of aluminum for ease of machining and low mass. The piston was two inches long with a

square cross section of 0.8 cm, leaving a one mm gap on either side of the piston to the sample chamber wall. The piston was machined to be smaller than the sample area to minimize pressure changes as the piston oscillated up and down.

IMAGING DEVICES

Three different imaging devices were used for this study. Two S-VHS video recorders were used to collect data on mechanical deformation. An infrared camera was used to measure temperature differences between the fibers.

The initial experimentation used a regular Panasonic 5100 30-hertz color video camera. The camera was attached to a low magnification, Bausch and Lomb dissecting microscope with a video adapter from Edmund Scientific in one of the ocular tubes. A fluorescent stain (Leucophor B-302) was applied selectively to either fiber type, and the stained fibers mixed into the unstained fibers. The imaging sequence was recorded in a darkened room to maximize the contrast for the light fluorescing from the stained fibers. A Spectronics high-intensity UV lamp was used to excite the fluorescent stain in these experiments. The cycling sequence was recorded to S-VHS videotapes.

High-speed video was required for high frequency studies of mechanical deformation. A 1000 HRC Kodak Ektapro Motion Analyzer was used in these experiments and Congo red stain was used on the fibers to identify fiber type. An Elicar VH-Q macro lens with a 2X-lens extender was used to image the fibers. This system had enough memory to store 1364 images and imaging rates of 250, 500, or 1000 frames-per-second for full size images. The images were then transferred to S-VHS videotape.

The infrared testing was performed at Oak Ridge National Laboratory using an Amber Galileo infrared imaging system. The camera has a 256 x 256 staring focal plane array with a maximum framing rate of 120 Hz. The temperature resolution is 0.025°C at 23°C. A 4X microscopic lens from Amber Raytheon was used to magnify the fibers for optimal spatial

resolution. Before testing began, a two-point external source correction was done on the focal plane array. The camera captured up to 200 images in a sequence (real-time acquisition of contiguous data). A counter device was used as a trigger for the infrared camera. After imaging, a linear two-point calibration curve was applied to each image selected for analysis to convert the data into temperatures. The images were saved on computer CDs or Zip discs.

Mechanical Deformation – Experimental

Low-Speed Video Experimental Technique

Initial tests were done at low frequencies (10 and 30 Hz) to see if there were any problems with the fiber sample holder, fiber bundles, or imaging systems. This initial testing was completed using an MTS servo-hydraulic testing system. The engineering drawings in Appendix 3 are for modifying the MTS for this testing purpose. An acrylic block holding a spectrophotometric cuvet was used to hold the fiber aggregates, and the Panasonic video recorder was used to record the compression sequence. Five percent by mass of the fiber aggregate was stained with the fluorescent stain and a Spectronics ultra violet lamp with a spot adapter shield supplied the only illumination. When the image was viewed, only the stained fibers were readily apparent.

The testing was carried out for 10,000 compressions. The average retention time for a fiber in a refiner was approximately one second (37). With typical bar crossing frequency of 10^4 Hz, the maximum number of compressions a fiber should experience would number in the 10,000s (37).

Initial testing was performed at 10 and 30 Hz using three aggregate densities and with either stained earlywood or latewood. The three densities of fiber aggregates tested were 0.084, 0.105, and 0.140g/cm^3. This was performed to determine if aggregate density affected the results of the experiments. Fiber aggregate density was determined by how far the piston was lowered

into the sample cell before testing. The three densities had the piston lowered to give the aggregate a starting height of five, four, and three millimeters, respectively. All testing used a one-millimeter peak-to-peak amplitude (stroke) distance.

Video Image Analysis

The images selected for analysis were the 0, 1, 10, 100, 1000, 10,000th cycle, and each half-stroke after. Selected fibers were analyzed for curl index using OPTIMAS image analysis software. Curl index is the ratio of the true length of a fiber to its longest projected dimension minus one (Figure 15) (57). Therefore, a straight fiber will have a curl index of zero and the greater the fiber deviation from a straight line, the greater the curl index. The curl index macro recorded true fiber length by tracing the pointer (cursor) over the length of the fiber. The longest projected dimension was determined by fitting the traced fiber within the smallest possible diameter circle. The diameter of the circle was then the longest projected dimension.

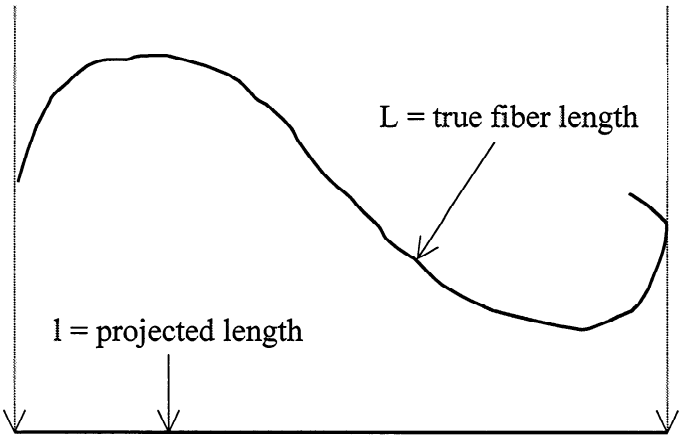

Curl index = (L/l) - 1

Figure 15. The measurements and formula for curl index (57).

Nine fibers from a single image were measured ten times to determine the reproducibility of this technique (Figure 16).

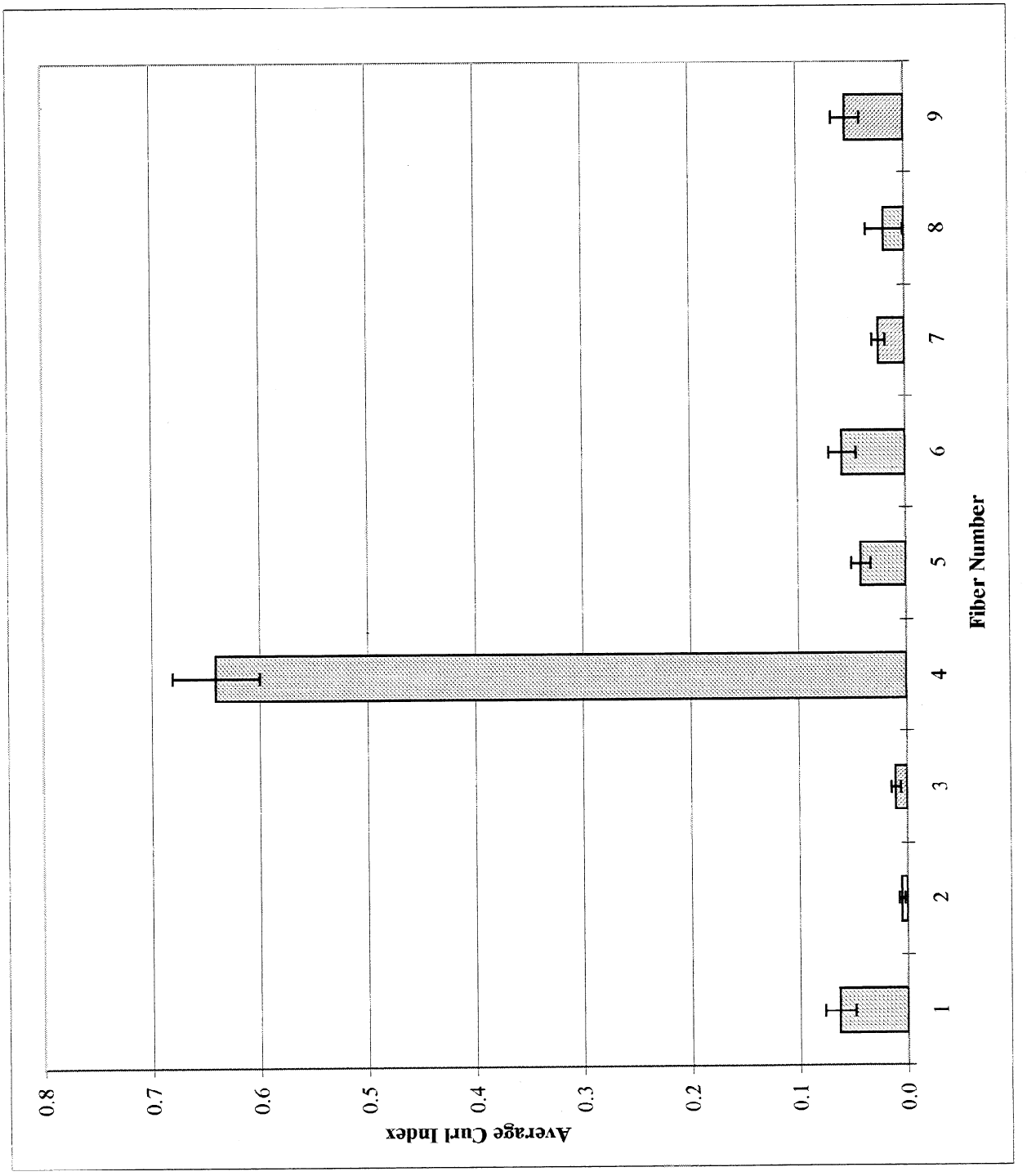

Figure 16. Reproducibility of the image analysis technique for curl index. The error bars show ±95% confidence limits.

Due to the friction between the fibers and the sample cell, there was concern whether the imaged fibers (those on the edge of the fiber aggregate) behave the same as those in the center of the aggregate. At a consistency of 30%, the fibers preferentially adhered to the rest of the aggregate and not the wall or window of the sample holder. Fibers that appeared to be adhering to the sample window were not selected for measurement of curl index. These fibers were easy to detect because they did not move with the rest of the aggregate.

A t-test was used to determine whether there was any statistical difference between the average absolute value change in curl index for the earlywood and latewood fibers.

High-Speed Video Experimental Technique

Final testing for fiber mechanical deformation used the electromagnetic shaker device and was carried out at frequencies of 10, 30, 50, 100, and 200 Hz using an aggregate density of 0.084 g/cm^3 (a 0.042 g OD in 0.5cm^3). The testing at 10 and 30 Hz was duplicated to determine reproducibility between the shaker apparatus and the MTS. Otherwise, testing was identical to the previous study using the MTS, other than the differences necessary due to use of the high-speed video system. These were the use of Congo red stain instead of the fluorescent stain, and performing the imaging in two stages due to the limited memory of the high-speed video system. The fluorescent stain did not work with the high-speed video camera because it required more light than the low-speed video camera.

The Kodak high-speed video system has enough memory to store 1364 images, but the slowest imaging rate was 250 frames per second. Due to the limited amount of memory, the imaging sequence had to be divided into two sections for recording. The first 200 cycles were recorded using the video system in the record mode and the images from 100 to 10,000 were recorded in record re-trigger mode. A counting device between the frequency generator and the camera triggered the camera for the record re-trigger mode. At every 100th cycle, the counter triggered the camera to take approximately 14 images (enough images to record the piston at its highest and lowest point within the compression cycle).

The data analysis was performed in the same manner as for the low-speed video experiments.

Thermal - Experimental

The thermal distribution was examined to determine whether the earlywood or the latewood fibers were absorbing energy in the compression cycling. This energy is from the hysteresis loop of a stress-strain cycle for a viscoelastic medium (30,41,58). Some of this absorbed energy is used in permanent plastic deformation and the rest is transformed to heat. The testing for thermal distribution was similar to the mechanical deformation testing with the high-speed video system.

The infrared camera could capture up to 200 images in a sequence (real-time acquisition of contiguous data). Therefore, the images had to be generated in two phases. The first phase collected one image of the first 200 cycles and the second phase collected a single image from cycle 100 to 10,000 but only every 100th cycle.

The fiber consistency had to be raised to 45%. At 30% consistency, when the fibers touched the sapphire window, the water blocked the infrared energy from reaching the camera.

Aggregates were weighed out prior to traveling to Oak Ridge National Laboratory (ORNL). The samples were conditioned for 24-48 hours for temperature in sealed bottles before testing. A 'snapshot' of the aggregate within the sample holder was taken before the testing began. The aggregates were then compressed following the same procedures as for mechanical deformation. Four aggregates were tested at each frequency and stained fiber type. The fiber aggregates were tested and weighed at ORNL, oven dried at IPST, and then reweighed to determine what the actual consistency was before and after testing. This was performed to ascertain whether the fiber temperature could be changing due to evaporational cooling.

The images were all converted to temperature and saved as .fts files at ORNL. The .fts files were then imported into Spyglass Transform where selected images were analyzed. Most of

the files were then saved as ASCI II files and imported into Labview for temperature analysis. Temperature measurements were collected on selected fibers within the images. Ten temperature observations per fiber were averaged to determine the temperature of a selected fiber. Temperature difference for each fiber was determined by comparison with the initial average temperature of that fiber. A t-test was used to determine whether there was any statistical difference between the average temperature change of earlywood and latewood fibers at the same frequency.

A single image with 10 fibers was measured ten times to determine the reproducibility of this averaging technique for fiber temperature (Figure 17).

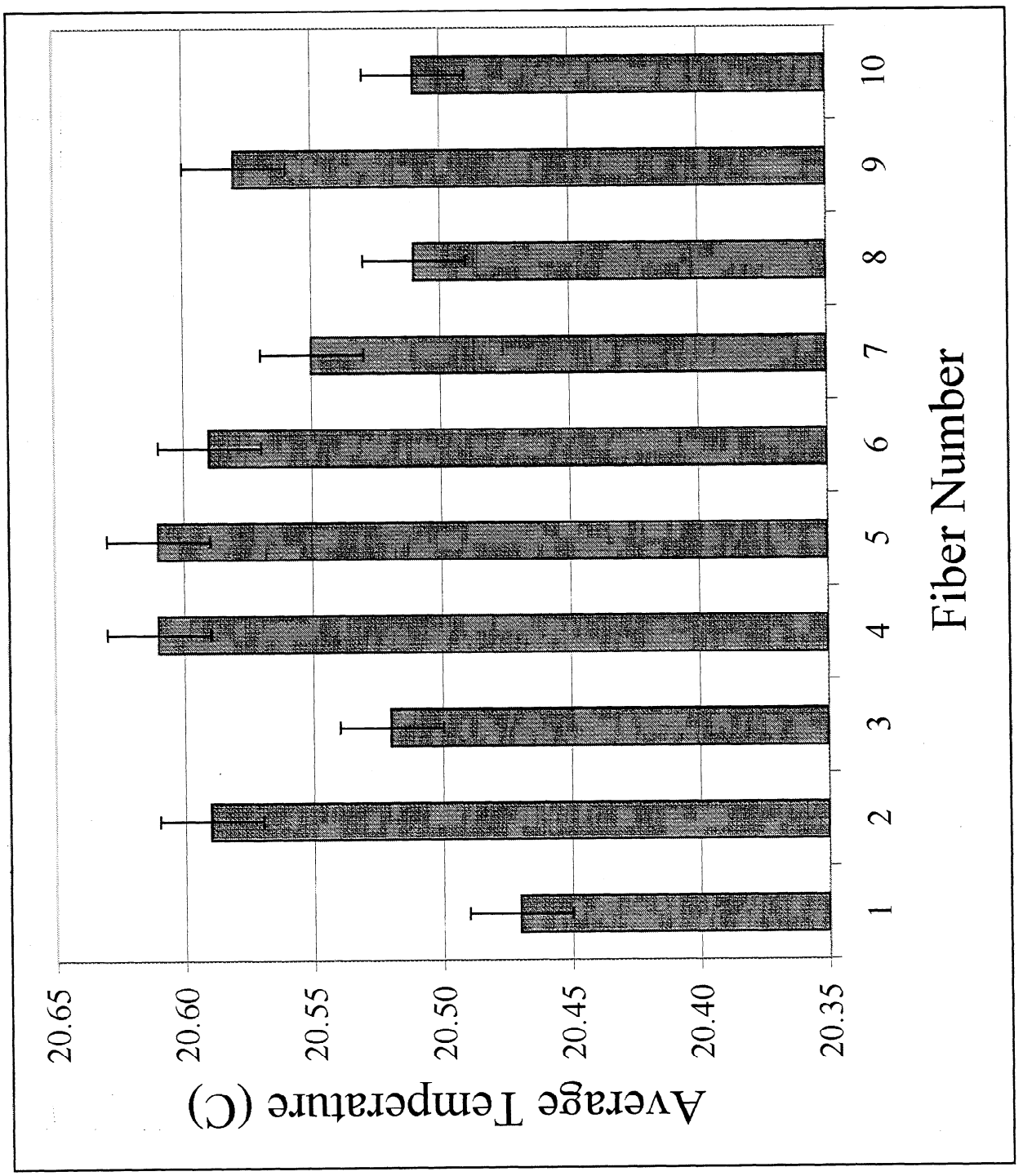

Figure 17. Reproducibility of the average fiber temperature technique. The error bars are ±95% confidence intervals.

Imaging Details

The experiments used three different cameras to record the images to either S-VHS video tape or digitally. Each camera was used to record the most information for a particular frequency. Table 4 has the camera recording frequency used for each piece of equipment at a particular cycling frequency.

Table 4. Cycle frequency vs. image frequency.

Cycling Frequency	Cycling Equipment	Camera	Camera Frequency
10	MTS	Panasonic video	60 Hz
30	MTS	Panasonic video	60 Hz
10	Shaker	Amber Galileo	120 Hz
30	Shaker	Amber Galileo	120 Hz
50	Shaker	Amber Galileo	120 Hz
100	Shaker	Amber Galileo	120 Hz
200	Shaker	Amber Galileo	120 Hz
10	Shaker	Kodak high speed	250 Hz
30	Shaker	Kodak high speed	250 Hz
50	Shaker	Kodak high speed	500 Hz
100	Shaker	Kodak high speed	1000 Hz
200	Shaker	Kodak high speed	1000 Hz

The spatial resolution of the infrared digital camera was greater than the cameras that recorded their information onto video tape. The Amber Galileo camera had approximately four pixels per 30 microns (about four pixels per fiber width). The S-VHS video tape (with approximately 480 lines of resolution) had about a 10 mm^2 image recorded on it. This gave a spatial resolution of about 20 microns per line.

Thermal Fiber Type Differentiation Technique

The technique used for fiber type identification during the mixed aggregate infrared testing used the Leucophor fluorescent stain. Stained earlywood or latewood was mixed 50/50 by mass with the opposite unstained fibers before testing. The fiber aggregates were brought to a consistency of about 45%. The aggregates were tested and the sequence of images taken with the infrared imaging system.

After testing, a single 'snapshot' image was taken without changing the final position of the fibers within the aggregate holder. Immediately after this image was acquired, another image was taken of the same aggregate but with ultra violet light focused on the fibers. The fibers without stain had larger temperature increases than the fibers with UV stain due to the lack of an efficient mode of radiating the energy absorbed from the UV lamp.

The difference was noted between the images with and without UV lighting, and the fibers with the larger differences were declared unstained. A test was performed to confirm this with stained and unstained fibers of either all earlywood or latewood in the same image, but separated on opposite sides of the sample holder. Figure 18 shows the difference of the images with and without the UV light. The fibers on the right of the image were stained while those on the left were not stained. The same holds true for the earlywood fibers.

Starting with the final image, the fibers were identified as earlywood or latewood, using this technique to identify the fiber types. Then in reverse order in the compression sequence, the same fibers were identified. After identification the fibers were analyzed for temperature and temperature differences.

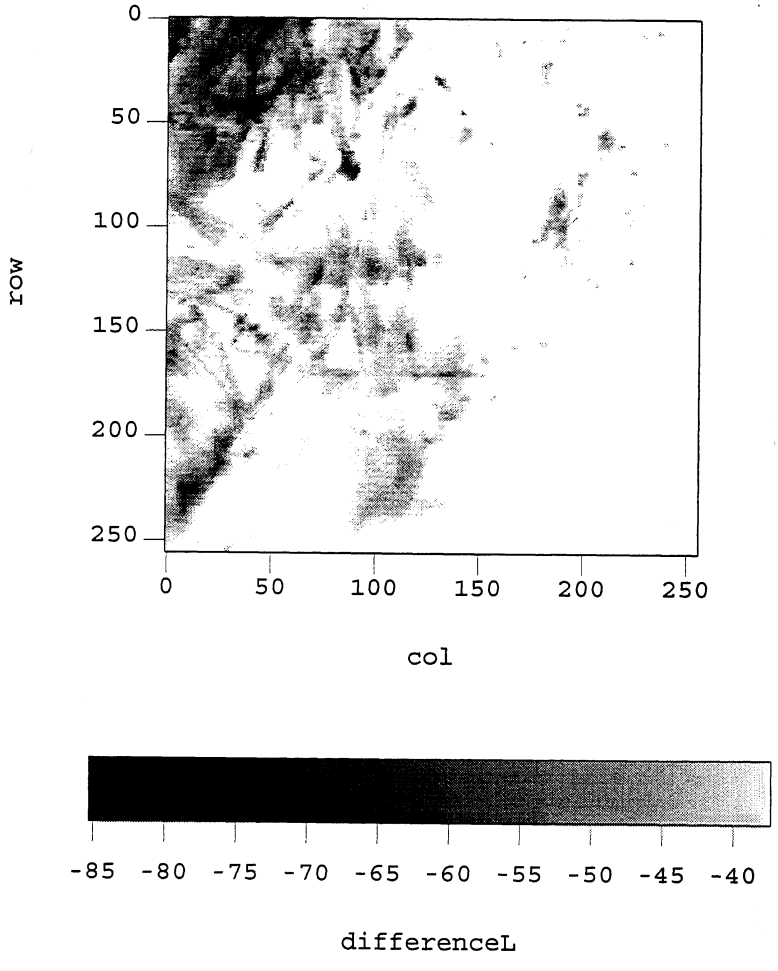

Figure 18. The difference (in intensity units) with the UV image subtracted from the pre-irradiation image baseline. The intensity difference between –85 and –40 is 1.1°C.

RESULTS AND DISCUSSION

MECHANICAL DEFORMATION - MTS

The first phase of the study of mechanical deformation of the fibers used the MTS servo-hydraulic testing apparatus modified for a small piston oscillating within a spectrophotometric cuvet. When work is applied to the fiber bundle, energy is absorbed by the flexing of the individual fibers of the aggregate within the cycle. A measure of mechanical deformation is obtained by determining the absolute difference of curl index within the cycle, measured when the piston reaches its highest and lowest points. Absolute difference was selected because it doesn't matter whether the fiber is straightened, curled, or kinked from the energy absorbed by the fiber. The data seen in Figure 19 show the difference between using the average curl index (the true average of all data at that cycle) and the average absolute change in curl index within a cycle. From this point onward, Δ curl index refers to the average absolute difference of curl index within a cycle for all fibers measured at that frequency at a specific cycle number. For example, a set of data taken from earlywood fibers at 30 hertz and the average absolute difference in curl index between the 100^{th} and 100-1/2 cycle.

$$\text{Average Curl Index} = \text{Sum}_i\,(\text{Curl Index}_{\text{piston high}}) / n_{i,} \text{ whereas} \quad (6)$$

$$\Delta\ \text{Curl Index} = \text{Sum}_i\,|\,\text{Curl Index}_{\text{piston high}} - \text{Curl Index}_{\text{piston low}}\,| / n_I \quad (7)$$

If there is a statically significant difference between the two fiber types using the Δ curl index method, this then supports the hypothesis that there is preferential energy absorption by the fiber type with the higher Δ curl index.

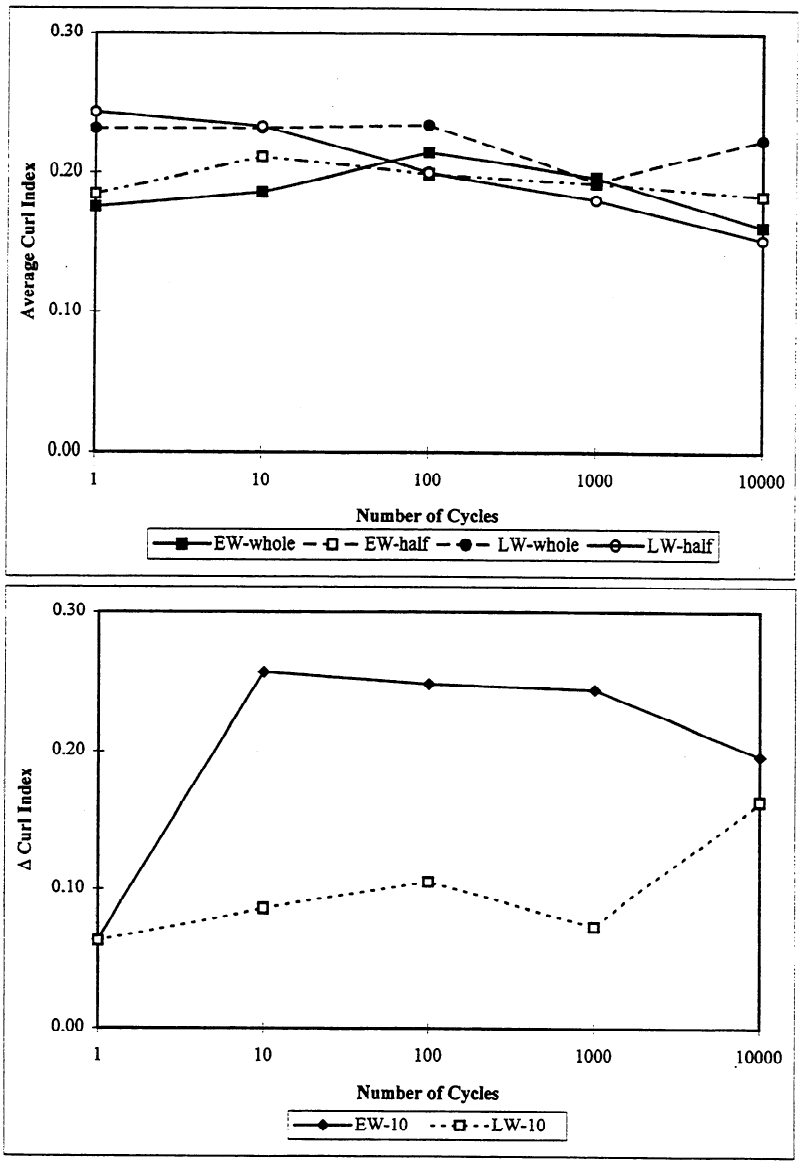

Figure 19. Difference between average curl index and average absolute difference of curl index within a cycle.

Fibers that shifted out of view or adhered to the viewing window during the cycling sequence were not included in the data pool. Multiple runs of each testing condition were performed to get curl index data for a minimum of 10 fibers (except at 200 Hz where there were problems with the equipment).

The MTS could only be used at the two lowest frequencies due to the high amplitude (one-millimeter peak-to-peak) chosen for the study. At this amplitude the machine could not control a sine wave greater than 30 hertz. Data taken at 10 hertz did show evidence of preferential energy absorption by the earlywood fibers (Figure 20 - the error bars are ± 95% confidence limits). The results of the t-tests as shown in Table 4, (see Appendix 4), confirm that at all but 10,000 cycles there is a high probability that the two average absolute differences in curl index within cycles are different for earlywood and latewood (H_o: $\mu_e = \mu_l$, $\alpha = 0.05$).

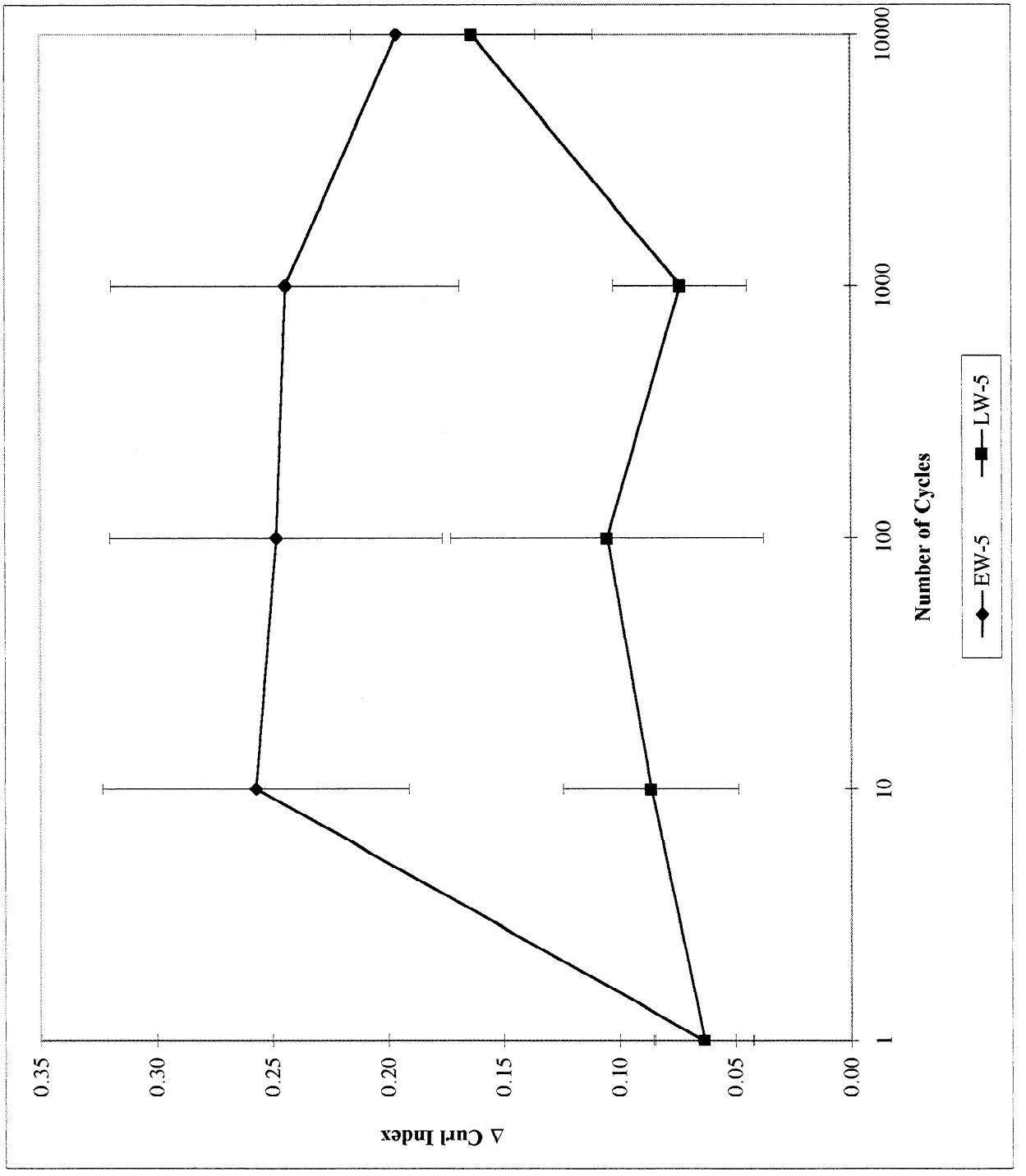

Figure 20. Change in curl index - 10 Hz, 5mm, MTS.

At 30 hertz, with the same aggregate density, there was evidence of preferential energy absorption by earlywood fibers, but only at the 90% confidence level for a couple of the measured cycles (Figure 60, Table 5). When the 10- and 30-hertz data are plotted together, the viscoelastic behavior of the fibers becomes evident (Figure 22). The higher the frequency, the less the fibers seem to change in curl index within cycles. This was apparently due to the fibers not having enough time to recover from one compression before the next compression was applied.

Some experiments were extended after the compression cycles stopped to see how quickly the fibers recovered from the applied stresses. This was done using the MTS setup, 10 and 30 Hz frequencies, earlywood and latewood stained aggregates, and cycling stopping after 10 or 1000 compression cycles. The 10 hertz data can be seen in Figure 21. There is still a significant amount of fiber movement after one second, which further reinforces the assumption of the fibers being prestressed prior to the application of the next compression. The 30 hertz data showed similar results.

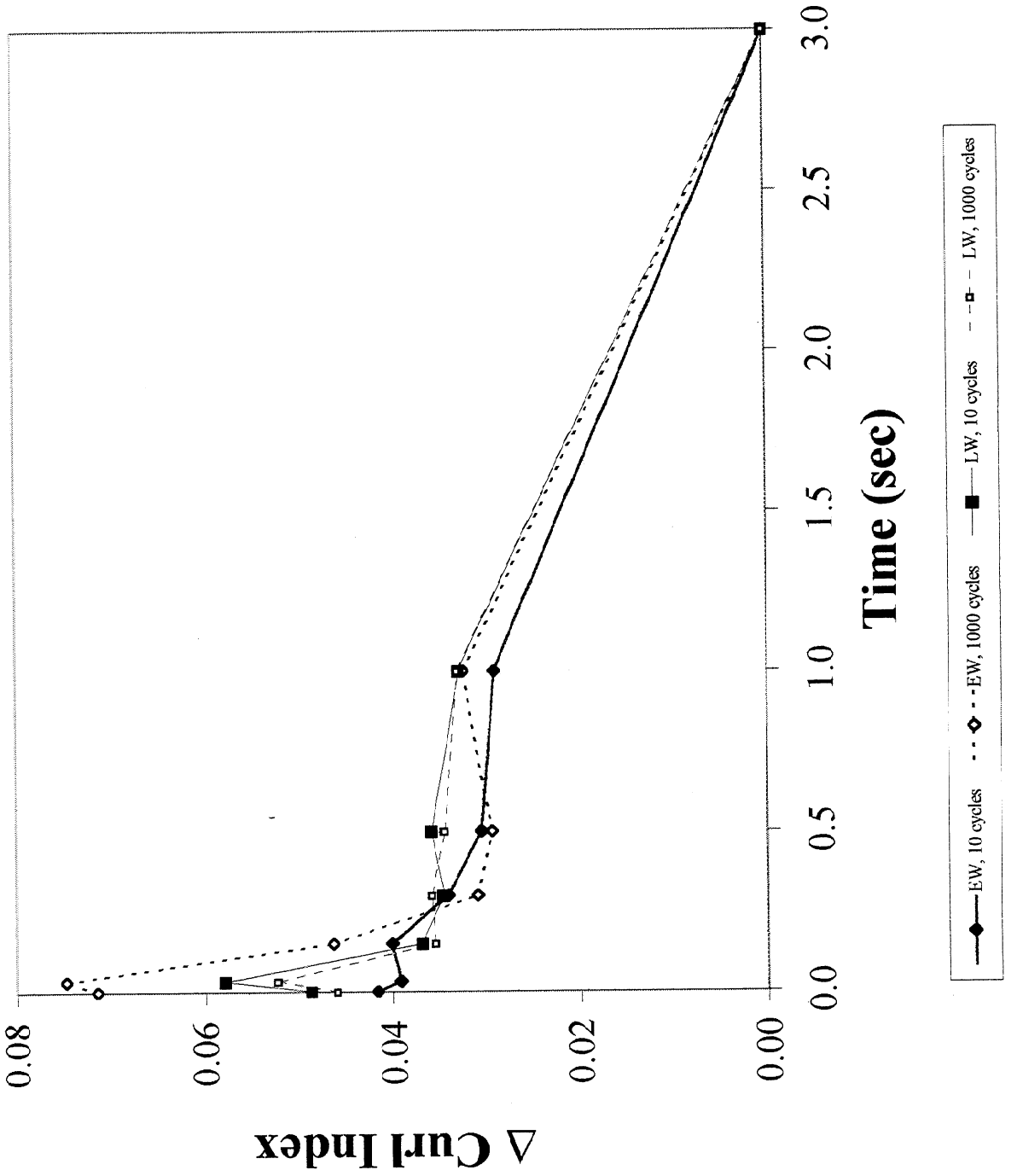

Figure 21. Relaxation of fibers after cycling, 10 Hz.

Two studies were carried out at 10 and 30 hertz to measure the effect of aggregate density on change in curl index. The spacer in the cuvet was raised from the normal distance of 5mm (between the spacer and the bottom of the piston before cycling) to 4mm and 3mm prior to cycling. The rest of the study was carried out the same as before. At 10 hertz, a noticeable drop occurred in Δ curl index between the 5mm data and the 4 and 3mm data (Figure 23) due to the increased density and less void volume in the aggregate. There was no observable pattern or difference in the data between the 4 and 3mm averages (Figure 61-64). The difference between earlywood and latewood at these new aggregate densities is not statistically significant (Table 6). At 30 hertz the result was the same, but without the large drop in average Δ curl index with increased aggregate density (Figures 24, 65-68, Table 7-8). The difference due to increased frequency of cycling was slight for these aggregates with higher density, but the Δ curl index for latewood appeared to be greater than Δ curl index for earlywood at these densities (Figure 67-70). At the highest aggregate density, the fibers may be hindered in their flexing due to increased fiber bonding and entanglement. This hypothesis agrees with the observation of the fiber aggregates upon removal from the cuvet. After the 3mm cycling, the fiber aggregate stayed compacted and did not recover while drying on the lab bench the way the other two density aggregates did.

To summarize the results of the low frequency work using the MTS, there does seem to be some preferential energy absorption by the earlywood fibers. The energy absorption appears to be less at the higher frequency and at higher aggregated densities.

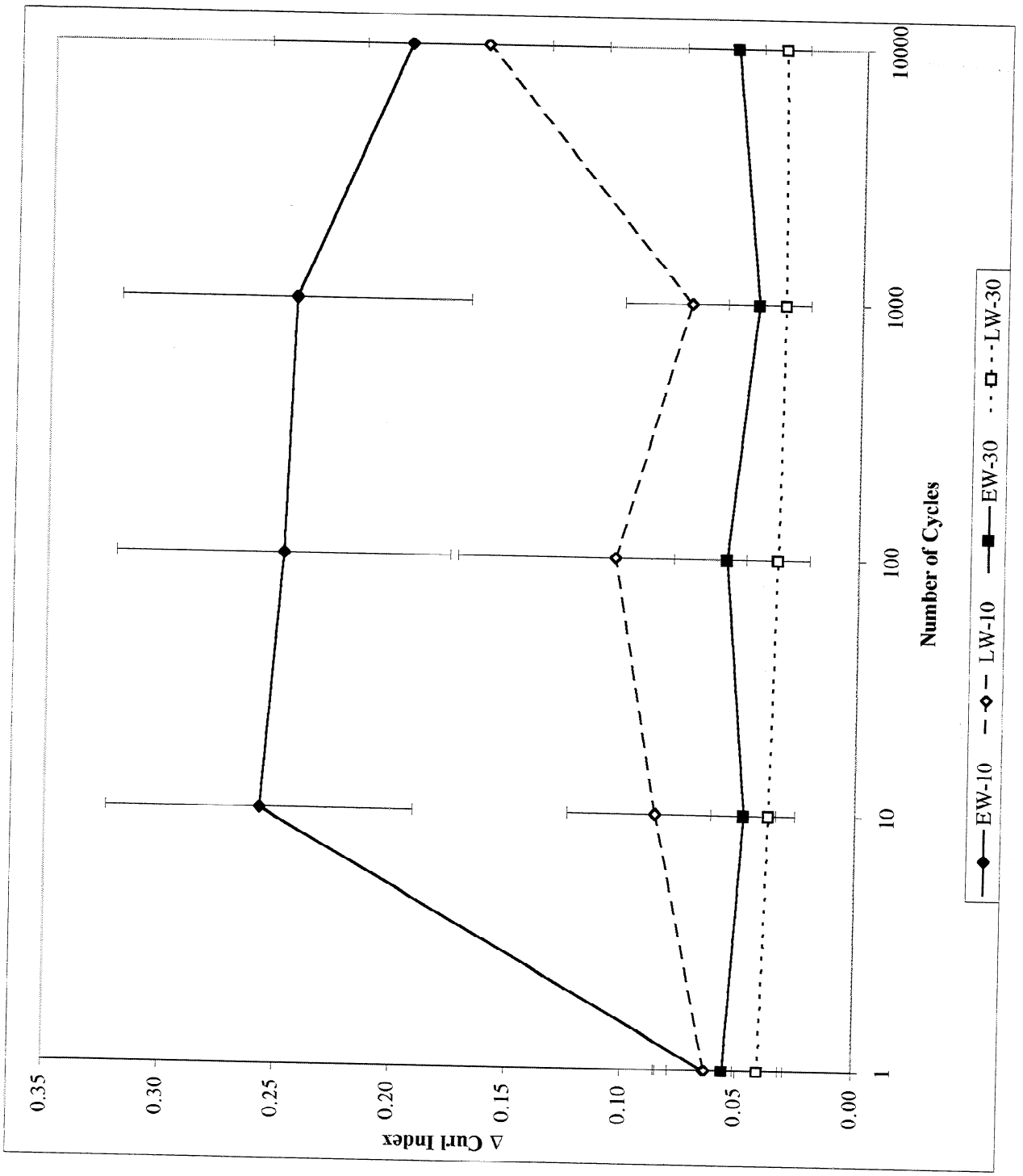

Figure 22. Comparison of 10 and 30 Hz change in curl index - 5mm, MTS.

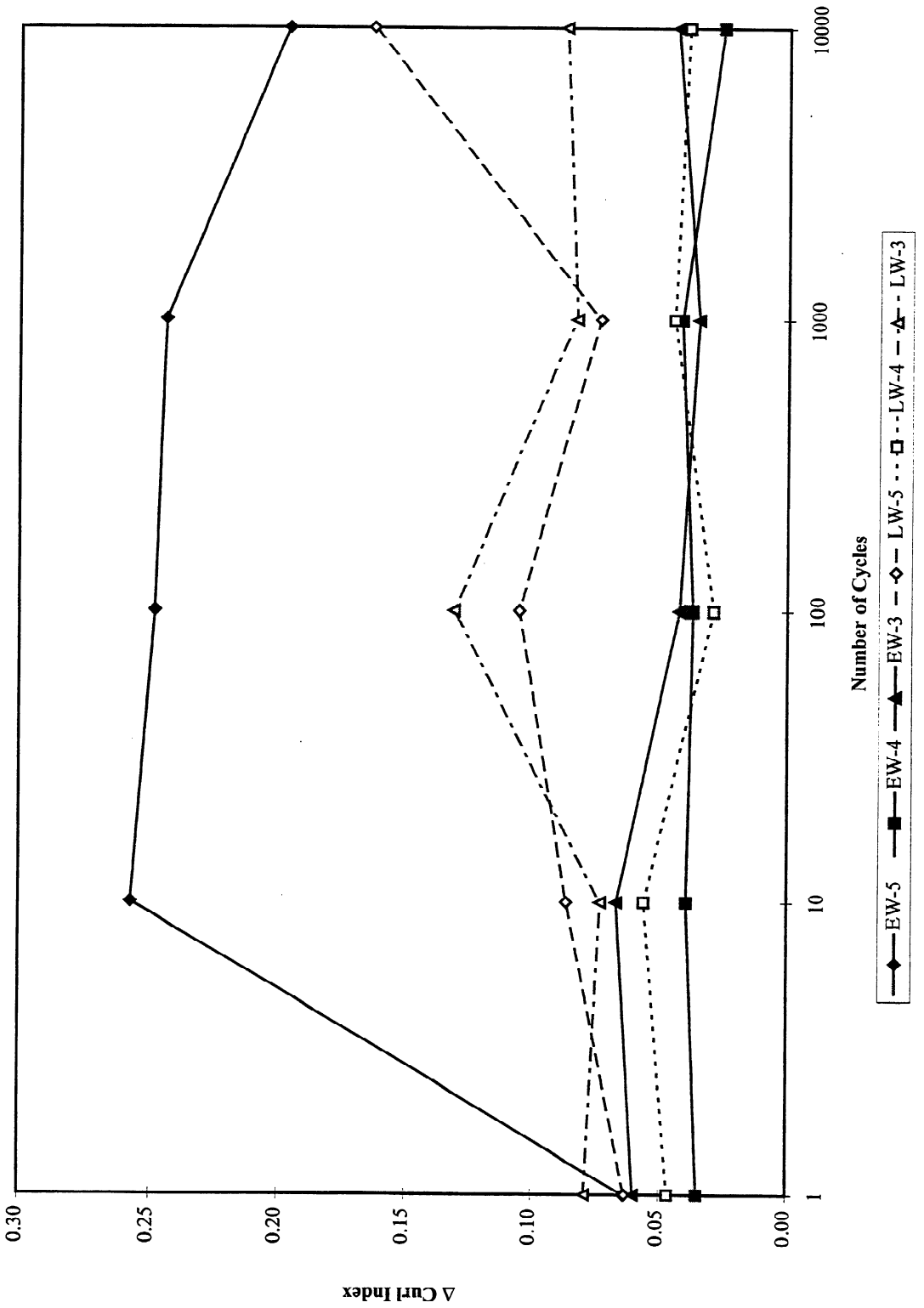

Figure 23. Change in curl index - 10 Hz, MTS (EW-5 means stained earlywood aggregates at an initial piston height of 5 mm in the sample chamber).

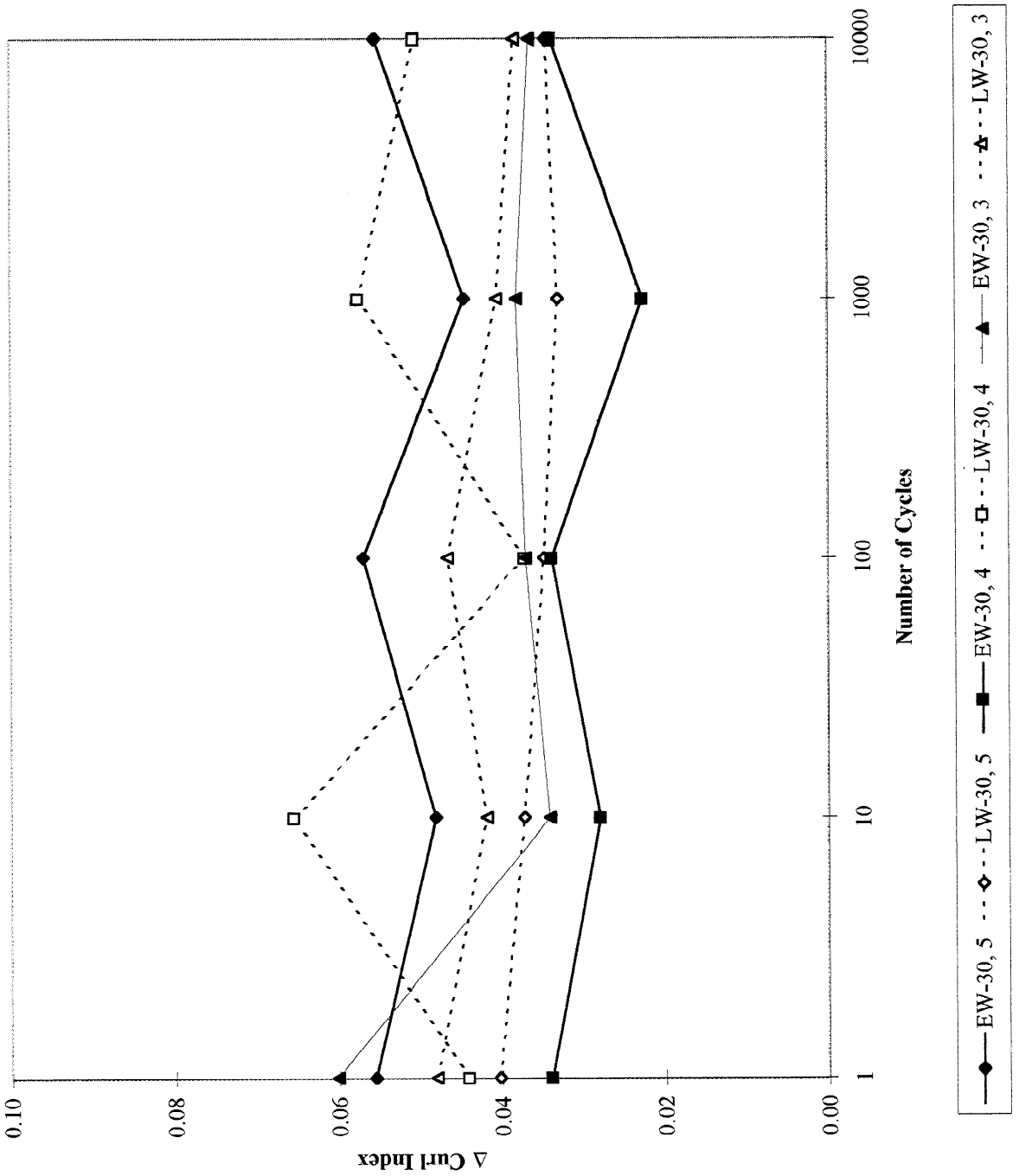

Figure 24. Change in curl index - 30 Hz, MTS.

SHAKER

The second phase of the studies used equipment developed to cyclically compress the fiber aggregate at higher frequencies than the MTS. A small electromagnetic shaker, amplifier, and function generator replaced the MTS and the spectrophotometric cuvet was replaced with an acrylic block with a sapphire window. The shaker was capable of moving the piston in a one-millimeter peak-to-peak amplitude at all frequencies up to 200 hertz. The piston position at the start of testing was estimated to be in up or uncompressed point of the cycle relative to the aggregate. Testing was increased to include the second and fifth cycle's absolute change in curl index to see the shape of the slope between the first and tenth cycle.

At 200 hertz, difficulties occurred resulting in shorting out the amplifier and then breaking the armature of the shaker (apparently due to the large amplitude at a high frequency). Therefore, the amplitude for this part of the study was adjusted to approximately 0.5mm.

The shaker movement is not as precise as the MTS. It had a tendency to stay in the down stroke slightly longer than the frequency generator dictated it should. This extra time in the first down stroke increased with higher frequencies. Within a couple of cycles, the shaker would move with the set frequency and amplitude.

The 10-hertz data using the shaker again showed a significantly larger average absolute difference of curl index for earlywood fibers compared to latewood fibers (Figure 25, Table 8). The measured values of Δ curl index were not as high as observed with the MTS equipment, but the two pieces of equipment do show the same trends of Δ curl index.

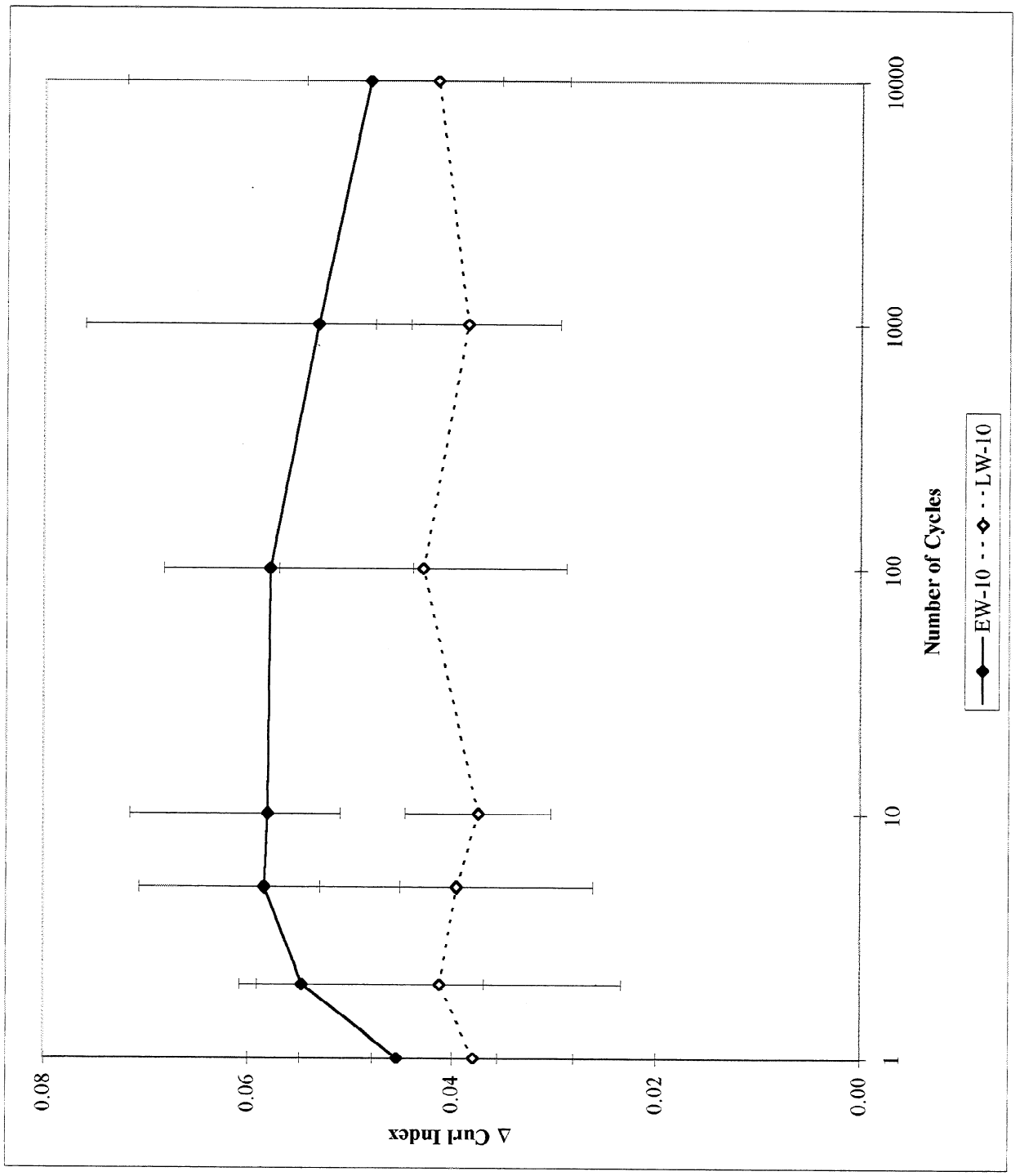

Figure 25. Change in curl index - 10 Hz, Shaker.

The 30-hertz data values were lower than those at 10 hertz and there was no significant difference between the earlywood and latewood fibers for Δ curl index (Figure 26, Table 9). Again, the values for Δ curl index were lower with the shaker equipment than those of the MTS.

The values for the shaker versus the MTS were graphed at each specified cycle at 10 and 30 hertz (Figure 27). These graphs show various levels of correlation of the data between the shaker and the MTS. The slopes at 10 hertz are low but very similar, and the slopes at 30 hertz were higher. This difference was probably due to the greater initial controllability of the MTS. The slightly longer time in the first down stroke may have given the fibers adequate time to form more entanglements and bonding between each other, thereby inhibiting flexing of the individual fibers.

The 50-, 100- and 200-hertz data show that no significant differences occur in Δ curl index between earlywood and latewood fibers (Figures 71-73, Tables 10-12). These data seem to suggest that at higher frequencies, such as frequencies found in a refiner, there was no significant difference in mechanical deformation or energy absorption between the earlywood and latewood fibers. Looking at Figures 28, 74-75, the trend due to higher frequency is seen. At lower frequencies there was greater deformation than at higher frequencies, due to the viscoelastic nature of the wood fibers. The fibers exhibit a need for time to recover from one compression before the next is applied for changes in Δ curl index per cycle to occur.

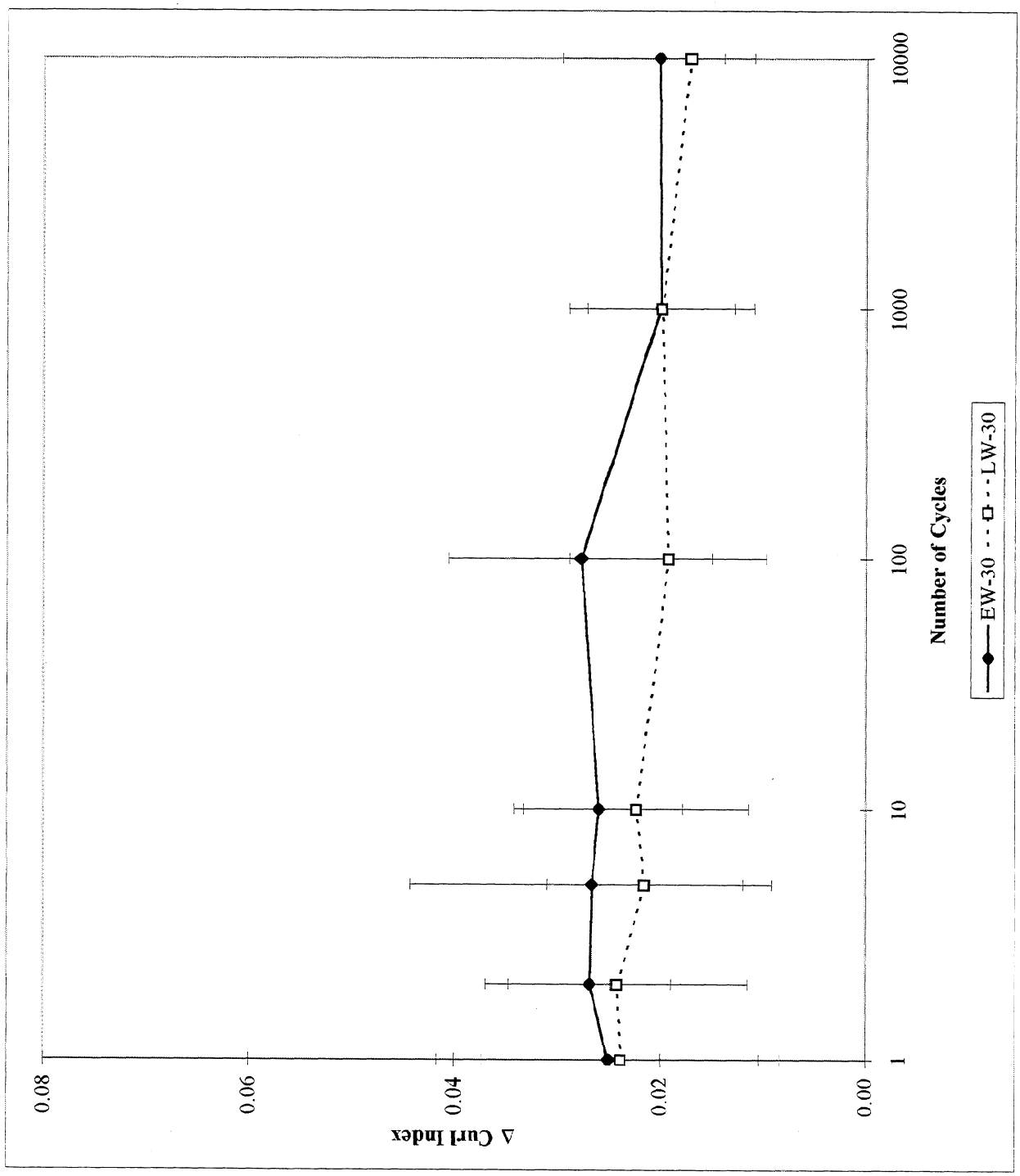

Figure 26. Change in curl index - 30 Hz, Shaker.

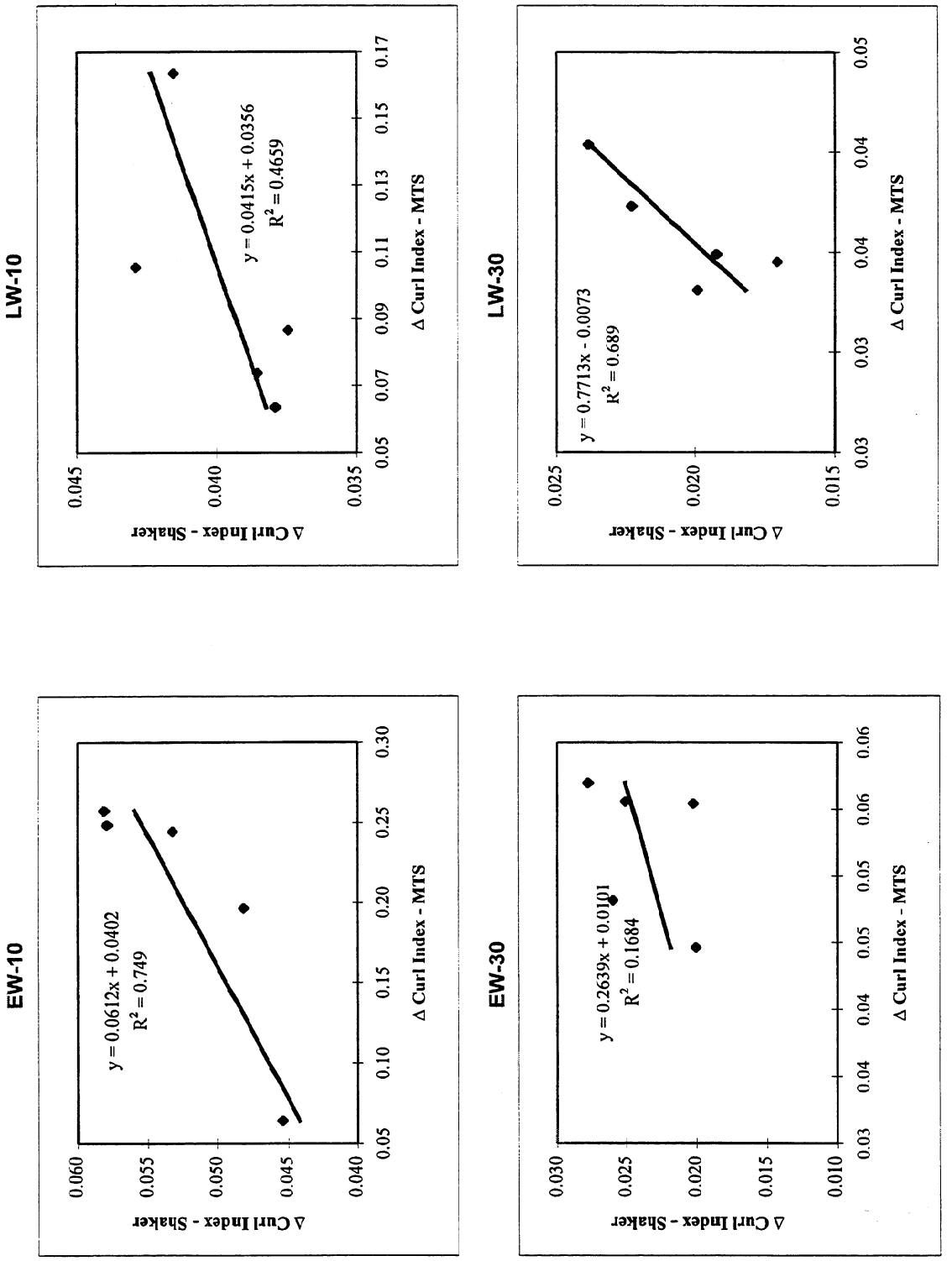

Figure 27. Correlations of curl index between MTS and Shaker.

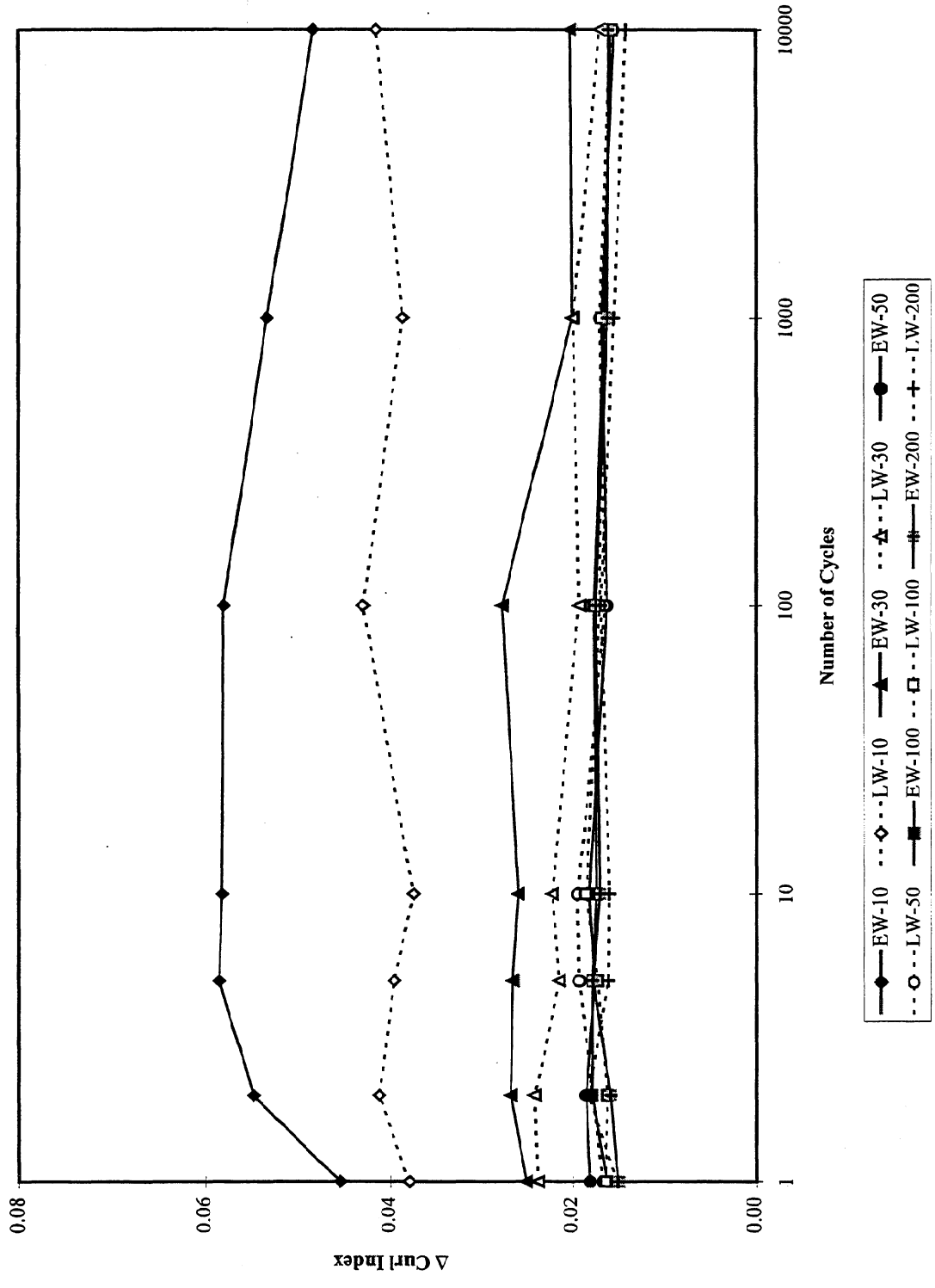

Figure 28. Change in curl index - Shaker.

THERMAL EXPERIMENTS

The thermal studies were all completed with the shaker equipment. An experiment was performed with small pieces of wood (toothpicks) to make sure there was a recordable temperature change, bridging the size difference between wooden blocks and fiber aggregates. Final studies were carried out on aggregates: mixed samples at 45% consistency, pure samples at 45% consistency, pure air-dried samples, and pure samples at 45% consistency with the piston cycling without touching the aggregate. The temperature differences were measured with the Amber Galileo infrared camera at Oak Ridge National Laboratories.

Small Wood Particles

These wood samples were from either the earlywood or latewood bands of a loblolly pine, with dimensions of approximately 1mm x 1mm x 9mm. The wood samples were all fully saturated with water and then placed in a small aluminum holder within the acrylic block (Figure 29). The sapphire window was removed in order to focus the IR camera on a sample placed in the middle of the acrylic block. The piston was modified to a single bar where it touched the wood sample to give a three-point bending test. The amplitude was decreased to 0.5 mm because the wood samples broke at the higher amplitude. It was cycled at 10 hertz for 100 seconds with an image collected every second. The data were analyzed at ORNL using the IR camera software. Figure 30 shows the average differences in temperatures recorded during this time interval, while Figures 76-77 show the individual data for the three samples of both wood type tested. As can be seen, a small half-a-degree Celsius temperature rise is seen with both the earlywood and latewood samples, confirming that the IR camera can detect the heating of wood particles. The temperature rise is not as large as Hickey observed with the wood blocks due to the smaller size particles. The size of the particle has an effect on the heat transfer rate (59) due to the amount of surface area per unit of mass. A smaller particle has a larger surface area than a

bigger particle, per unit of mass. The shape of the curves are typical for deflection-controlled cyclic testing.

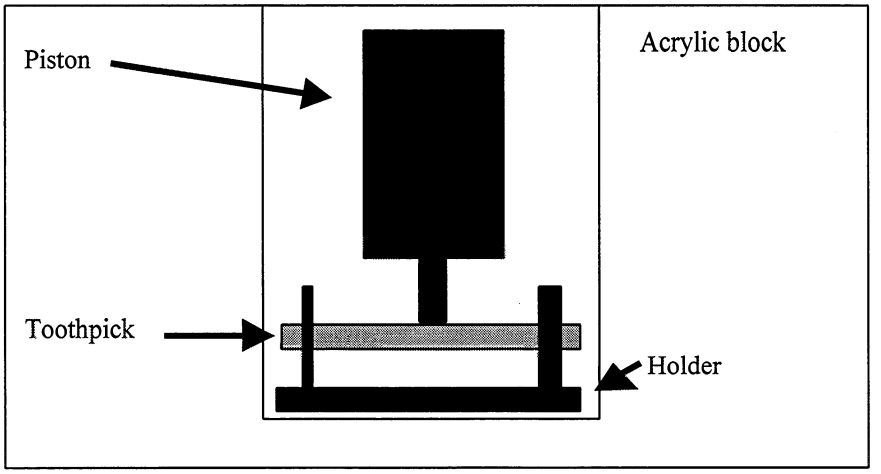

Figure 29. Wood particle sample holding apparatus.

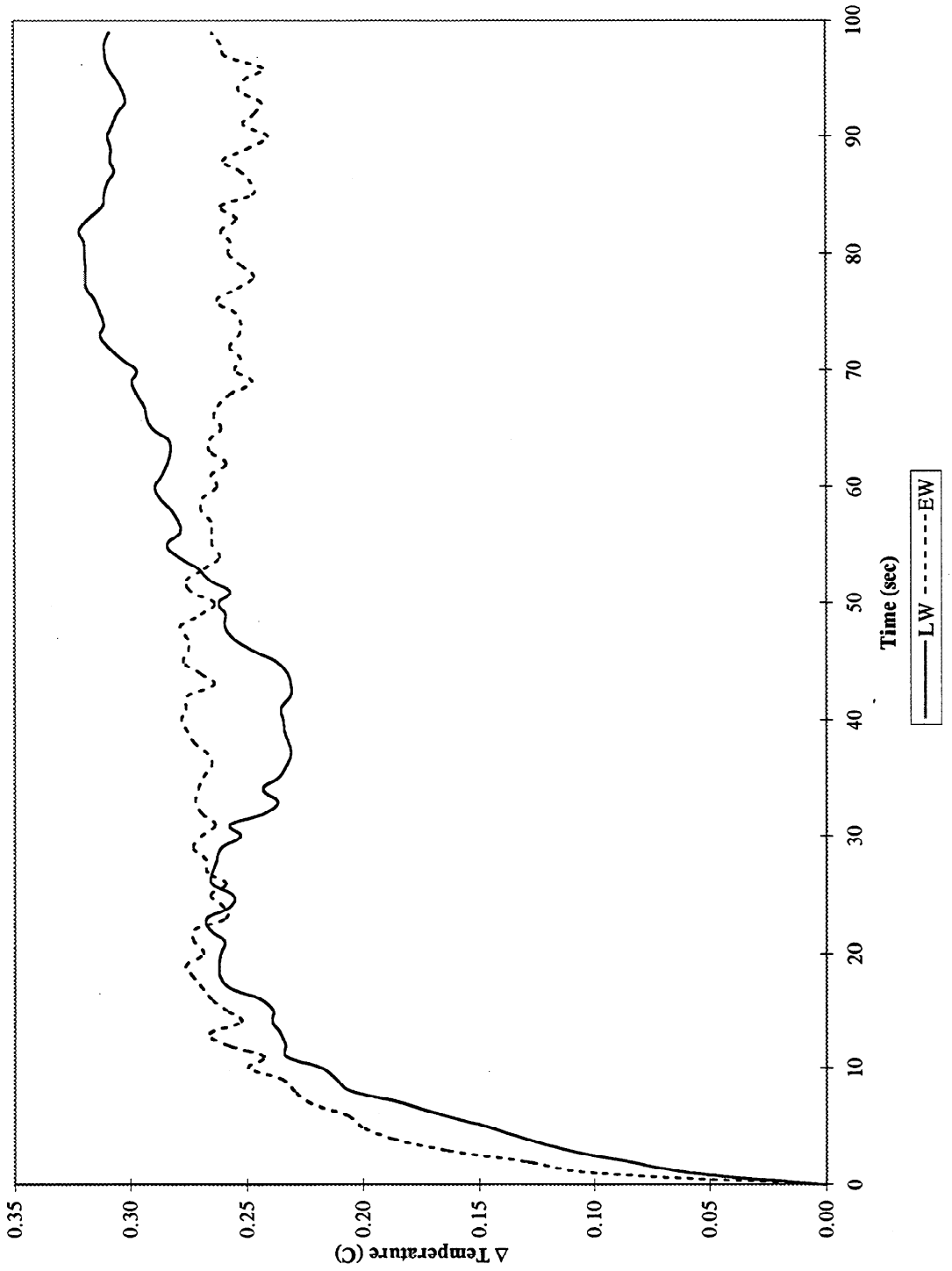

Figure 30. Change in temperature – average earlywood and latewood wood samples.

Fiber Aggregates

Mixed Aggregates at 45% Consistency

The initial study on the thermal history of cyclically compressed fiber aggregates demonstrated a need for drier consistency than the testing for curl index. At 30% consistency there was too much surface water and when a fiber touched the sapphire window water remained on the window and blocked the transmission of the infrared energy. Therefore, all IR studies were completed with fiber aggregates at 45% consistency. This consistency is still within the range found in mechanical pulping refiners (17).

This study used fiber samples with mixed fiber type. The fibers were identified by type using a fluorescent stain.

The study performed at 10 hertz showed an overall lack of statistical significance of temperature change between the two fiber types (Figure 31, Table 13). It is interesting to note that the first cycle did show a significant difference between earlywood and latewood fibers, with the earlywood having a larger temperature rise. After the first cycle the temperature dropped to below the initial temperature and then slowly rose until approximately the 500th cycle, followed by a large drop in temperature at 10,000 cycles. This temperature rise between the fifth and 500th cycle was more pronounced with the earlywood fibers.

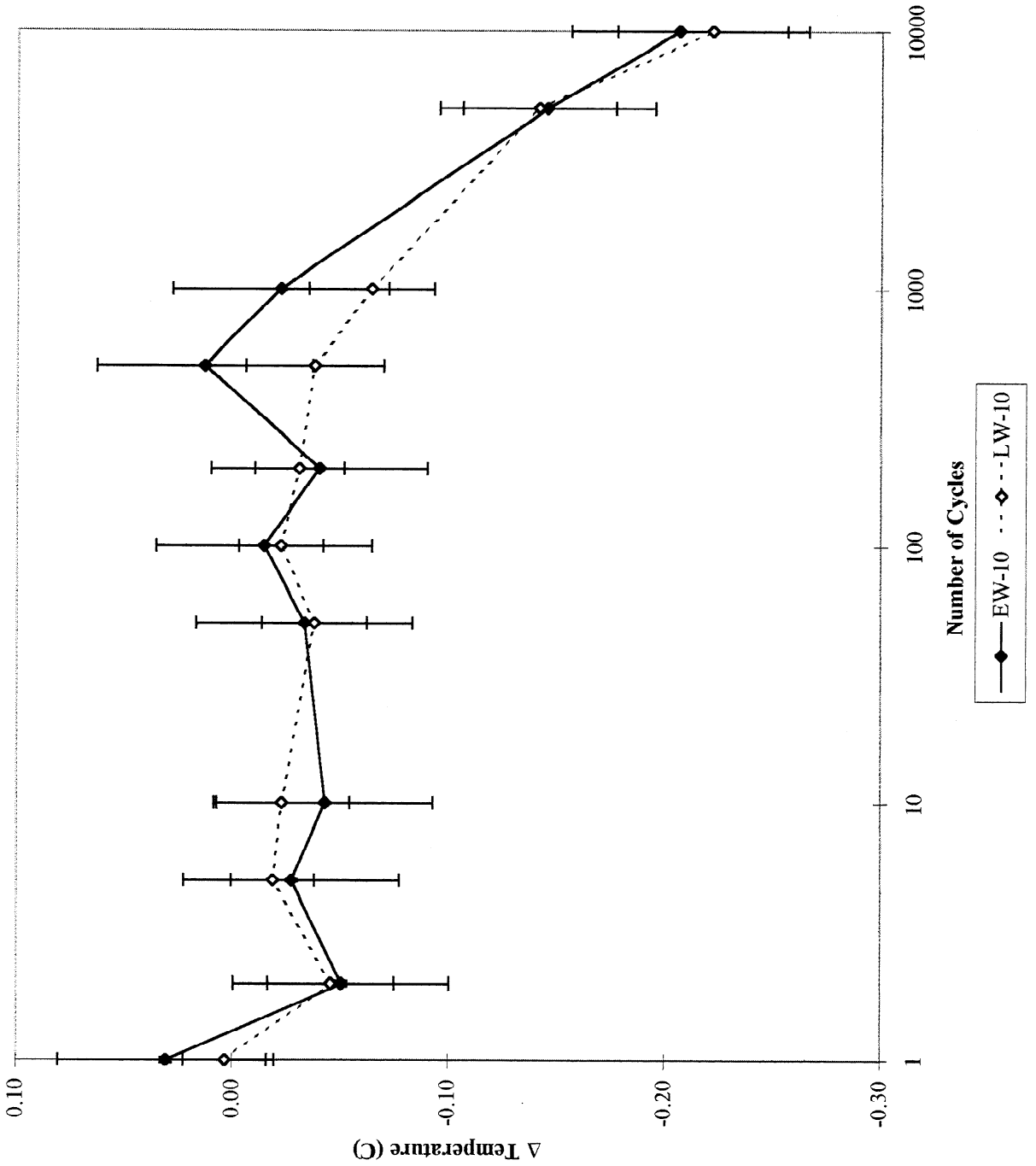

Figure 31. Change in temperature - mixed aggregates, 10 Hz.

At 30 hertz the same overall trend was seen but with a very small drop in temperature as soon as cycling began (Figure 32, Table 14). At 30 hertz there were no cycles where there was a significant difference in change in temperature between the two fiber types. The curves were best fit with a polynomial, but a difference between earlywood and latewood was seen in the later cycles. The temperature began to drop more quickly with the latewood fibers.

At 50 hertz the temperature again dropped immediately upon start of cycling (Figure 33, Table 15). The decrease in temperature difference was larger, and the rise was slower with the earlywood fibers (after the first cycle) until the 200 cycle. There was a 90% statistical difference between the two fiber types at the 10th cycle indicating the latewood is hotter. The change in temperature leveled out and then began dropping much earlier for the latewood fibers (there is a significant difference between the 200 and 500 cycles change in temperature). The best-fit curves show this longer 'increase' and later decrease in temperature.

The 100-hertz data are very similar to the 50-hertz data, but with no significant differences between the two data sets (Figure 34, Table 16). Earlywood decreased in temperature longer before starting to heat, but continued heating longer into the compression sequence. Other than the initial cooling, the latewood data could almost be fit with a linear curve.

The 200-hertz data are presented in the Appendix. This data set had some problems due to its high frequency. The fibers were hit by the piston fast enough that the water within the fiber was shaken out and sprayed on the sapphire window. This made analyzing the fibers for type impossible to differentiate.

Another possible explanation for the lack of preferential energy absorption by the earlywood fibers is that maybe within the fiber aggregate the latewood fibers form a supporting network that the earlywood fibers cannot bridge or support. Therefore, when a force is applied to the aggregate, the latewood fibers are actually absorbing more energy than the earlywood fibers. This possibility can also be dismissed by looking at the thermal data and observing no signs of latewood preferential energy absorption (significantly higher latewood temperatures).

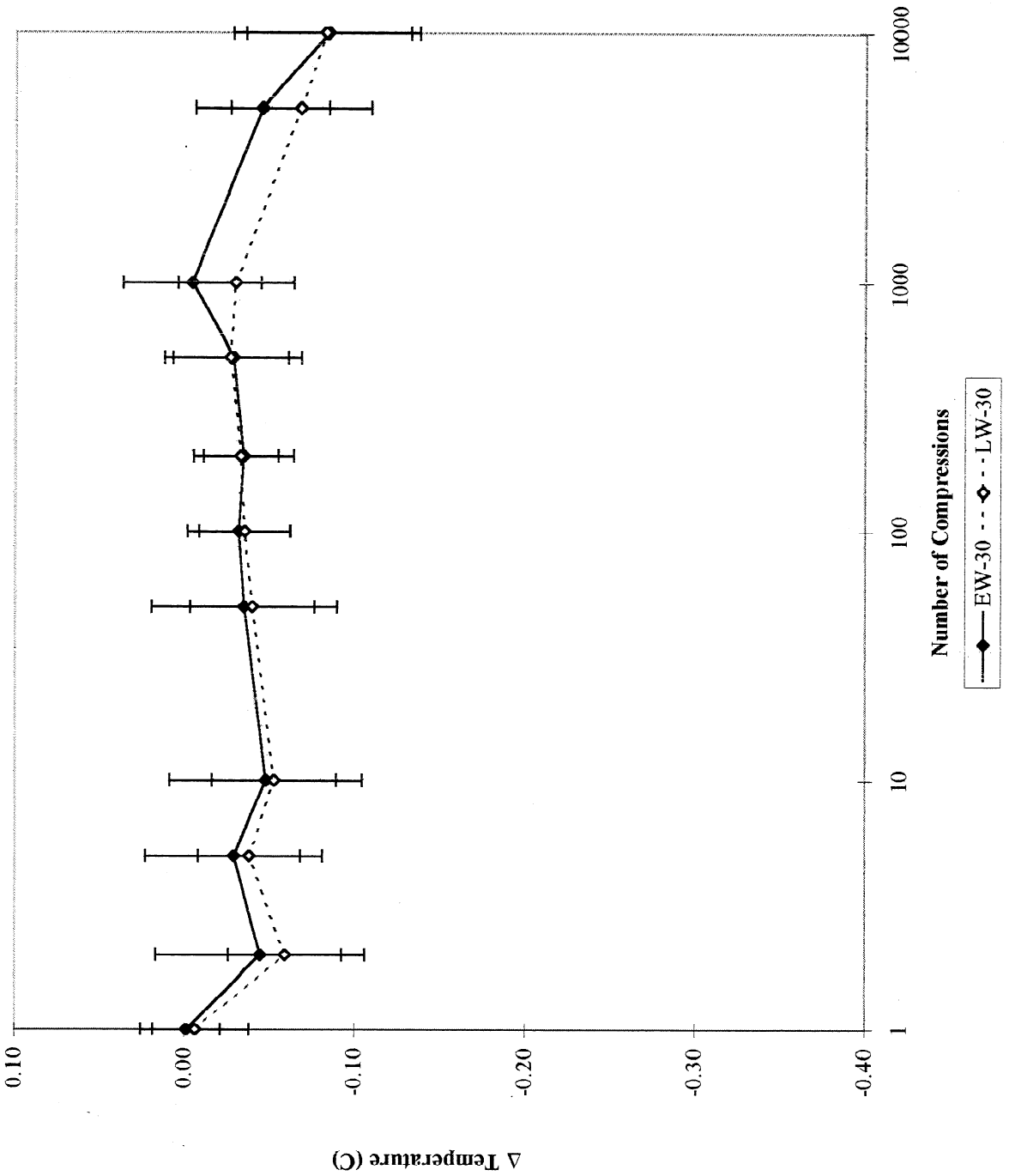

Figure 32. Change in temperature - mixed aggregates, 30 Hz.

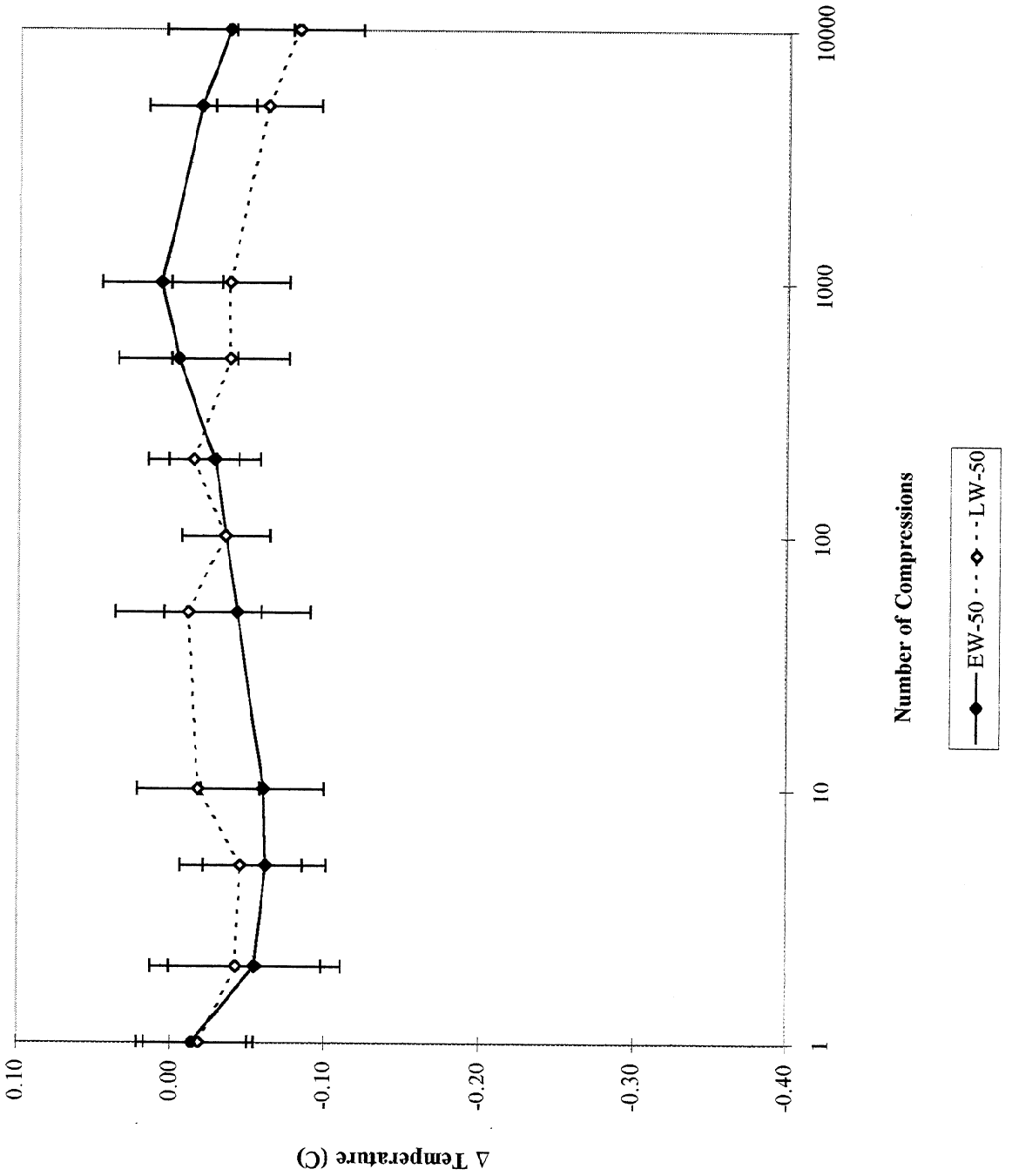

Figure 33. Change in temperature - mixed aggregates, 50 Hz.

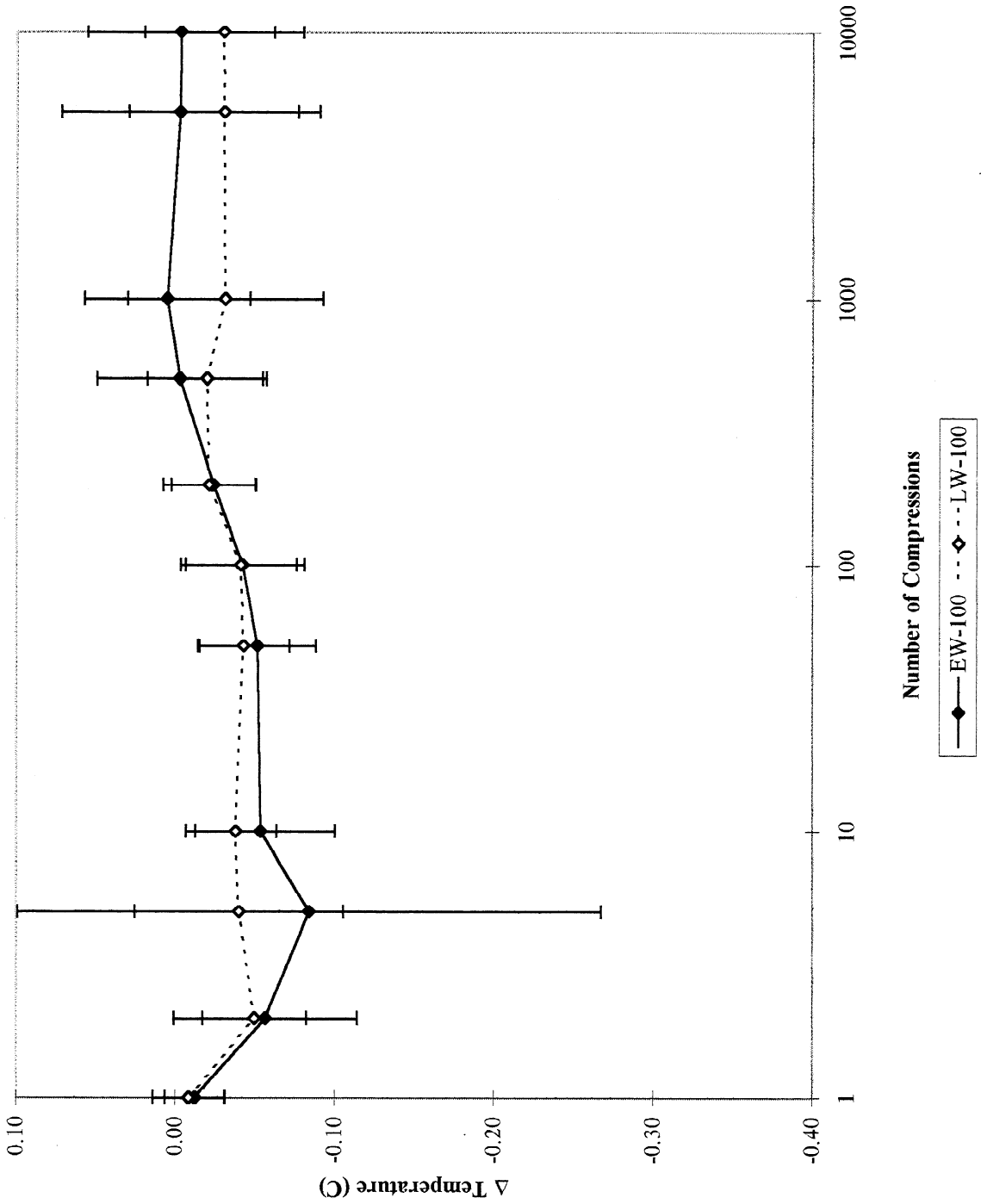

Figure 34. Change in temperature - mixed aggregates, 100 Hz.

The complete set of data for this initial mixed aggregate testing is shown in Figures 35-36 (except for 200 Hz). Up to approximately 1000 cycles, the fibers follow a similar trend, regardless of type or frequency. After 1000 cycles, fiber type and frequency show their effects. Earlywood fibers show signs of continued heating with increased frequency. This is similar to Hickey's findings (23). Earlywood took longer to reach the plateau temperature, and that temperature was higher than the latewood fibers' temperature. Figures 34-35 show the point-to-point fit and best-fit polynomial (second order) curve for the earlywood fibers. The latewood curves (Figures 37-38) follow a similar trend but with less temperature increase between cycles 5 and 1000. The curves definitely follow the trend of a larger initial temperature drop and a longer temperature rise with increasing frequency.

The decrease in temperature after approximately 1000 cycles is thought to be from the forced convection and evaporation that occurs within the cuvet when the piston is moving. At this point the fibers appear to be losing their viscoelastic heating capabilities and the effect of evaporation and convection overwhelm any heating.

Figure 39 shows the correlation between the earlywood and latewood temperature change at a specified cycle and frequency. The slope decreases with increasing frequency meaning that the latewood absorbs more energy and earlywood absorbs less at higher frequencies, probably due to latewoods' stiffer fibers with better recovery capabilities.

Figure 40 has the correlation graphs between the change in temperature and change in curl index for fiber type at a specified frequency and cycle number (all experiments using the shaker equipment). There is little correlation between them. Because the temperature did not rise as expected, and the cooling was not linear, there is little reason for these figures to show a correlation.

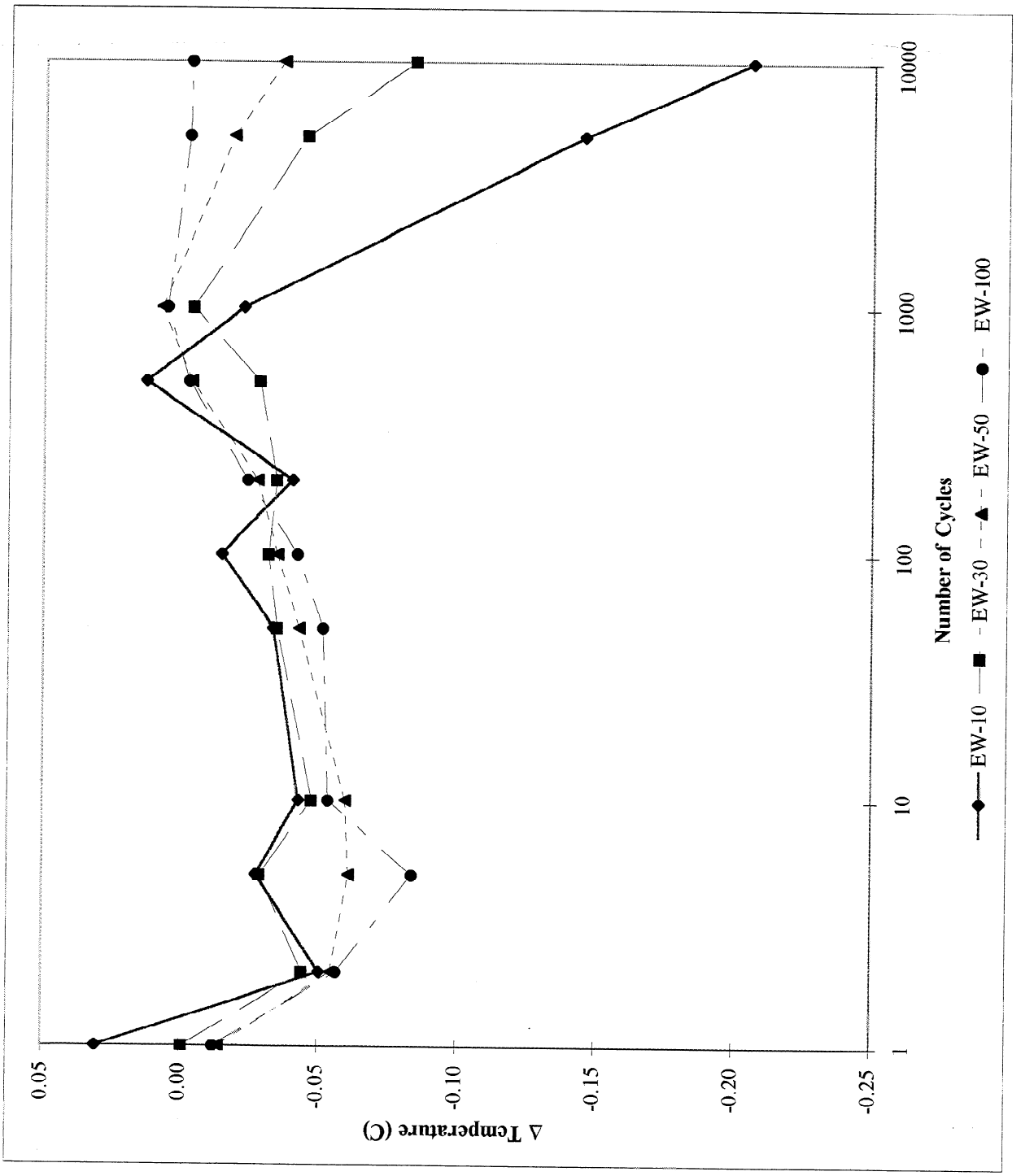

Figure 35. Change in temperature - mixed aggregates, Earlywood, point to point.

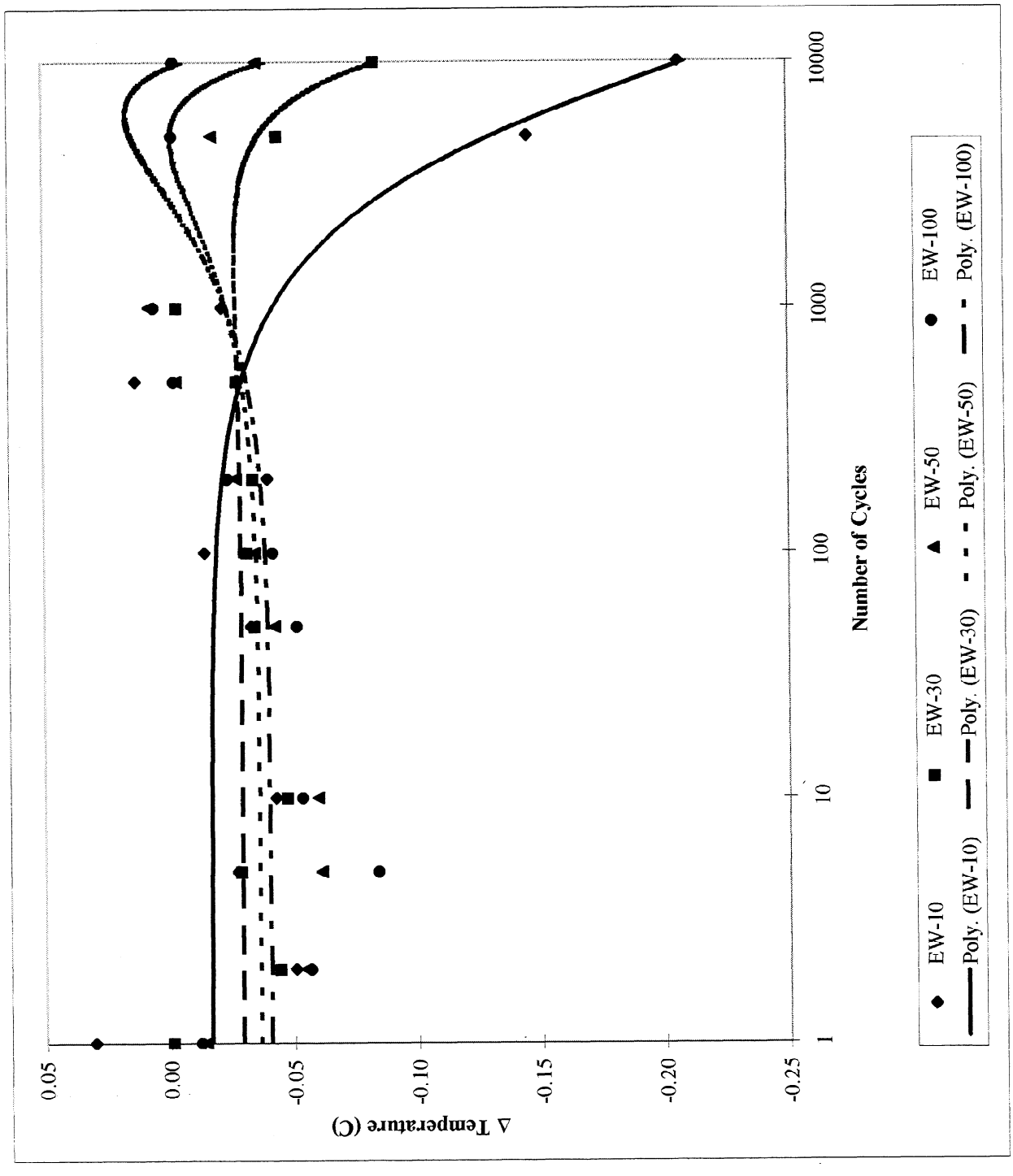

Figure 36. Change in temperature - mixed aggregates, Earlywood, best fit.

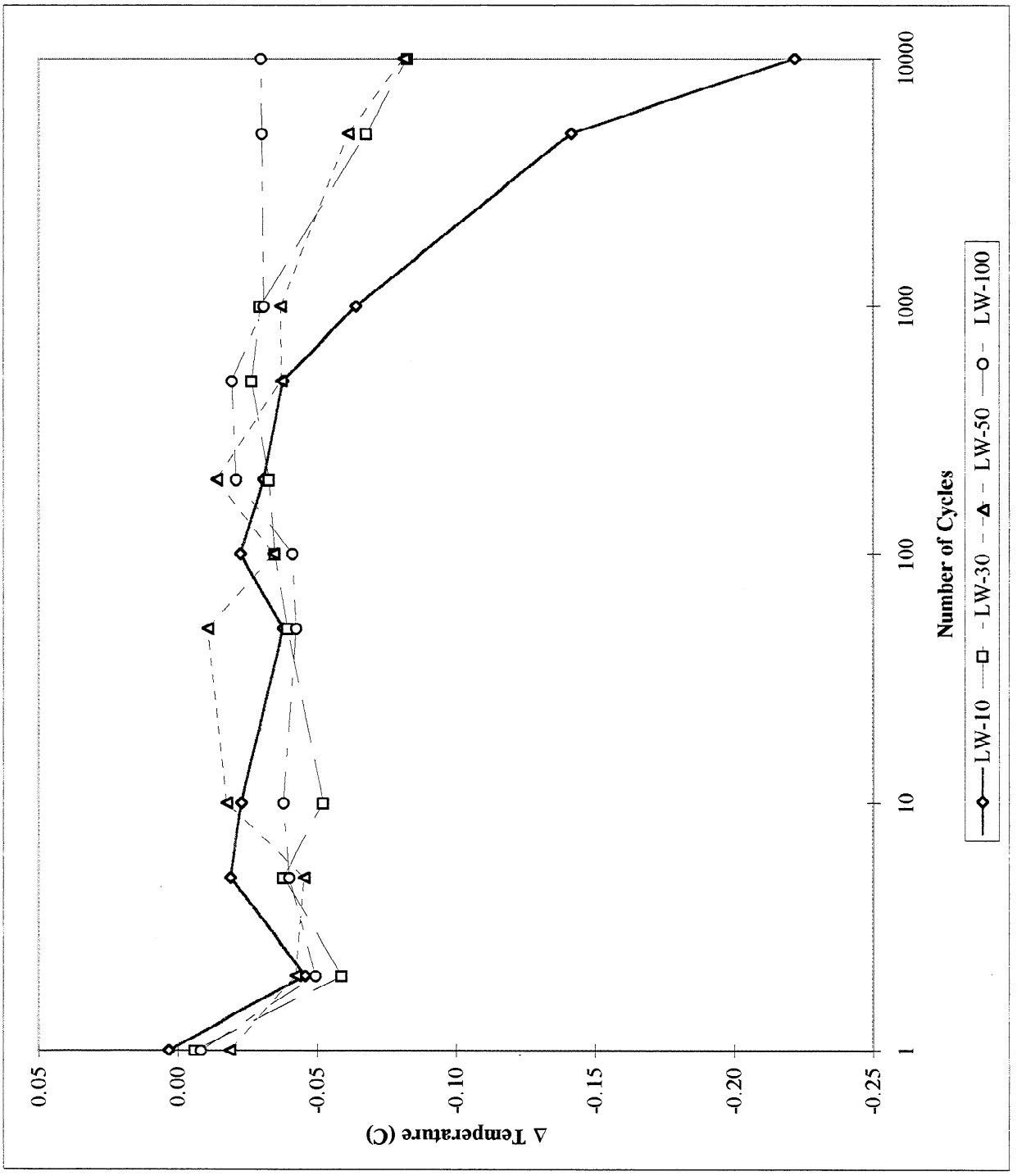

Figure 37. Change in temperature - mixed aggregates, Latewood, point to point.

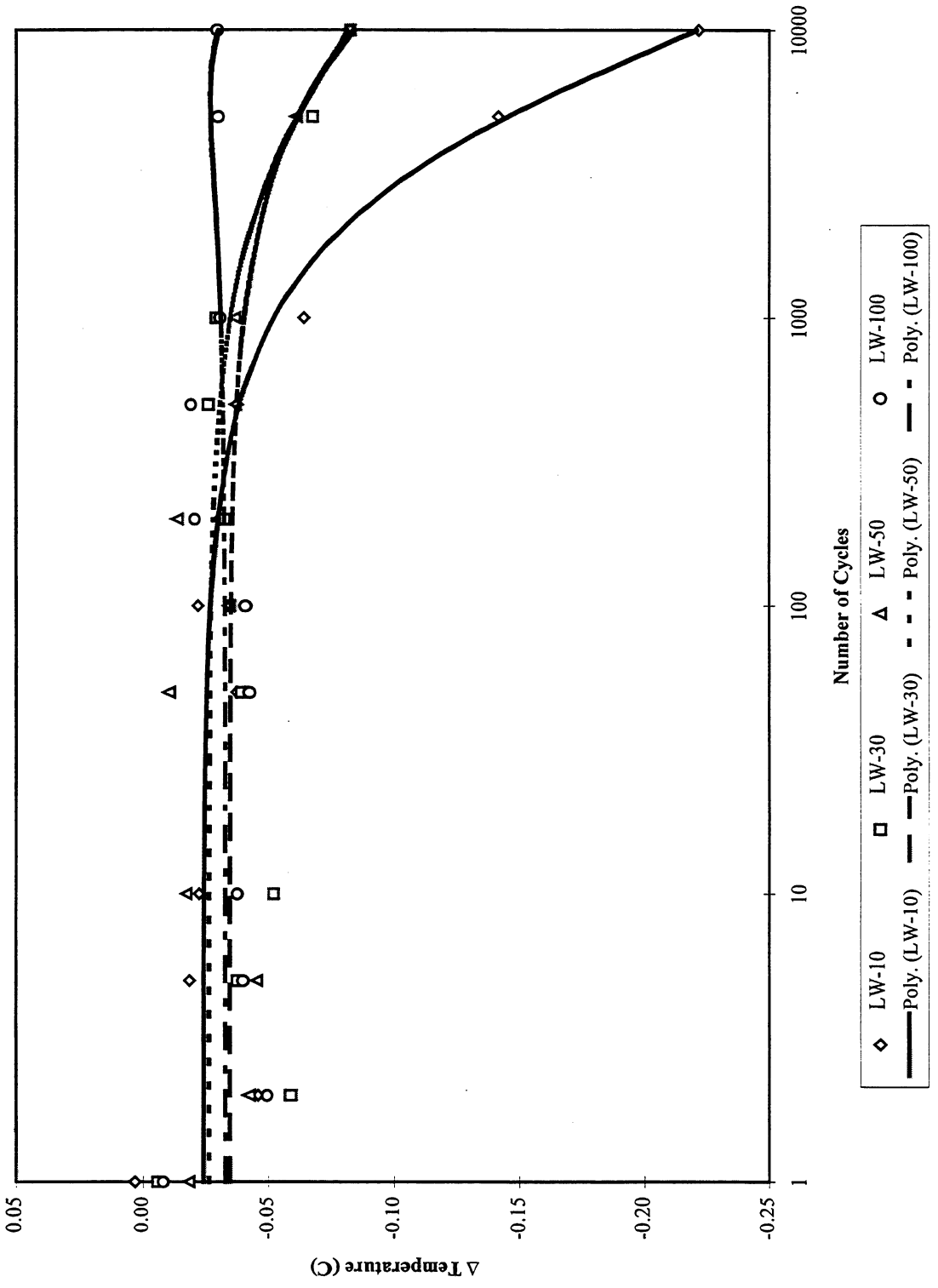

Figure 38. Change in temperature - mixed aggregates, Latewood, best fit.

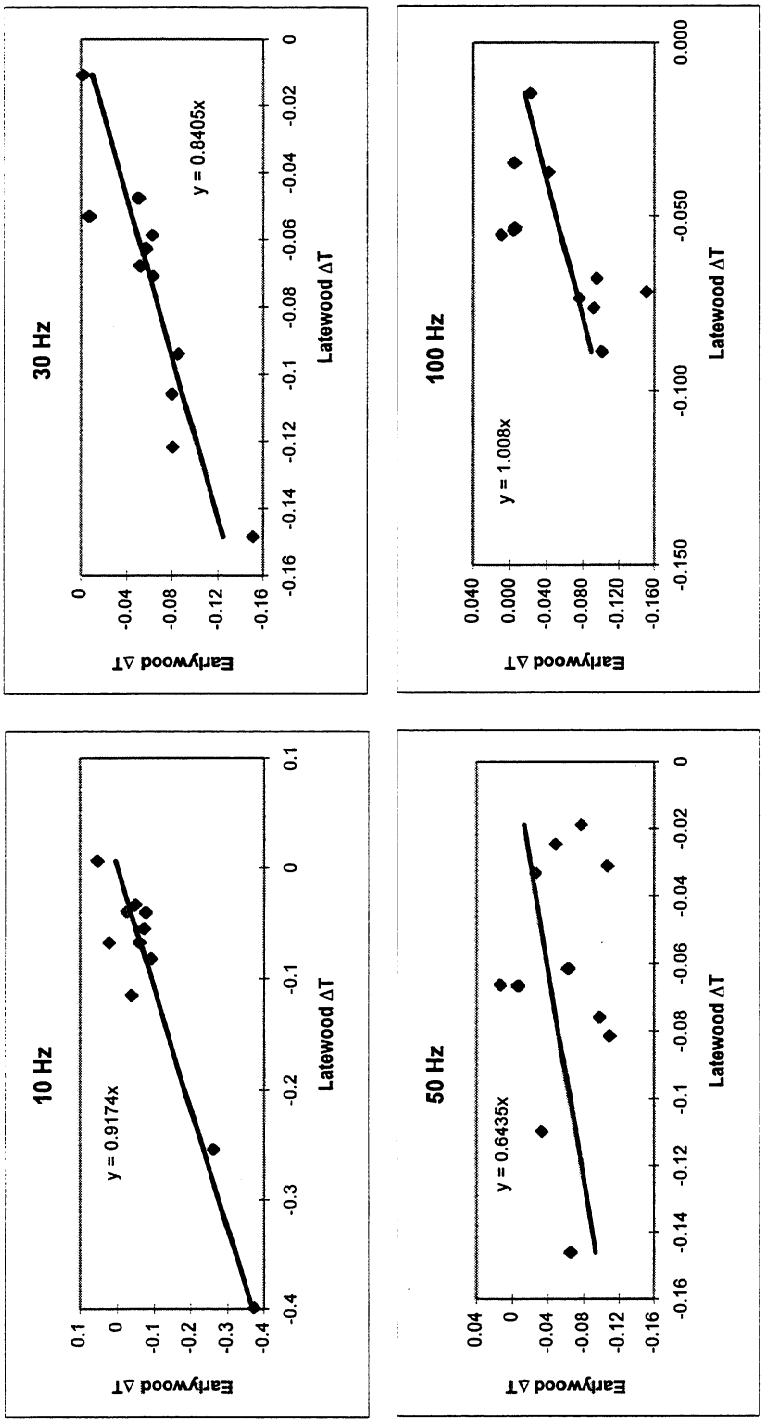

Figure 39. Correlation between earlywood and latewood change in temperature at a specific frequency.

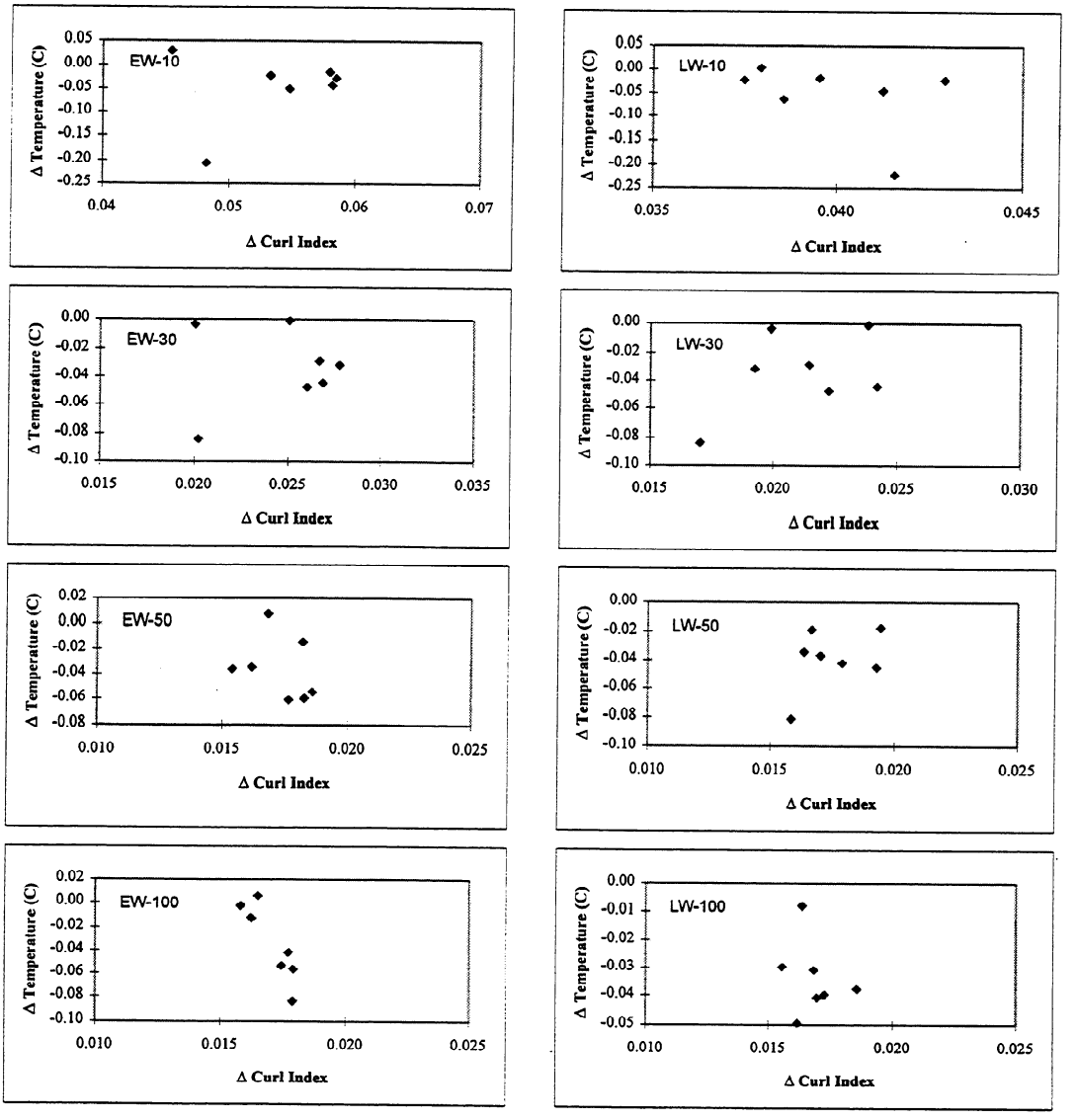

Figure 40. Correlation between change in temperature and change in curl index for a specific fiber type and frequency.

Pure Aggregates at 45% Consistency

Experimentation was also carried out to see the impact of aggregate makeup (mixed fiber type or pure aggregates) and whether the same trends and temperature changes occurred. The same procedures were followed as before, other than the fiber aggregates were either all (pure) earlywood or latewood, and testing was done at 10, 50, and 100 hertz.

The results are very similar to the initial infrared data set (Figures 41, 78-82, Tables 17-19). The best-fit curves follow the same trends, and the t-tests show very little significant difference between the fiber types. Temperature decreases initially, followed by a slow temperature rise, and then a fast decrease after approximately 1000 cycles. The effect of frequency is seen at the cycles between 1000 and 10,000. Ten-hertz fibers cool sooner than do the higher frequencies, as seen with the mixed aggregates.

The earlywood data show a very good correlation between the two data sets, but the latewood (other than at 10 hertz) is weak (Figure 42). The difference is probably due to the technique used in determining sample size. Even though the samples were the sample mass (density), the pure latewood aggregate took up less volume within the cuvet compared to a mixed fiber aggregate. This is due to fewer fibers per gram of latewood compared to mixed or pure earlywood samples (59). After the first few compressions, the aggregate compressed to the point where it did not get much stress with each cycle.

In five of the six correlation graphs, the slope of the linear curve-fit is greater than one. This states that the fibers in the pure aggregates were hotter than the fibers in the mixed aggregates. By being hotter, the pure aggregates absorbed more energy and more energy absorption equates to more flexible fibers for papermaking.

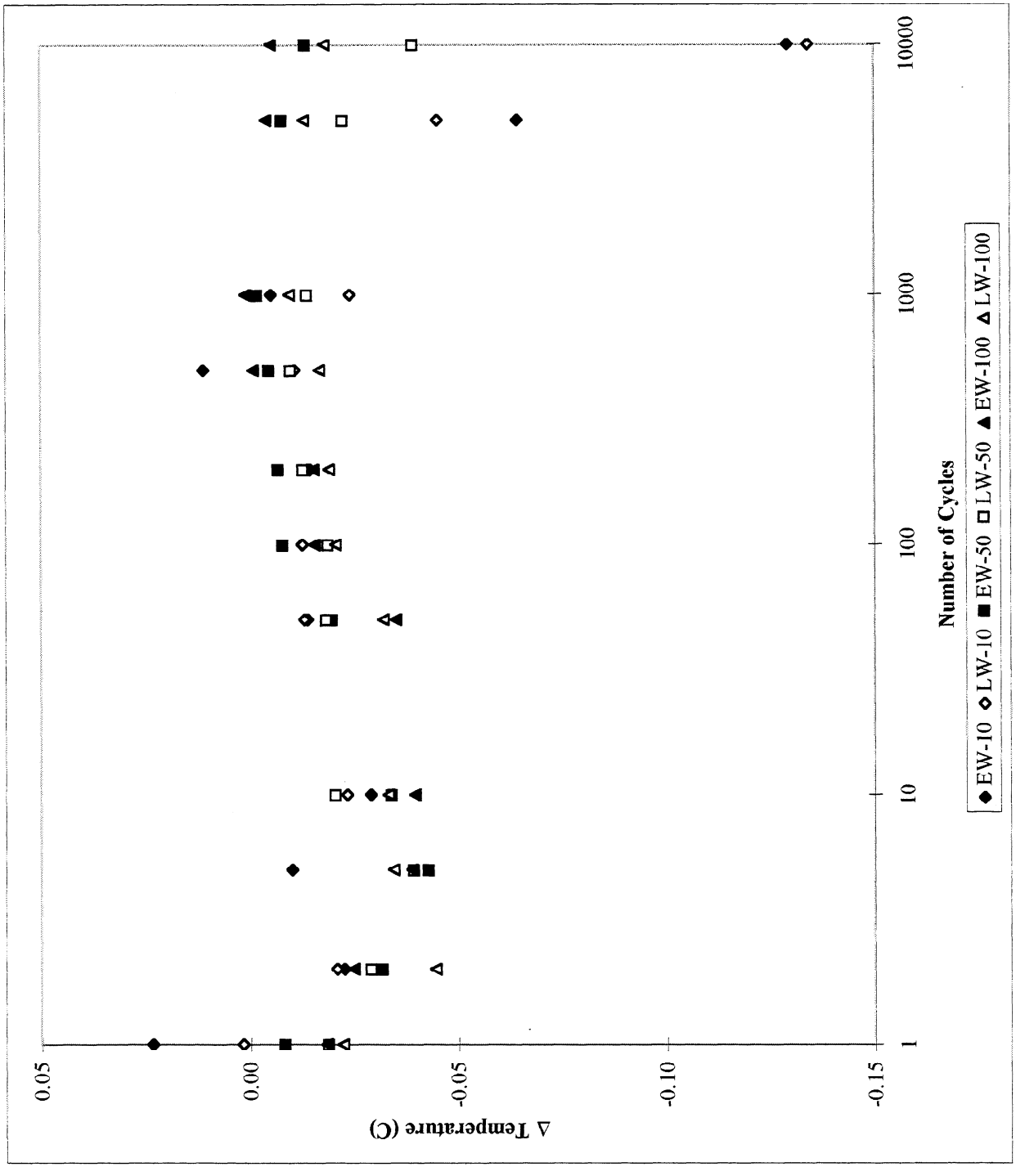

Figure 41. Change in temperature - pure aggregates.

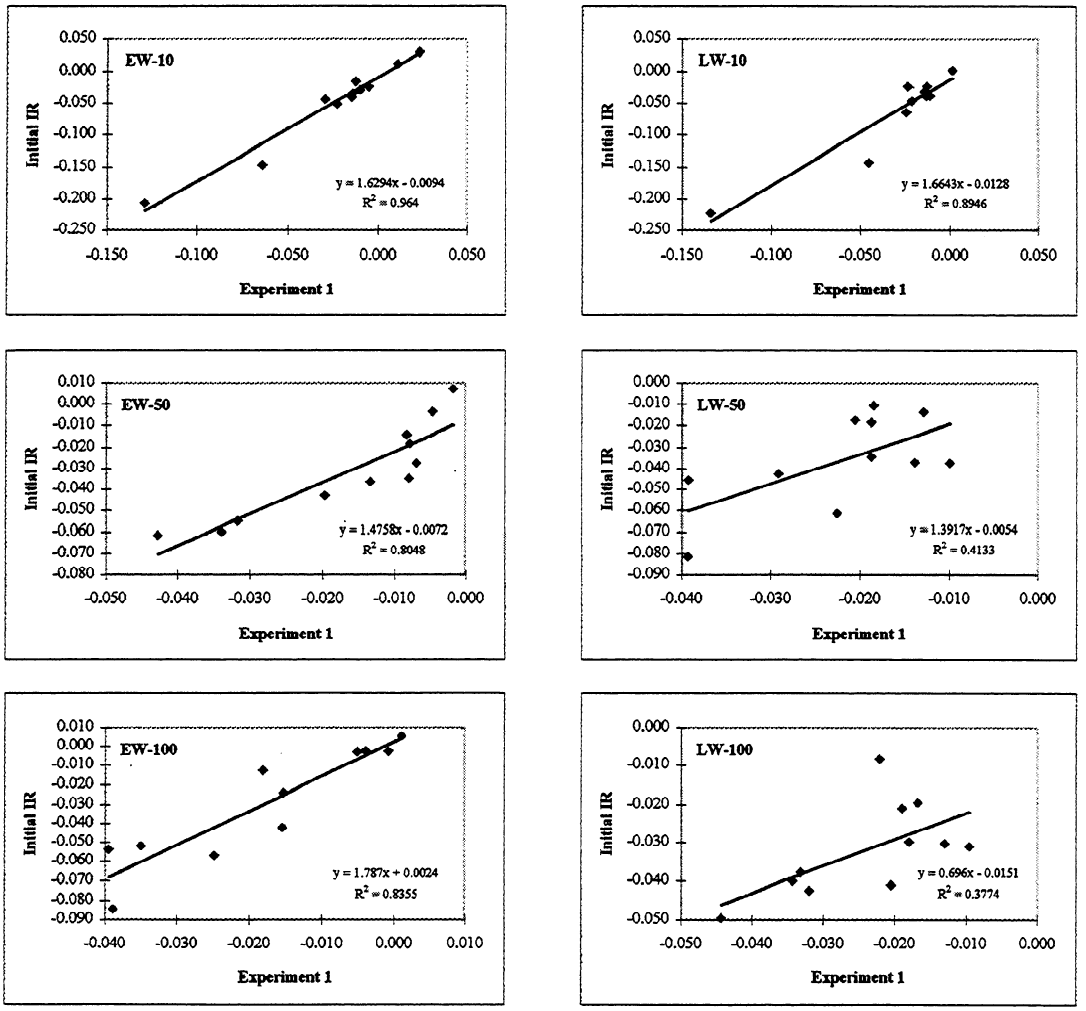

Figure 42. Correlation of initial mixed aggregate IR study to pure aggregate study.

Pure Aggregates - Air Dried

Another set of testing was completed to record the thermal history of samples that had reached moisture equilibrium with the environment. These experiments were performed to eliminate evaporation and its cooling effect from the fibers. Samples were conditioned for 48 hours in an open container at room conditions: approximately 60% relative humidity and 25°C. The samples were treated the same as the mixed and pure aggregates, but were only tested at 10 and 50 hertz up to 2000 cycles. This testing was performed on pure samples of latewood fibers.

The data from the 10 and 50 hertz testing are presented in Figures 43 and 83. As can be seen the fiber aggregates do increase in temperature when evaporation is eliminated. The difference between these two frequencies is very significant after approximately 200 cycles (Table 20). The 50-hertz aggregate reached the plateau temperature quickly, but the 10-hertz aggregate temperature is still climbing at 2000 cycles. Apparently, the dynamic modulus has not decreased as much as the damping capacity has increased, referring to relationship 2 for temperature increase to occur in deflection-controlled testing.

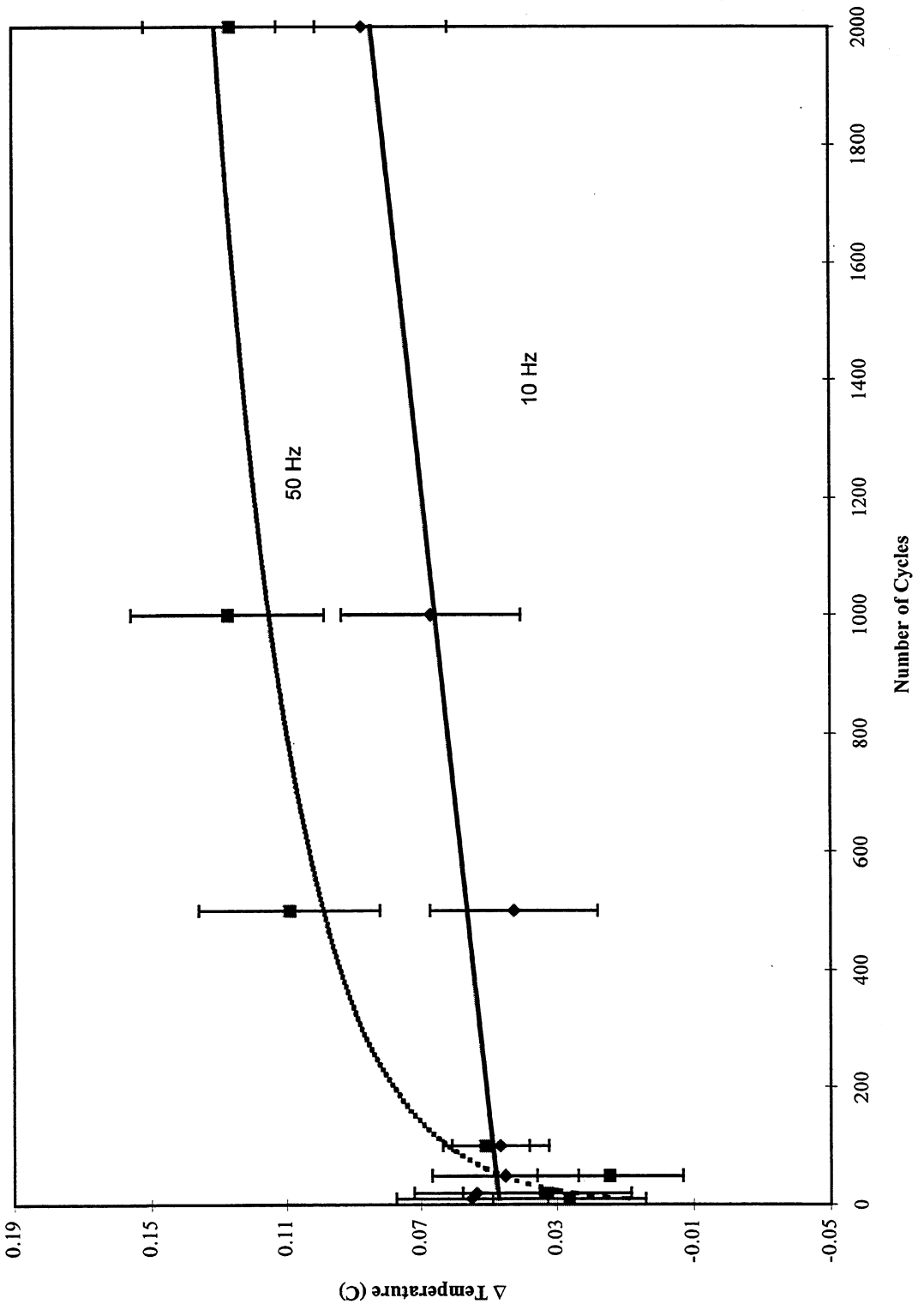

Figure 43. Change in temperature - pure, air-dried.

Pure Aggregates at 45% Consistency, Cycling Above Aggregate

This study was carried out to evaluate the effect of evaporative cooling with no fiber work involved. Pure latewood aggregates were placed into the acrylic block. The fiber mass was initially crushed to just beyond the lowest point the piston would reach in its cycling. The piston then cycled above the fiber aggregate, and images were collected at 100, 500, 1000, 5000, and 10,000 cycles.

The data show that without fiber work performed on the aggregates, there is no intermediate heating occurring (Figures 44, 84). The cooling is achieved through two modes: evaporation of some of the moisture in the fibers and forced convection from the air being pumped through the fiber mass by the movement of the piston. The assumption is that the fibers cool at a rate that slows due to attaining moisture equilibrium with the air present in the acrylic block. The impact of frequency on a per cycle basis is small but the cooling is larger with a higher frequency. The difference in the temperature between the two frequencies is significant at 500 cycles (Table 21). When looking at the same data on a time basis, the differences appear to be much greater (Figure 84). This is probably due to the speed at which the 50-hertz cycling is forcing air through the fiber mass.

Evaporative cooling was expected after analysis of the initial thermal study. If this were discounted, the temperature of the initial thermal study, that study would have shown an increase instead of having a negative temperature change (Figure 45). This was concluded from data taken from latewood aggregates that were weighed, compressed for a number of compressions, removed from the sample chamber, and reweighed. The theoretical temperature increase was calculated from the normalized water lost per cycle for both 10 and 50 hertz for a 0.042 gram aggregate at 45% consistency. The amount of energy required to evaporate this amount of water was calculated, and that amount of energy was applied to the aggregate under the assumption that the saturated fibers would have a specific heat similar to water. The temperature rises higher with the lower frequencies. This is consistent with the idea of the higher frequencies having

smaller hysteresis loops and less energy absorbed due to the strain not being completely removed between cycles and the next stress cycles starting from a prestrained position.

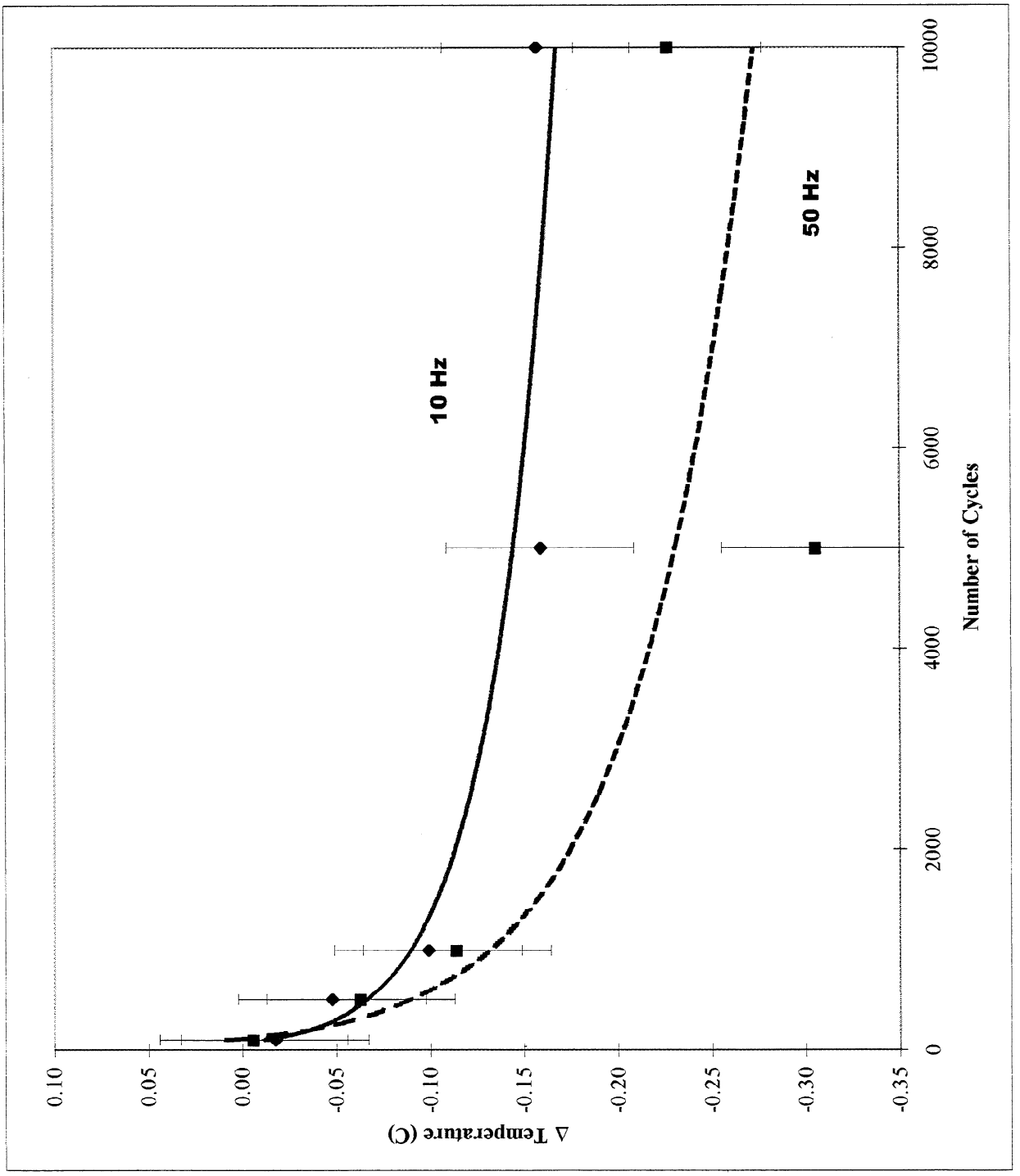

Figure 44. Change in temperature – pure latewood, no fiber work.

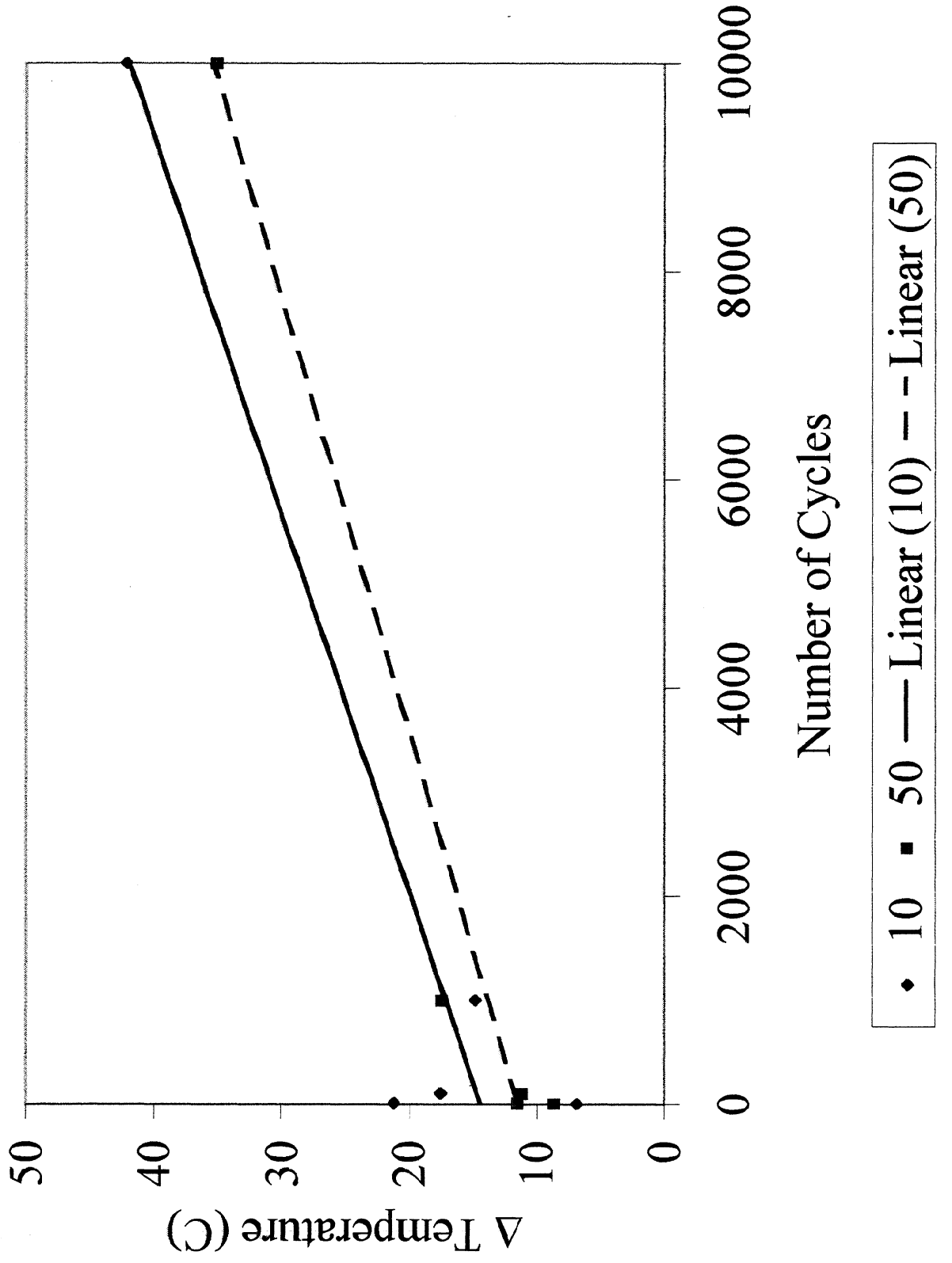

Figure 45. Calculated change in temperature of latewood without evaporation – 10 and 50 Hz.

Evaporation Study without Cycling

A three-phase experiment to understand when, where, and how much water was being lost due to evaporation was also undertaken. The first phase was to see how much evaporation could occur in the fiber aggregate in the cuvet with the piston in place but static. The second phase was to ascertain how much water could evaporate from the fiber aggregate if left in an uncovered weighing dish. The third phase was to find out how much water was lost by moving the fiber aggregate from the sample bottle to the acrylic block and back to the sample bottle. Phases one and two introduced a new factor - some of the aggregates were saturated in polyethylene glycol (PEG, MW=200) to hinder evaporation at room temperature.

The amount of water evaporated with the fibers in the cuvet and piston in place was extremely small for both the regular fiber aggregates and the aggregate with PEG (Figure 46). The regular aggregate only lost approximately 0.001g of water in 20 minutes. The PEG sample lost one-tenth of that amount in the same amount of time. Therefore, little water would evaporate without cycling the piston. A spectrophotometric cuvet was used in place of the acrylic block in this experiment because its mass was smaller, so the balance could measure the difference in aggregate mass.

The amount of water evaporated in an uncovered weighing dish in stagnant air was much larger than in phase one (Figure 45). The regular aggregates lost approximately 0.019 g of water. This amount of water would theoretically require a temperature change of almost 10°C if all the energy to evaporate the water came from the fibers. The PEG samples also lost more water than before (0.004 g). This is probably due to incomplete exchange of the water for PEG in the fiber sample.

The third phase of testing in this evaporation study was simply to measure the loss in mass that occurred while taking the fibers to and from the sample bottle (Figure 46). The second mass was measured two minutes after the initial weighing in the sample bottle for continuity. The aggregate average was approximately 0.003 g of water lost in the two-minute time period.

Besides losing water in this phase, lost fiber could also account for some of the mass difference. Every effort was made to put all fibers back into the bottle, but that was impossible to achieve. Phases one and two did not have this problem because the initial weighing occurred after the aggregate was placed into the appropriate container.

Evaporation Study with Cycling

Another experiment was completed to understand how much water was being lost in the process of cycling. It was performed at 10 and 50 hertz with mixed aggregates of fibers. The samples were weighed in the sample bottles, cycled, and then reweighed. The samples were cycled for 0, 10, 100, 1000, and 10,000 cycles. The zero-cycle samples were taken out of the bottle, placed into the block, the block placed under the piston, and then the sample was removed.

Water loss and average change in consistency was greater in the 10-hertz samples (Figures 47,85). This is probably due to the longer time to reach the same number of cycles. It is interesting to note that the amount of water lost is almost half the amount that was lost in the phase-three study of evaporation without cycling when the fibers were checked to see how much was lost in just the fiber transfer and setup time prior to testing. If one were to take the total mass of water lost with the piston in place but not moving and add it too the amount of water lost due to aggregate transfer then subtract the amount of water lost during cycling, theoretically the temperature of the fiber should drop by two degrees Celsius. However, the temperature of the fibers never decreased by two degrees in any of the experiments, so it is highly probable that there is another mechanism for water removal from the fiber aggregate. The obvious answer is the physical transfer of the water from the fiber to the aggregate chamber walls. This was actually seen with the infrared camera during the first attempts at the lower consistency and with the higher frequencies with the higher consistency experiments. Water droplets were adhering to the sapphire window blocking the infrared energy to the camera.

Comparing this study to the experiment with fiber aggregates without fiber work, it is noteworthy that the temperature difference is greater in the 50-hertz testing, but this study shows that the 50-hertz aggregates lose less water than those tested at 10 hertz. Therefore, it is apparent that more than just evaporation of some of the fiber water is causing the cooling to occur.

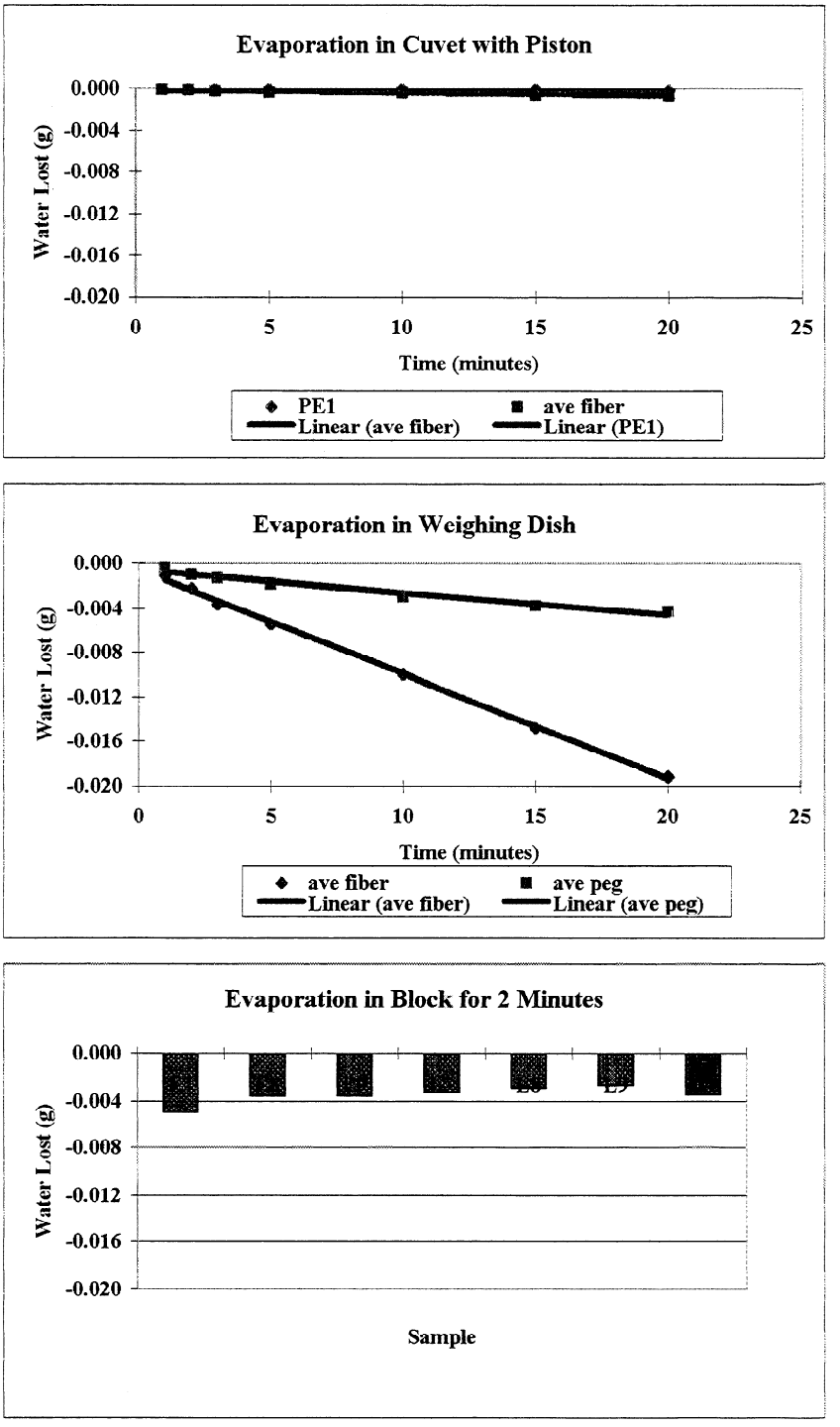

Figure 46. Evaporation study without cycling - phase 1, phase 2, and phase 3.

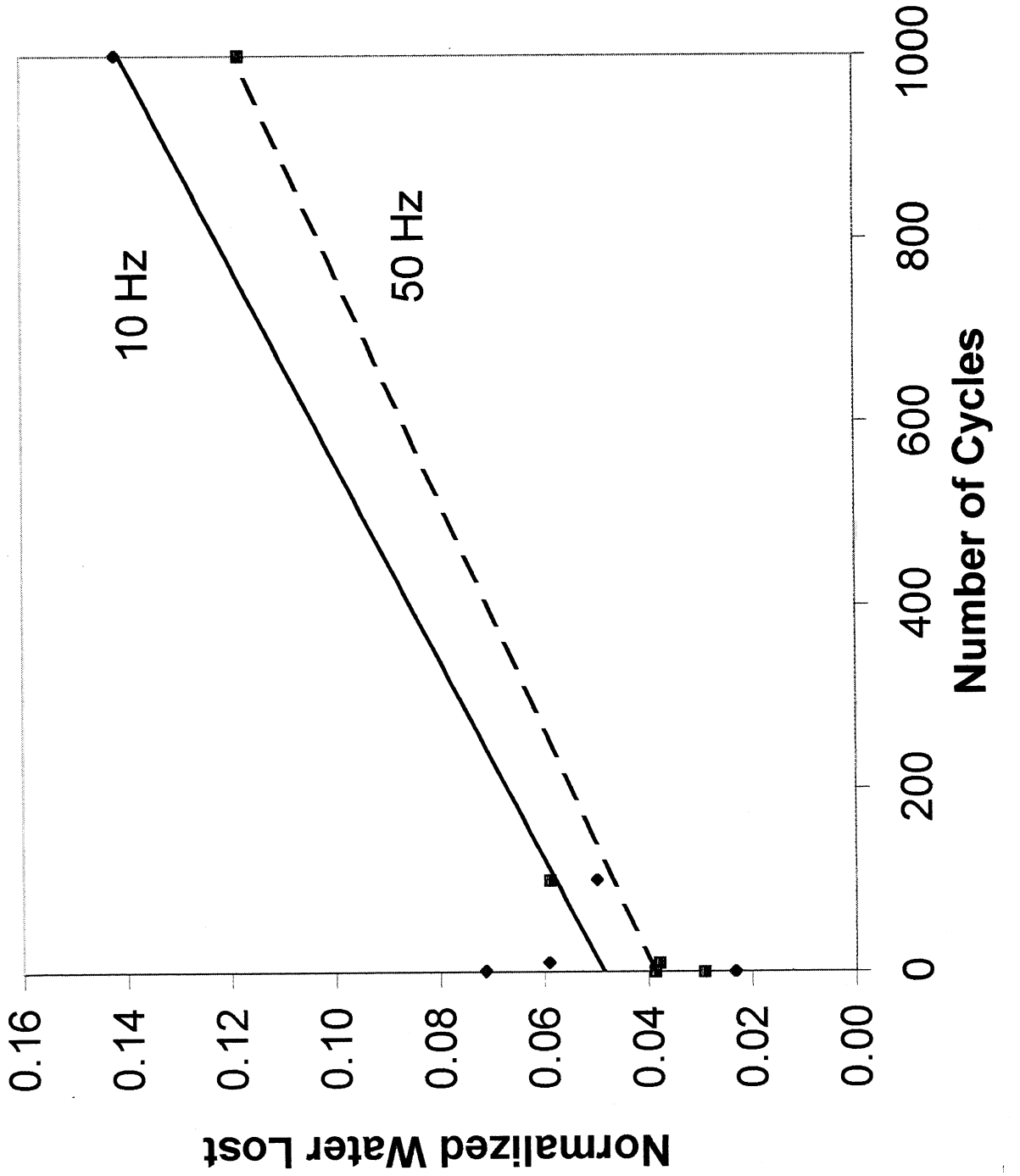

Figure 47. Evaporation study with cycling - average water lost.

CONCLUSIONS

The main purpose of this thesis was to evaluate whether fiber morphology caused earlywood fibers to preferentially absorb energy compared to latewood fibers in cyclic compression simulating a disk refiner. At the fiber aggregate level there is no evidence of a preferential strain, with the possible exception of the lowest frequencies and first cycle of compression. Once the fibers were cycled above 30 hertz, the fiber types showed no difference in their energy absorption behaviors, as seen with a change in curl index within cycles or a change in temperature. These frequencies are still to a factor of 100 lower than the frequencies found in an actual mill refiner.

The change in curl index within a cycle showed that the fibers have viscoelastic behaviors at these frequencies. This is seen in the way change in curl index decreases with higher frequency. The MTS and shaker experimental devices both showed the same tendencies, though the shakers' values in curl index were significantly lower than those of the MTS. This is probably due to the problem with the starting of the cycling and lower force of the shaker.

The change in temperature shows no differences between the earlywood and latewood fibers. An increase in temperature is not present except with the first cycle of the ten-hertz experimentation. This is important in itself due to the way fibers move through a refiner. Fibers are continually in a process of joining and leaving fiber aggregates. The data seen at one or two cycles is probably closer to what may be happening in a true refiner than that at cycles above 100.

The temperatures follow a pattern of immediate cooling, followed by an intermediate section of increasing temperature, and finally rapid cooling. The cooling appears to be due to evaporation. Initially, evaporative cooling occurs more quickly than the temperature rises in the fibers from the fatigue/hysteresis effects of the cyclic compressions. As the rate of temperature increase becomes higher than the rate of cooling, the slope of the curve of temperature change begins to be positive. When the plateau of the heating effect from fatigue/hysteresis of the fiber

is attained, evaporative cooling of the wet fibers dominates the temperature change. At this point, the negative slope of the change in temperature curve returns.

The first stage of temperature change within fibers due to cyclic compression shows the tendency of higher frequencies to result in lower temperatures and more cycles until the slope of the temperature change curve begins to be positive. The second stage shows some heating (but overall still at a lower temperature than the initial temperature), due to fiber work from the energy absorbed from the cyclic compression. A lower frequency allows viscoelastic fibers time to respond to a force and absorb more energy per hysteresis cycle. The larger energy absorption will also bring about more fractures and fiber surface area development than lower energy absorption. This should cause a more slowly cycled fiber to have a higher temperature in the same number of cycles.

Looking at the change in curl index, Δ curl index generally plateaus by the end of the 10,000th compression cycle. This decrease in flexing will then lower the amount of energy absorbed (and heating) of the fibers. The change in temperature data does show a trend of reaching the maximum temperature after fewer cycles with lower frequency. There is also less within cycle flexing with higher frequency. Figure 48 shows this trend. This figure was made by averaging the Δ curl index values for a number of cycles at a specific frequency per fiber type. As frequency increases, both fiber types are reacting very similarly to the applied stress. Beyond 30 hertz, the fibers show no significant differences between fiber types. The frequency has now exceeded the viscous attributes of stress response time.

The third stage thermal response is due to the plateau of fiber temperature increase and continued fiber cooling from evaporation. This can be demonstrated by taking some of the data and adding the temperature change values. The oven-dried aggregates and the 45% consistency aggregates without fiber work data (both at 50 hertz) were added together (Figure 49). Missing points were added using the best-fit trendline calculation. While this figure is not a perfect fit for the thermal change of 45% consistency fiber aggregates with fiber work, the basic form is there.

This suggests that fiber work does increase the temperature and that evaporative cooling is occurring from the cycling of the air through the sample.

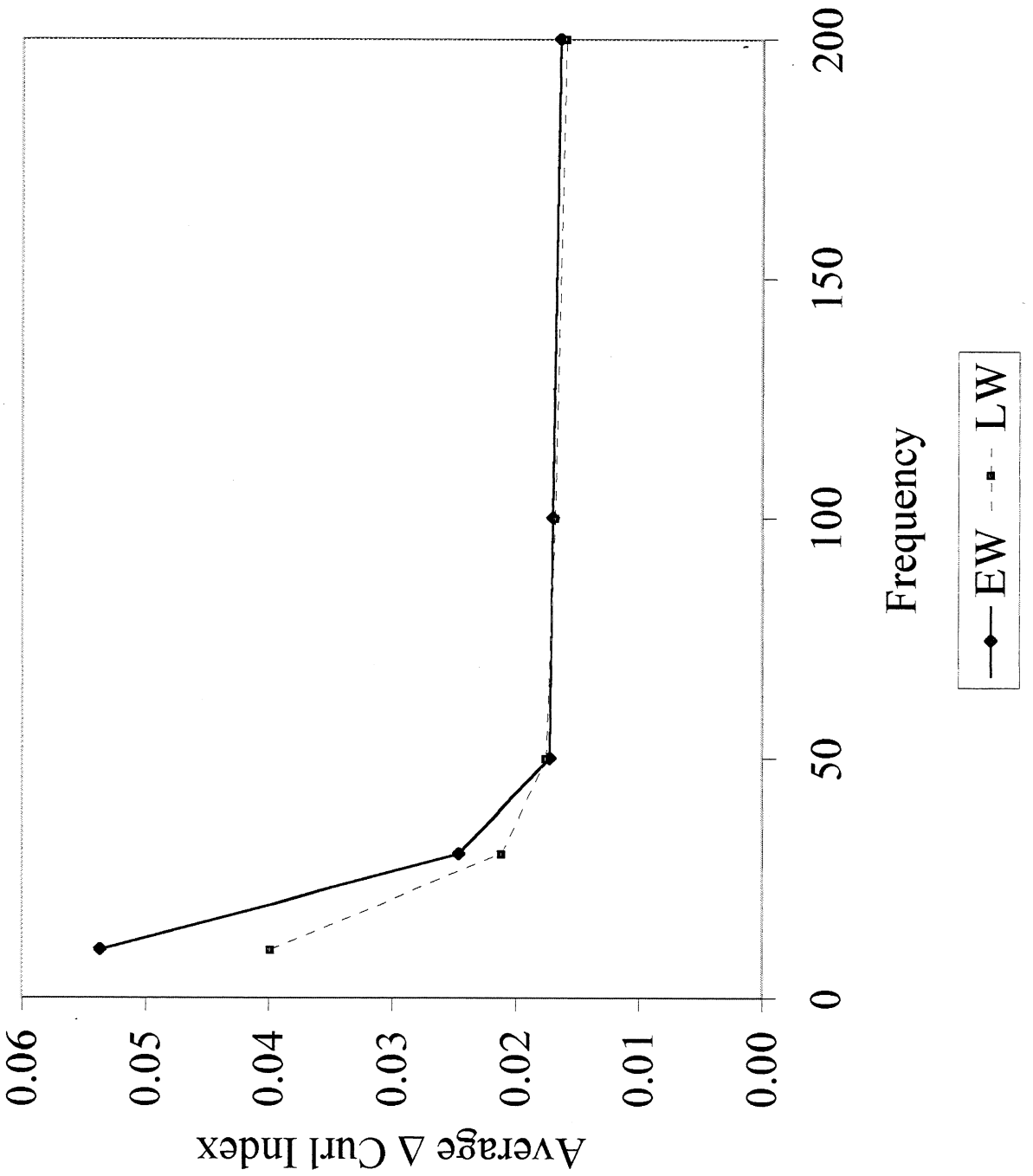

Figure 48. Average Δ curl index at a frequency per fiber type.

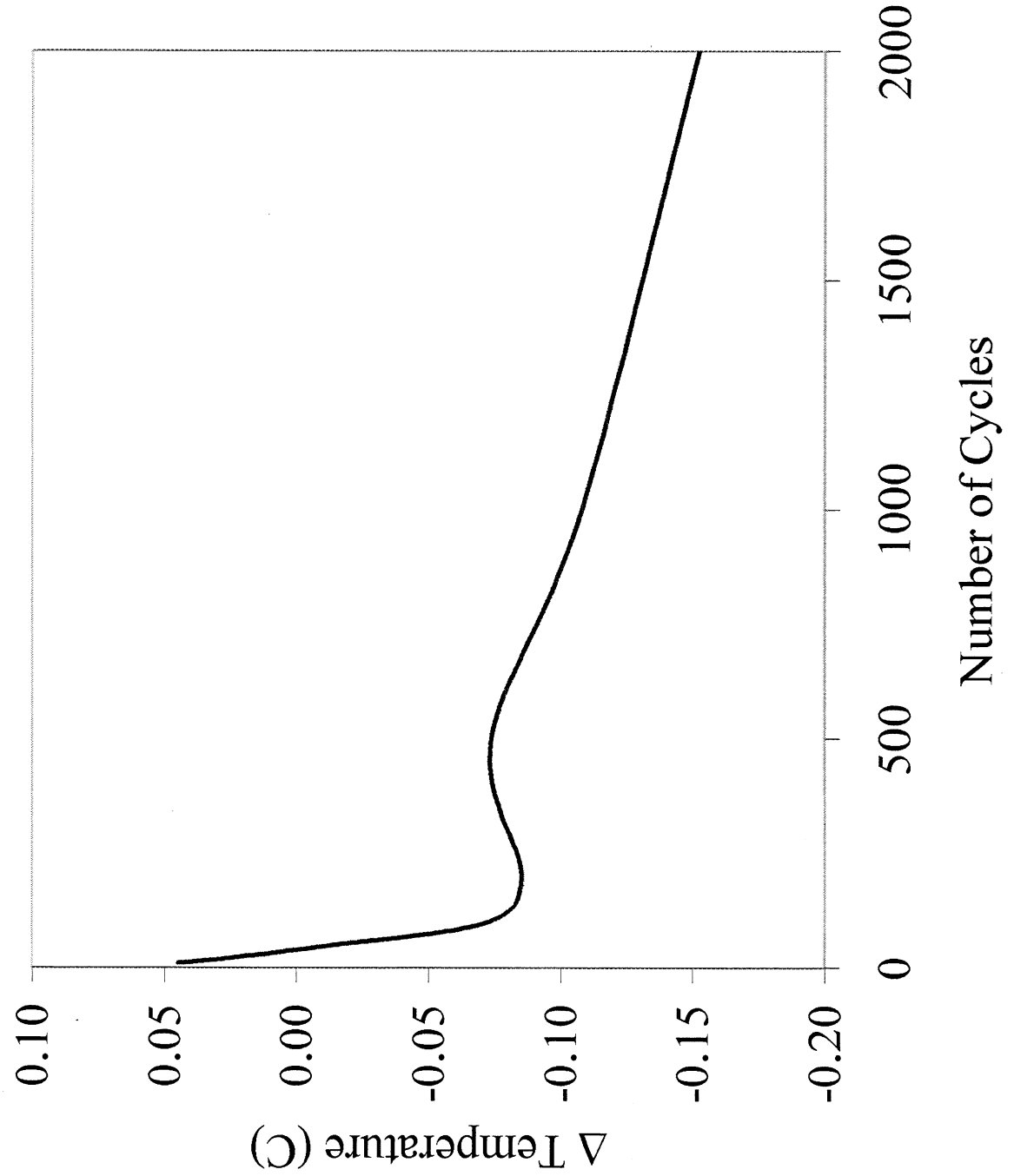

Figure 49. Addition of fiber work and evaporative cooling.

SUGGESTIONS FOR FUTURE WORK

There are three possible next steps for this area of study. The first would be to follow up on the possible significance of the first cycle preferential energy absorption. This is probably more important in the scheme of 'real-world' research than a cyclic compression sequence due to the high probability that a fiber aggregate does not exist as an entity unto itself in its progress through the refiner. A fiber aggregate is more likely to have fibers added and subtracted with each compression.

The second idea is to do more cyclic compression studies, but to see whether there is a difference in crack, kinks, etc., due to the plastic deformations. When energy is absorbed by a fiber most of that energy is lost as heat, but some is absorbed in permanent changes. This thesis finds that the amount of energy lost as heat is not significantly different between the two fiber types. But does the energy used in deformations have a preference for fiber type?

The third idea would be to try to do an energy balance of the system. This would need to account for the energy added to the system by the fiber work due to hysteresis and the evaporation of moisture from the fibers and the physical transfer of water shaken off the aggregate during cycling.

ACKNOWLEDGMENTS

I would like to acknowledge the IPST member companies for the money they contribute to the academic program of the Institute. These funds make it possible for students to receive a great education without ending up with an incredible debt upon graduation.

My advisor, Dr. Alan Rudie, needs to be recognized for his never-ending patience and open-door policy, which helped the learning process along.

The rest of my standing thesis committee, Dr. Earl Malcolm and Dr. Pierre Brodeur, should be credited for their many questions and subtle proddings to get me thinking in the right direction to solve the many problems that arise during thesis experimentation.

This thesis would have never been finished without the scholarship at the MPLUS (Metals Processing Laboratory User Facility) at Oak Ridge National Laboratory. With the scholarship, I was able to acquire the thermal data of this study. I would like to thank three people at Oak Ridge for their help: Dr. Ralph Dinwiddie, Dr. Gail Mackiewica-Ludkta, and Dr. Sheng Hu.

I would like to thank the many people at IPST (fellow students, staff and faculty) who helped make a Microbiologist and former high school Science teacher capable of solving the many problems that occur every day in the thesis process.

It is due to the support of my husband, Larry, that I came to the Institute. He was there when times were tough and hours very irregular, and also there when I needed a kick in the butt to quit procrastinating.

My dogs get credit for keeping me sane, Mistletoe, Brother, and Rastle. These dogs gave me a hobby and got me away from almost anyone who knows something about paper.

Lastly I would like to acknowledge my son, Samuel Rueckert, born during this process of earning a Ph.D. It is due to him that I now know there are more frustrating things than an experiment gone wrong, and more wonder than the first time your analysis turns out as expected.

LITERATURE CITED

1. Koch, P. Utilization of the Southern Pines, Vol. 1. U.S. Department of Agriculture Forest Service. (1972).

2. Pulp and Paper Manufacture, Vol. 2. Joint Textbook Committee of the Paper Industry. Leask, R.A.; Kocurek, M.J. – ed. 1987.

3. Panshin, A.J.; DeZeeuw, C. Textbook of Wood Technology. McGraw-Hill. 1980.

4. Kennedy, R.W.; Ifju, G. Applications of Microtensile Testing to Thin Wood Sections. TAPPI Journal. 45(9):725(1962).

5. Kennedy, R.W. Intra-increment Variation and Heritability of Specific Gravity, Parallel-to-Grain Tensile Strength, Stiffness, and Tracheid Length, in Clonal Norway Spruce. Tappi Journal. 49(7):292(1966).

6. Ifju, G. Within-Growth-Ring Variation in Some Physical Properties of Southern Pine Wood. Wood Science. 2(1):11(1969).

7. Nordman, L.S.; Qvickstrom, B. Variability of the mechanical properties of fibers within a growth period. The Physics and Chemistry of Wood Pulp Fibers. TAPPI Press. Page, D.H. – ed 1970.

8. Biblis, E.J. Transitional Variation and Relationships Among Properties Within Loblolly Pine Growth Rings. Wood Science and Technology. (3):14(1969).

9. Wellwood, R.W. Tensile Testing of Small Wood Samples. Pulp and Paper Magazine of Canada. (2):T61(1962).

10. Koran, Z. Some aspects of mechanical separation of wood fibers. Pulp and Paper Research Institute of Canada. Trend 11:14.

11. Rudie, A.W.; Morra, J.; St. Laurent, J.; Hickey, K.L. The Influence of Wood and Fiber Properties on Mechanical Pulping. Tappi Journal. 77(6):86(1994).

12. Page, D.H.; El-Hosseiny, F.; Winkler, K.; Lancaster, A.P.S. Elastic Modulus of Single Wood Pulp Fibers. Tappi Journal. 60(4):114(1977).

13. Schniewind, A.P. Mechanical Behavior of Wood in the Light of Its Anatomic Structure. Proceedings of the Conference on the Mechanical Behavior of Wood. p. 136 (1962).

14. Asplund, A. The origin and development of the defibrator process. Svensk Papperstidning. 56(7):550(1950).

15. Breck, D.H.; May, W.D.; Tremblay, M.N. Thermomechanical Pulping – A Preliminary Optimization. Transactions. 1(3):89(1975).

16. Atack, D. Towards a theory of refiner mechanical pulping. APPITA. 34(3):223(1980).

17. Rudie, A.W. A384 Special Topics in Mechanical Pulping class notes. 1993.

18. Pearson, A.J. Towards a more unified theory of mechanical pulping and refining. 1983 International Mechanical Pulping Conference. p. 131.

19. Hattula, T.; Mannstrom, B. Wood structure as a limiting factor in mechanical pulping. 1981 International Mechanical Pulping Conference Preprints. p. 1.

20. Atack, D.; May, W.D. Mechanical pulping studies with a model steel wheel. Tappi Journal. 45(2):145(1962).

21. Karnis, A.; Atack, D.; Stationwala, M.I. What happens in refining - Part II. Pulp and Paper Canada. 87(11):T416(1986).

22. Lai, Y. Z.; Iwamida, T. Effects of Chemical Treatments on Ultra-High-Yield Pulping 1. Fiber Separation. Wood Science and Technology. (27):195(1993).

23. Hickey, K.L.; Rudie, A.W. EUCEPA, 18th International Mechanical Pulping Conference - Poster Presentation, Oslo, Norway, 1993. Preferential Energy Absorption by Earlywood in Cyclic Compression of Loblolly Pine. p. 81.

24. Thiruvengadaswamy, R.; Ouellet, D. On the generation of structural damage in wood by cyclic compressive loading. 1997 International Mechanical Pulping Conference. p. 183.

25. Salmen, L.; Fellers, C.; Tigerstrom, A. The effect of loading mode on the energy consumption during mechanical treatment of wood. 1983 International Mechanical Pulping Proceedings. p. 109.

26. Nielsen, L.E.; Landel, R.F. Mechanical Properties of Polymers and Composites. Marcel Dekker, Inc. (1994).

27. Van Vleack, L.H. Materials for Engineering, Concepts and Applications. Addison Wesley. (1982).

28. Bodig, J.; Jayne, B.A. Mechanics of Wood and Wood Composites. Van Nostrand Reinhold Company. (1982).

29. Thorndike, E.L.; Barnhart, C.L. Scott, Foresman Advanced Dictionary. Scott, Foresman and Company. (1988).

30. Hertzberg, R.W.; Manson, J.A. Fatigue of Engineering Plastics. Academic Press. (1980).

31. Aklonis, J.J., MacKnight, W.J. Introduction to Polymer Viscoelasticity. John Wiley & Sons. (1983).

32. Salmen, L.; Olsson, A.-M. Interaction Between Hemicelluloses, Lignin and Cellulose: Structure – Property Relationships. Journal of Pulp and Paper Science. 24(3):99(1998).

33. Mataki, Y. Internal Structure of Fiberboard and Its Relation to Mechanical Properties. Theory and Design of Wood and Fiber Composite Materials. Syracuse University Press. Jayne, B.A. – ed. (1972).

34. Salmen, L. Chip refining: Influence of mechanical and chemical treatments on the energy consumption during fatigue of wood. STFI - meddelande serie. A Nr 964, Dec. 1986, 1-41.

35. Van Der Akker, J.A. Energy considerations in the beating of pulp. Fundamentals of Papermaking Fibers. F. Technical Section, B.P. & B.M.A. Bolam – ed. (1958).

36. Lamb, G.E. R. Energy consumption in mechanical pulping. Tappi Journal. 45(5):364(1962).

37. Miles, K.B.; May, W.D.; Karnis, A. Refining Intensity, Energy Consumption, and Pulp Quality in Two-Stage Chip Refining. TAPPI Journal. 74(3):221(1991).

38. Stone, J.E.; Scallan, A.M.; Abrahamson, B. Influence of beating on cell wall swelling and internal fibrillation. Svensk Papperstidning. 71(12):687(1968).

39. Attalla, R.H.; Wahren, D. On the energy requirement in refining. Tappi Journal. 63(6):121(1980).

40. Nissan, A.H. Lectures on Fibre Science in Paper. Joint Textbook Committee of the Paper Industry. (1977).

41. Salmen, L.; Tigerstrom, A.; Fellers, C. Fatigue of wood - characterization of mechanical defibration. Journal of Pulp and Paper Science. 11(5):J68(1985).

42. Salmen, N.L.; Fellers, C. The fundamentals of energy consumption during viscoelastic and plastic deformation of wood. TAPPI Transactions. (12):TR93(1982).

43. Salmen, L. The effect of the frequency of a mechanical deformation on the fatigue of wood. 1985 International Mechanical Pulping Conference. p. 146.

44. Tam Doo, P.A.; Kerekes, R.J. The Effect of Beating and Low-Amplitude Flexing on Pulp Fibre Flexibility. Journal of Pulp and Paper Science. 15(1):J36(1989).

45. Goring, D.A.I. Thermal softening of lignin, hemicellulose and cellulose. Pulp and Paper Magazine of Canada. 64(12):T517(1963).

46. Hoglund, H.; Sohlin, U. The effect of physical properties of the wood on chip refining. 1975 International Mechanical Pulping Conference Proceedings. 47.

47. de Montmorency, W.H. The relationship of wood characteristics to mechanical pulping. Pulp and Paper Magazine of Canada. 66(6):T325(1965).

48. Corson, S.R. Thermomechanical and refiner mechanical pulps of New Zealand grown Radiata pine. 1983 International Mechanical Pulping Conference. p. 1.

49. Corson, S.R. Wood characteristics influence pine TMP quality. Tappi Journal. (11):135(1991).

50. Wynne-Roberts, R.I. Grinding characteristics of various woods. Technical Association Papers, Series XX. 258(1937).

51. Corson, S.R. Fibre and fines fractions influence strength of TMP. Pulp & Paper Canada. 81(5):T108(1980).

52. Uhmeier, A. Some Aspects on Solid and Fluid Mechanics of Wood in Relation to Mechanical Pulping. Doctors Thesis, Royal Institute of Technology.

53. Felder, R.M.; Rousseau, R.W. Elementary Principles of Chemical Processes. John Wiley & Sons. (1986).

54. Law, K.N.; Valade, J.L.; Yang, K.C. Fibre Development in Thermomechanical Pulping: Comparison Between Black Spruce and Jack Pine. Journal of Pulp and Paper Science. 24(2):73(1998).

55. Alahautala, T.; Vattulainen, J.; Hernberg, R. Visualization of Pulp Refining in a Rotating Disk Refiner. File:///E|/DOCUMENT/TOPIC/709/709.000_htm.

56. Unholtz-Dickie Corporation. Vibration and Vibration Testing.

57. Jordan, B.L.; Nguyen, N.G. Curvature, Kink and Curl. Paperi ja Puu. (4):313(1986).

58. Hearle, J.W.S. Polymers and Their Properties – Vol. 1: Fundamentals of Structure and Mechanics. John Wiley & Sons. (1982).

59. Horn, R.A.; Coens, C.L. Rapid Determination of the Number of Fibers per Gram of Pulp. TAPPI Journal. 53(11):2120(1970).

60. Trepanier, R.J. The Infrared Emissivity of Wet Webs. Journal of Pulp and Paper Science. (11):J166(1984).

61. Hull, D. An Introduction to Composite Materials. Cambridge University Press. 1981.

62. Koran, Z. Tensile properties of spruce under different conditions. Wood and Fiber. 11(1):38(1979).

63. Koran, Z. Electron microscopy of radial tracheid surfaces of black spruce separated by tensile failure at various temperatures. Tappi Journal. 50(2):60(1967).

64. Irvine, G.M. The significance of the glass transition of lignin in thermomechanical pulping. Wood Science and Technology. 19:139(1985).

65. Atack, D.; May, D.; Morris, E.L.; Sproule, R.N. The energy of tensile and cleavage fracture of black spruce. TAPPI Journal. 44(8):555(1961).

66. Kolseth, P.; De Ruvo, A. The measurement of viscoelastic behavior for the characterization of time-, temperature-, and humidity-dependent properties. Handbook of Physical and Mechanical Testing of Paper and Paperboard —Vol. 1. Marcel Dekker, Inc. Mark, R.E. – ed. (1983).

67. Steadman, R.; Lunar, P. The effect of wet fibre flexibility of sheet apparent density. Papermaking Raw Materials – Vol. 1. Mechanical Engineering Publications Limited. Punton, V. – ed. (1985).

68. Young, R.J.; Lovell, P.A. Introduction to Polymers. Chapman & Hall. (1991).

69. Ferry, J.D. Viscoelastic Properties of Polymers. John Wiley & Sons, Inc. (1980).

70. Jones, R.M. Mechanics of Composite Materials. McGraw-Hill Book Company. (1975).

71. Mark, R.E. Cell Wall Mechanics of Tracheids. Yale University Press. (1967).

72. Rudie, A.W. Personal correspondence, 1996.

73. Smook, G.A. Handbook for Pulp and Paper Technologists. Joint Textbook Committee of the Paper Industry. (1982).

APPENDIX 1: FIBER DIMENSIONS OF THE SELECTED FRACTION FOR TESTING

Fiber Width (FW) and Lumen Diameter (ID)
Project A-490
Sampler: Cheryl Rueckert
Sample ID: EW

	FW	ID		FW	ID		FW	ID		FW	ID
1	35.68	16.65	26	26.19	17.86	51	40.41	32.09	76	46.45	39.32
2	45.14	34.46	27	55.81	46.31	52	27.36	17.84	77	28.47	21.36
3	32.04	24.92	28	16.66	5.96	53	34.50	11.89	78	14.27	8.33
4	41.53	30.85	29	33.27	23.77	54	41.55	34.43	79	34.41	13.05
5	40.49	30.97	30	29.74	21.42	55	47.50	38.00	80	30.88	23.75
6	34.45	21.38	31	38.11	29.76	56	35.65	26.14	81	33.23	24.93
7	49.95	40.44	32	36.80	27.30	57	27.36	3.56	82	42.74	30.87
8	41.60	29.73	33	17.79	10.67	58	43.98	34.47	83	28.49	20.20
9	30.90	22.58	34	38.12	19.06	59	41.62	29.73	84	38.00	28.51
10	36.87	29.72	35	32.10	17.84	60	33.23	20.17	85	34.49	23.78
11	23.75	15.44	36	52.18	41.53	61	52.38	21.43	86	32.12	27.36
12	13.06	8.32	37	35.67	24.97	62	47.55	38.04	87	22.62	10.72
13	30.89	19.02	38	37.97	24.91	63	59.48	42.82	88	10.67	7.11
14	24.96	11.89	39	39.22	32.09	64	59.38	43.94	89	30.97	25.01
15	27.32	16.63	40	33.33	26.19	65	32.05	27.31	90	13.05	4.75
16	30.87	22.57	41	35.61	14.25	66	39.26	32.14	91	38.04	29.72
17	35.62	26.11	42	27.29	9.49	67	34.48	26.15	92	35.59	29.65
18	23.74	15.42	43	33.25	26.13	68	41.65	32.14	93	41.58	33.26
19	14.24	2.37	44	47.55	38.03	69	25.01	16.67	94	49.86	43.93
20	20.22	7.13	45	36.87	19.02	70	60.57	51.07	95	36.84	27.34
21	35.62	26.12	46	20.19	11.87	71	45.14	30.88	96	39.23	32.10
22	38.01	29.69	47	48.77	41.64	72	42.78	33.27	97	43.91	34.41
23	45.21	36.88	48	26.15	11.89	73	44.03	36.90	98	41.55	30.86
24	28.53	14.27	49	21.40	8.32	74	33.22	26.10	99	21.37	11.87
25	42.82	35.67	50	46.37	21.40	75	35.60	27.29	100	14.24	7.12

Arithmetic average fiber width (W)	=	35.19 microns
Arithmetic average lumen diameter (L)	=	24.65 microns
Arithmetic average cell wall thickness	=	5.27 microns
Runkel ratio (W-L)/Average lumen width	=	0.43 microns
Perimeter (2xW) + (4x(W-L)/2)	=	91.46 microns
Standard Deviation (fiber width)	=	10.507 microns
Standard Deviation (lumen width)	=	10.667 microns

Fiber Width (FW) and Lumen Diameter (ID)
Project A-490
Sampler: Cheryl Rueckert
Sample ID: LW

	FW	ID		FW	ID		FW	ID		FW	ID
1	27.36	8.32	26	34.50	16.66	51	17.82	3.57	76	22.59	4.76
2	23.75	5.95	27	27.28	13.04	52	33.21	16.61	77	23.80	3.57
3	23.77	5.94	28	35.69	21.40	53	33.22	7.11	78	30.87	8.31
4	27.35	9.51	29	26.13	8.30	54	28.57	13.09	79	29.70	14.25
5	26.13	8.32	30	36.89	23.81	55	32.04	8.31	80	29.72	5.94
6	34.50	13.09	31	22.55	4.75	56	28.51	15.44	81	27.28	8.29
7	28.48	9.49	32	29.76	9.53	57	29.67	16.61	82	33.33	10.72
8	30.90	9.51	33	15.47	4.75	58	35.60	18.99	83	27.29	8.31
9	21.41	4.76	34	29.72	17.84	59	26.17	4.76	84	29.70	8.30
10	35.68	10.70	35	30.90	14.25	60	37.98	17.81	85	41.54	19.00
11	36.78	27.30	36	27.35	9.52	61	30.94	14.28	86	29.71	13.07
12	26.13	9.51	37	51.09	41.58	62	28.54	9.52	87	29.79	11.91
13	42.71	33.22	38	26.16	4.75	63	33.29	14.26	88	26.19	7.15
14	27.34	11.89	39	29.66	18.98	64	32.07	15.44	89	27.33	7.14
15	20.19	8.31	40	20.20	4.75	65	30.90	11.88	90	24.95	5.94
16	24.91	7.12	41	11.92	2.38	66	21.36	7.11	91	27.33	9.51
17	34.45	15.44	42	28.52	17.83	67	26.14	9.50	92	28.55	9.52
18	26.18	8.32	43	29.69	14.25	68	23.77	13.08	93	27.32	5.94
19	22.54	9.49	44	26.15	3.57	69	26.14	13.08	94	23.76	7.12
20	26.16	7.12	45	32.16	10.72	70	19.01	7.13	95	27.31	11.87
21	29.68	5.93	46	29.68	17.81	71	19.06	4.77	96	27.32	3.57
22	25.01	9.53	47	33.37	9.53	72	32.07	15.44	97	34.47	14.26
23	13.06	2.37	48	30.85	11.87	73	34.46	13.07	98	23.76	3.56
24	22.58	8.32	49	22.62	8.34	74	18.99	4.75	99	34.42	10.68
25	36.83	23.77	50	27.34	4.75	75	27.31	8.31	100	23.77	4.76

Arithmetic average fiber width (W)	=	28.28 microns
Arithmetic average lumen diameter (L)	=	10.90 microns
Arithmetic average cell wall thickness	=	8.69 microns
Runkel ratio (W-L)/Average lumen width	=	1.60 microns
Perimeter (2xW) + (4x(W-L)/2)	=	91.34 microns
Standard Deviation (fiber width)	=	5.9303 microns
Standard Deviation (lumen width)	=	6.347 microns

APPENDIX 2: ASSORTED IMAGES

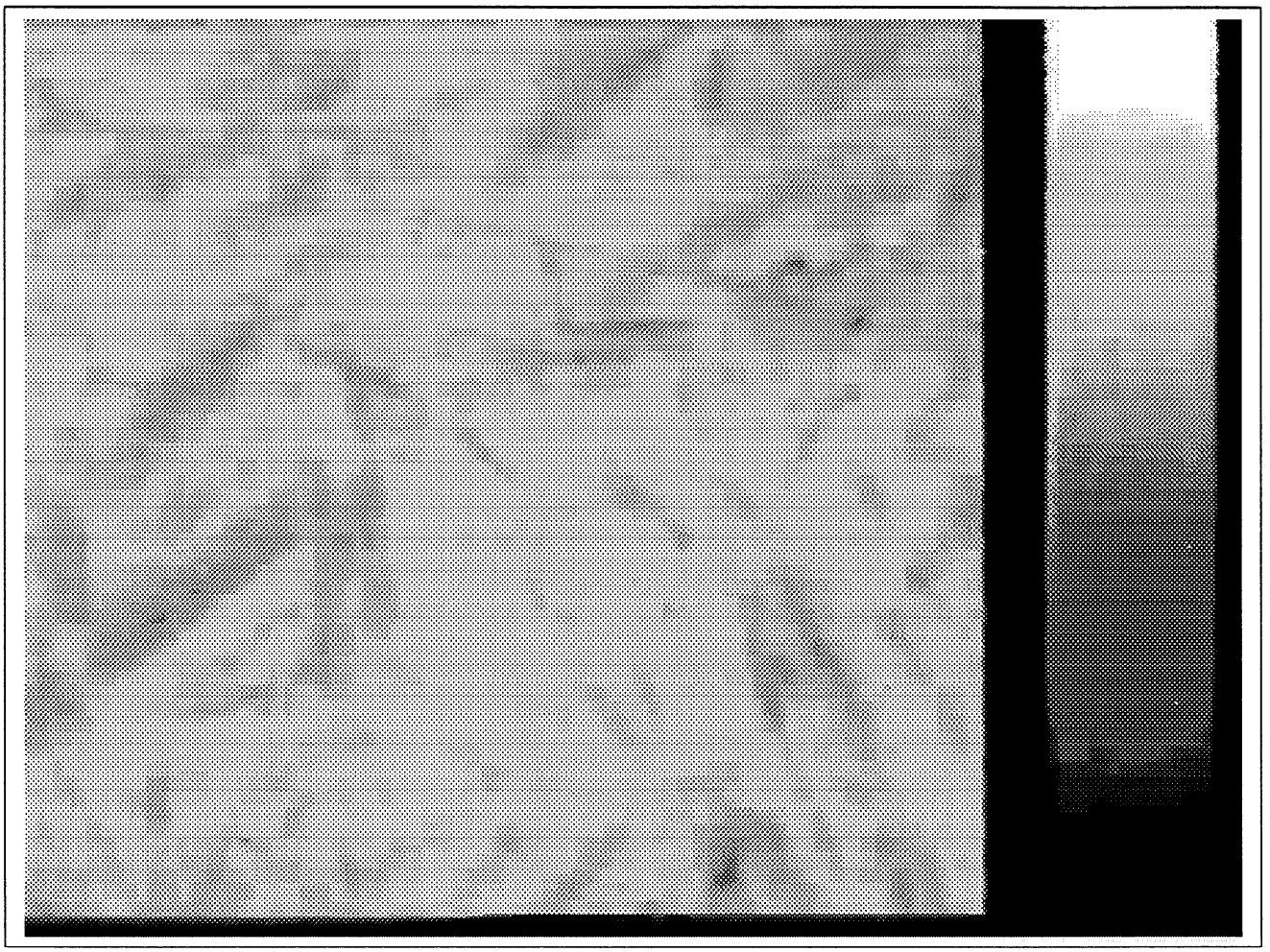

Figure 50. Compressed fiber aggregate within the sample chamber

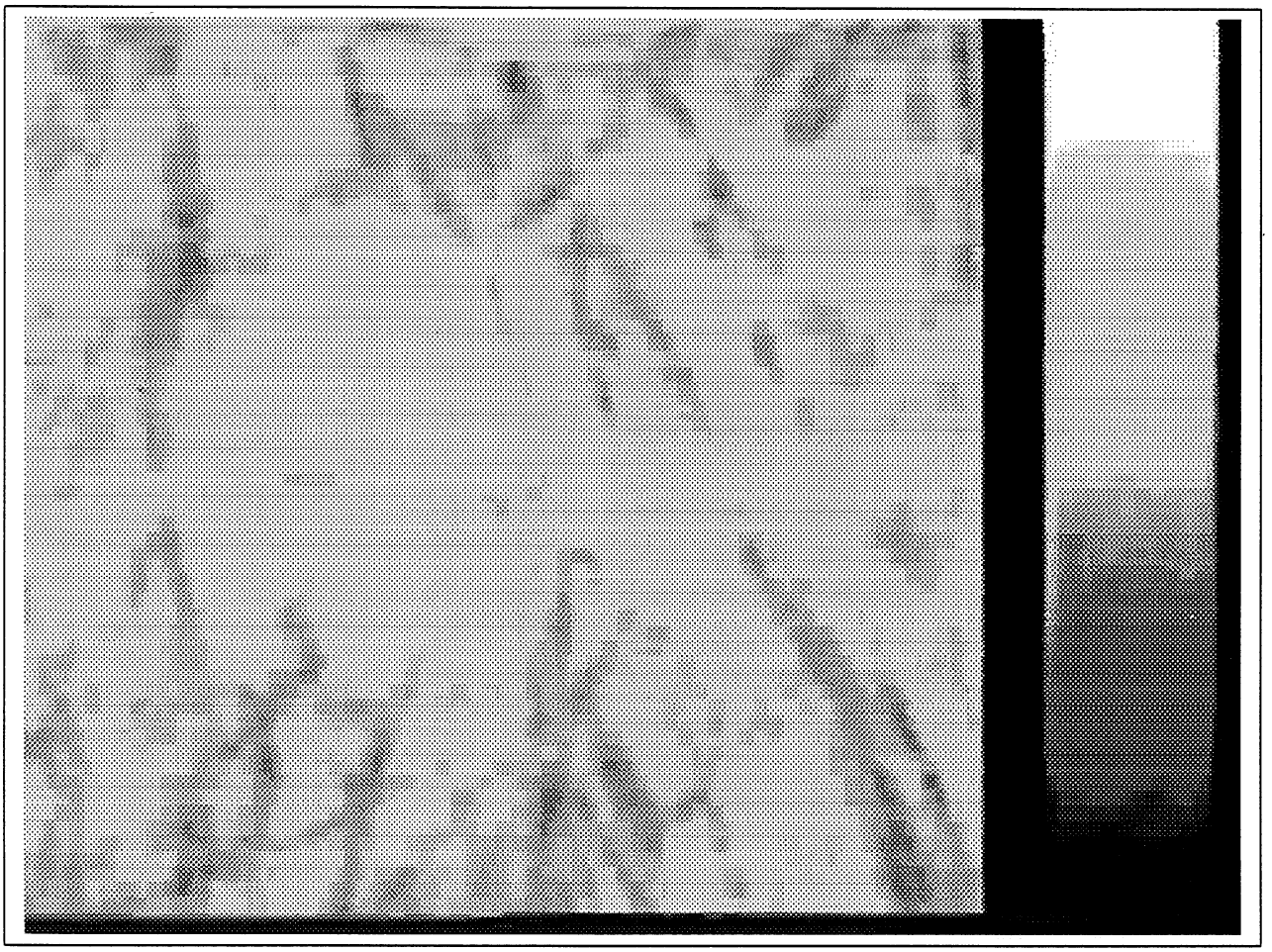

Figure 51. Uncompressed fiber aggregate within the sample chamber.

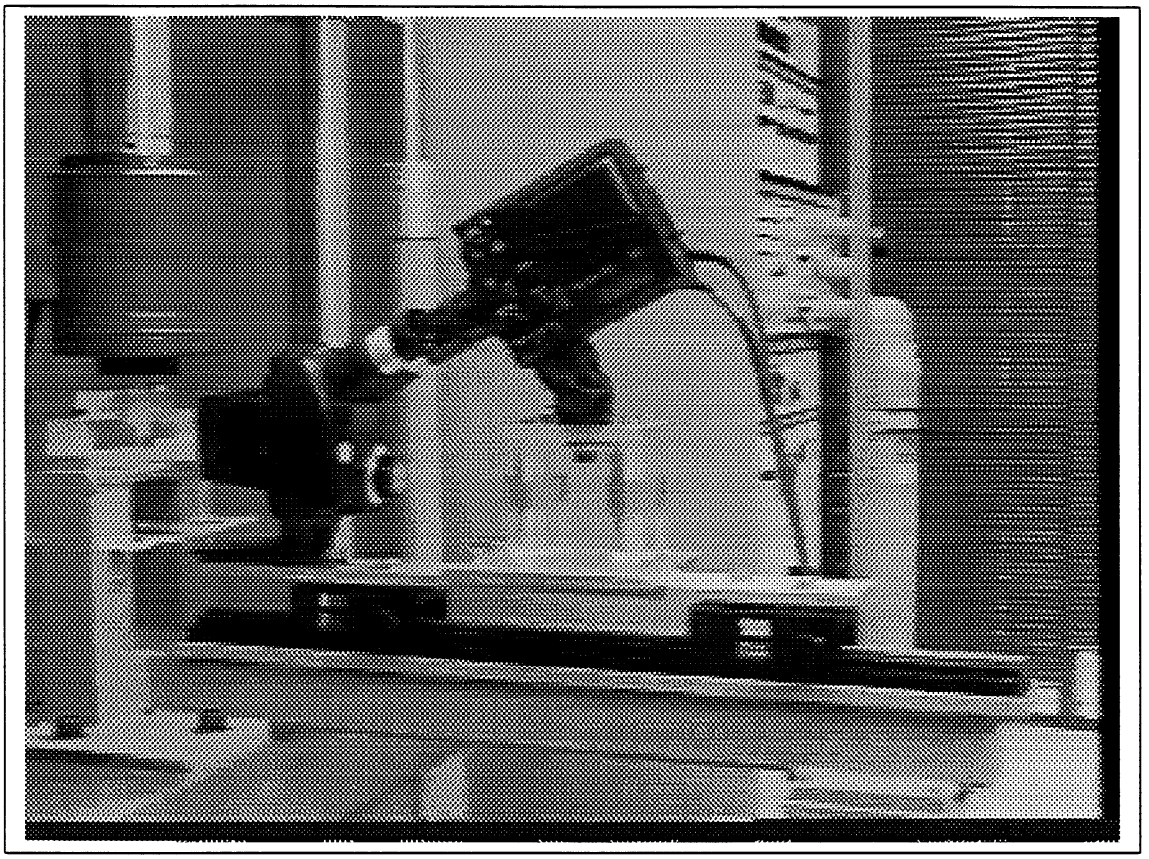

Figure 52. Image of experimental apparatus showing the camera (top), camera mount, microscope (center) and sample holder (left). The MTS control panel is in the background.

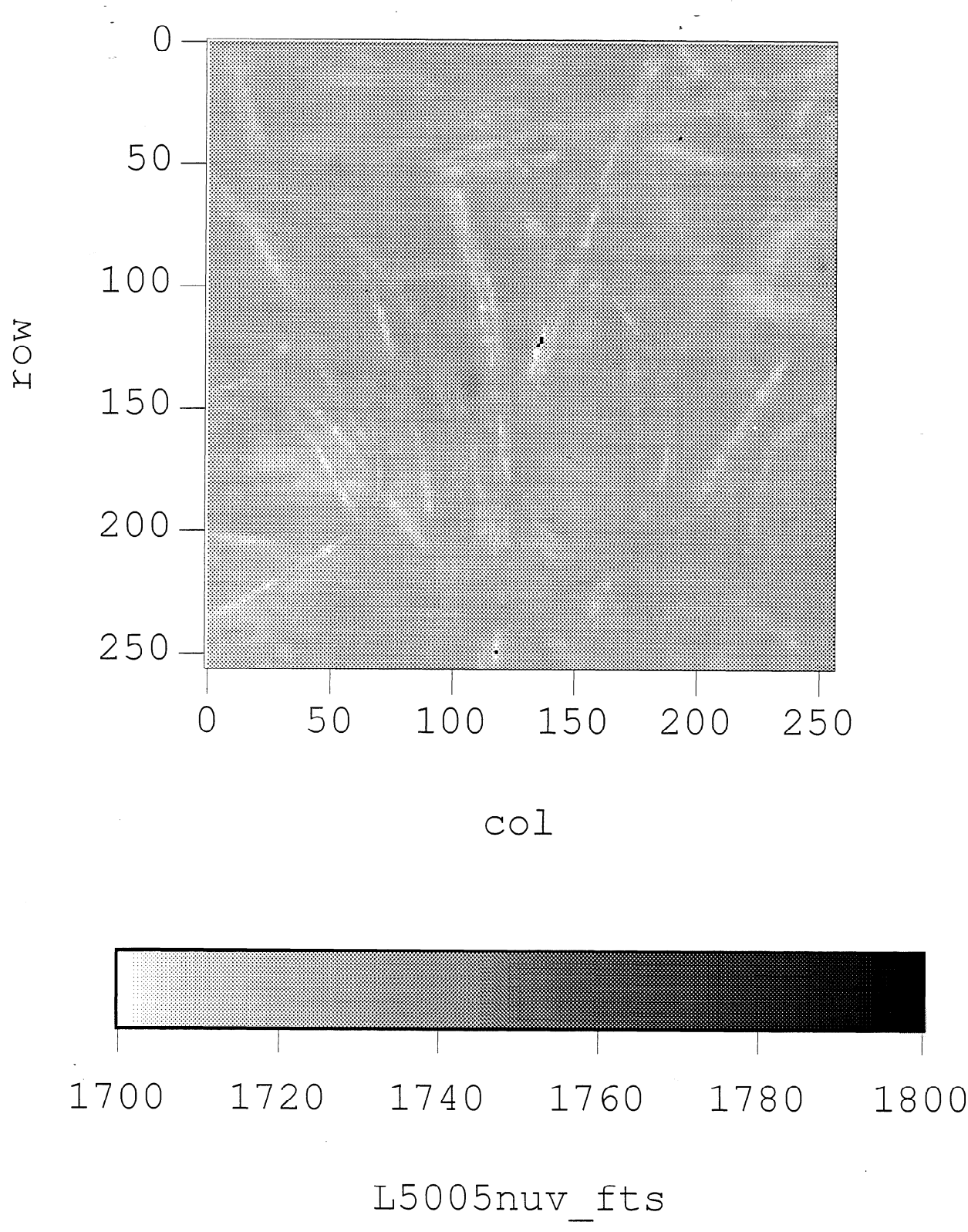

Figure 53. Infrared image of fibers prior to exposure to ultraviolet light to identify stained fibers.

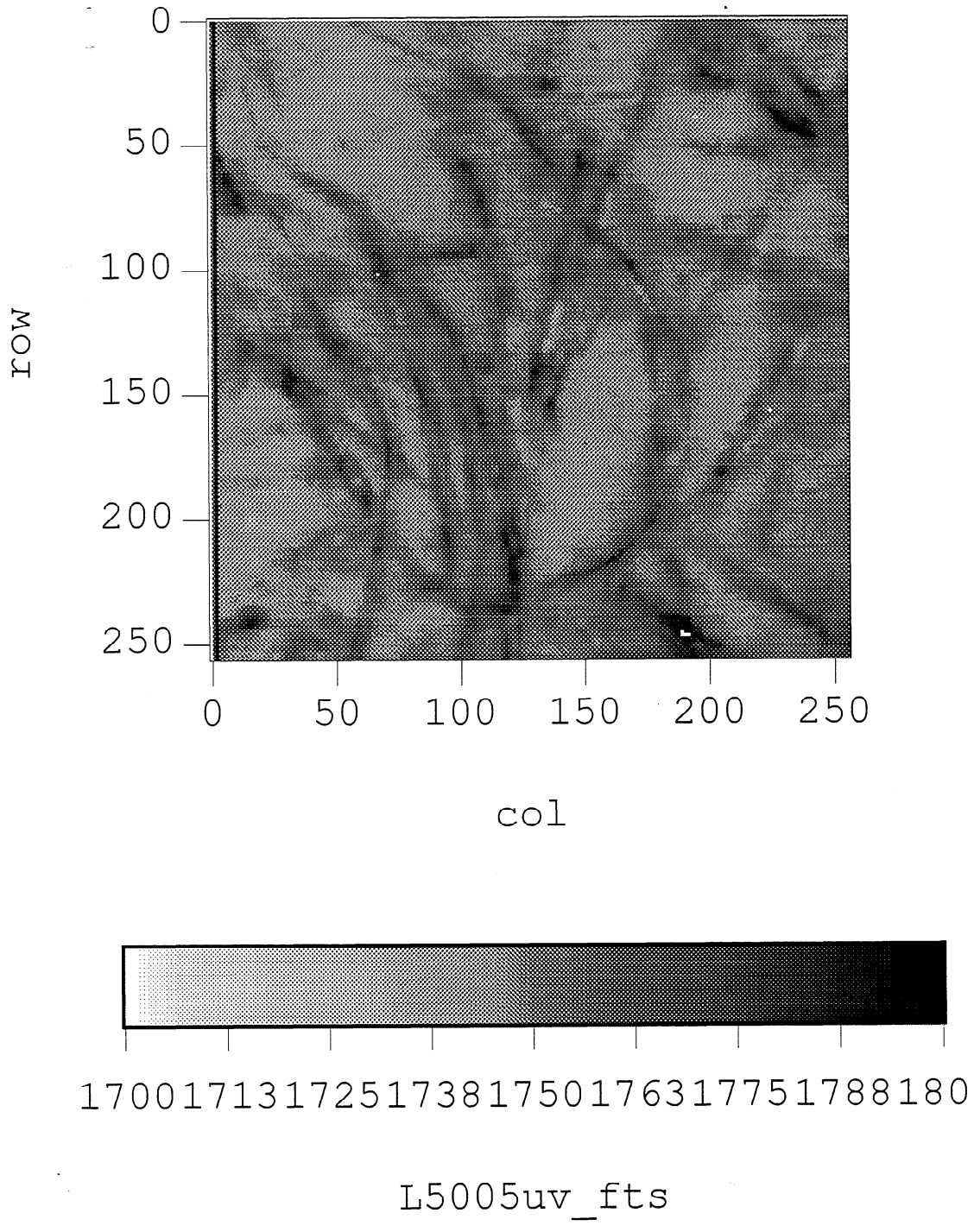

Figure 54. Infrared image of fibers after exposure to UV light to identify stained fibers.

APPENDIX 3: SHAKER DESIGN DRAWINGS

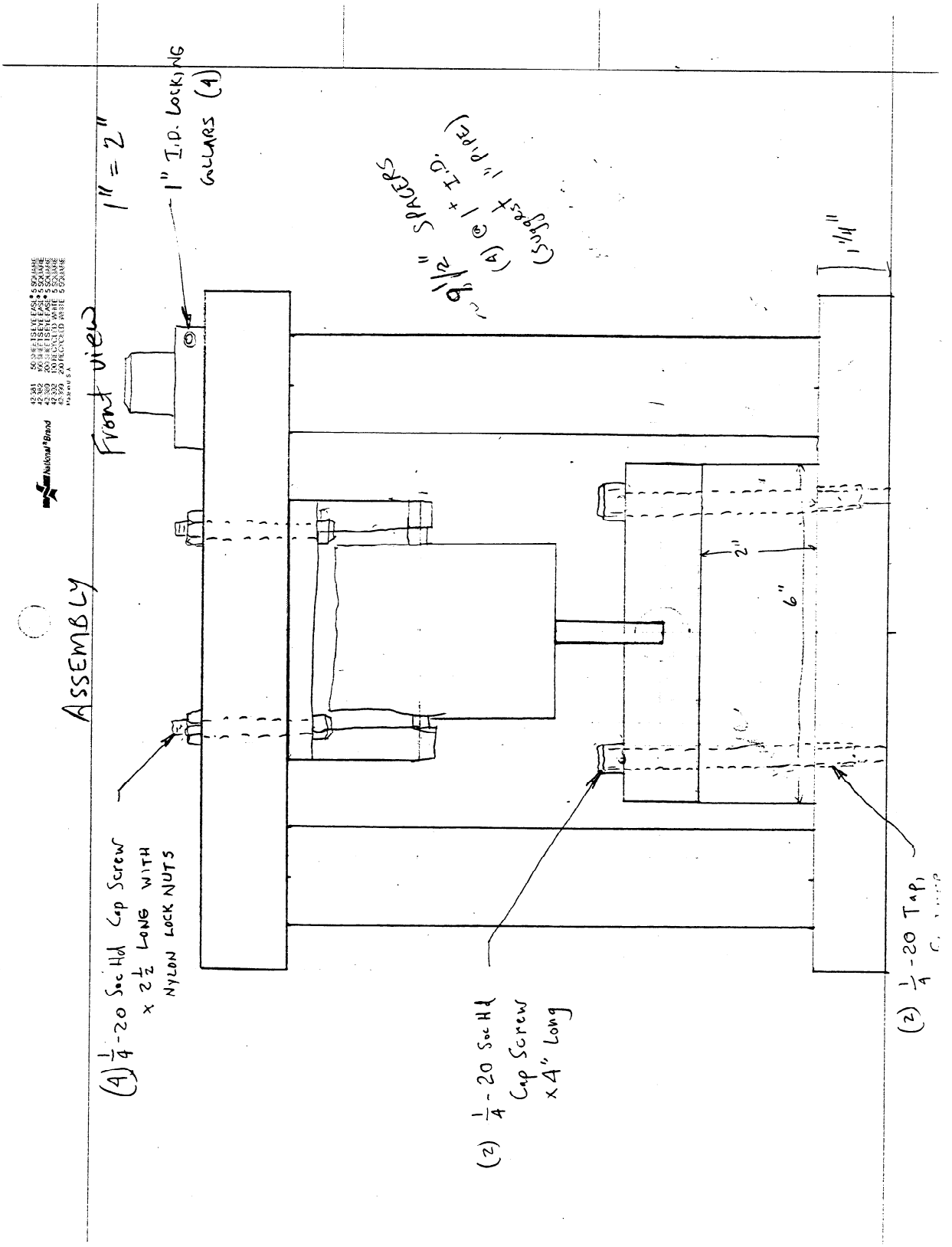

top plate

1" = 2"

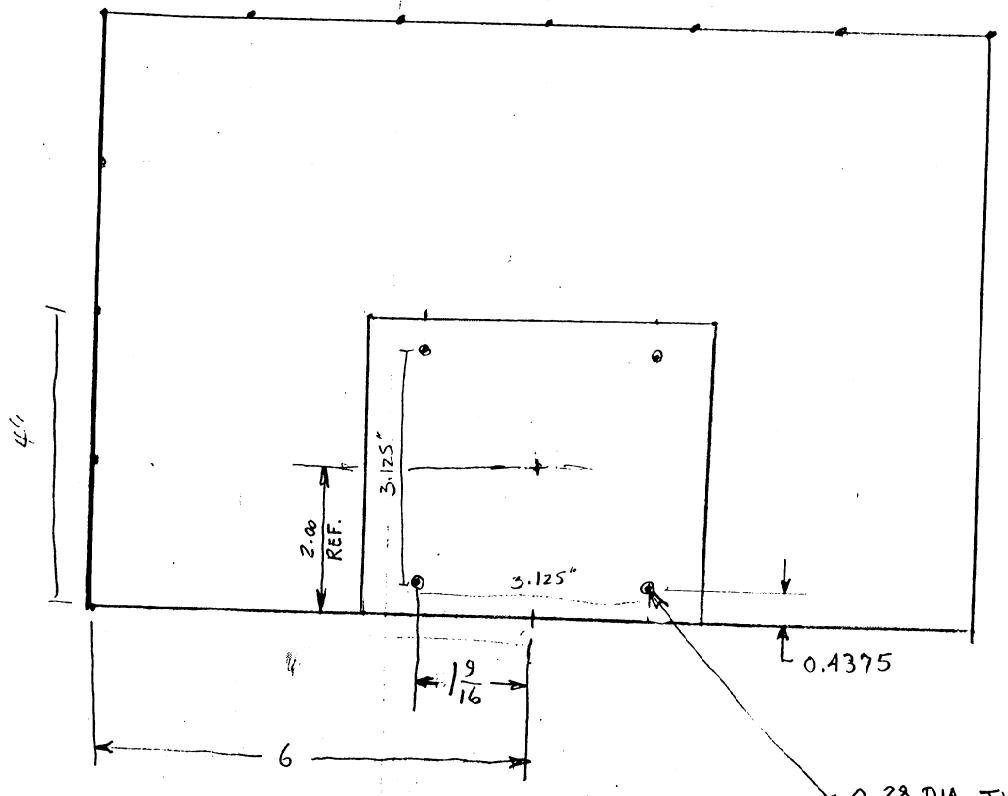

the 4 holes in the trunnion are 7mm (0.28") in diameter

bottom plate

1"=2"

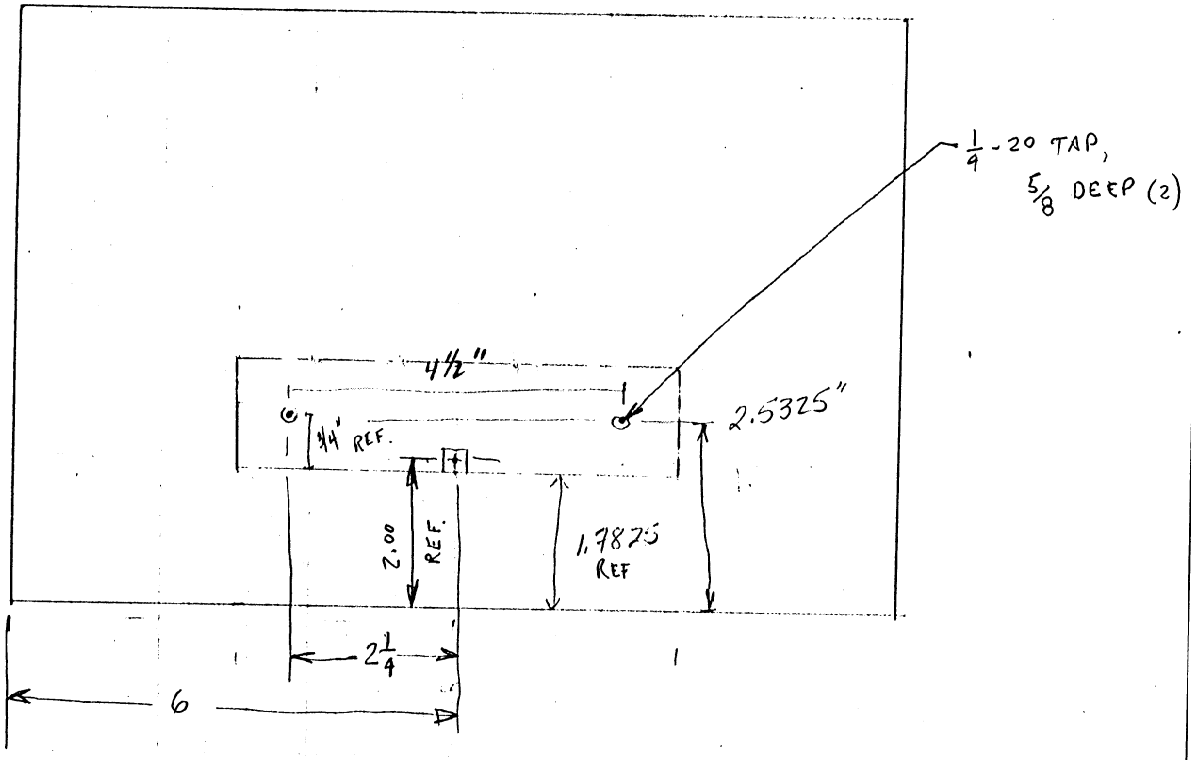

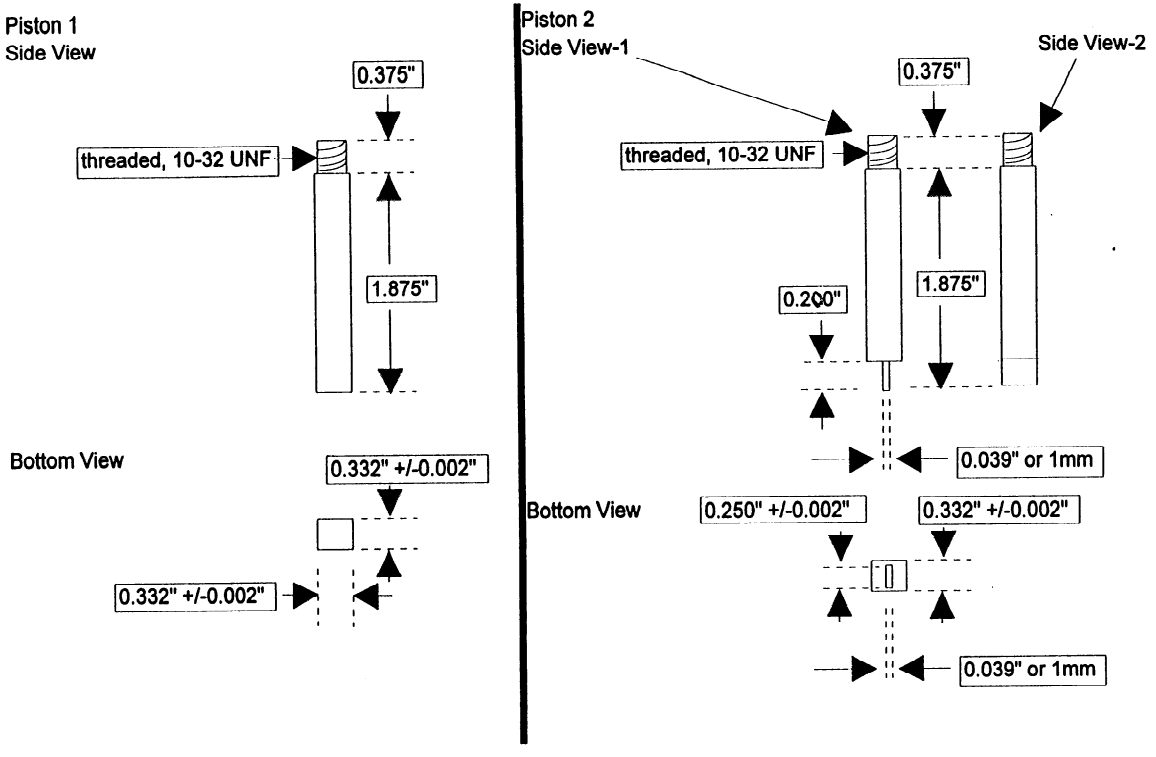
Piston 1
Side View
0.375"
threaded, 10-32 UNF
1.875"
Bottom View
0.332" +/-0.002"
0.332" +/-0.002"
Piston 2
Side View-1
Side View-2
0.375"
threaded, 10-32 UNF
0.200"
1.875"
0.039" or 1mm
Bottom View
0.250" +/-0.002"
0.332" +/-0.002"
0.039" or 1mm

"Tooth-pick" Holder
Front View

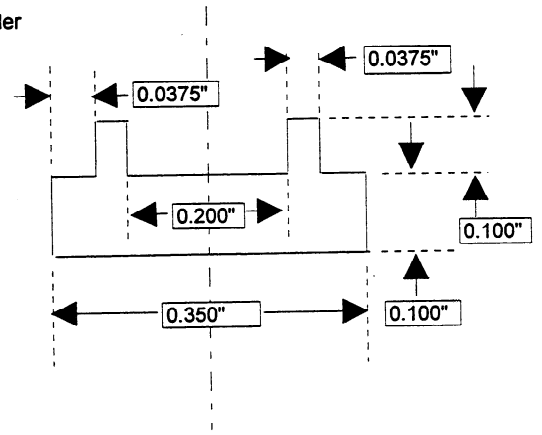

Bottom View

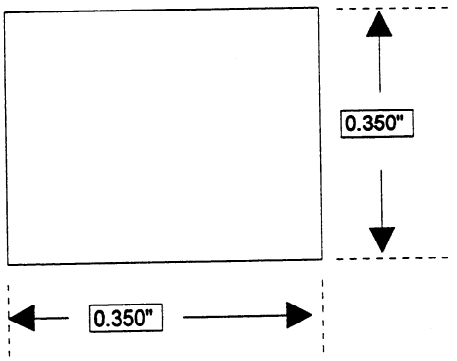

Side View

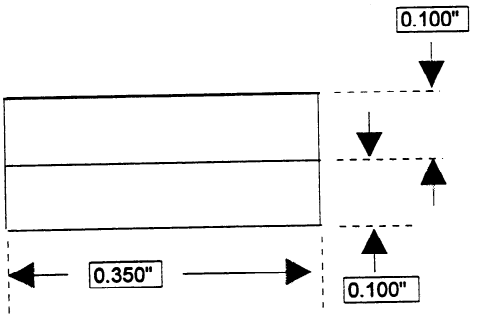

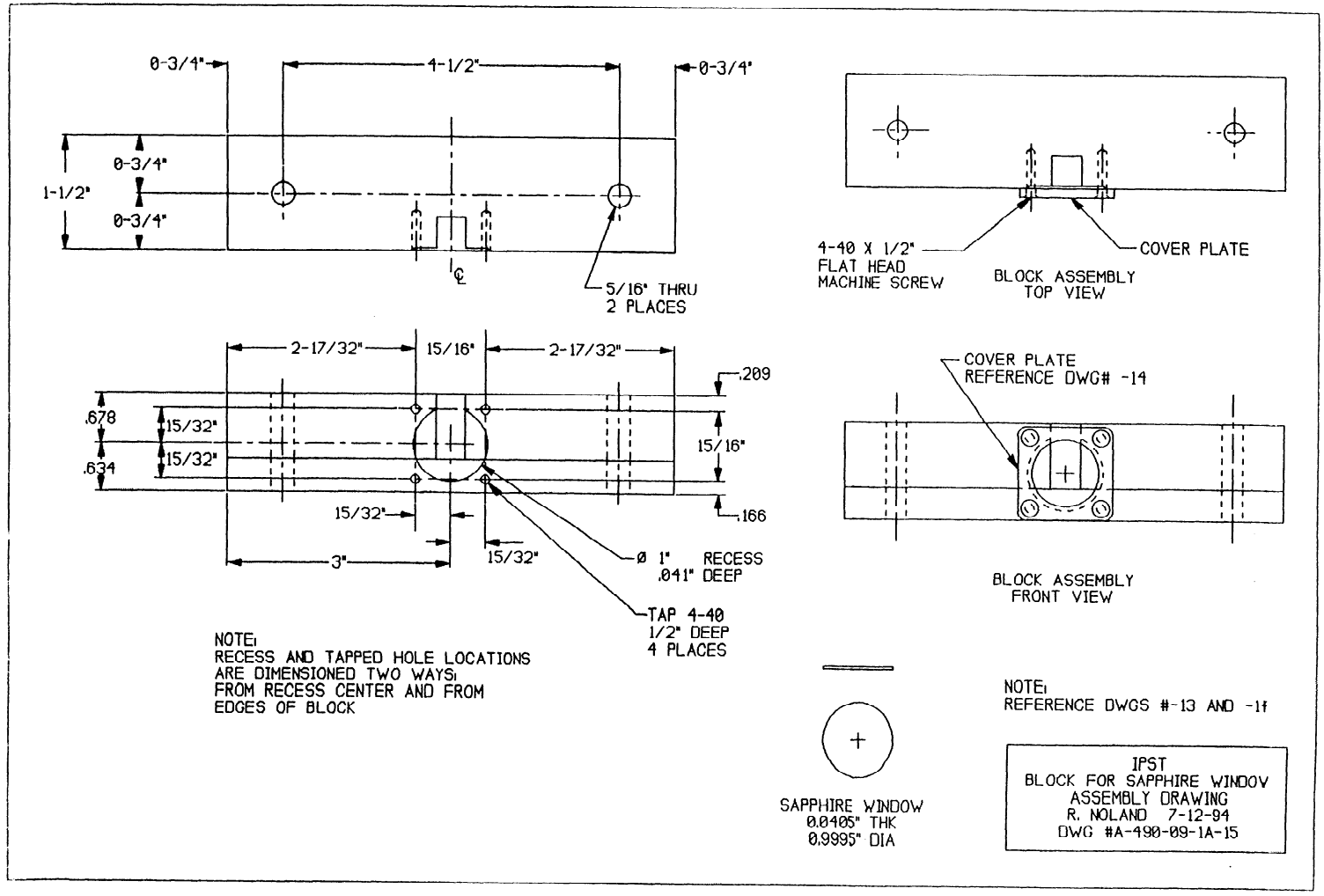
0-3/4"
4-1/2"
0-3/4"
1-1/2"
0-3/4"
0-3/4"
℄
5/16" THRU
2 PLACES
2-17/32"
15/16"
2-17/32"
.209
.678
15/32"
.634
15/32"
15/16"
.166
15/32"
3"
15/32"
Ø 1" RECESS
.041" DEEP
TAP 4-40
1/2" DEEP
4 PLACES
NOTE:
RECESS AND TAPPED HOLE LOCATIONS
ARE DIMENSIONED TWO WAYS:
FROM RECESS CENTER AND FROM
EDGES OF BLOCK
4-40 X 1/2"
FLAT HEAD
MACHINE SCREW
COVER PLATE
BLOCK ASSEMBLY
TOP VIEW
COVER PLATE
REFERENCE DWG# -14
BLOCK ASSEMBLY
FRONT VIEW
SAPPHIRE WINDOW
0.0405" THK
0.9995" DIA
NOTE:
REFERENCE DWGS #-13 AND -14
IPST
BLOCK FOR SAPPHIRE WINDOW
ASSEMBLY DRAWING
R. NOLAND 7-12-94
DWG #A-490-09-1A-15

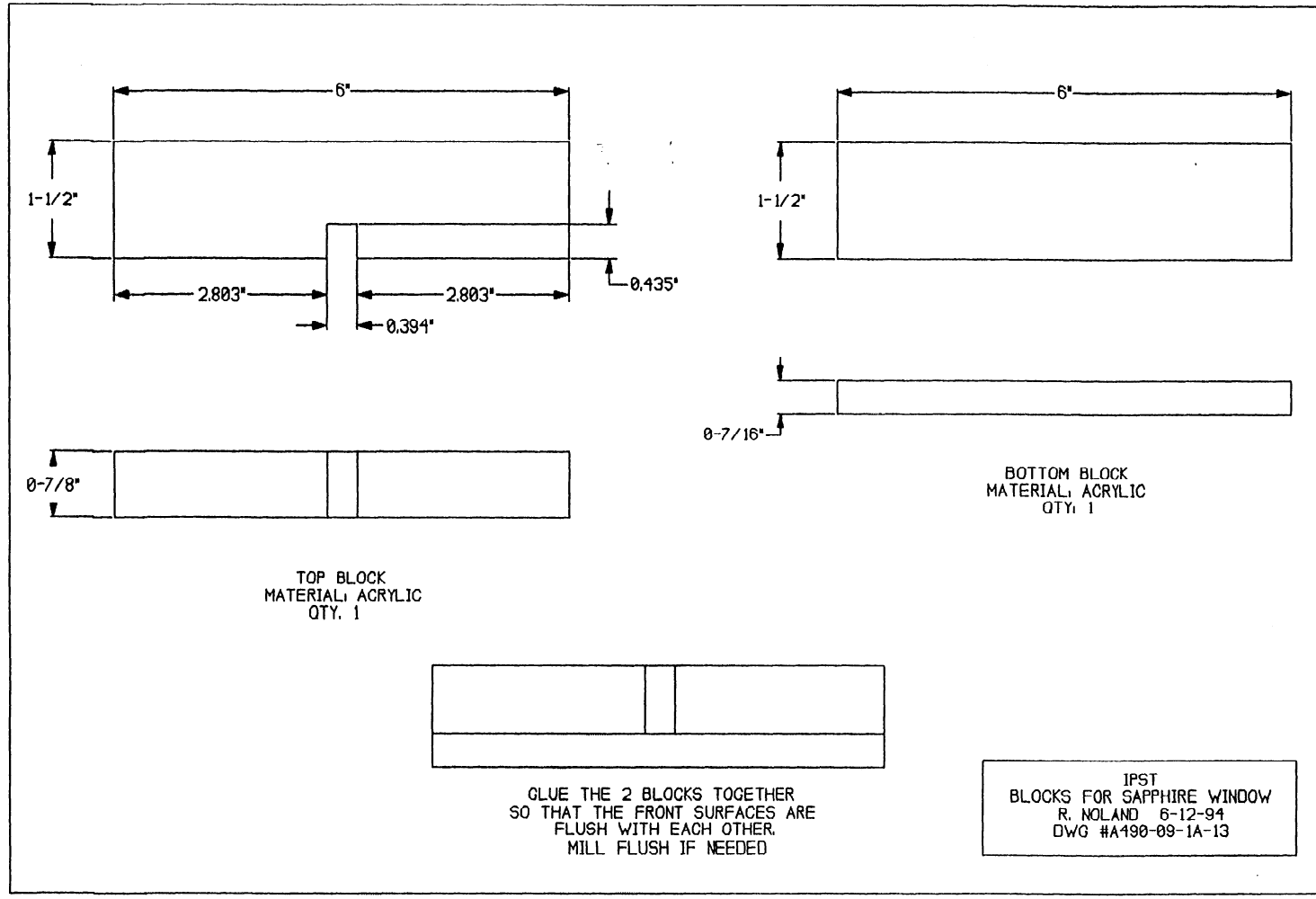
6"
1-1/2"
2.803"
2.803"
0.435"
0.394"
0-7/8"
TOP BLOCK
MATERIAL: ACRYLIC
QTY. 1
6"
1-1/2"
0-7/16"
BOTTOM BLOCK
MATERIAL: ACRYLIC
QTY: 1
GLUE THE 2 BLOCKS TOGETHER
SO THAT THE FRONT SURFACES ARE
FLUSH WITH EACH OTHER.
MILL FLUSH IF NEEDED
IPST
BLOCKS FOR SAPPHIRE WINDOW
R. NOLAND 6-12-94
DWG #A490-09-1A-13

APPENDIX 4: MTS ENGINEERING DRAWINGS

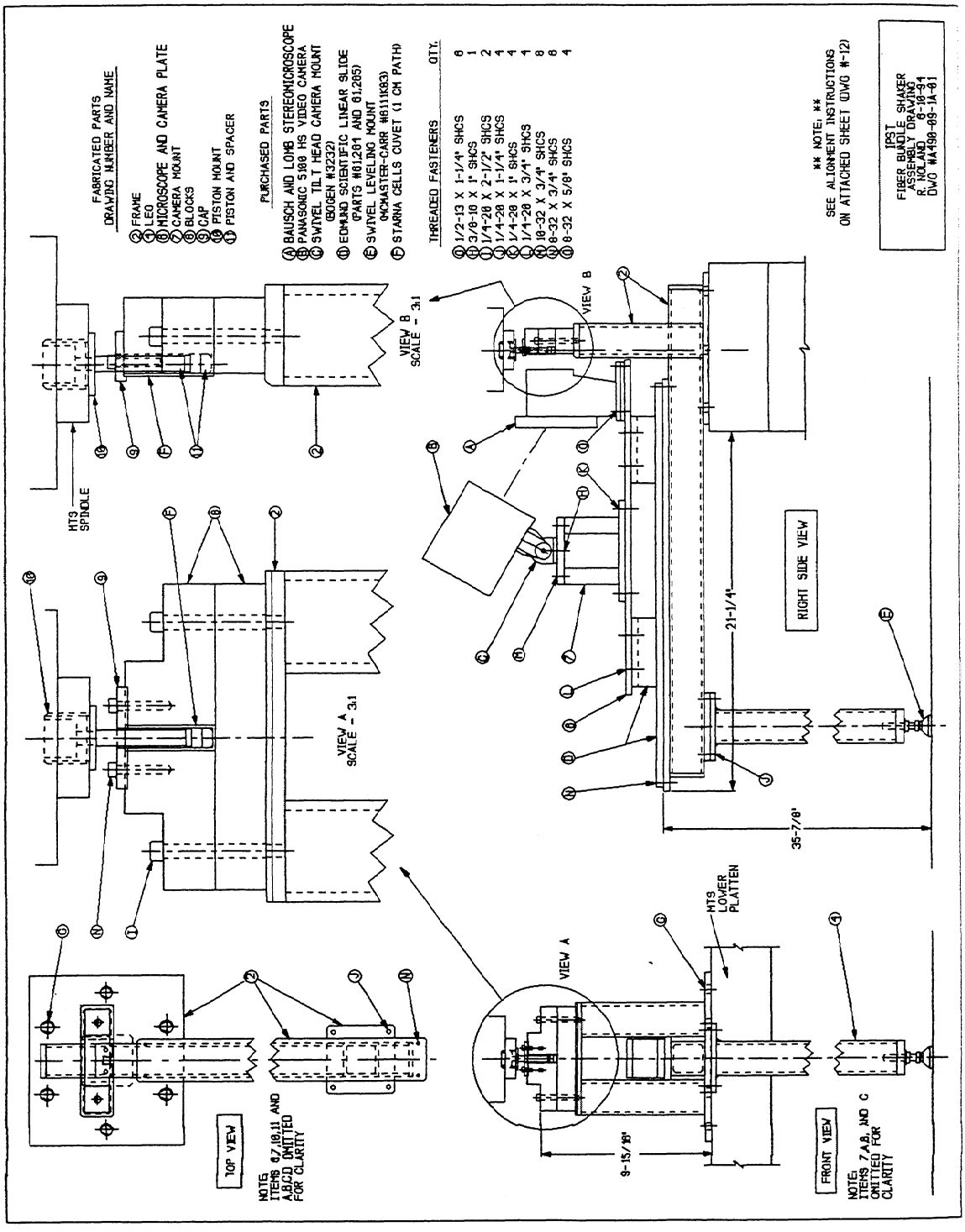

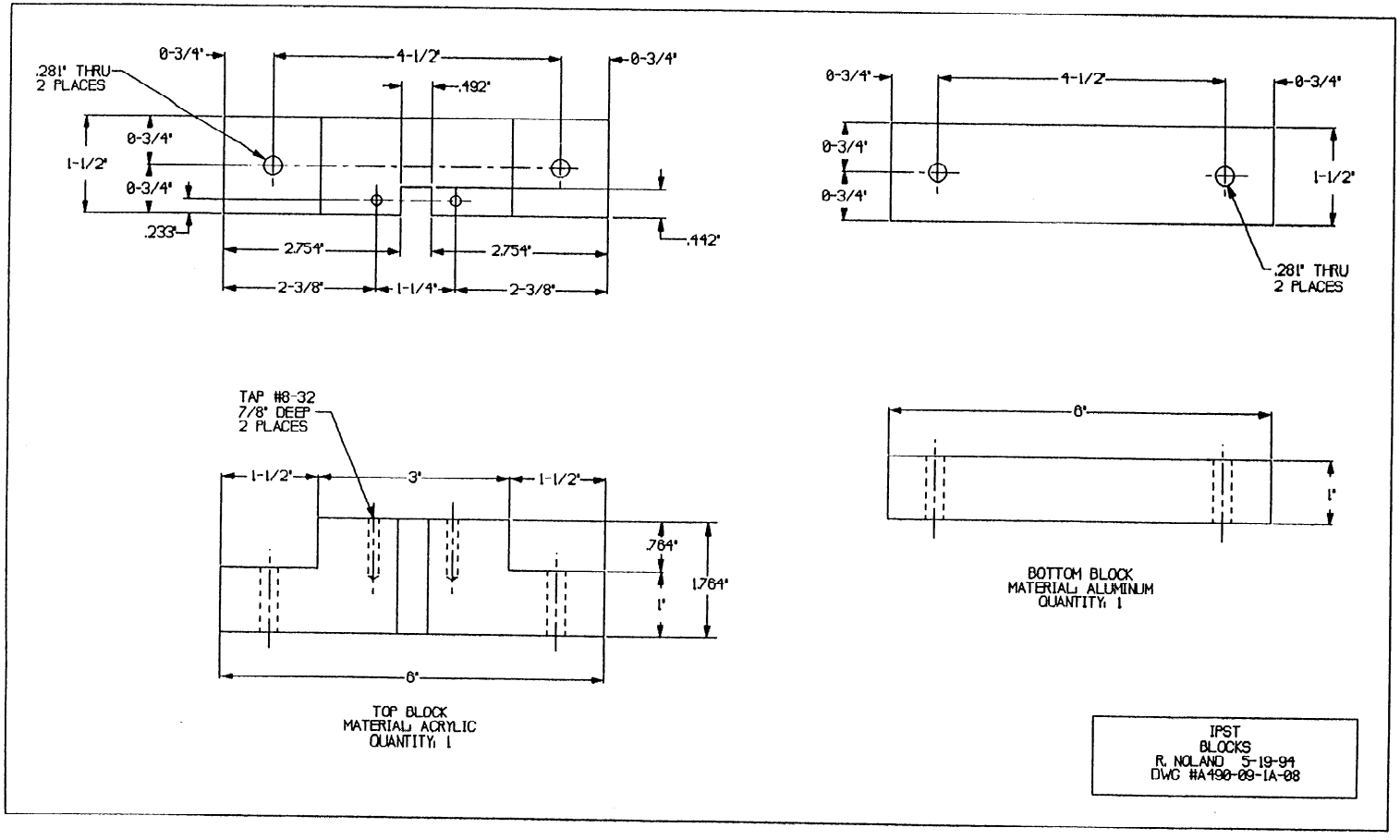
.281" THRU
2 PLACES
0-3/4"
4-1/2"
0-3/4"
.192"
0-3/4"
1-1/2"
0-3/4"
.233"
.442"
2.754"
2.754"
2-3/8"
1-1/4"
2-3/8"
0-3/4"
4-1/2"
0-3/4"
0-3/4"
0-3/4"
1-1/2"
.281" THRU
2 PLACES
TAP #8-32
7/8" DEEP
2 PLACES
1-1/2"
3"
1-1/2"
.764"
1"
1.764"
6"
TOP BLOCK
MATERIAL: ACRYLIC
QUANTITY: 1
6"
1"
BOTTOM BLOCK
MATERIAL: ALUMINUM
QUANTITY: 1
IPST
BLOCKS
R. NOLAND 5-19-94
DWG #A490-09-1A-08

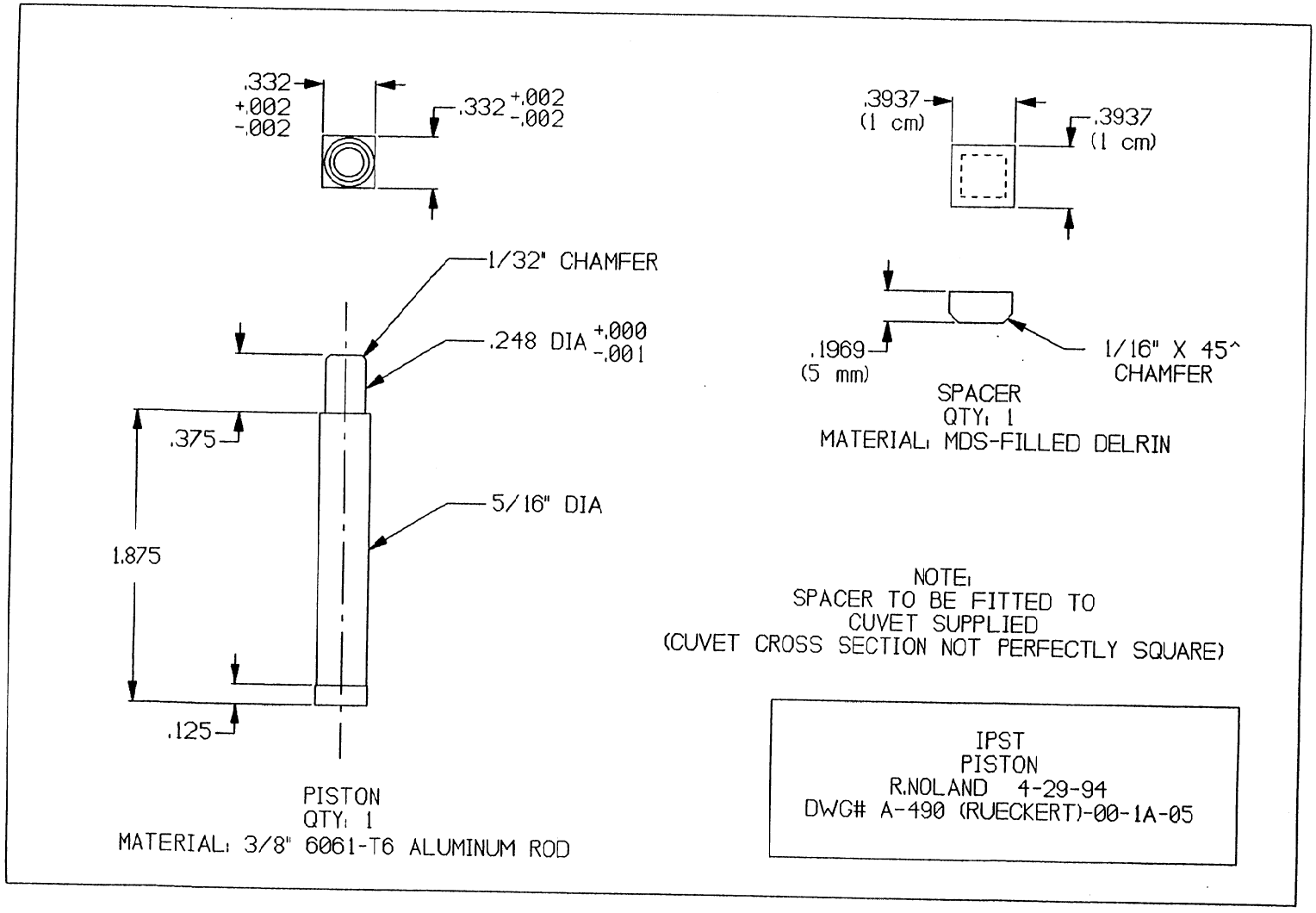
.332 +.002 -.002
.332 +.002 -.002
1/32" CHAMFER
.248 DIA +.000 -.001
.375
1.875
5/16" DIA
.125
PISTON
QTY: 1
MATERIAL: 3/8" 6061-T6 ALUMINUM ROD
.3937 (1 cm)
.3937 (1 cm)
.1969 (5 mm)
1/16" X 45^ CHAMFER
SPACER
QTY: 1
MATERIAL: MDS-FILLED DELRIN
NOTE:
SPACER TO BE FITTED TO CUVET SUPPLIED
(CUVET CROSS SECTION NOT PERFECTLY SQUARE)
IPST
PISTON
R.NOLAND 4-29-94
DWG# A-490 (RUECKERT)-00-1A-05

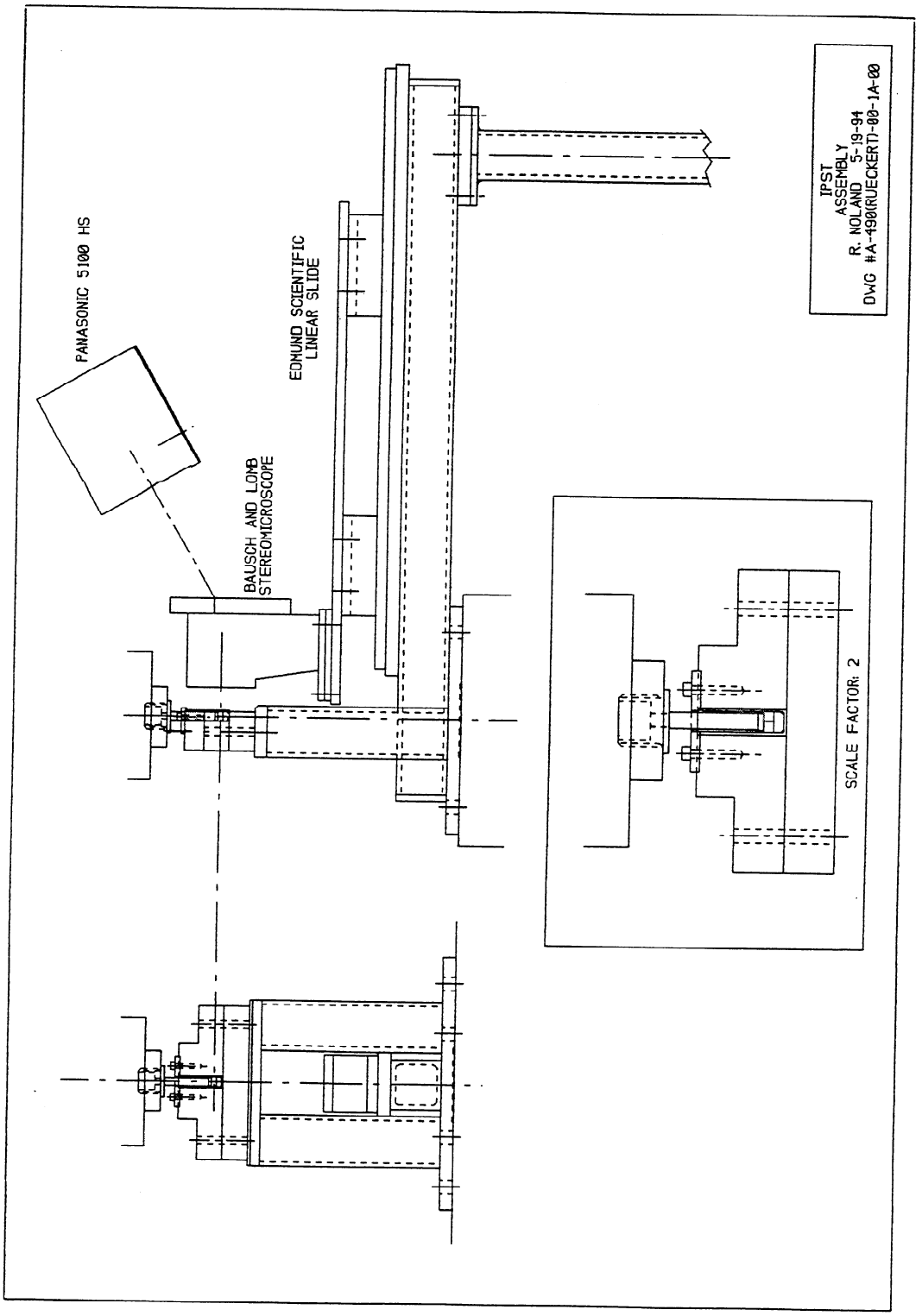
PANASONIC 5100 HS
BAUSCH AND LOMB
STEREOMICROSCOPE
EDMUND SCIENTIFIC
LINEAR SLIDE
IPST
ASSEMBLY
R. NOLAND 5-19-94
DWG #A-490(RUECKERT)-00-1A-00
SCALE FACTOR: 2

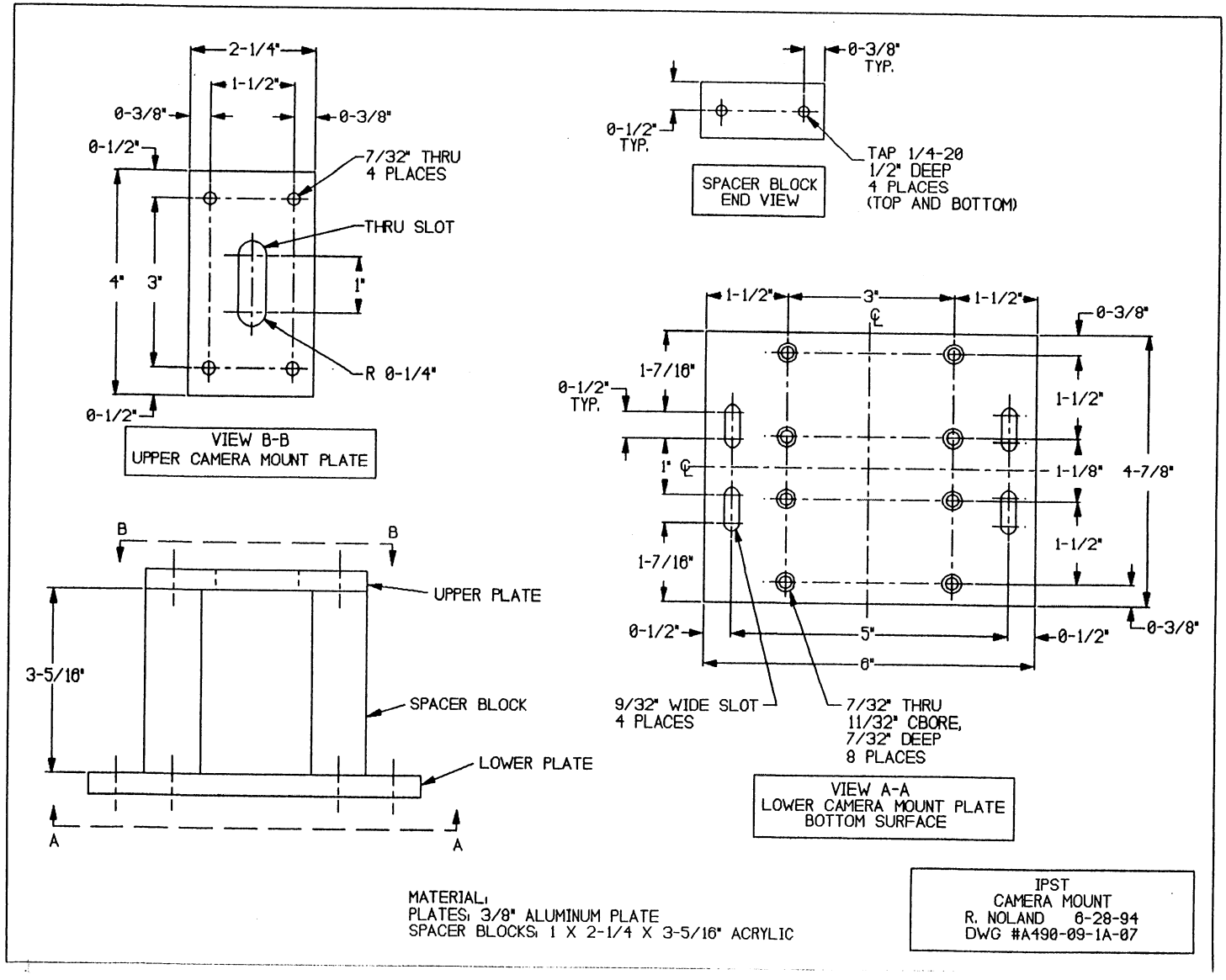
2-1/4"
1-1/2"
0-3/8"
0-3/8"
0-1/2"
7/32" THRU
4 PLACES
THRU SLOT
4"
3"
1"
R 0-1/4"
0-1/2"
VIEW B-B
UPPER CAMERA MOUNT PLATE
0-3/8"
TYP.
0-1/2"
TYP.
TAP 1/4-20
1/2" DEEP
4 PLACES
(TOP AND BOTTOM)
SPACER BLOCK
END VIEW
B
B
UPPER PLATE
3-5/16"
SPACER BLOCK
LOWER PLATE
A
A
1-1/2"
3"
1-1/2"
0-3/8"
1-7/16"
0-1/2"
TYP.
1-1/2"
1"
1-1/8"
4-7/8"
1-1/2"
1-7/16"
0-1/2"
5"
0-1/2"
0-3/8"
6"
9/32" WIDE SLOT
4 PLACES
7/32" THRU
11/32" CBORE,
7/32" DEEP
8 PLACES
VIEW A-A
LOWER CAMERA MOUNT PLATE
BOTTOM SURFACE
MATERIAL:
PLATES: 3/8" ALUMINUM PLATE
SPACER BLOCKS: 1 X 2-1/4 X 3-5/16" ACRYLIC
IPST
CAMERA MOUNT
R. NOLAND 6-28-94
DWG #A490-09-1A-07

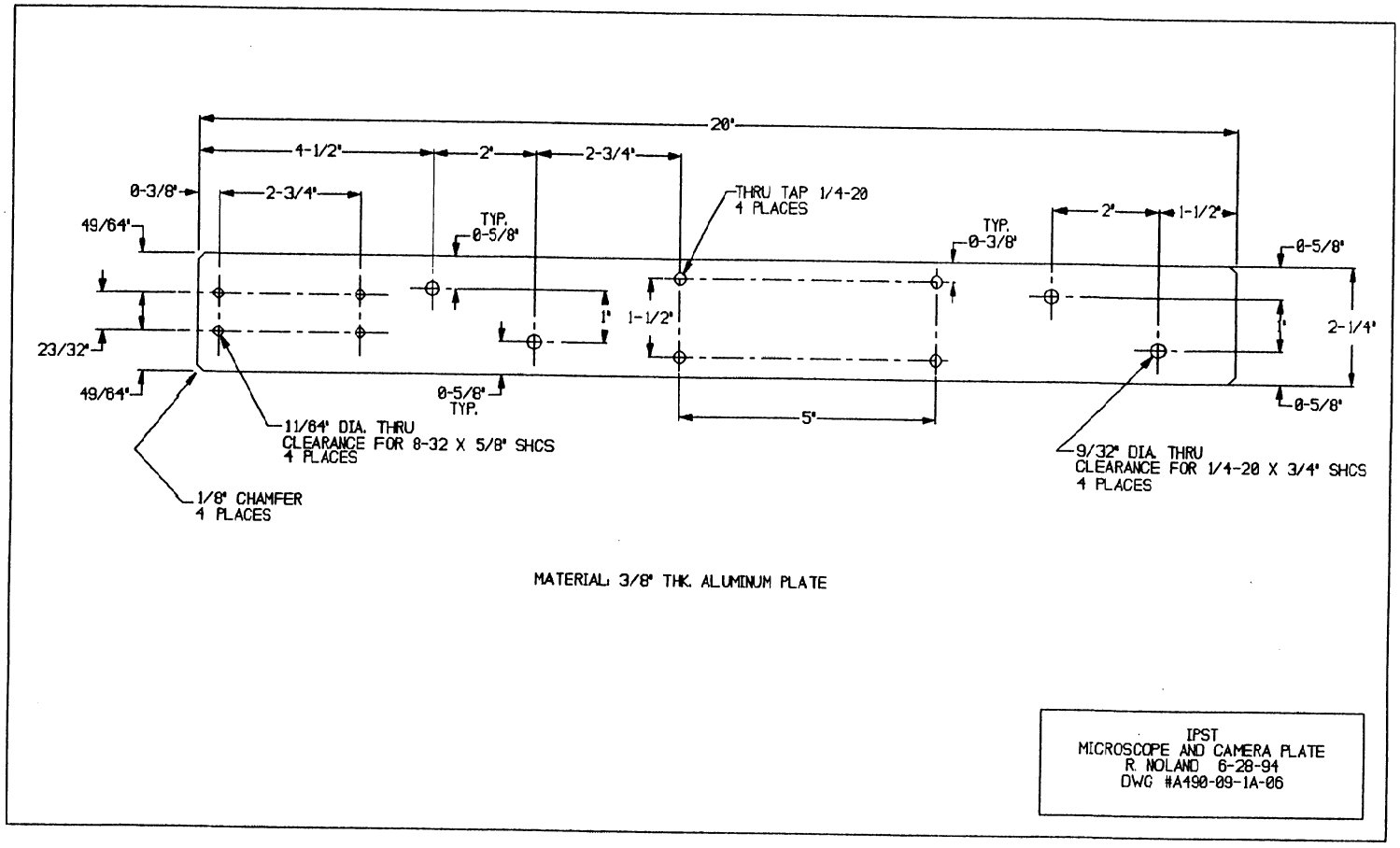
20"
4-1/2"
2"
2-3/4"
0-3/8"
2-3/4"
49/64"
TYP.
0-5/8"
THRU TAP 1/4-20
4 PLACES
TYP.
0-3/8"
2"
1-1/2"
0-5/8"
1"
1-1/2"
2-1/4"
23/32"
49/64"
0-5/8"
TYP.
5"
0-5/8"
11/64" DIA. THRU
CLEARANCE FOR 8-32 X 5/8" SHCS
4 PLACES
9/32" DIA. THRU
CLEARANCE FOR 1/4-20 X 3/4" SHCS
4 PLACES
1/8" CHAMFER
4 PLACES
MATERIAL: 3/8" THK. ALUMINUM PLATE
IPST
MICROSCOPE AND CAMERA PLATE
R. NOLAND 6-28-94
DWG #A190-09-1A-06

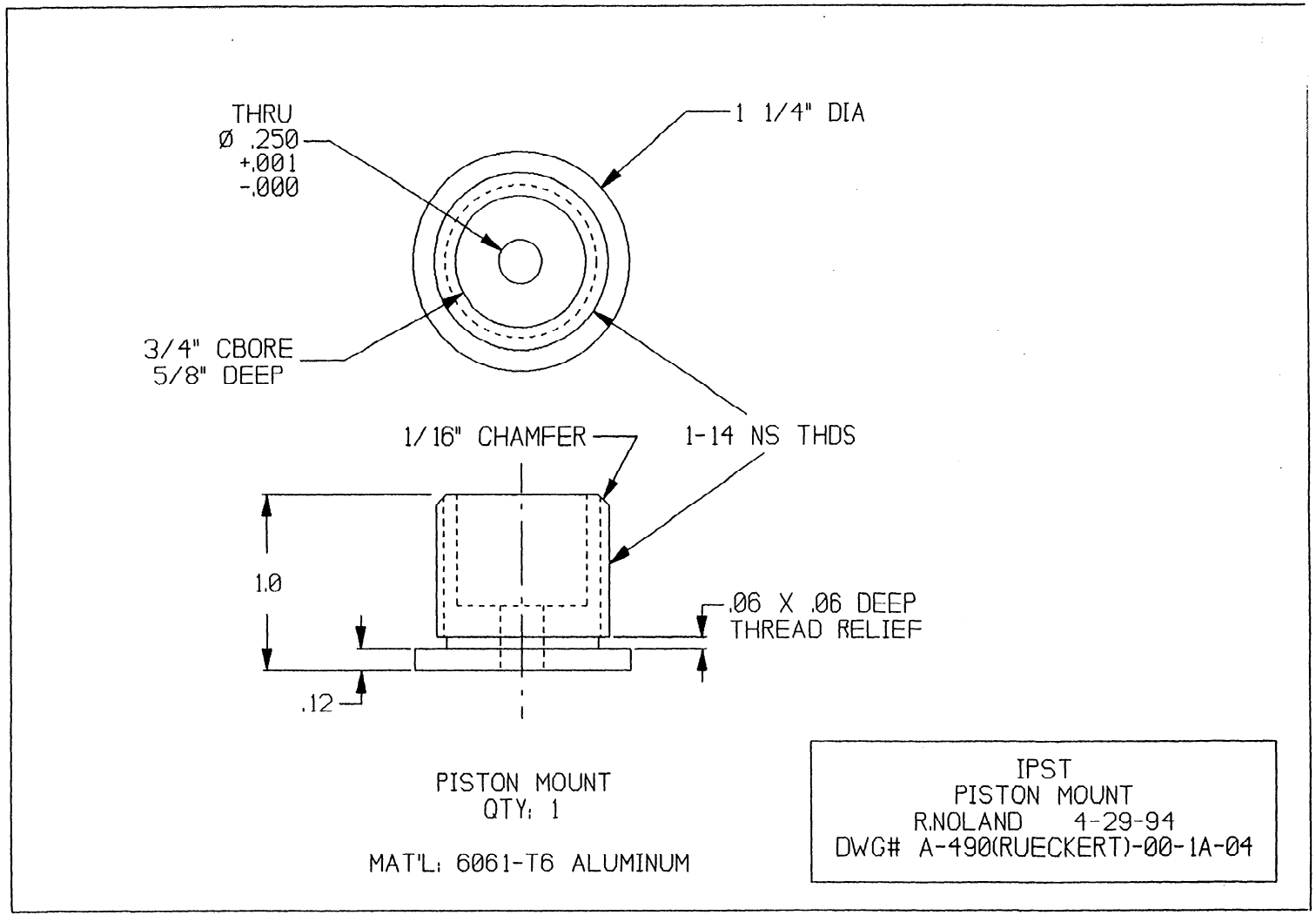
THRU
Ø .250
+.001
-.000
1 1/4" DIA
3/4" CBORE
5/8" DEEP
1/16" CHAMFER
1-14 NS THDS
1.0
.06 X .06 DEEP
THREAD RELIEF
.12
PISTON MOUNT
QTY: 1
MAT'L: 6061-T6 ALUMINUM
IPST
PISTON MOUNT
R.NOLAND 4-29-94
DWG# A-490(RUECKERT)-00-1A-04

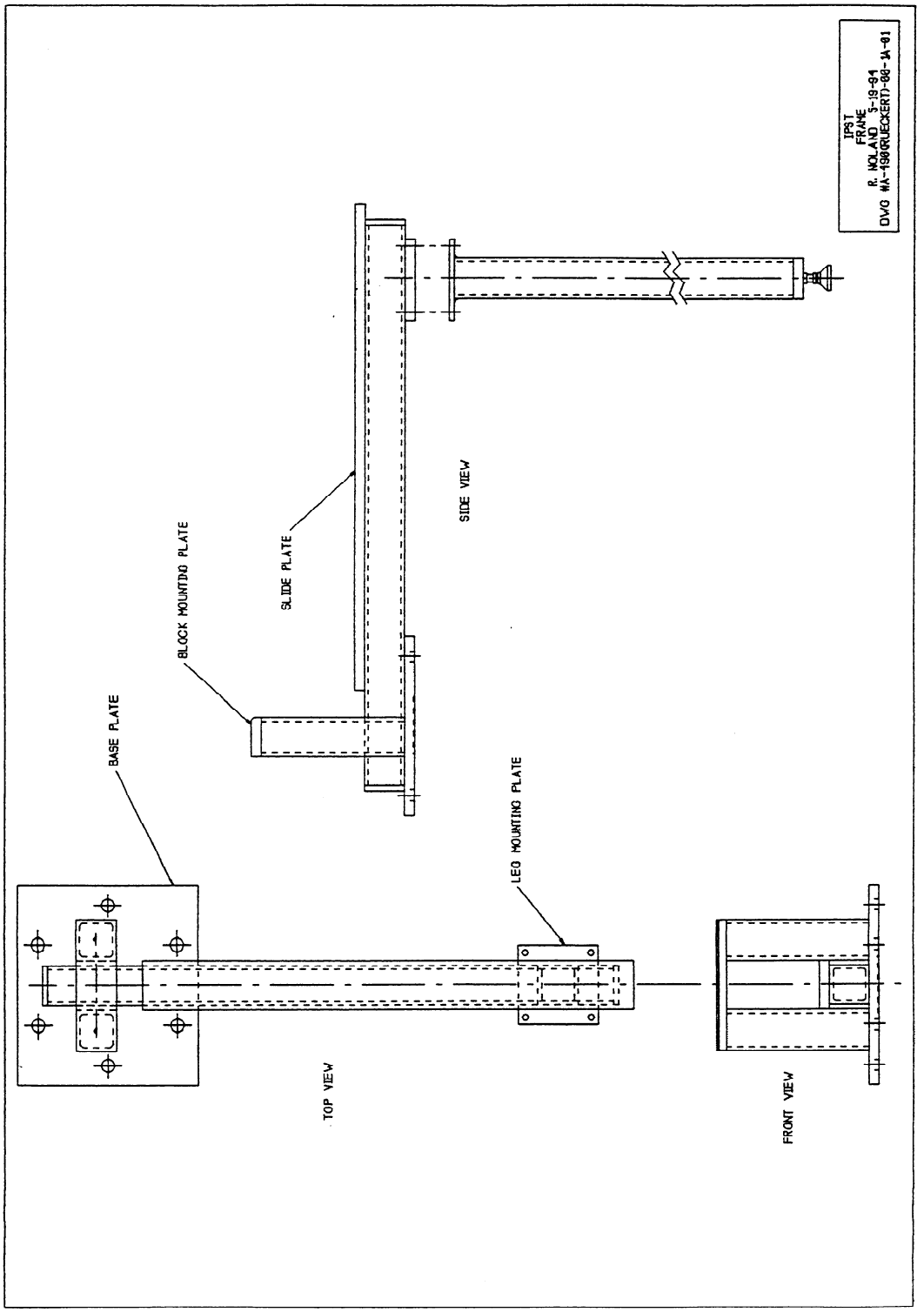
IPGT
FRAME
R. HOLAND 5-19-94
DWG #A-190GRUEOCERT)-00-A-01
SIDE VIEW
SLIDE PLATE
BLOCK MOUNTING PLATE
BASE PLATE
LEG MOUNTING PLATE
TOP VIEW
FRONT VIEW

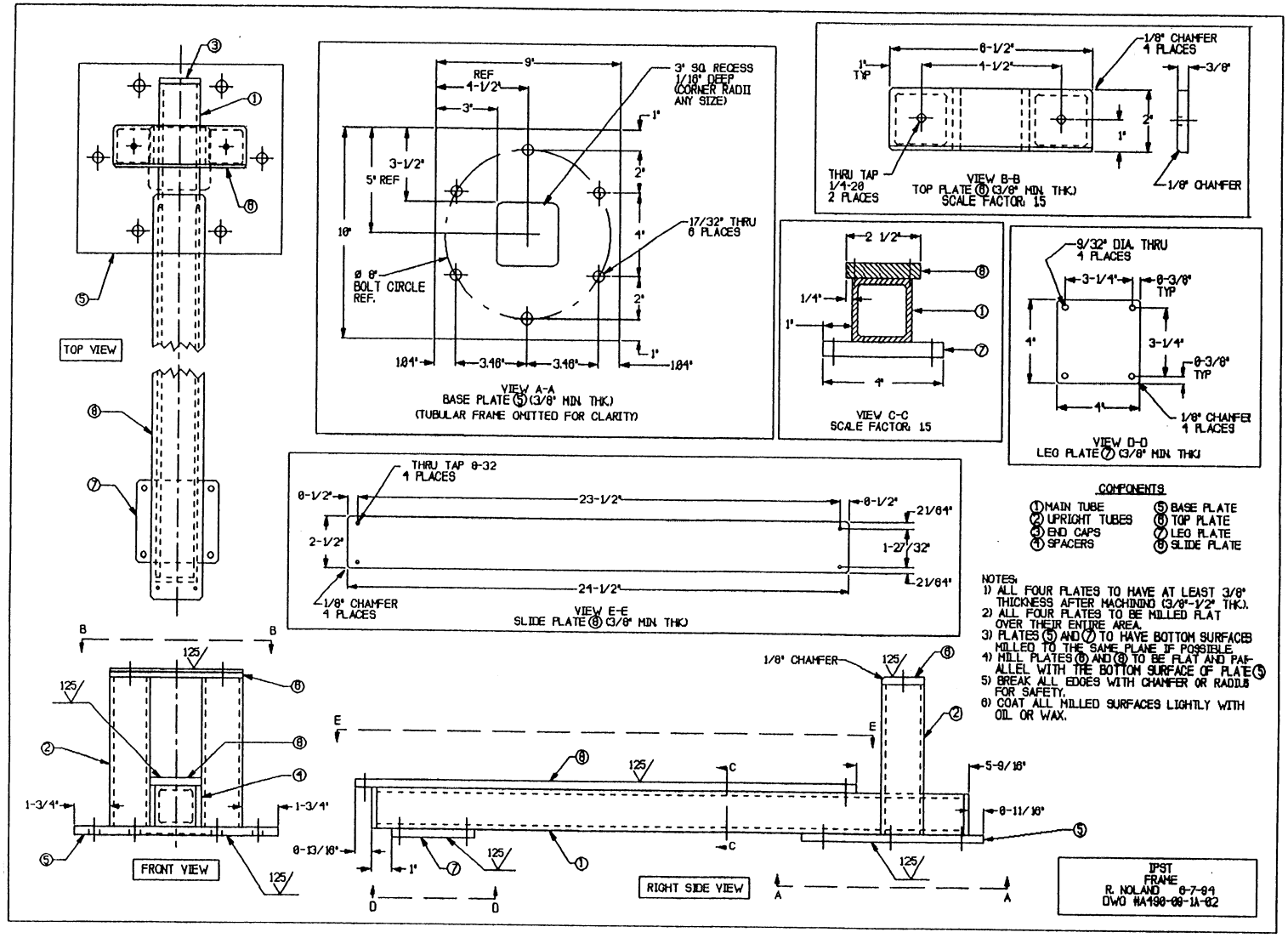
TOP VIEW
VIEW A-A
BASE PLATE ⑤ (3/8" MIN. THK.)
(TUBULAR FRAME OMITTED FOR CLARITY)
3" SQ. RECESS 1/16" DEEP (CORNER RADII ANY SIZE)
17/32" THRU 8 PLACES
Ø 8" BOLT CIRCLE REF.
VIEW B-B
TOP PLATE ⑥ (3/8" MIN. THK.)
SCALE FACTOR: 1.5
1/8" CHAMFER 4 PLACES
THRU TAP 1/4-20 2 PLACES
VIEW C-C
SCALE FACTOR: 1.5
9/32" DIA. THRU 4 PLACES
VIEW D-D
LEG PLATE ⑦ (3/8" MIN. THK.)
THRU TAP 8-32 4 PLACES
VIEW E-E
SLIDE PLATE ⑧ (3/8" MIN. THK.)
1/8" CHAMFER 4 PLACES
COMPONENTS
① MAIN TUBE
② UPRIGHT TUBES
③ END CAPS
④ SPACERS
⑤ BASE PLATE
⑥ TOP PLATE
⑦ LEG PLATE
⑧ SLIDE PLATE
NOTES:
1) ALL FOUR PLATES TO HAVE AT LEAST 3/8" THICKNESS AFTER MACHINING (3/8"-1/2" THK.).
2) ALL FOUR PLATES TO BE MILLED FLAT OVER THEIR ENTIRE AREA.
3) PLATES ⑤ AND ⑦ TO HAVE BOTTOM SURFACES MILLED TO THE SAME PLANE IF POSSIBLE.
4) MILL PLATES ⑥ AND ⑧ TO BE FLAT AND PARALLEL WITH THE BOTTOM SURFACE OF PLATE ⑤
5) BREAK ALL EDGES WITH CHAMFER OR RADIUS FOR SAFETY.
6) COAT ALL MILLED SURFACES LIGHTLY WITH OIL OR WAX.
FRONT VIEW
RIGHT SIDE VIEW
IPST
FRAME
R. NOLAND 8-7-99
DWG #A190-00-1A-02

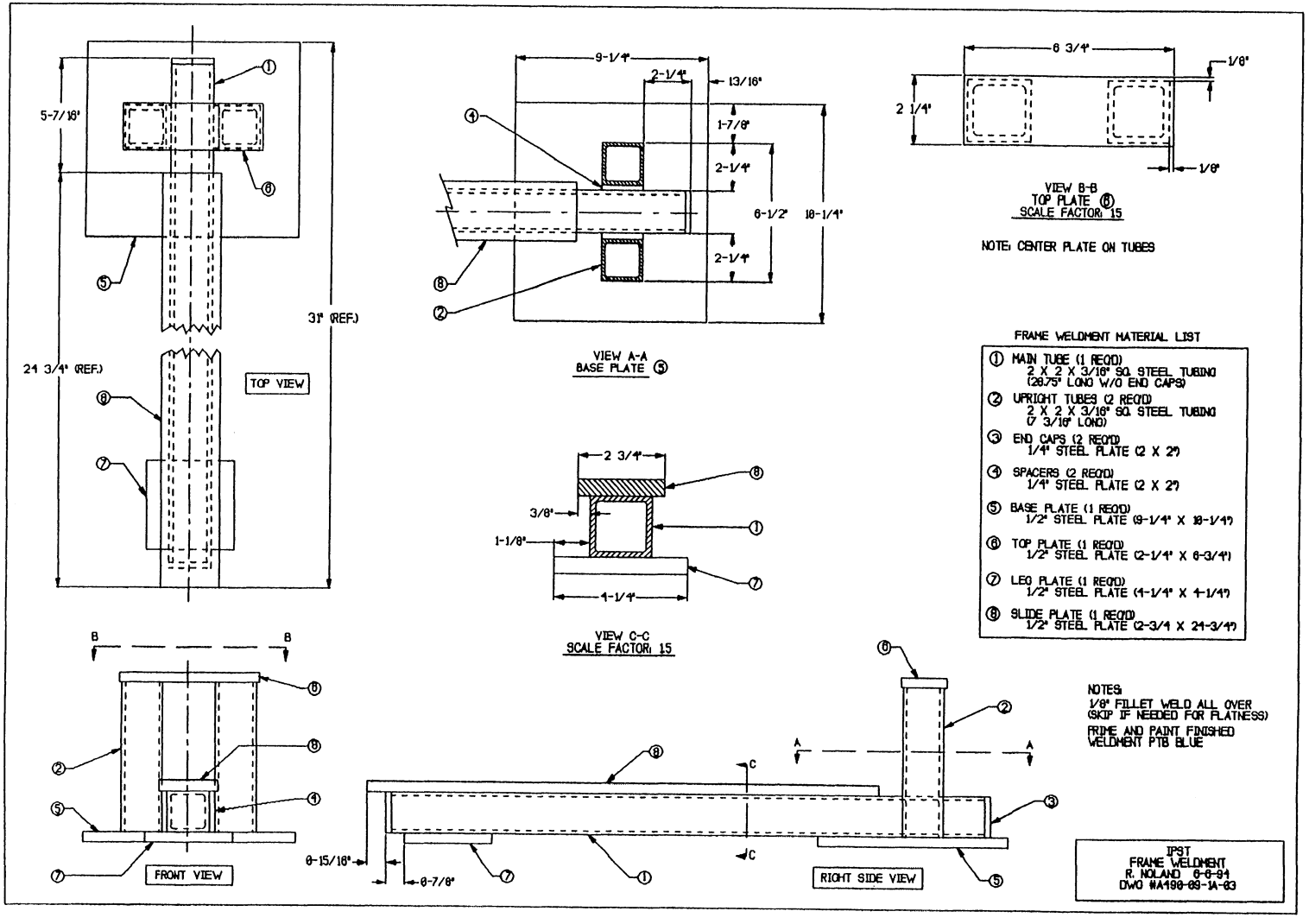
5-7/16"
31" (REF.)
24 3/4" (REF.)
TOP VIEW
FRONT VIEW
9-1/4"
2-1/4"
13/16"
1-7/8"
2-1/4"
6-1/2"
10-1/4"
2-1/4"
VIEW A-A
BASE PLATE ⑤
2 3/4"
3/8"
1-1/8"
1-1/4"
VIEW C-C
SCALE FACTOR: 15
0-15/16"
0-7/8"
RIGHT SIDE VIEW
6 3/4"
1/8"
2 1/4"
1/8"
VIEW B-B
TOP PLATE ⑥
SCALE FACTOR: 15
NOTE: CENTER PLATE ON TUBES
FRAME WELDMENT MATERIAL LIST
① MAIN TUBE (1 REQ'D)
2 X 2 X 3/16" SQ. STEEL TUBING
(28.75" LONG W/O END CAPS)
② UPRIGHT TUBES (2 REQ'D)
2 X 2 X 3/16" SQ. STEEL TUBING
(7 3/16" LONG)
③ END CAPS (2 REQ'D)
1/4" STEEL PLATE (2 X 2")
④ SPACERS (2 REQ'D)
1/4" STEEL PLATE (2 X 2")
⑤ BASE PLATE (1 REQ'D)
1/2" STEEL PLATE (9-1/4" X 10-1/4")
⑥ TOP PLATE (1 REQ'D)
1/2" STEEL PLATE (2-1/4" X 6-3/4")
⑦ LEG PLATE (1 REQ'D)
1/2" STEEL PLATE (1-1/4" X 1-1/4")
⑧ SLIDE PLATE (1 REQ'D)
1/2" STEEL PLATE (2-3/4 X 24-3/4")
NOTES:
1/8" FILLET WELD ALL OVER
(SKIP IF NEEDED FOR FLATNESS)
PRIME AND PAINT FINISHED
WELDMENT PTB BLUE
IPST
FRAME WELDMENT
R. NOLAND 6-6-94
DWG #A190-09-1A-03

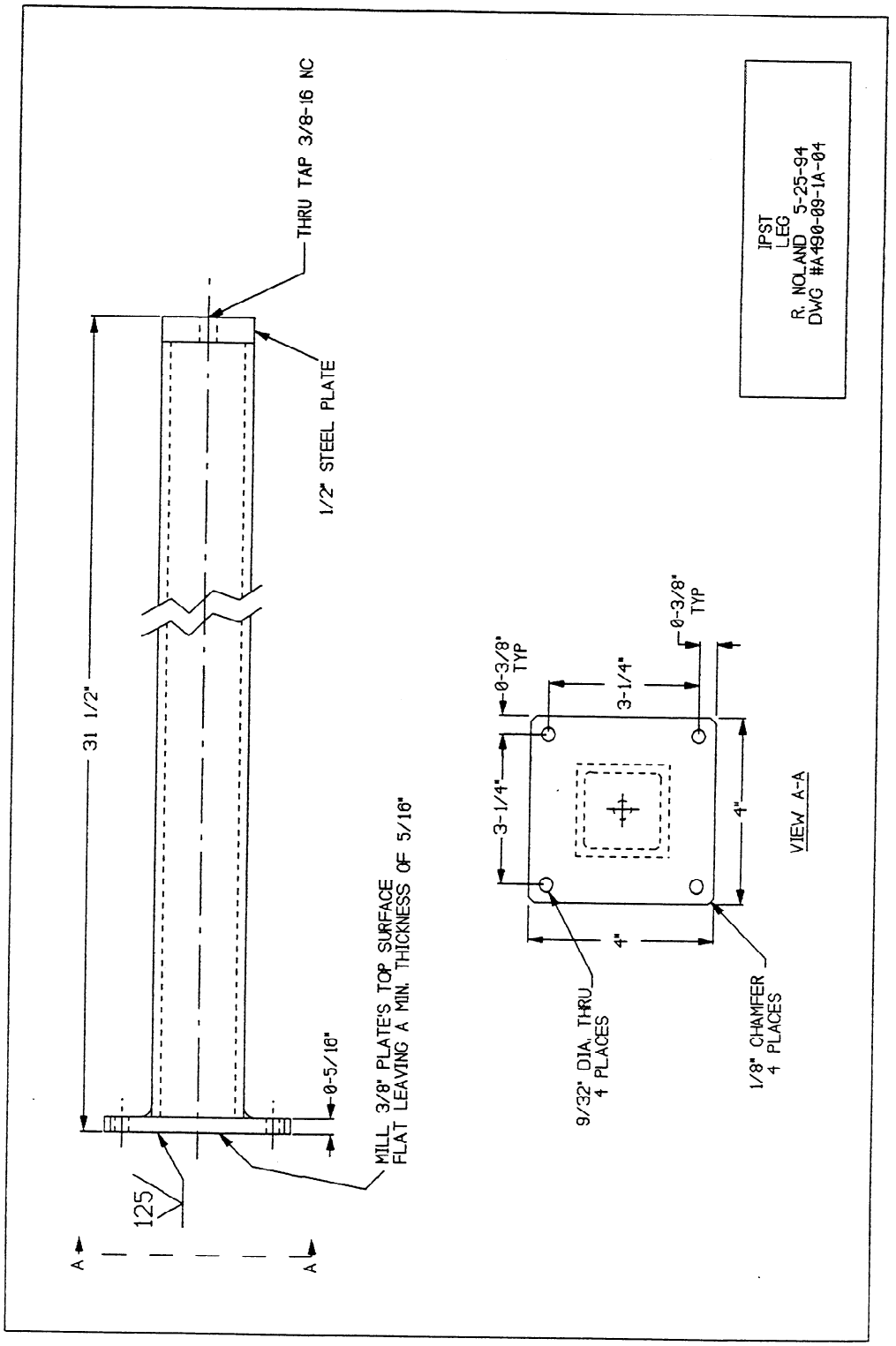
IPST
LEG
R. NOLAND 5-25-94
DWG #A490-09-1A-04
THRU TAP 3/8-16 NC
1/2" STEEL PLATE
31 1/2"
0-5/16"
MILL 3/8" PLATE'S TOP SURFACE
FLAT LEAVING A MIN. THICKNESS OF 5/16"
125
A
A
0-3/8" TYP
3-1/4"
0-3/8" TYP
3-1/4"
4"
4"
9/32" DIA. THRU
4 PLACES
1/8" CHAMFER
4 PLACES
VIEW A-A

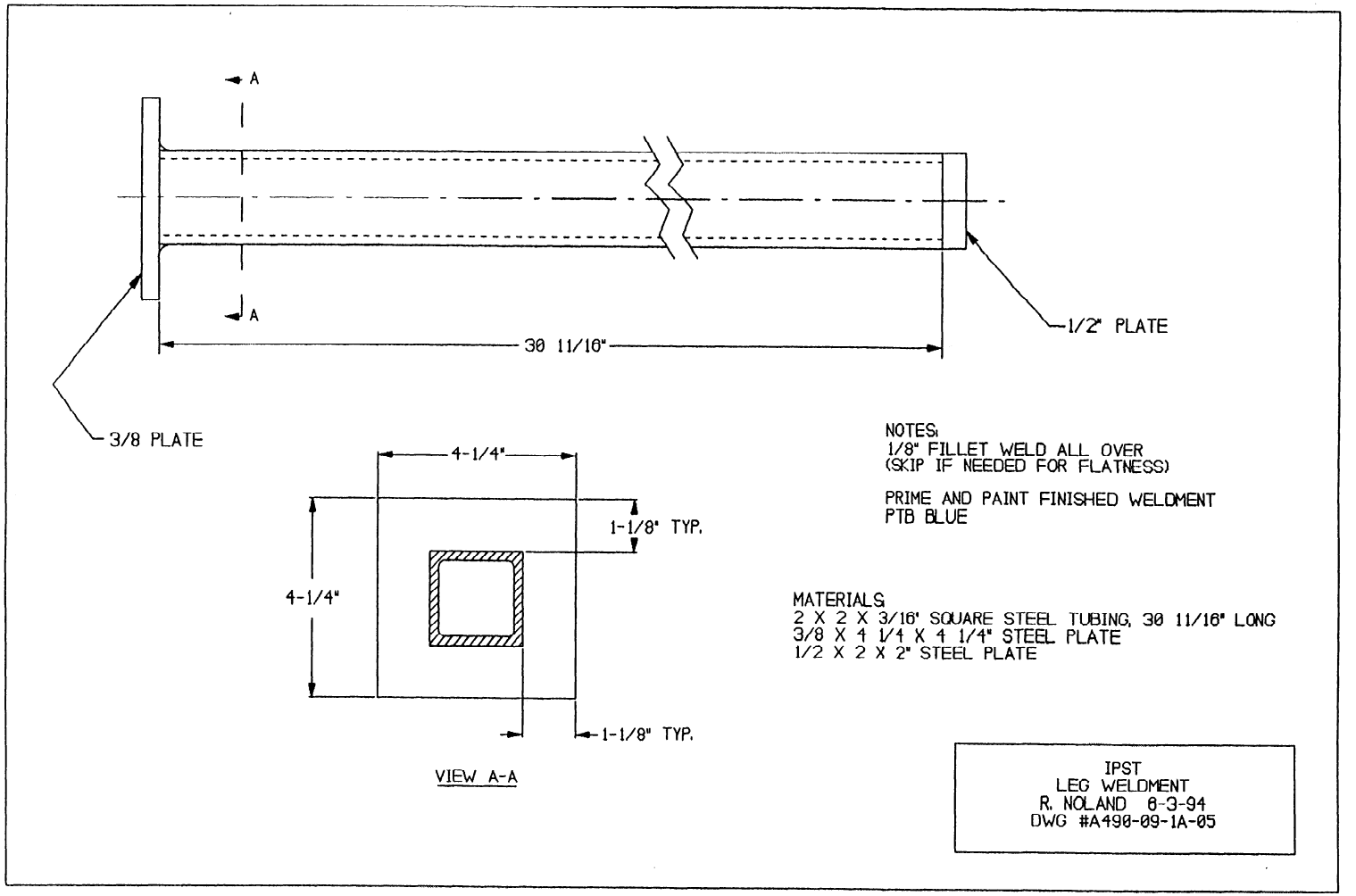
A
A
30 11/16"
1/2" PLATE
3/8 PLATE
4-1/4"
1-1/8" TYP.
4-1/4"
1-1/8" TYP.
VIEW A-A
NOTES:
1/8" FILLET WELD ALL OVER
(SKIP IF NEEDED FOR FLATNESS)
PRIME AND PAINT FINISHED WELDMENT
PTB BLUE
MATERIALS:
2 X 2 X 3/16" SQUARE STEEL TUBING, 30 11/16" LONG
3/8 X 4 1/4 X 4 1/4" STEEL PLATE
1/2 X 2 X 2" STEEL PLATE
IPST
LEG WELDMENT
R. NOLAND 6-3-94
DWG #A490-09-1A-05

APPENDIX 5: T-TESTS OF MECHANICAL DEFORMATION AND TEMPERATURE DATA

Table 5. t-Test for change in curl index - 10 Hz, 5mm, MTS.

Δ Curl Index - 10 Hz, 5mm, MTS						
t-Test: Two-Sample Assuming Unequal Variances						
1	*EW*	*LW*		*1000*	*EW*	*LW*
Mean	0.064	0.063		Mean	0.244	0.074
Variance	0.005	0.009		Variance	0.068	0.011
Observations	46	52		Observations	46	52
Hypothesized Mean Difference	0			Hypothesized Mean Difference	0	
df	95			df	58	
t Stat	0.031			t Stat	4.144	
P(T<=t) one-tail	0.488			P(T<=t) one-tail	0.000	
t Critical one-tail	1.661			t Critical one-tail	1.672	
P(T<=t) two-tail	0.975			P(T<=t) two-tail	0.000	
t Critical two-tail	1.985			t Critical two-tail	2.002	
10	*EW*	*LW*		*10,000*	*EW*	*LW*
Mean	0.257	0.086		Mean	0.196	0.163
Variance	0.052	0.019		Variance	0.043	0.037
Observations	46	52		Observations	46	52
Hypothesized Mean Difference	0			Hypothesized Mean Difference	0	
df	72			df	92	
t Stat	4.391			t Stat	0.808	
P(T<=t) one-tail	0.000			P(T<=t) one-tail	0.211	
t Critical one-tail	1.666			t Critical one-tail	1.662	
P(T<=t) two-tail	0.000			P(T<=t) two-tail	0.421	
t Critical two-tail	1.993			t Critical two-tail	1.986	
100	*EW*	*LW*				
Mean	0.248	0.105				
Variance	0.062	0.062				
Observations	46	52				
Hypothesized Mean Difference	0					
df	95					
t Stat	2.839					
P(T<=t) one-tail	0.003					
t Critical one-tail	1.661					
P(T<=t) two-tail	0.006					
t Critical two-tail	1.985					

Table 6. t-Test of change in curl index - 30 Hz, 5mm, MTS.

Δ Curl Index - 30 Hz, 5mm, MTS						
t-Test: Two-Sample Assuming Unequal Variances				t-Test: Two-Sample Assuming Unequal Variances		
1	*EW*	*LW*		*1000*	*EW*	*LW*
Mean	0.05559	0.04036		Mean	0.0446	0.0331
Variance	0.00576	0.00136		Variance	0.0019	0.0013
Observations	39	45		Observations	39	45
Hypothesized Mean Difference	0			Hypothesized Mean Difference	0	
df	53			df	75	
t Stat	1.1425			t Stat	1.3068	
P(T<=t) one-tail	0.1292			P(T<=t) one-tail	0.0976	
t Critical one-tail	1.6741			t Critical one-tail	1.6654	
P(T<=t) two-tail	0.2584			P(T<=t) two-tail	0.1953	
t Critical two-tail	2.0057			t Critical two-tail	1.9921	
t-Test: Two-Sample Assuming Unequal Variances				t-Test: Two-Sample Assuming Unequal Variances		
10	*EW*	*LW*		*10,000*	*EW*	*LW*
Mean	0.0481	0.0373		Mean	0.0554	0.0345
Variance	0.0020	0.0015		Variance	0.0049	0.0011
Observations	39	45		Observations	39	45
Hypothesized Mean Difference	0			Hypothesized Mean Difference	0	
df	76			df	53	
t Stat	1.1785			t Stat	1.6976	
P(T<=t) one-tail	0.1211			P(T<=t) one-tail	0.0477	
t Critical one-tail	1.6652			t Critical one-tail	1.6741	
P(T<=t) two-tail	0.2423			P(T<=t) two-tail	0.0955	
t Critical two-tail	1.9917			t Critical two-tail	2.0057	
t-Test: Two-Sample Assuming Unequal Variances						
100	*EW*	*LW*				
Mean	0.0570	0.0349				
Variance	0.0053	0.0022				
Observations	39	45				
Hypothesized Mean Difference	0					
df	63					
t Stat	1.6259					
P(T<=t) one-tail	0.0545					
t Critical one-tail	1.6694					
P(T<=t) two-tail	0.1090					
t Critical two-tail	1.9983					

Table 7. t-Test of difference in curl index - 10 Hz, 3 and 4mm, MTS.

t-Test: Two-Sample Assuming Unequal Variances

3mm	EW	LW
	1	*1*
Mean	0.060016	0.079209
Variance	0.003027	0.007046
Observations	15	24
Hypothesized Mean Difference	0	
df	37	
t Stat	-0.862344	
P(T<=t) one-tail	0.197027	
t Critical one-tail	1.687094	
P(T<=t) two-tail	0.394053	
t Critical two-tail	2.02619	

t-Test: Two-Sample Assuming Unequal Variances

4mm	EW	LW
	1	*1*
Mean	0.035162	0.046556
Variance	0.002361	0.002765
Observations	26	25
Hypothesized Mean Difference	0	
df	48	
t Stat	-0.802851	
P(T<=t) one-tail	0.213009	
t Critical one-tail	1.677224	
P(T<=t) two-tail	0.426018	
t Critical two-tail	2.010634	

t-Test: Two-Sample Assuming Unequal Variances

	10	*10*
Mean	0.067087	0.073304
Variance	0.009366	0.008577
Observations	15	24
Hypothesized Mean Difference	0	
df	29	
t Stat	-0.198417	
P(T<=t) one-tail	0.422052	
t Critical one-tail	1.699127	
P(T<=t) two-tail	0.844103	
t Critical two-tail	2.045231	

t-Test: Two-Sample Assuming Unequal Variances

	10	*10*
Mean	0.039618	0.056215
Variance	0.001681	0.002212
Observations	26	25
Hypothesized Mean Difference	0	
df	48	
t Stat	-1.341187	
P(T<=t) one-tail	0.093086	
t Critical one-tail	1.677224	
P(T<=t) two-tail	0.186172	
t Critical two-tail	2.010634	

t-Test: Two-Sample Assuming Unequal Variances

	100	*100*
Mean	0.042469	0.131132
Variance	0.00286	0.022857
Observations	15	24
Hypothesized Mean Difference	0	
df	31	
t Stat	-2.622439	
P(T<=t) one-tail	0.006708	
t Critical one-tail	1.695519	
P(T<=t) two-tail	0.013415	
t Critical two-tail	2.039515	

t-Test: Two-Sample Assuming Unequal Variances

	100	*100*
Mean	0.037265	0.029167
Variance	0.00148	0.002042
Observations	26	25
Hypothesized Mean Difference	0	
df	47	
t Stat	0.687813	
P(T<=t) one-tail	0.247476	
t Critical one-tail	1.677927	
P(T<=t) two-tail	0.494951	
t Critical two-tail	2.011739	

t-Test: Two-Sample Assuming Unequal Variances

	1000	*1000*
Mean	0.035294	0.083025
Variance	0.002207	0.013496
Observations	15	24
Hypothesized Mean Difference	0	
df	33	
t Stat	-1.792054	
P(T<=t) one-tail	0.041149	
t Critical one-tail	1.69236	
P(T<=t) two-tail	0.082298	
t Critical two-tail	2.034517	

t-Test: Two-Sample Assuming Unequal Variances

	1000	*1000*
Mean	0.04188	0.044846
Variance	0.002576	0.002944
Observations	26	25
Hypothesized Mean Difference	0	
df	48	
t Stat	-0.201409	
P(T<=t) one-tail	0.420615	
t Critical one-tail	1.677224	
P(T<=t) two-tail	0.84123	
t Critical two-tail	2.010634	

t-Test: Two-Sample Assuming Unequal Variances

	10000	*10000*
Mean	0.043866	0.087494
Variance	0.002927	0.014678
Observations	15	24
Hypothesized Mean Difference	0	
df	34	
t Stat	-1.536059	
P(T<=t) one-tail	0.066889	
t Critical one-tail	1.690923	
P(T<=t) two-tail	0.133779	
t Critical two-tail	2.032243	

t-Test: Two-Sample Assuming Unequal Variances

	10000	*10000*
Mean	0.025835	0.039458
Variance	0.000801	0.002722
Observations	26	25
Hypothesized Mean Difference	0	
df	37	
t Stat	-1.152611	
P(T<=t) one-tail	0.128231	
t Critical one-tail	1.687094	
P(T<=t) two-tail	0.256463	
t Critical two-tail	2.02619	

Table 8. t-Test of differences in curl index - 30 Hz, 4mm, MTS.

Δ Curl Index - 30 Hz, 4mm, MTS						
t-Test: Two-Sample Assuming Unequal Variances				t-Test: Two-Sample Assuming Unequal Variances		
1	EW	LW		1000	EW	LW
Mean	0.0340	0.0442		Mean	0.0227	0.0575
Variance	0.0006	0.0039		Variance	0.0004	0.0022
Observations	20	16		Observations	20	16
Hypothesized Mean Difference	0			Hypothesized Mean Difference	0	
df	19			df	19	
t Stat	-0.6142			t Stat	-2.7868	
P(T<=t) one-tail	0.2732			P(T<=t) one-tail	0.0059	
t Critical one-tail	1.7291			t Critical one-tail	1.7291	
P(T<=t) two-tail	0.5464			P(T<=t) two-tail	0.0118	
t Critical two-tail	2.0930			t Critical two-tail	2.0930	
t-Test: Two-Sample Assuming Unequal Variances				t-Test: Two-Sample Assuming Unequal Variances		
10	EW	LW		10,000	EW	LW
Mean	0.0280	0.0655		Mean	0.0340	0.0506
Variance	0.0010	0.0057		Variance	0.0014	0.0036
Observations	20	16		Observations	20	16
Hypothesized Mean Difference	0			Hypothesized Mean Difference	0	
df	19			df	24	
t Stat	-1.8634			t Stat	-0.9699	
P(T<=t) one-tail	0.0390			P(T<=t) one-tail	0.1709	
t Critical one-tail	1.7291			t Critical one-tail	1.7109	
P(T<=t) two-tail	0.0779			P(T<=t) two-tail	0.3417	
t Critical two-tail	2.0930			t Critical two-tail	2.0639	
t-Test: Two-Sample Assuming Unequal Variances						
100	EW	LW				
Mean	0.0339	0.0373				
Variance	0.0021	0.0034				
Observations	20	16				
Hypothesized Mean Difference	0					
df	28					
t Stat	-0.1894					
P(T<=t) one-tail	0.4256					
t Critical one-tail	1.7011					
P(T<=t) two-tail	0.8511					
t Critical two-tail	2.0484					

Table 9. t-Test of differences in curl index - 30 Hz, 3mm, MTS.

Δ Curl Index - 30 Hz, 3mm, MTS						
t-Test: Two-Sample Assuming Unequal Variances						
1	EW	LW		1000	EW	LW
Mean	0.0602	0.0489		Mean	0.0382	0.0407
Variance	0.0036	0.0076		Variance	0.0030	0.0034
Observations	24	24		Observations	24	24
Hypothesized Mean Differenc	0			Hypothesized Mean Differenc	0	
df	41			df	46	
t Stat	0.5238			t Stat	-0.1502	
P(T<=t) one-tail	0.3016			P(T<=t) one-tail	0.4406	
t Critical one-tail	1.6829			t Critical one-tail	1.6787	
P(T<=t) two-tail	0.6032			P(T<=t) two-tail	0.8812	
t Critical two-tail	2.0195			t Critical two-tail	2.0129	
10	EW	LW		10000	EW	LW
Mean	0.0342	0.0419		Mean	0.0366	0.0384
Variance	0.0014	0.0019		Variance	0.0056	0.0020
Observations	24	24		Observations	24	24
Hypothesized Mean Differenc	0			Hypothesized Mean Differenc	0	
df	45			df	38	
t Stat	-0.6582			t Stat	-0.1032	
P(T<=t) one-tail	0.2569			P(T<=t) one-tail	0.4592	
t Critical one-tail	1.6794			t Critical one-tail	1.6860	
P(T<=t) two-tail	0.5138			P(T<=t) two-tail	0.9184	
t Critical two-tail	2.0141			t Critical two-tail	2.0244	
100	EW	LW				
Mean	0.03713	0.04667				
Variance	0.00237	0.00599				
Observations	24	24				
Hypothesized Mean Differenc	0					
df	39					
t Stat	-0.5111					
P(T<=t) one-tail	0.3061					
t Critical one-tail	1.6849					
P(T<=t) two-tail	0.6122					
t Critical two-tail	2.0227					

Table 10. t-Test of differences in curl index - 10 Hz, Shaker.

Δ Curl Index - 10 Hz, 5mm, Shaker						
t-Test: Two-Sample Assuming Unequal Variances				t-Test: Two-Sample Assuming Unequal Variances		
1	*EW*	*LW*		*100*	*EW*	*LW*
Mean	0.04542	0.03792		Mean	0.05792	0.0429
Variance	0.00029	0.00037		Variance	0.00035	0.00075
Observations	15	17		Observations	13	15
Hypothesized Mean Difference	0			Hypothesized Mean Difference	0	
df	30			df	25	
t Stat	1.16566			t Stat	1.71429	
P(T<=t) one-tail	0.12647			P(T<=t) one-tail	0.04942	
t Critical one-tail	1.69726			t Critical one-tail	1.70814	
P(T<=t) two-tail	0.25294			P(T<=t) two-tail	0.09885	
t Critical two-tail	2.04227			t Critical two-tail	2.05954	
t-Test: Two-Sample Assuming Unequal Variances				t-Test: Two-Sample Assuming Unequal Variances		
2	*EW*	*LW*		*1000*	*EW*	*LW*
Mean	0.05473	0.04123		Mean	0.05322	0.03856
Variance	0.00012	0.00121		Variance	0.0017	0.00031
Observations	15	17		Observations	13	15
Hypothesized Mean Difference	0			Hypothesized Mean Difference	0	
df	19			df	16	
t Stat	1.51949			t Stat	1.19204	
P(T<=t) one-tail	0.07255			P(T<=t) one-tail	0.12531	
t Critical one-tail	1.72913			t Critical one-tail	1.74588	
P(T<=t) two-tail	0.1451			P(T<=t) two-tail	0.25063	
t Critical two-tail	2.09302			t Critical two-tail	2.1199	
t-Test: Two-Sample Assuming Unequal Variances				t-Test: Two-Sample Assuming Unequal Variances		
5	*EW*	*LW*		*10,000*	*EW*	*LW*
Mean	0.05842	0.03954		Mean	0.0482	0.04155
Variance	0.00049	0.00068		Variance	0.00185	0.00063
Observations	15	17		Observations	13	15
Hypothesized Mean Difference	0			Hypothesized Mean Difference	0	
df	30			df	19	
t Stat	2.21888			t Stat	0.48905	
P(T<=t) one-tail	0.0171			P(T<=t) one-tail	0.3152	
t Critical one-tail	1.69726			t Critical one-tail	1.72913	
P(T<=t) two-tail	0.0342			P(T<=t) two-tail	0.63041	
t Critical two-tail	2.04227			t Critical two-tail	2.09302	
t-Test: Two-Sample Assuming Unequal Variances						
10	*EW*	*LW*				
Mean	0.05812	0.03747				
Variance	0.00059	0.00019				
Observations	15	17				
Hypothesized Mean Difference	0					
df	22					
t Stat	2.89578					
P(T<=t) one-tail	0.00419					
t Critical one-tail	1.71714					
P(T<=t) two-tail	0.00839					
t Critical two-tail	2.07388					

Table 11. t-Test of differences in curl index - 30 Hz, Shaker.

Δ Curl Index - 30 Hz, 5mm, Shaker						
t-Test: Two-Sample Assuming Unequal Variances				t-Test: Two-Sample Assuming Unequal Variances		
1	*EW*	*LW*		*100*	*EW*	*LW*
Mean	0.02506	0.02384		Mean	0.02775	0.01924
Variance	0.00127	0.0006		Variance	0.00075	0.0003
Observations	20	15		Observations	13	17
Hypothesized Mean Difference	0			Hypothesized Mean Difference	0	
df	33			df	19	
t Stat	0.12036			t Stat	0.98242	
P(T<=t) one-tail	0.45247			P(T<=t) one-tail	0.16912	
t Critical one-tail	1.69236			t Critical one-tail	1.72913	
P(T<=t) two-tail	0.90493			P(T<=t) two-tail	0.33824	
t Critical two-tail	2.03452			t Critical two-tail	2.09302	
t-Test: Two-Sample Assuming Unequal Variances				t-Test: Two-Sample Assuming Unequal Variances		
2	*EW*	*LW*		*1000*	*EW*	*LW*
Mean	0.02685	0.02422		Mean	0.02003	0.0199
Variance	0.00029	0.00053		Variance	0.00023	0.00026
Observations	20	15		Observations	14	17
Hypothesized Mean Difference	0			Hypothesized Mean Difference	0	
df	25			df	28	
t Stat	0.37423			t Stat	0.02212	
P(T<=t) one-tail	0.35569			P(T<=t) one-tail	0.49126	
t Critical one-tail	1.70814			t Critical one-tail	1.70113	
P(T<=t) two-tail	0.71139			P(T<=t) two-tail	0.98251	
t Critical two-tail	2.05954			t Critical two-tail	2.04841	
t-Test: Two-Sample Assuming Unequal Variances				t-Test: Two-Sample Assuming Unequal Variances		
5	*EW*	*LW*		*10,000*	*EW*	*LW*
Mean	0.02666	0.02149		Mean	0.02023	0.01706
Variance	0.00141	0.0003		Variance	0.0004	3.3E-05
Observations	20	15		Observations	14	11
Hypothesized Mean Difference	0			Hypothesized Mean Difference	0	
df	28			df	16	
t Stat	0.54353			t Stat	0.56736	
P(T<=t) one-tail	0.29553			P(T<=t) one-tail	0.28917	
t Critical one-tail	1.70113			t Critical one-tail	1.74588	
P(T<=t) two-tail	0.59107			P(T<=t) two-tail	0.57834	
t Critical two-tail	2.04841			t Critical two-tail	2.1199	
t-Test: Two-Sample Assuming Unequal Variances						
10	*EW*	*LW*				
Mean	0.026	0.02229				
Variance	0.00031	0.00039				
Observations	20	15				
Hypothesized Mean Difference	0					
df	28					
t Stat	0.57858					
P(T<=t) one-tail	0.28375					
t Critical one-tail	1.70113					
P(T<=t) two-tail	0.5675					
t Critical two-tail	2.04841					

Table 12. t-Test of differences in curl index - 50 Hz, Shaker.

Δ Curl Index - 50 Hz, 5mm, Shaker						
t-Test: Two-Sample Assuming Unequal Variances				t-Test: Two-Sample Assuming Unequal Variances		
1	*EW*	*LW*		*100*	*EW*	*LW*
Mean	0.01819	0.01671		Mean	0.01618	0.01639
Variance	0.00013	0.00011		Variance	0.00013	0.00016
Observations	14	14		Observations	12	11
Hypothesized Mean Difference	0			Hypothesized Mean Difference	0	
df	26			df	20	
t Stat	0.35647			t Stat	-0.0412	
P(T<=t) one-tail	0.36218			P(T<=t) one-tail	0.48377	
t Critical one-tail	1.70562			t Critical one-tail	1.72472	
P(T<=t) two-tail	0.72436			P(T<=t) two-tail	0.96754	
t Critical two-tail	2.05553			t Critical two-tail	2.08596	
t-Test: Two-Sample Assuming Unequal Variances				t-Test: Two-Sample Assuming Unequal Variances		
2	*EW*	*LW*		*1000*	*EW*	*LW*
Mean	0.01858	0.01792		Mean	0.01682	0.01706
Variance	0.00023	0.00026		Variance	0.00013	0.00016
Observations	14	14		Observations	12	11
Hypothesized Mean Difference	0			Hypothesized Mean Difference	0	
df	26			df	20	
t Stat	0.11239			t Stat	-0.04815	
P(T<=t) one-tail	0.45569			P(T<=t) one-tail	0.48104	
t Critical one-tail	1.70562			t Critical one-tail	1.72472	
P(T<=t) two-tail	0.91138			P(T<=t) two-tail	0.96208	
t Critical two-tail	2.05553			t Critical two-tail	2.08596	
t-Test: Two-Sample Assuming Unequal Variances				t-Test: Two-Sample Assuming Unequal Variances		
5	*EW*	*LW*		*10,000*	*EW*	*LW*
Mean	0.01764	0.01929		Mean	0.0154	0.01587
Variance	0.00024	0.00047		Variance	0.00016	0.00014
Observations	14	14		Observations	12	11
Hypothesized Mean Difference	0			Hypothesized Mean Difference	0	
df	24			df	21	
t Stat	-0.23073			t Stat	-0.093	
P(T<=t) one-tail	0.40974			P(T<=t) one-tail	0.46339	
t Critical one-tail	1.71088			t Critical one-tail	1.72074	
P(T<=t) two-tail	0.81948			P(T<=t) two-tail	0.92678	
t Critical two-tail	2.0639			t Critical two-tail	2.07961	
t-Test: Two-Sample Assuming Unequal Variances						
10	*EW*	*LW*				
Mean	0.01826	0.01959				
Variance	0.00031	0.0004				
Observations	14	14				
Hypothesized Mean Difference	0					
df	26					
t Stat	-0.18745					
P(T<=t) one-tail	0.42638					
t Critical one-tail	1.70562					
P(T<=t) two-tail	0.85276					
t Critical two-tail	2.05553					

Table 13. t-Test of differences in curl index - 100 Hz, Shaker.

Δ Curl Index - 100 Hz, 5 mm, Shaker						
t-Test: Two-Sample Assuming Unequal Variances				t-Test: Two-Sample Assuming Unequal Variances		
1	*EW*	*LW*		*100*	*EW*	*LW*
Mean	0.01624	0.01639		Mean	0.0177	0.017
Variance	8.1E-05	0.00011		Variance	0.00011	0.00032
Observations	12	7		Observations	15	10
Hypothesized Mean Difference	0			Hypothesized Mean Difference	0	
df	11			df	13	
t Stat	-0.03053			t Stat	0.11253	
P(T<=t) one-tail	0.48809			P(T<=t) one-tail	0.45606	
t Critical one-tail	1.79588			t Critical one-tail	1.77093	
P(T<=t) two-tail	0.97619			P(T<=t) two-tail	0.91213	
t Critical two-tail	2.20099			t Critical two-tail	2.16037	
t-Test: Two-Sample Assuming Unequal Variances				t-Test: Two-Sample Assuming Unequal Variances		
2	*EW*	*LW*		*1000*	*EW*	*LW*
Mean	0.0179	0.0162		Mean	0.0165	0.01688
Variance	0.00026	0.00019		Variance	0.00013	0.00022
Observations	12	7		Observations	15	10
Hypothesized Mean Difference	0			Hypothesized Mean Difference	0	
df	14			df	16	
t Stat	0.24072			t Stat	-0.06892	
P(T<=t) one-tail	0.40663			P(T<=t) one-tail	0.47295	
t Critical one-tail	1.76131			t Critical one-tail	1.74588	
P(T<=t) two-tail	0.81326			P(T<=t) two-tail	0.94591	
t Critical two-tail	2.14479			t Critical two-tail	2.1199	
t-Test: Two-Sample Assuming Unequal Variances				t-Test: Two-Sample Assuming Unequal Variances		
5	*EW*	*LW*		*10,000*	*EW*	*LW*
Mean	0.01788	0.01729		Mean	0.01581	0.01557
Variance	0.0002	9.4E-05		Variance	0.00029	5.7E-05
Observations	12	7		Observations	15	10
Hypothesized Mean Difference	0			Hypothesized Mean Difference	0	
df	16			df	21	
t Stat	0.10712			t Stat	0.04839	
P(T<=t) one-tail	0.45801			P(T<=t) one-tail	0.48093	
t Critical one-tail	1.74588			t Critical one-tail	1.72074	
P(T<=t) two-tail	0.91602			P(T<=t) two-tail	0.96186	
t Critical two-tail	2.1199			t Critical two-tail	2.07961	
t-Test: Two-Sample Assuming Unequal Variances						
10	*EW*	*LW*				
Mean	0.01743	0.01859				
Variance	0.00016	0.00011				
Observations	12	7				
Hypothesized Mean Difference	0					
df	15					
t Stat	-0.21584					
P(T<=t) one-tail	0.41601					
t Critical one-tail	1.75305					
P(T<=t) two-tail	0.83202					
t Critical two-tail	2.13145					

Table 14. t-Test of differences in curl index - 200 Hz, Shaker.

Δ Curl Index - 200 Hz, 5mm, Shaker						
t-Test: Two-Sample Assuming Unequal Variances				t-Test: Two-Sample Assuming Unequal Variances		
1	*EW*	*LW*		*100*	*EW*	*LW*
Mean	0.01502	0.01509		Mean	0.01748	0.0169
Variance	0.00011	2.8E-05		Variance	7.6E-05	6.2E-05
Observations	17	4		Observations	11	11
Hypothesized Mean Difference	0			Hypothesized Mean Difference	0	
df	10			df	20	
t Stat	-0.02109			t Stat	0.16404	
P(T<=t) one-tail	0.4918			P(T<=t) one-tail	0.43567	
t Critical one-tail	1.81246			t Critical one-tail	1.72472	
P(T<=t) two-tail	0.98359			P(T<=t) two-tail	0.87134	
t Critical two-tail	2.22814			t Critical two-tail	2.08596	
t-Test: Two-Sample Assuming Unequal Variances				t-Test: Two-Sample Assuming Unequal Variances		
2	*EW*	*LW*		*1000*	*EW*	*LW*
Mean	0.01581	0.01838		Mean	0.01618	0.01543
Variance	0.00013	0.00013		Variance	0.00017	6.7E-05
Observations	17	4		Observations	11	11
Hypothesized Mean Difference	0			Hypothesized Mean Difference	0	
df	5			df	17	
t Stat	-0.40259			t Stat	0.16035	
P(T<=t) one-tail	0.35194			P(T<=t) one-tail	0.43725	
t Critical one-tail	2.01505			t Critical one-tail	1.73961	
P(T<=t) two-tail	0.70388			P(T<=t) two-tail	0.87449	
t Critical two-tail	2.57058			t Critical two-tail	2.10982	
t-Test: Two-Sample Assuming Unequal Variances				t-Test: Two-Sample Assuming Unequal Variances		
5	*EW*	*LW*		*10,000*	*EW*	*LW*
Mean	0.01783	0.01608		Mean	0.01604	0.01418
Variance	0.00012	4.7E-05		Variance	0.00027	7.7E-05
Observations	11	4		Observations	11	11
Hypothesized Mean Difference	0			Hypothesized Mean Difference	0	
df	9			df	15	
t Stat	0.36546			t Stat	0.32784	
P(T<=t) one-tail	0.3616			P(T<=t) one-tail	0.37378	
t Critical one-tail	1.83311			t Critical one-tail	1.75305	
P(T<=t) two-tail	0.72321			P(T<=t) two-tail	0.74757	
t Critical two-tail	2.26216			t Critical two-tail	2.13145	
t-Test: Two-Sample Assuming Unequal Variances						
10	*EW*	*LW*				
Mean	0.01703	0.01596				
Variance	0.00027	4.9E-05				
Observations	12	4				
Hypothesized Mean Difference	0					
df	13					
t Stat	0.18143					
P(T<=t) one-tail	0.42941					
t Critical one-tail	1.77093					
P(T<=t) two-tail	0.85883					
t Critical two-tail	2.16037					

Table 15. t-Test of differences in change in temperature - mixed aggregates, 10 Hz.

IR - 10 Hz					
t-Test: Two-Sample Assuming Unequal Variances			t-Test: Two-Sample Assuming Unequal Variances		
1	*LW*	*EW*	*200*	*LW*	*EW*
Mean	0.0034	0.0307	Mean	-0.0306	-0.0398
Variance	0.0016	0.0016	Variance	0.0050	0.0098
Observations	19	12	Observations	45	28
Hypothesized Mean Difference	0		Hypothesized Mean Difference	0	
df	23		df	44	
t Stat	-1.853		t Stat	0.429	
P(T<=t) one-tail	0.038		P(T<=t) one-tail	0.335	
t Critical one-tail	1.714		t Critical one-tail	1.680	
P(T<=t) two-tail	0.077		P(T<=t) two-tail	0.670	
t Critical two-tail	2.069		t Critical two-tail	2.015	
t-Test: Two-Sample Assuming Unequal Variances			t-Test: Two-Sample Assuming Unequal Variances		
2	*LW*	*EW*	*500*	*LW*	*EW*
Mean	-0.0456	-0.0504	Mean	-0.0376	0.0133
Variance	0.0037	0.0043	Variance	0.0060	0.0181
Observations	19	12	Observations	25	16
Hypothesized Mean Difference	0		Hypothesized Mean Difference	0	
df	22		df	21	
t Stat	0.204		t Stat	-1.375	
P(T<=t) one-tail	0.420		P(T<=t) one-tail	0.092	
t Critical one-tail	1.717		t Critical one-tail	1.721	
P(T<=t) two-tail	0.840		P(T<=t) two-tail	0.184	
t Critical two-tail	2.074		t Critical two-tail	2.080	
t-Test: Two-Sample Assuming Unequal Variances			t-Test: Two-Sample Assuming Unequal Variances		
5	*LW*	*EW*	*1000*	*LW*	*EW*
Mean	-0.0187	-0.0273	Mean	-0.0640	-0.0218
Variance	0.0016	0.0049	Variance	0.0050	0.0140
Observations	19	12	Observations	25	16
Hypothesized Mean Difference	0		Hypothesized Mean Difference	0	
df	16		df	22	
t Stat	0.388		t Stat	-1.286	
P(T<=t) one-tail	0.352		P(T<=t) one-tail	0.106	
t Critical one-tail	1.746		t Critical one-tail	1.717	
P(T<=t) two-tail	0.703		P(T<=t) two-tail	0.212	
t Critical two-tail	2.120		t Critical two-tail	2.074	
t-Test: Two-Sample Assuming Unequal Variances			t-Test: Two-Sample Assuming Unequal Variances		
10	*LW*	*EW*	*5000*	*LW*	*EW*
Mean	-0.0227	-0.0426	Mean	-0.0141	-0.1451
Variance	0.0042	0.0052	Variance	0.0074	0.0139
Observations	19	12	Observations	25	16
Hypothesized Mean Difference	0		Hypothesized Mean Difference	0	
df	22		df	25	
t Stat	0.778		t Stat	0.114	
P(T<=t) one-tail	0.222		P(T<=t) one-tail	0.455	
t Critical one-tail	1.717		t Critical one-tail	1.708	
P(T<=t) two-tail	0.445		P(T<=t) two-tail	0.910	
t Critical two-tail	2.074		t Critical two-tail	2.060	
t-Test: Two-Sample Assuming Unequal Variances			t-Test: Two-Sample Assuming Unequal Variances		
50	*LW*	*EW*	*10,000*	*LW*	*EW*
Mean	-0.0375	-0.0330	Mean	-0.2217	-0.2061
Variance	0.0025	0.0049	Variance	0.0000	0.0138
Observations	19	12	Observations	25	16
Hypothesized Mean Difference	0		Hypothesized Mean Difference	0	
df	18		df	30	
t Stat	-0.195		t Stat	-0.4274	
P(T<=t) one-tail	0.424		P(T<=t) one-tail	0.3361	
t Critical one-tail	1.734		t Critical one-tail	1.6973	
P(T<=t) two-tail	0.847		P(T<=t) two-tail	0.6721	
t Critical two-tail	2.101		t Critical two-tail	2.0423	
t-Test: Two-Sample Assuming Unequal Variances					
100	*Variable 1*	*Variable 2*			
Mean	-0.0222	-0.0143			
Variance	0.0045	0.0091			
Observations	45	28			
Hypothesized Mean Difference	0				
df	43				
t Stat	-0.382				
P(T<=t) one-tail	0.352				
t Critical one-tail	1.681				
P(T<=t) two-tail	0.705				
t Critical two-tail	2.017				

Table 16. t-Test of differences in change in temperature - mixed aggregates, 30 Hz.

IR - 30 Hz

t-Test: Two-Sample Assuming Unequal Variances

1	LW	EW
Mean	-0.0060	-0.0010
Variance	0.0030	0.0007
Observations	14	9
Hypothesized Mean Difference	0	
df	20	
t Stat	-0.294	
P(T<=t) one-tail	0.386	
t Critical one-tail	1.725	
P(T<=t) two-tail	0.771	
t Critical two-tail	2.086	

t-Test: Two-Sample Assuming Unequal Variances

2	LW	EW
Mean	-0.0590	-0.0440
Variance	0.0033	0.0064
Observations	14	9
Hypothesized Mean Difference	0	
df	13	
t Stat	-0.474	
P(T<=t) one-tail	0.322	
t Critical one-tail	1.771	
P(T<=t) two-tail	0.644	
t Critical two-tail	2.160	

t-Test: Two-Sample Assuming Unequal Variances

5	LW	EW
Mean	-0.0380	-0.0290
Variance	0.0027	0.0046
Observations	14	9
Hypothesized Mean Difference	0	
df	14	
t Stat	-0.340	
P(T<=t) one-tail	0.370	
t Critical one-tail	1.761	
P(T<=t) two-tail	0.739	
t Critical two-tail	2.145	

t-Test: Two-Sample Assuming Unequal Variances

10	LW	EW
Mean	-0.0520	-0.0470
Variance	0.0040	0.0054
Observations	14	9
Hypothesized Mean Difference	0	
df	15	
t Stat	-0.161	
P(T<=t) one-tail	0.437	
t Critical one-tail	1.753	
P(T<=t) two-tail	0.874	
t Critical two-tail	2.131	

t-Test: Two-Sample Assuming Unequal Variances

50	LW	EW
Mean	-0.0390	-0.0350
Variance	0.0038	0.0050
Observations	13	9
Hypothesized Mean Difference	0	
df	16	
t Stat	-0.159	
P(T<=t) one-tail	0.438	
t Critical one-tail	1.746	
P(T<=t) two-tail	0.876	
t Critical two-tail	2.120	

t-Test: Two-Sample Assuming Unequal Variances

100	LW	EW
Mean	-0.0350	-0.0140
Variance	0.0074	0.0082
Observations	40	34
Hypothesized Mean Difference	0	
df	69	
t Stat	-0.163	
P(T<=t) one-tail	0.435	
t Critical one-tail	1.667	
P(T<=t) two-tail	0.871	
t Critical two-tail	1.995	

t-Test: Two-Sample Assuming Unequal Variances

200	LW	EW
Mean	-0.0330	-0.0190
Variance	0.0050	0.0077
Observations	40	34
Hypothesized Mean Difference	0	
df	63	
t Stat	0.084	
P(T<=t) one-tail	0.467	
t Critical one-tail	1.669	
P(T<=t) two-tail	0.933	
t Critical two-tail	1.998	

t-Test: Two-Sample Assuming Unequal Variances

500	LW	EW
Mean	-0.0270	-0.0190
Variance	0.0071	0.0095
Observations	26	25
Hypothesized Mean Difference	0	
df	47	
t Stat	0.055	
P(T<=t) one-tail	0.478	
t Critical one-tail	1.678	
P(T<=t) two-tail	0.956	
t Critical two-tail	2.012	

t-Test: Two-Sample Assuming Unequal Variances

1000	LW	EW
Mean	-0.0300	0.0080
Variance	0.0071	0.0097
Observations	26	25
Hypothesized Mean Difference	0	
df	47	
t Stat	-1.005	
P(T<=t) one-tail	0.160	
t Critical one-tail	1.678	
P(T<=t) two-tail	0.320	
t Critical two-tail	2.012	

t-Test: Two-Sample Assuming Unequal Variances

5000	LW	EW
Mean	-0.0680	-0.0320
Variance	0.0105	0.0090
Observations	26	25
Hypothesized Mean Difference	0	
df	49	
t Stat	-0.826	
P(T<=t) one-tail	0.206	
t Critical one-tail	1.677	
P(T<=t) two-tail	0.413	
t Critical two-tail	2.010	

t-Test: Two-Sample Assuming Unequal Variances

10,000	LW	EW
Mean	-0.0820	-0.0620
Variance	0.0169	0.0128
Observations	23	22
Hypothesized Mean Difference	0	
df	43	
t Stat	0.033	
P(T<=t) one-tail	0.487	
t Critical one-tail	1.681	
P(T<=t) two-tail	0.974	
t Critical two-tail	2.017	

Table 17. t-Test of differences in change of temperature - mixed aggregates, 50 Hz.

IR - 50 Hz						
t-Test: Two-Sample Assuming Unequal Variances				t-Test: Two-Sample Assuming Unequal Variances		
1	*LW*	*EW*		*200*	*LW*	*EW*
Mean	-0.0185	-0.01397		Mean	-0.01368	-0.02726
Variance	0.00227	0.00356		Variance	0.00902	0.00609
Observations	10	13		Observations	27	29
Hypothesized Mean Difference	0			Hypothesized Mean Difference	0	
df	21			df	50	
t Stat	-0.20227			t Stat	0.58213	
P(T<=t) one-tail	0.42082			P(T<=t) one-tail	0.28155	
t Critical one-tail	1.72074			t Critical one-tail	1.67591	
P(T<=t) two-tail	0.84165			P(T<=t) two-tail	0.5631	
t Critical two-tail	2.07961			t Critical two-tail	2.00856	
t-Test: Two-Sample Assuming Unequal Variances				t-Test: Two-Sample Assuming Unequal Variances		
2	*LW*	*EW*		*500*	*LW*	*EW*
Mean	-0.04217	-0.05449		Mean	-0.03709	-0.00323
Variance	0.0089	0.00843		Variance	0.00901	0.00525
Observations	10	13		Observations	17	16
Hypothesized Mean Difference	0			Hypothesized Mean Difference	0	
df	19			df	30	
t Stat	0.31406			t Stat	-1.15587	
P(T<=t) one-tail	0.37845			P(T<=t) one-tail	0.12843	
t Critical one-tail	1.72913			t Critical one-tail	1.69726	
P(T<=t) two-tail	0.75689			P(T<=t) two-tail	0.25686	
t Critical two-tail	2.09302			t Critical two-tail	2.04227	
t-Test: Two-Sample Assuming Unequal Variances				t-Test: Two-Sample Assuming Unequal Variances		
5	*LW*	*EW*		*1000*	*LW*	*EW*
Mean	-0.04522	-0.06098		Mean	-0.03686	0.00767
Variance	0.00749	0.00433		Variance	0.01023	0.0053
Observations	10	13		Observations	17	16
Hypothesized Mean Difference	0			Hypothesized Mean Difference	0	
df	16			df	29	
t Stat	0.47897			t Stat	-1.45819	
P(T<=t) one-tail	0.31922			P(T<=t) one-tail	0.07777	
t Critical one-tail	1.74588			t Critical one-tail	1.69913	
P(T<=t) two-tail	0.63844			P(T<=t) two-tail	0.15553	
t Critical two-tail	2.1199			t Critical two-tail	2.04523	
t-Test: Two-Sample Assuming Unequal Variances				t-Test: Two-Sample Assuming Unequal Variances		
10	*LW*	*EW*		*5000*	*LW*	*EW*
Mean	-0.01733	-0.05953		Mean	-0.06098	-0.01806
Variance	0.00556	0.00433		Variance	0.00713	0.00427
Observations	10	13		Observations	17	16
Hypothesized Mean Difference	0			Hypothesized Mean Difference	0	
df	18			df	30	
t Stat	1.4154			t Stat	-1.63862	
P(T<=t) one-tail	0.08701			P(T<=t) one-tail	0.05587	
t Critical one-tail	1.73406			t Critical one-tail	1.69726	
P(T<=t) two-tail	0.17402			P(T<=t) two-tail	0.11174	
t Critical two-tail	2.10092			t Critical two-tail	2.04227	
t-Test: Two-Sample Assuming Unequal Variances				t-Test: Two-Sample Assuming Unequal Variances		
50	*LW*	*EW*		*10,000*	*LW*	*EW*
Mean	-0.0105	-0.04256		Mean	-0.08118	-0.03604
Variance	0.0057	0.00613		Variance	0.01111	0.006
Observations	10	13		Observations	17	16
Hypothesized Mean Difference	0			Hypothesized Mean Difference	0	
df	20			df	29	
t Stat	0.99368			t Stat	-1.40746	
P(T<=t) one-tail	0.16613			P(T<=t) one-tail	0.08496	
t Critical one-tail	1.72472			t Critical one-tail	1.69913	
P(T<=t) two-tail	0.33225			P(T<=t) two-tail	0.16992	
t Critical two-tail	2.08596			t Critical two-tail	2.04523	
t-Test: Two-Sample Assuming Unequal Variances						
100	*LW*	*EW*				
Mean	-0.03422	-0.03454				
Variance	0.00734	0.00566				
Observations	27	29				
Hypothesized Mean Difference	0					
df	52					
t Stat	0.01491					
P(T<=t) one-tail	0.49408					
t Critical one-tail	1.67469					
P(T<=t) two-tail	0.98816					
t Critical two-tail	2.00665					

Table 18. t-Test of differences in change in temperature - mixed aggregates, 100 Hz.

IR - 100 Hz						
t-Test: Two-Sample Assuming Unequal Variances				t-Test: Two-Sample Assuming Unequal Variances		
1	*LW*	*EW*		*200*	*LW*	*EW*
Mean	-0.008	-0.012		Mean	-0.021	-0.024
Variance	0.00154	0.0006		Variance	0.00514	0.0034
Observations	14	9		Observations	26	21
Hypothesized Mean Difference	0			Hypothesized Mean Difference	0	
df	21			df	45	
t Stat	0.30306			t Stat	0.14677	
P(T<=t) one-tail	0.38241			P(T<=t) one-tail	0.44199	
t Critical one-tail	1.72074			t Critical one-tail	1.67943	
P(T<=t) two-tail	0.76482			P(T<=t) two-tail	0.88397	
t Critical two-tail	2.07961			t Critical two-tail	2.0141	
t-Test: Two-Sample Assuming Unequal Variances				t-Test: Two-Sample Assuming Unequal Variances		
2	*LW*	*EW*		*500*	*LW*	*EW*
Mean	-0.049	-0.056		Mean	-0.019	-0.002
Variance	0.0032	0.00561		Variance	0.00345	0.00673
Observations	14	9		Observations	11	11
Hypothesized Mean Difference	0			Hypothesized Mean Difference	0	
df	14			df	18	
t Stat	0.24363			t Stat	-0.55942	
P(T<=t) one-tail	0.40553			P(T<=t) one-tail	0.29139	
t Critical one-tail	1.76131			t Critical one-tail	1.73406	
P(T<=t) two-tail	0.81105			P(T<=t) two-tail	0.58277	
t Critical two-tail	2.14479			t Critical two-tail	2.10092	
t-Test: Two-Sample Assuming Unequal Variances				t-Test: Two-Sample Assuming Unequal Variances		
5	*LW*	*EW*		*1000*	*LW*	*EW*
Mean	-0.04	-0.084		Mean	-0.031	0.006
Variance	0.00501	0.01326		Variance	0.00931	0.00672
Observations	7	4		Observations	12	12
Hypothesized Mean Difference	0			Hypothesized Mean Difference	0	
df	4			df	21	
t Stat	0.69364			t Stat	-0.9995	
P(T<=t) one-tail	0.26304			P(T<=t) one-tail	0.16447	
t Critical one-tail	2.13185			t Critical one-tail	1.72074	
P(T<=t) two-tail	0.52608			P(T<=t) two-tail	0.32893	
t Critical two-tail	2.77645			t Critical two-tail	2.07961	
t-Test: Two-Sample Assuming Unequal Variances				t-Test: Two-Sample Assuming Unequal Variances		
10	*LW*	*EW*		*5000*	*LW*	*EW*
Mean	-0.038	-0.053		Mean	-0.03	-0.002
Variance	0.00194	0.00369		Variance	0.00887	0.01372
Observations	14	9		Observations	12	12
Hypothesized Mean Difference	0			Hypothesized Mean Difference	0	
df	13			df	21	
t Stat	0.66457			t Stat	-0.64332	
P(T<=t) one-tail	0.25897			P(T<=t) one-tail	0.26349	
t Critical one-tail	1.77093			t Critical one-tail	1.72074	
P(T<=t) two-tail	0.51794			P(T<=t) two-tail	0.52698	
t Critical two-tail	2.16037			t Critical two-tail	2.07961	
t-Test: Two-Sample Assuming Unequal Variances				t-Test: Two-Sample Assuming Unequal Variances		
50	*LW*	*EW*		*10,000*	*LW*	*EW*
Mean	-0.042	-0.051		Mean	-0.03	-0.003
Variance	0.00249	0.00228		Variance	0.00621	0.00851
Observations	14	9		Observations	11	12
Hypothesized Mean Difference	0			Hypothesized Mean Difference	0	
df	18			df	21	
t Stat	0.42921			t Stat	-0.75945	
P(T<=t) one-tail	0.33643			P(T<=t) one-tail	0.22801	
t Critical one-tail	1.73406			t Critical one-tail	1.72074	
P(T<=t) two-tail	0.67286			P(T<=t) two-tail	0.45602	
t Critical two-tail	2.10092			t Critical two-tail	2.07961	
t-Test: Two-Sample Assuming Unequal Variances						
100	*LW*	*EW*				
Mean	-0.041	-0.042				
Variance	0.00741	0.00725				
Observations	26	21				
Hypothesized Mean Difference	0					
df	43					
t Stat	0.03582					
P(T<=t) one-tail	0.48579					
t Critical one-tail	1.68107					
P(T<=t) two-tail	0.97159					
t Critical two-tail	2.01669					

Table 19. t-Test of change in temperature - pure aggregates, 10 Hz.

Experiment 1 - 10 Hz						
t-Test: Two-Sample Assuming Unequal Variances				t-Test: Two-Sample Assuming Unequal Variances		
1	*LW*	*EW*		*200*	*LW*	*EW*
Mean	0.002	0.024		Mean	-0.014	-0.014
Variance	0.0004	0.005		Variance	0.0019	0.001
Observations	5	8		Observations	9	15
Hypothesized Mean Difference	0			Hypothesized Mean Difference	0	
df	9			df	10	
t Stat	-0.81539			t Stat	0.03366	
P(T<=t) one-tail	0.21795			P(T<=t) one-tail	0.48691	
t Critical one-tail	1.83311			t Critical one-tail	1.81246	
P(T<=t) two-tail	0.4359			P(T<=t) two-tail	0.97381	
t Critical two-tail	2.26216			t Critical two-tail	2.22814	
t-Test: Two-Sample Assuming Unequal Variances				t-Test: Two-Sample Assuming Unequal Variances		
2	*LW*	*EW*		*500*	*LW*	*EW*
Mean	-0.021	-0.022		Mean	-0.019	0.011
Variance	0.0005	0.0000		Variance	0.0017	0.002
Observations	5	8		Observations	4	7
Hypothesized Mean Difference	0			Hypothesized Mean Difference	0	
df	8			df	7	
t Stat	0.13911			t Stat	-1.1393	
P(T<=t) one-tail	0.4464			P(T<=t) one-tail	0.14603	
t Critical one-tail	1.85955			t Critical one-tail	1.89458	
P(T<=t) two-tail	0.8928			P(T<=t) two-tail	0.29206	
t Critical two-tail	2.30601			t Critical two-tail	2.36462	
t-Test: Two-Sample Assuming Unequal Variances				t-Test: Two-Sample Assuming Unequal Variances		
10	*LW*	*EW*		*1000*	*LW*	*EW*
Mean	-0.023	-0.029		Mean	-0.038	-0.005
Variance	0.0018	0.001		Variance	0.0018	0.001
Observations	5	8		Observations	4	7
Hypothesized Mean Difference	0			Hypothesized Mean Difference	0	
df	6			df	4	
t Stat	0.2793			t Stat	-1.38727	
P(T<=t) one-tail	0.3947			P(T<=t) one-tail	0.11882	
t Critical one-tail	1.94318			t Critical one-tail	2.13185	
P(T<=t) two-tail	0.78939			P(T<=t) two-tail	0.23765	
t Critical two-tail	2.44691			t Critical two-tail	2.77645	
t-Test: Two-Sample Assuming Unequal Variances				t-Test: Two-Sample Assuming Unequal Variances		
50	*LW*	*EW*		*5000*	*LW*	*EW*
Mean	-0.013	-0.014		Mean	-0.059	-0.064
Variance	0.0002	0.0000		Variance	0.0009	0.001
Observations	5	8		Observations	4	7
Hypothesized Mean Difference	0			Hypothesized Mean Difference	0	
df	9			df	8	
t Stat	0.09417			t Stat	0.25312	
P(T<=t) one-tail	0.46352			P(T<=t) one-tail	0.40328	
t Critical one-tail	1.83311			t Critical one-tail	1.85955	
P(T<=t) two-tail	0.92703			P(T<=t) two-tail	0.80656	
t Critical two-tail	2.26216			t Critical two-tail	2.30601	
t-Test: Two-Sample Assuming Unequal Variances				t-Test: Two-Sample Assuming Unequal Variances		
100	*LW*	*EW*		*10,000*	*LW*	*EW*
Mean	-0.013	-0.011		Mean	-0.134	-0.129
Variance	0.001	0.001		Variance	0.0006	0.003
Observations	4	7		Observations	4	7
Hypothesized Mean Difference	0			Hypothesized Mean Difference	0	
df	7			df	9	
t Stat	-0.00517			t Stat	-0.21219	
P(T<=t) one-tail	0.49801			P(T<=t) one-tail	0.41834	
t Critical one-tail	1.89458			t Critical one-tail	1.83311	
P(T<=t) two-tail	0.99602			P(T<=t) two-tail	0.83669	
t Critical two-tail	2.36462			t Critical two-tail	2.26216	

Table 20. t-Test of differences in change in temperature - pure aggregates, 50 Hz.

Experiment 1 - 50 Hz					
t-Test: Two-Sample Assuming Unequal Variances			t-Test: Two-Sample Assuming Unequal Variances		
1	*LW*	*EW*	*200*	*LW*	*EW*
Mean	-0.019	-0.008	Mean	-0.013	-0.007
Variance	0.00008	0.00032	Variance	0.00129	0.00075
Observations	8	7	Observations	16	17
Hypothesized Mean Difference	0		Hypothesized Mean Difference	0	
df	9		df	28	
t Stat	-1.39562		t Stat	-0.5327	
P(T<=t) one-tail	0.09815		P(T<=t) one-tail	0.29922	
t Critical one-tail	1.83311		t Critical one-tail	1.70113	
P(T<=t) two-tail	0.1963		P(T<=t) two-tail	0.59845	
t Critical two-tail	2.26216		t Critical two-tail	2.04841	
t-Test: Two-Sample Assuming Unequal Variances			t-Test: Two-Sample Assuming Unequal Variances		
2	*LW*	*EW*	*500*	*LW*	*EW*
Mean	-0.029	-0.032	Mean	-0.01	-0.005
Variance	0.00126	0.0003	Variance	0.00186	0.00093
Observations	8	7	Observations	8	10
Hypothesized Mean Difference	0		Hypothesized Mean Difference	0	
df	10		df	12	
t Stat	0.18759		t Stat	-0.29189	
P(T<=t) one-tail	0.42747		P(T<=t) one-tail	0.38768	
t Critical one-tail	1.81246		t Critical one-tail	1.78229	
P(T<=t) two-tail	0.85495		P(T<=t) two-tail	0.77535	
t Critical two-tail	2.22814		t Critical two-tail	2.17881	
t-Test: Two-Sample Assuming Unequal Variances			t-Test: Two-Sample Assuming Unequal Variances		
5	*LW*	*EW*	*1000*	*LW*	*EW*
Mean	-0.039	-0.043	Mean	-0.014	-0.002
Variance	0.00167	0.00074	Variance	0.00079	0.00114
Observations	8	7	Observations	8	10
Hypothesized Mean Difference	0		Hypothesized Mean Difference	0	
df	12		df	16	
t Stat	0.19976		t Stat	-0.82613	
P(T<=t) one-tail	0.42251		P(T<=t) one-tail	0.21044	
t Critical one-tail	1.78229		t Critical one-tail	1.74588	
P(T<=t) two-tail	0.84501		P(T<=t) two-tail	0.42088	
t Critical two-tail	2.17881		t Critical two-tail	2.1199	
t-Test: Two-Sample Assuming Unequal Variances			t-Test: Two-Sample Assuming Unequal Variances		
10	*LW*	*EW*	*5000*	*LW*	*EW*
Mean	-0.02	-0.034	Mean	-0.023	-0.008
Variance	0.00062	0.00036	Variance	0.00126	0.00052
Observations	8	7	Observations	8	10
Hypothesized Mean Difference	0		Hypothesized Mean Difference	0	
df	13		df	11	
t Stat	1.1834		t Stat	-1.00955	
P(T<=t) one-tail	0.12892		P(T<=t) one-tail	0.1672	
t Critical one-tail	1.77093		t Critical one-tail	1.79588	
P(T<=t) two-tail	0.25784		P(T<=t) two-tail	0.3344	
t Critical two-tail	2.16037		t Critical two-tail	2.20099	
t-Test: Two-Sample Assuming Unequal Variances			t-Test: Two-Sample Assuming Unequal Variances		
50	*LW*	*EW*	*10,000*	*LW*	*EW*
Mean	-0.018	-0.02	Mean	-0.039	-0.013
Variance	0.00041	0.00058	Variance	0.0006	0.00028
Observations	8	7	Observations	8	10
Hypothesized Mean Difference	0		Hypothesized Mean Difference	0	
df	12		df	12	
t Stat	0.11087		t Stat	-2.56223	
P(T<=t) one-tail	0.45678		P(T<=t) one-tail	0.01245	
t Critical one-tail	1.78229		t Critical one-tail	1.78229	
P(T<=t) two-tail	0.91355		P(T<=t) two-tail	0.0249	
t Critical two-tail	2.17881		t Critical two-tail	2.17881	
t-Test: Two-Sample Assuming Unequal Variances					
100	*LW*	*EW*			
Mean	-0.019	-0.008			
Variance	0.00333	0.00098			
Observations	8	10			
Hypothesized Mean Difference	0				
df	10				
t Stat	-0.47366				
P(T<=t) one-tail	0.32296				
t Critical one-tail	1.81246				
P(T<=t) two-tail	0.64592				
t Critical two-tail	2.22814				

Table 21. t-Test of difference in change in temperature - pure aggregates, 100 Hz.

Experiment 1 - 100 Hz					
t-Test: Two-Sample Assuming Unequal Variances			t-Test: Two-Sample Assuming Unequal Variances		
1	*LW*	*EW*	*200*	*LW*	*EW*
Mean	-0.022	-0.018	Mean	-0.019	-0.015
Variance	0.0001	0.0002	Variance	0.0009	0.001
Observations	8	5	Observations	16	13
Hypothesized Mean Difference	0		Hypothesized Mean Difference	0	
df	7		df	25	
t Stat	-0.48267		t Stat	-0.31229	
P(T<=t) one-tail	0.32203		P(T<=t) one-tail	0.3787	
t Critical one-tail	1.89458		t Critical one-tail	1.70814	
P(T<=t) two-tail	0.64406		P(T<=t) two-tail	0.75741	
t Critical two-tail	2.36462		t Critical two-tail	2.05954	
t-Test: Two-Sample Assuming Unequal Variances			t-Test: Two-Sample Assuming Unequal Variances		
2	*LW*	*EW*	*500*	*LW*	*EW*
Mean	-0.044	-0.025	Mean	-0.017	-0.001
Variance	0.0003	0.0005	Variance	0.0004	0.001
Observations	8	5	Observations	8	8
Hypothesized Mean Difference	0		Hypothesized Mean Difference	0	
df	7		df	11	
t Stat	-1.69735		t Stat	-1.21677	
P(T<=t) one-tail	0.06672		P(T<=t) one-tail	0.12458	
t Critical one-tail	1.89458		t Critical one-tail	1.79588	
P(T<=t) two-tail	0.13344		P(T<=t) two-tail	0.24915	
t Critical two-tail	2.36462		t Critical two-tail	2.20099	
t-Test: Two-Sample Assuming Unequal Variances			t-Test: Two-Sample Assuming Unequal Variances		
5	*LW*	*EW*	*1000*	*LW*	*EW*
Mean	-0.034	-0.039	Mean	-0.01	0.001
Variance	0.0005	0.0008	Variance	0.0021	0.0005
Observations	8	5	Observations	8	8
Hypothesized Mean Difference	0		Hypothesized Mean Difference	0	
df	7		df	10	
t Stat	0.296		t Stat	-0.59808	
P(T<=t) one-tail	0.38791		P(T<=t) one-tail	0.28154	
t Critical one-tail	1.89458		t Critical one-tail	1.81246	
P(T<=t) two-tail	0.77582		P(T<=t) two-tail	0.56309	
t Critical two-tail	2.36462		t Critical two-tail	2.22814	
t-Test: Two-Sample Assuming Unequal Variances			t-Test: Two-Sample Assuming Unequal Variances		
10	*LW*	*EW*	*5000*	*LW*	*EW*
Mean	-0.033	-0.039	Mean	-0.013	-0.004
Variance	0.0016	0.0004	Variance	0.0017	0.0004
Observations	8	5	Observations	8	8
Hypothesized Mean Difference	0		Hypothesized Mean Difference	0	
df	11		df	10	
t Stat	0.38781		t Stat	-0.56646	
P(T<=t) one-tail	0.35278		P(T<=t) one-tail	0.29179	
t Critical one-tail	1.79588		t Critical one-tail	1.81246	
P(T<=t) two-tail	0.70555		P(T<=t) two-tail	0.58357	
t Critical two-tail	2.20099		t Critical two-tail	2.22814	
t-Test: Two-Sample Assuming Unequal Variances			t-Test: Two-Sample Assuming Unequal Variances		
50	*LW*	*EW*	*10,000*	*LW*	*EW*
Mean	-0.032	-0.035	Mean	-0.018	-0.005
Variance	0.0016	0.0007	Variance	0.0014	0.0001
Observations	8	5	Observations	8	8
Hypothesized Mean Difference	0		Hypothesized Mean Difference	0	
df	11		df	8	
t Stat	0.16372		t Stat	-0.92412	
P(T<=t) one-tail	0.43646		P(T<=t) one-tail	0.19123	
t Critical one-tail	1.79588		t Critical one-tail	1.85955	
P(T<=t) two-tail	0.87292		P(T<=t) two-tail	0.38245	
t Critical two-tail	2.20099		t Critical two-tail	2.30601	
t-Test: Two-Sample Assuming Unequal Variances					
100	*LW*	*EW*			
Mean	-0.02	-0.015			
Variance	0.0013	0.0018			
Observations	8	8			
Hypothesized Mean Difference	0				
df	14				
t Stat	-0.25263				
P(T<=t) one-tail	0.40211				
t Critical one-tail	1.76131				
P(T<=t) two-tail	0.80423				
t Critical two-tail	2.14479				

Table 22. t-Test of differences due to frequency - pure, air-dried.

Experiment 4						
t-Test: Two-Sample Assuming Unequal Variances				t-Test: Two-Sample Assuming Unequal Variances		
10	*50 Hz*	*10 Hz*		*500*	*50 Hz*	*10 Hz*
Mean	0.02635	0.05496		Mean	0.10896	0.04248
Variance	0.00177	0.00149		Variance	0.00258	0.00183
Observations	16	14		Observations	16	14
Hypothesized Mean Difference	0			Hypothesized Mean Difference	0	
df	28			df	28	
t Stat	-1.93957			t Stat	3.8936	
P(T<=t) one-tail	0.03128			P(T<=t) one-tail	0.00028	
t Critical one-tail	1.70113			t Critical one-tail	1.70113	
P(T<=t) two-tail	0.06257			P(T<=t) two-tail	0.00056	
t Critical two-tail	2.04841			t Critical two-tail	2.04841	
t-Test: Two-Sample Assuming Unequal Variances				t-Test: Two-Sample Assuming Unequal Variances		
20	*50 Hz*	*10 Hz*		*1000*	*50 Hz*	*10 Hz*
Mean	0.03288	0.05353		Mean	0.12708	0.06679
Variance	0.00215	0.00102		Variance	0.00287	0.0021
Observations	16	14		Observations	8	14
Hypothesized Mean Difference	0			Hypothesized Mean Difference	0	
df	27			df	13	
t Stat	-1.43417			t Stat	2.67405	
P(T<=t) one-tail	0.0815			P(T<=t) one-tail	0.00956	
t Critical one-tail	1.70329			t Critical one-tail	1.77093	
P(T<=t) two-tail	0.163			P(T<=t) two-tail	0.01912	
t Critical two-tail	2.05183			t Critical two-tail	2.16037	
t-Test: Two-Sample Assuming Unequal Variances				t-Test: Two-Sample Assuming Unequal Variances		
50	*50 Hz*	*10 Hz*		*2000*	*50 Hz*	*10 Hz*
Mean	0.01441	0.04516		Mean	0.12618	0.08679
Variance	0.00161	0.00139		Variance	0.00226	0.00195
Observations	16	14		Observations	16	14
Hypothesized Mean Difference	0			Hypothesized Mean Difference	0	
df	28			df	28	
t Stat	-2.17545			t Stat	2.35095	
P(T<=t) one-tail	0.0191			P(T<=t) one-tail	0.013	
t Critical one-tail	1.70113			t Critical one-tail	1.70113	
P(T<=t) two-tail	0.0382			P(T<=t) two-tail	0.026	
t Critical two-tail	2.04841			t Critical two-tail	2.04841	
t-Test: Two-Sample Assuming Unequal Variances						
100	*50 Hz*	*10 Hz*				
Mean	0.05076	0.04655				
Variance	0.00057	0.0006				
Observations	8	14				
Hypothesized Mean Difference	0					
df	15					
t Stat	0.39461					
P(T<=t) one-tail	0.34934					
t Critical one-tail	1.75305					
P(T<=t) two-tail	0.69868					
t Critical two-tail	2.13145					

Table 23. t-Test of differences due to frequency - pure, no fiber work.

Experiment 6						
t-Test: Two-Sample Assuming Unequal Variances				t-Test: Two-Sample Assuming Unequal Variances		
100	*10 Hz*	*50 Hz*		*5000*	*10 Hz*	*50 Hz*
Mean	-0.01712	-0.00587		Mean	-0.159	-0.153
Variance	0.00071	0.00048		Variance	0.00179	0.02646
Observations	17	14		Observations	17	7
Hypothesized Mean Difference	0			Hypothesized Mean Difference	0	
df	29			df	9	
t Stat	-1.28728			t Stat	6.44385	
P(T<=t) one-tail	0.10409			P(T<=t) one-tail	5.9E-05	
t Critical one-tail	1.69913			t Critical one-tail	1.83311	
P(T<=t) two-tail	0.20818			P(T<=t) two-tail	0.00012	
t Critical two-tail	2.04523			t Critical two-tail	2.26216	
t-Test: Two-Sample Assuming Unequal Variances				t-Test: Two-Sample Assuming Unequal Variances		
500	*10 Hz*	*50 Hz*		*10,000*	*10 Hz*	*50 Hz*
Mean	-0.048	-0.063		Mean	-0.157	-0.227
Variance	0.00092	0.00515		Variance	0.0014	0.02578
Observations	17	14		Observations	17	14
Hypothesized Mean Difference	0			Hypothesized Mean Difference	0	
df	17			df	14	
t Stat	0.74537			t Stat	1.59612	
P(T<=t) one-tail	0.23312			P(T<=t) one-tail	0.06639	
t Critical one-tail	1.73961			t Critical one-tail	1.76131	
P(T<=t) two-tail	0.46623			P(T<=t) two-tail	0.13278	
t Critical two-tail	2.10982			t Critical two-tail	2.14479	
t-Test: Two-Sample Assuming Unequal Variances						
1000	*10 Hz*	*50 Hz*				
Mean	-0.099	-0.114				
Variance	0.00151	0.00706				
Observations	17	14				
Hypothesized Mean Difference	0					
df	18					
t Stat	0.62878					
P(T<=t) one-tail	0.2687					
t Critical one-tail	1.73406					
P(T<=t) two-tail	0.53739					
t Critical two-tail	2.10092					

APPENDIX 6: OTHER INFRARED TESTING AND ANALYSIS

Pure aggregates – Oven-dried

Other infrared testing was done to show heating. Oven-dried fibers were cycled at 10 and 50 hertz. As can be seen in Figure 49-50, there were significant differences in temperature increase between the two frequencies (Table 23). A higher frequency caused a faster and higher temperature increase. Internal friction of the dry fibers may be higher at the higher frequency.

Pure aggregates - Wet and Dry

Testing examined whether evaporation did cause cooling when there was no cycling. Fiber aggregates (45% consistency) were placed in the sample chamber and placed in position under the piston. Images were taken a various times over a 20-minute period. Figure 57 shows that the infrared camera saw evaporational cooling.

If evaporation causes cooling, then absorption of water into the fiber should cause the fiber to heat. Oven dried fibers were placed in the sample chamber, and the block placed under the piston. The piston was not cycled. Images were collected for 20 minutes. There is a temperature rise from water absorption into a fiber (Figure 57). Table 24 shows the t-test and significant differences in temperature between wet and oven-dried aggregates, with no cycling.

PEG Fiber Aggregates

A few fiber aggregates that had their intra-fiber water exchanged for polyethylene glycol were cycled at 10 hertz. If evaporation was stopped then the temperature decrease would also be stopped if only evaporation was cooling the fibers. This technique did not work well because the PEG coated the sapphire window where the fibers touched, obscuring any acquisition of IR radiation. The data points seen in Figure 58 are from whole image averaging done by Spyglass Transform. The data points may be showing a trend towards increasing to higher temperatures but it can not be stated with any certainty with only two images of data.

Mixed aggregates - 200 Hz

This is the data gathered during the initial infrared testing with mixed fiber aggregates at 45% consistency. The data is included in the Appendix because of the already stated problems with technique. The aggregates were at the normal 45% consistency, but when cycling began water started to appear on the sapphire window. By the time the sequence was finished there was enough water on the window that the UV light difference technique could not tell the difference between the fiber types. Therefore, the data was pooled for earlywood and latewood fiber types. This would give an adequate estimate because the other frequencies showed no differences between the earlywood and latewood fiber types. The data was analyzed, but it was hard to find the same fibers, due to the water on the window obscuring the fibers. Figure 59 shows the gathered data. These are the only images where temperature increased; therefore, the water on the window caused an apparently faulty temperature reading. Water has a much larger emissivity that wet fibers (0.96 vs. 0.65 (60)). The emissivity is the thermal energy radiated by an object relative to that of a black body at the same temperature. When the water is calibrated with the same calibration for wet fibers, the water on the window will show higher temperatures than actual.

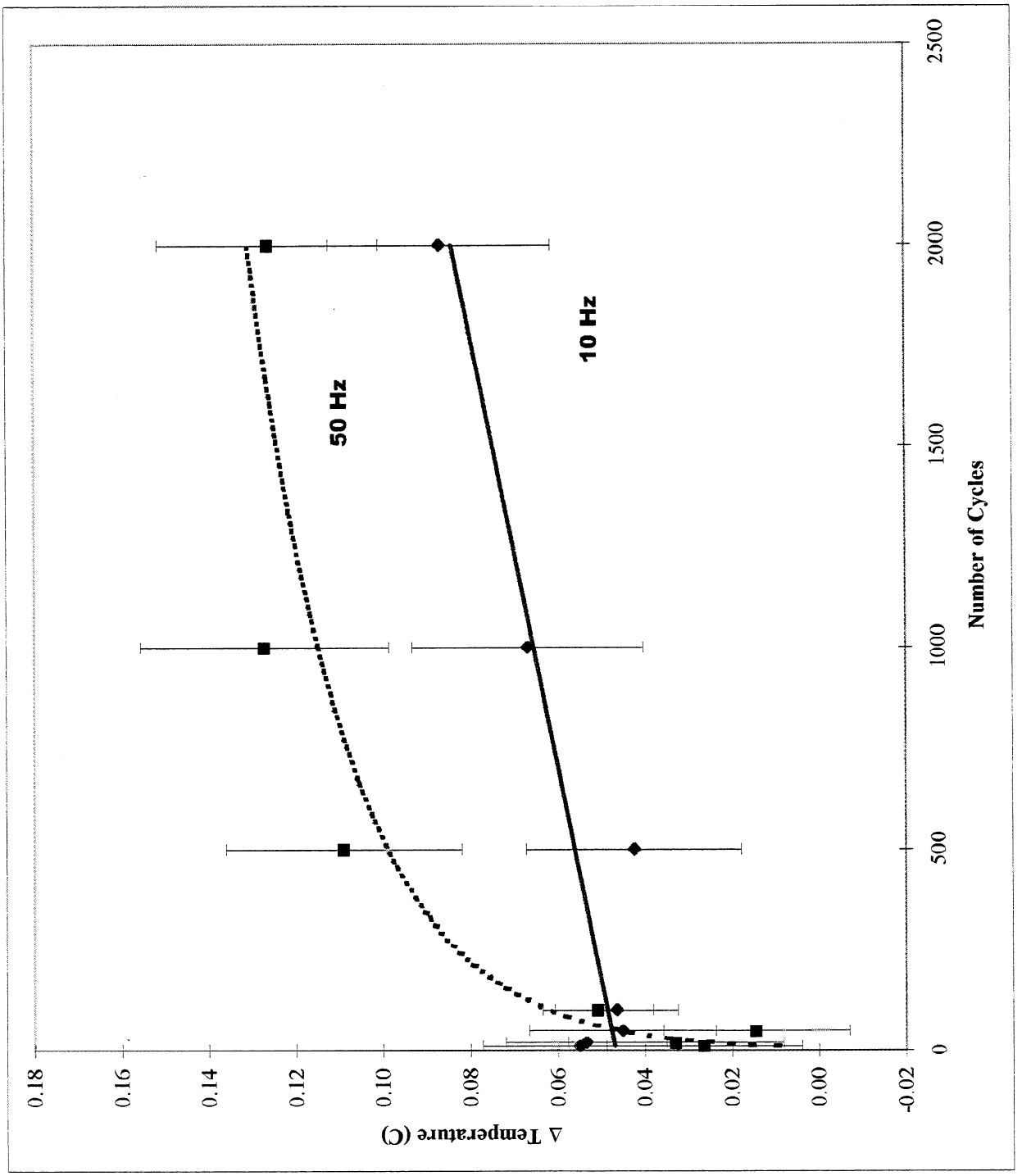

Figure 55. Pure aggregates – oven-dried, 10 and 50 Hz.

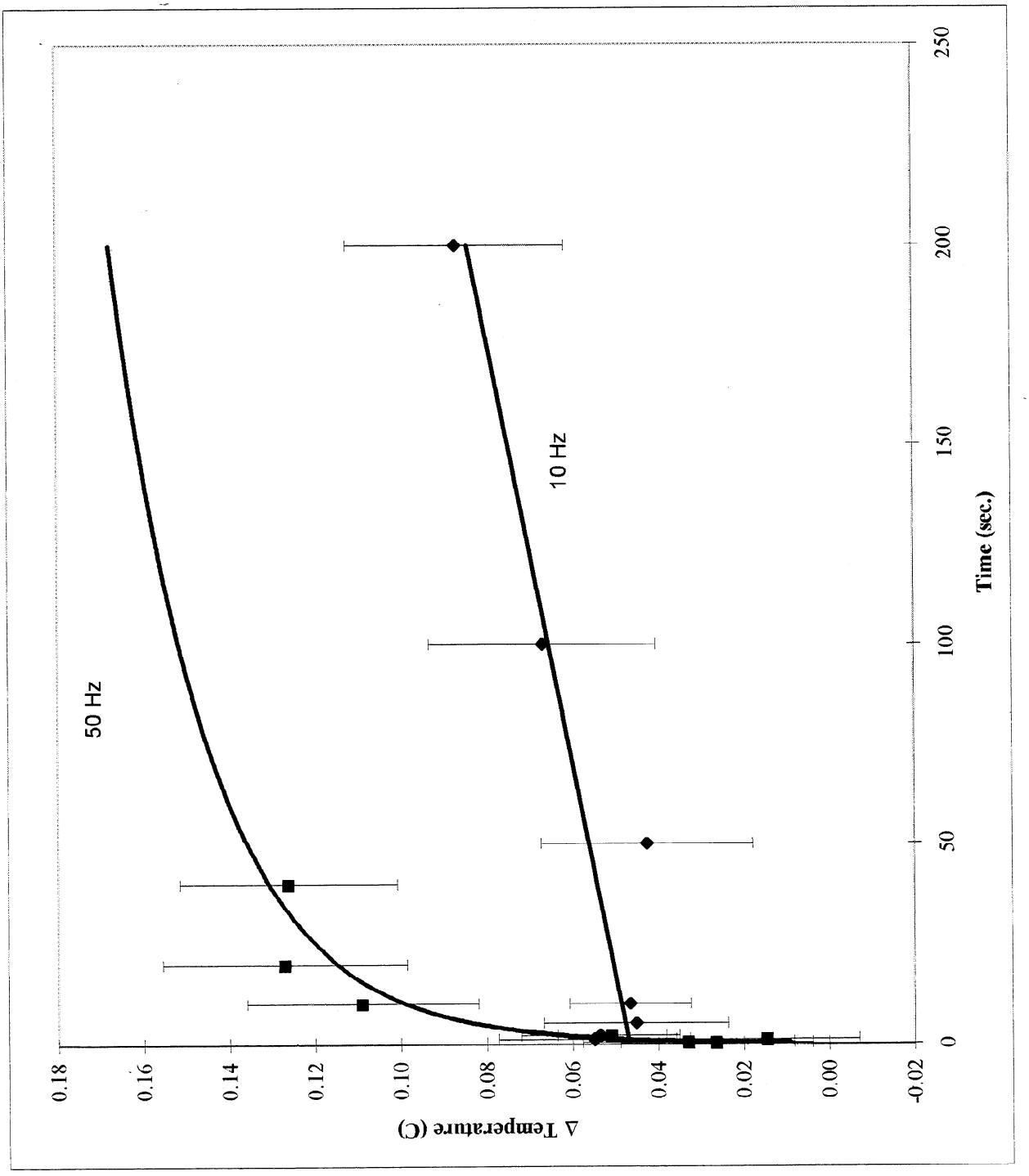

Figure 56. Pure aggregates - oven dried, 10 and 50 Hz, time basis.

Table 24. t-Test of difference in change in temperature due to frequency.

Experiment 3						
t-Test: Two-Sample Assuming Unequal Variances				t-Test: Two-Sample Assuming Unequal Variances		
10	*50 Hz*	*10 Hz*		*500*	*50 Hz*	*10 Hz*
Mean	0.04878	0.02025		Mean	0.1563	0.01827
Variance	0.00609	0.0013		Variance	0.0199	0.00208
Observations	15	9		Observations	15	9
Hypothesized Mean Difference	0			Hypothesized Mean Difference	0	
df	21			df	18	
t Stat	1.21649			t Stat	3.4977	
P(T<=t) one-tail	0.11865			P(T<=t) one-tail	0.00128	
t Critical one-tail	1.72074			t Critical one-tail	1.73406	
P(T<=t) two-tail	0.2373			P(T<=t) two-tail	0.00257	
t Critical two-tail	2.07961			t Critical two-tail	2.10092	
t-Test: Two-Sample Assuming Unequal Variances				t-Test: Two-Sample Assuming Unequal Variances		
20	*50 Hz*	*10 Hz*		*1000*	*50 Hz*	*10 Hz*
Mean	0.06044	-0.01		Mean	0.16456	0.02531
Variance	0.00613	0.00115		Variance	0.02479	0.00254
Observations	15	9		Observations	15	9
Hypothesized Mean Difference	0			Hypothesized Mean Difference	0	
df	21			df	18	
t Stat	3.04028			t Stat	3.16556	
P(T<=t) one-tail	0.00311			P(T<=t) one-tail	0.00268	
t Critical one-tail	1.72074			t Critical one-tail	1.73406	
P(T<=t) two-tail	0.00622			P(T<=t) two-tail	0.00535	
t Critical two-tail	2.07961			t Critical two-tail	2.10092	
t-Test: Two-Sample Assuming Unequal Variances				t-Test: Two-Sample Assuming Unequal Variances		
100	*50 Hz*	*10 Hz*		*2000*	*50 Hz*	*10 Hz*
Mean	0.06004	-0.00975		Mean	0.16252	0.05179
Variance	0.00665	0.00144		Variance	0.01679	0.00253
Observations	15	9		Observations	15	9
Hypothesized Mean Difference	0			Hypothesized Mean Difference	0	
df	21			df	20	
t Stat	2.84145			t Stat	2.95864	
P(T<=t) one-tail	0.00489			P(T<=t) one-tail	0.00388	
t Critical one-tail	1.72074			t Critical one-tail	1.72472	
P(T<=t) two-tail	0.00978			P(T<=t) two-tail	0.00777	
t Critical two-tail	2.07961			t Critical two-tail	2.08596	
t-Test: Two-Sample Assuming Unequal Variances						
200	*50 Hz*	*10 Hz*				
Mean	0.08863	0.00926				
Variance	0.00512	0.0017				
Observations	15	9				
Hypothesized Mean Difference	0					
df	22					
t Stat	3.4481					
P(T<=t) one-tail	0.00115					
t Critical one-tail	1.71714					
P(T<=t) two-tail	0.00229					
t Critical two-tail	2.07388					

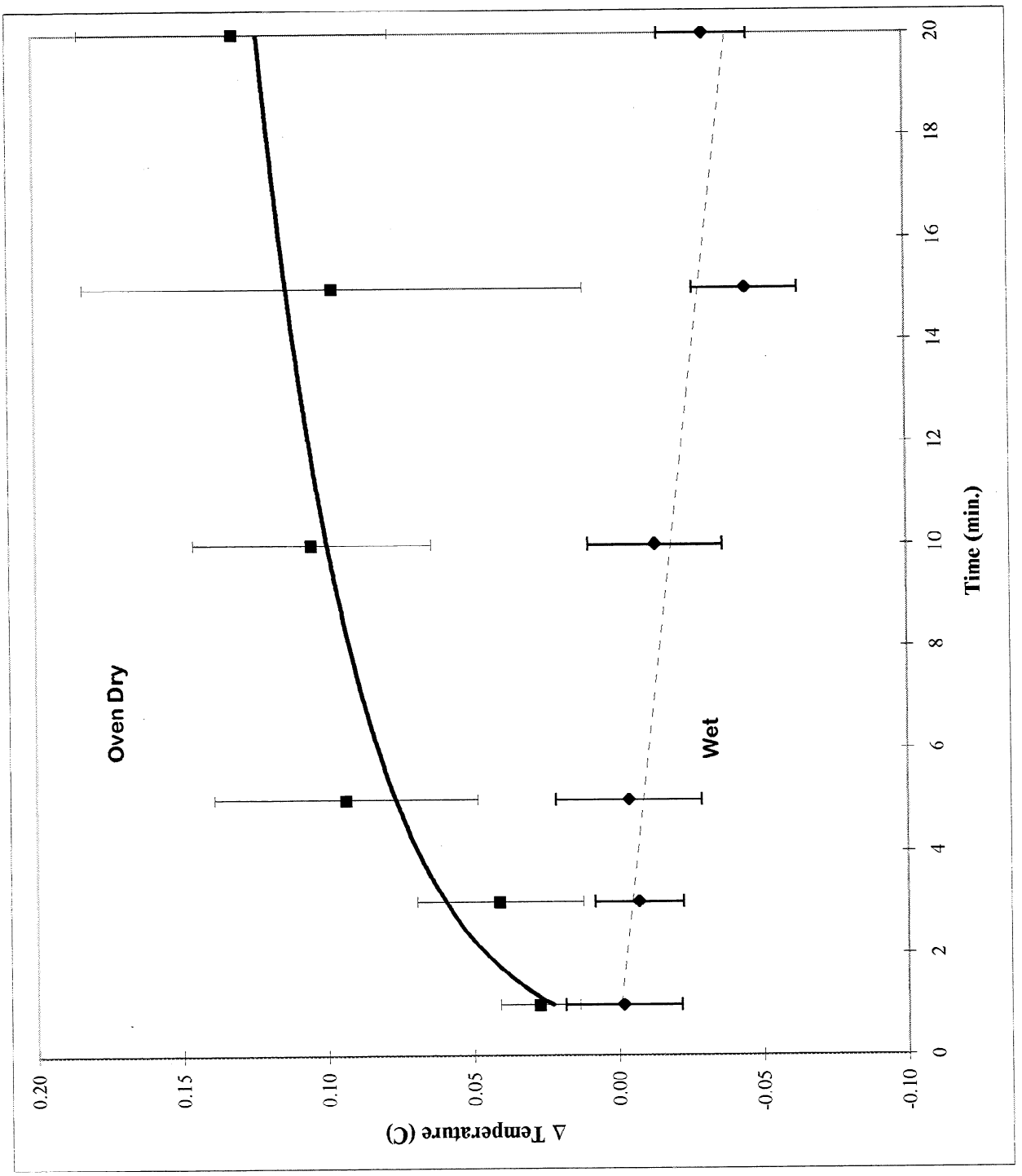

Figure 57. Pure aggregates - wet and dry.

Table 25. t-Test of differences in change in temperature - wet and oven-dry.

Experiment 5						
t-Test: Two-Sample Assuming Unequal Variances				t-Test: Two-Sample Assuming Unequal Variances		
1 min.	*wet*	*dry*		*10 min.*	*wet*	*dry*
Mean	-0.0015	0.027135		Mean	-0.01331	0.104854
Variance	0.001839	0.000811		Variance	0.002461	0.00724
Observations	20	19		Observations	20	19
Hypothesized Mean Differenc	0			Hypothesized Mean Differenc	0	
df	33			df	29	
t Stat	-2.46805			t Stat	-5.26278	
P(T<=t) one-tail	0.00947			P(T<=t) one-tail	6.11E-06	
t Critical one-tail	1.69236			t Critical one-tail	1.699127	
P(T<=t) two-tail	0.01894			P(T<=t) two-tail	1.22E-05	
t Critical two-tail	2.034517			t Critical two-tail	2.045231	
t-Test: Two-Sample Assuming Unequal Variances				t-Test: Two-Sample Assuming Unequal Variances		
3 min.	*wet*	*dry*		*15 min.*	*wet*	*dry*
Mean	-0.007	0.040819		Mean	-0.04489	0.097222
Variance	0.001067	0.003525		Variance	0.001493	0.031986
Observations	20	19		Observations	20	19
Hypothesized Mean Differenc	0			Hypothesized Mean Differenc	0	
df	28			df	20	
t Stat	-3.09415			t Stat	-3.38927	
P(T<=t) one-tail	0.002222			P(T<=t) one-tail	0.001456	
t Critical one-tail	1.70113			t Critical one-tail	1.724718	
P(T<=t) two-tail	0.004444			P(T<=t) two-tail	0.002913	
t Critical two-tail	2.048409			t Critical two-tail	2.085962	
t-Test: Two-Sample Assuming Unequal Variances				t-Test: Two-Sample Assuming Unequal Variances		
5 min.	*wet*	*dry*		*20 min.*	*wet*	*dry*
Mean	-0.00358	0.093626		Mean	-0.03083	0.130965
Variance	0.002897	0.008883		Variance	0.001088	0.012356
Observations	20	19		Observations	20	19
Hypothesized Mean Differenc	0			Hypothesized Mean Differenc	0	
df	28			df	21	
t Stat	-3.92815			t Stat	-6.09501	
P(T<=t) one-tail	0.000255			P(T<=t) one-tail	2.38E-06	
t Critical one-tail	1.70113			t Critical one-tail	1.720744	
P(T<=t) two-tail	0.000509			P(T<=t) two-tail	4.77E-06	
t Critical two-tail	2.048409			t Critical two-tail	2.079614	

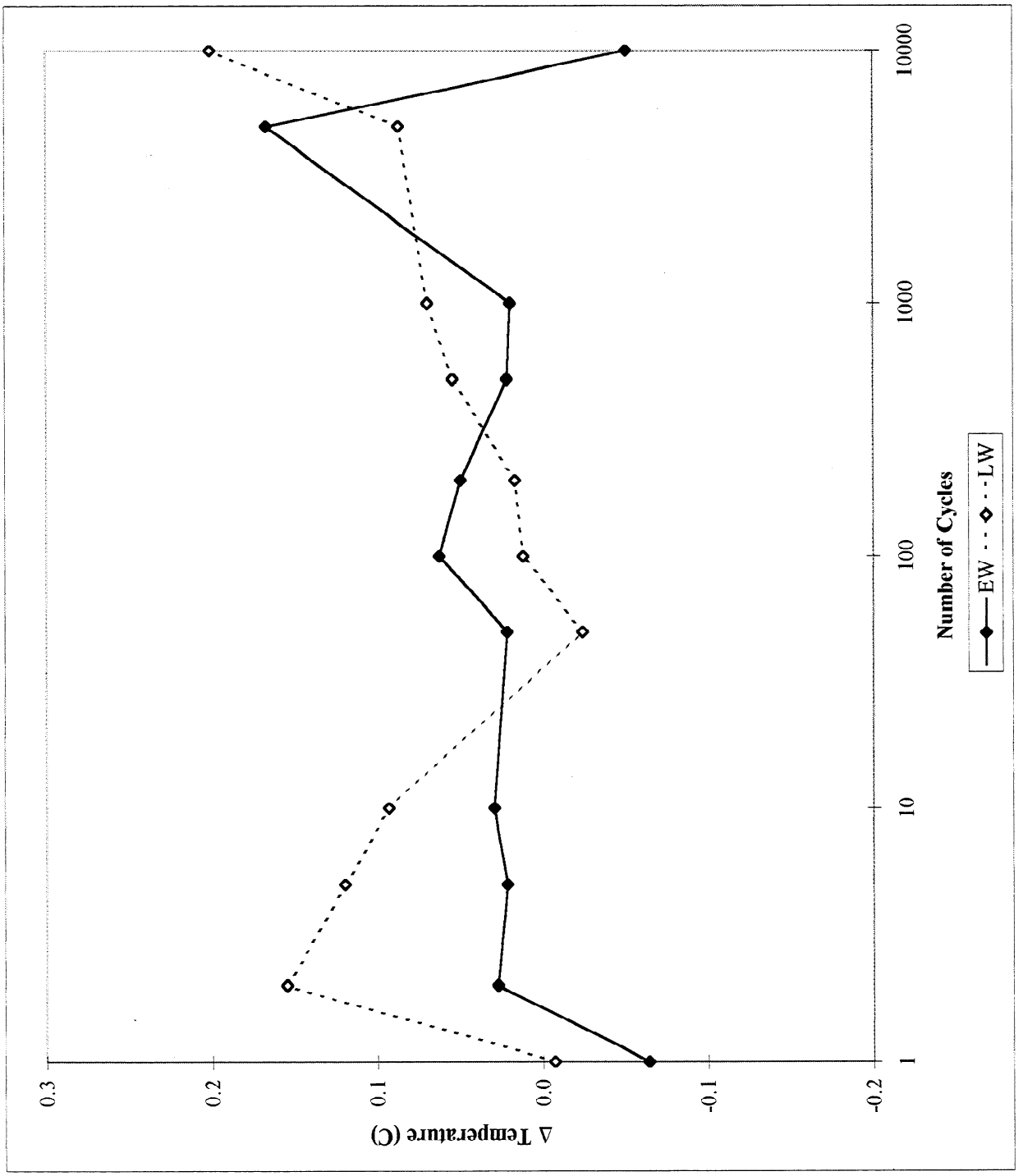

Figure 58. Change in temperature - PEG.

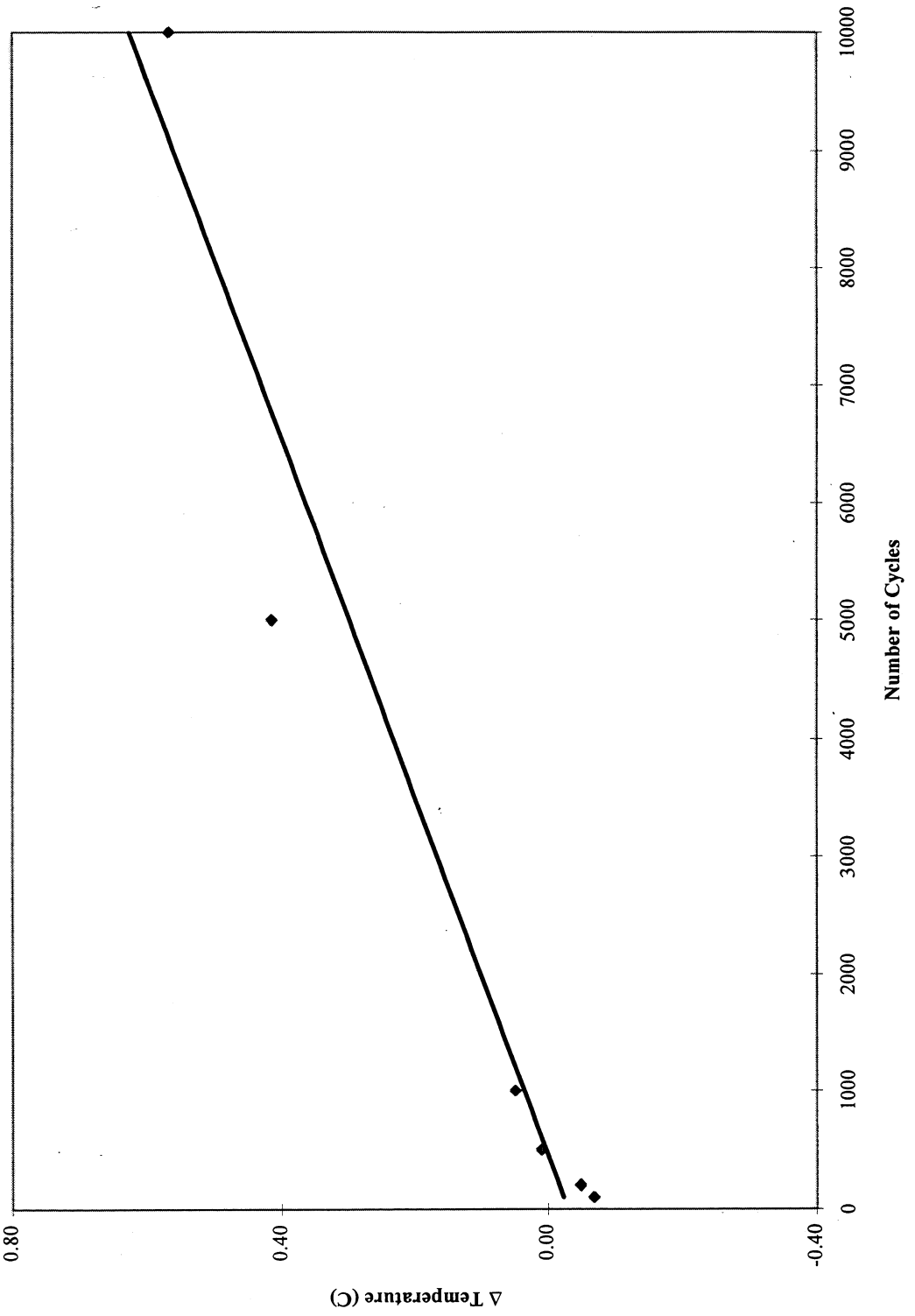

Figure 59. Change in temperature - mixed aggregates, 200 Hz.

APPENDIX 7: OTHER FIGURES

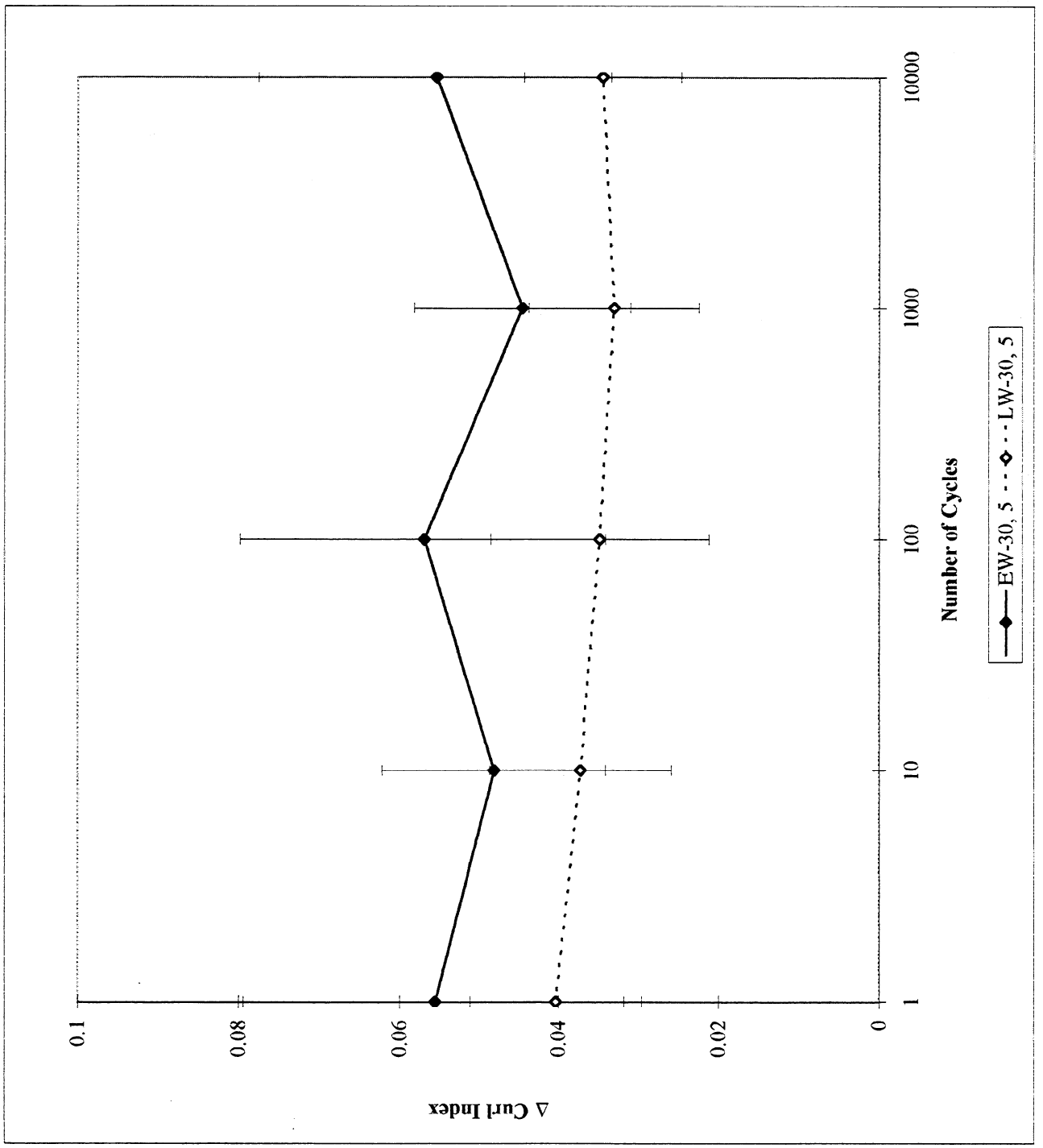

Figure 60. Change in curl index – 30 Hz, 5 mm, MTS.

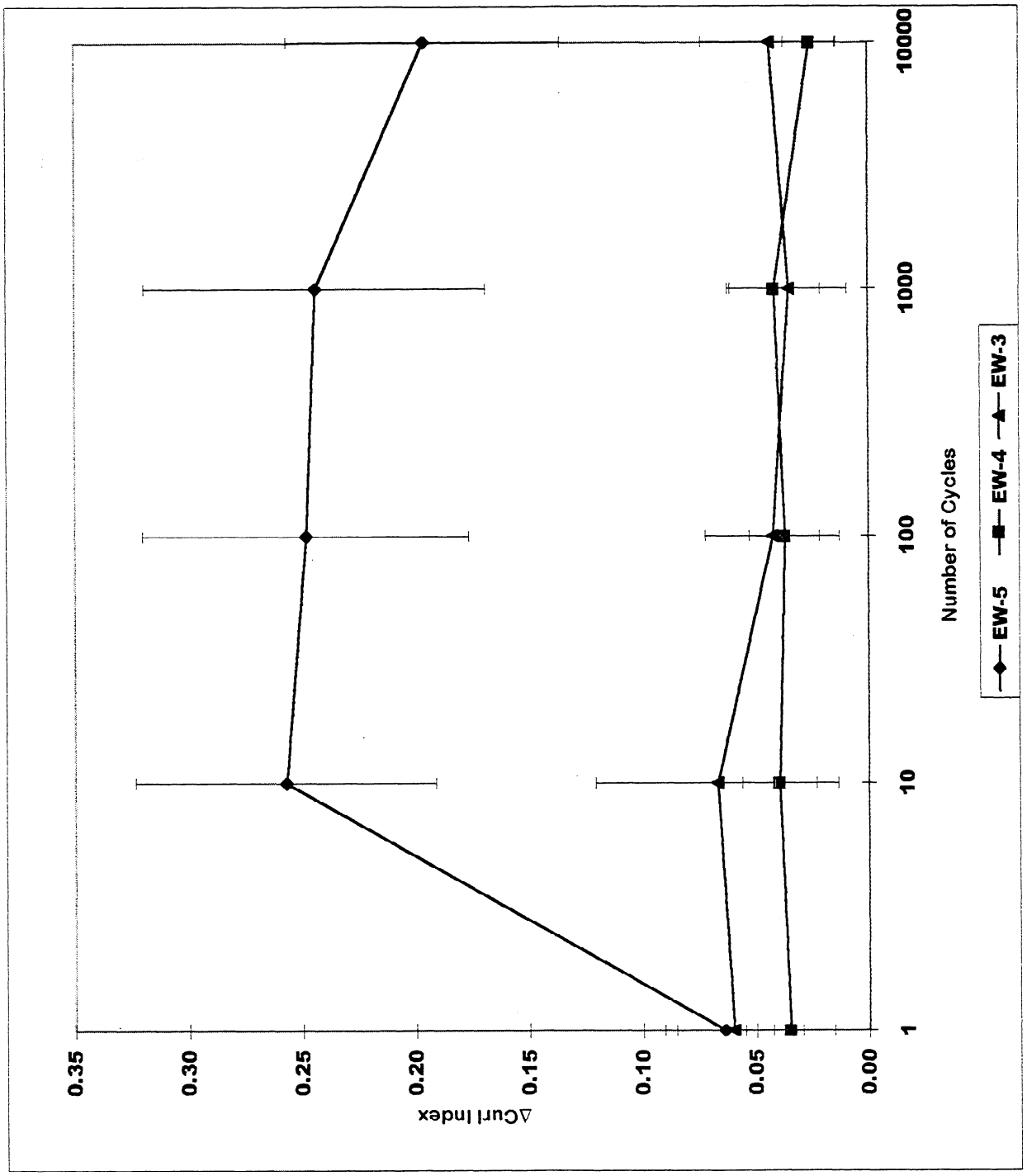

Figure 61. Change in curl index – 10 Hz, Earlywood, MTS.

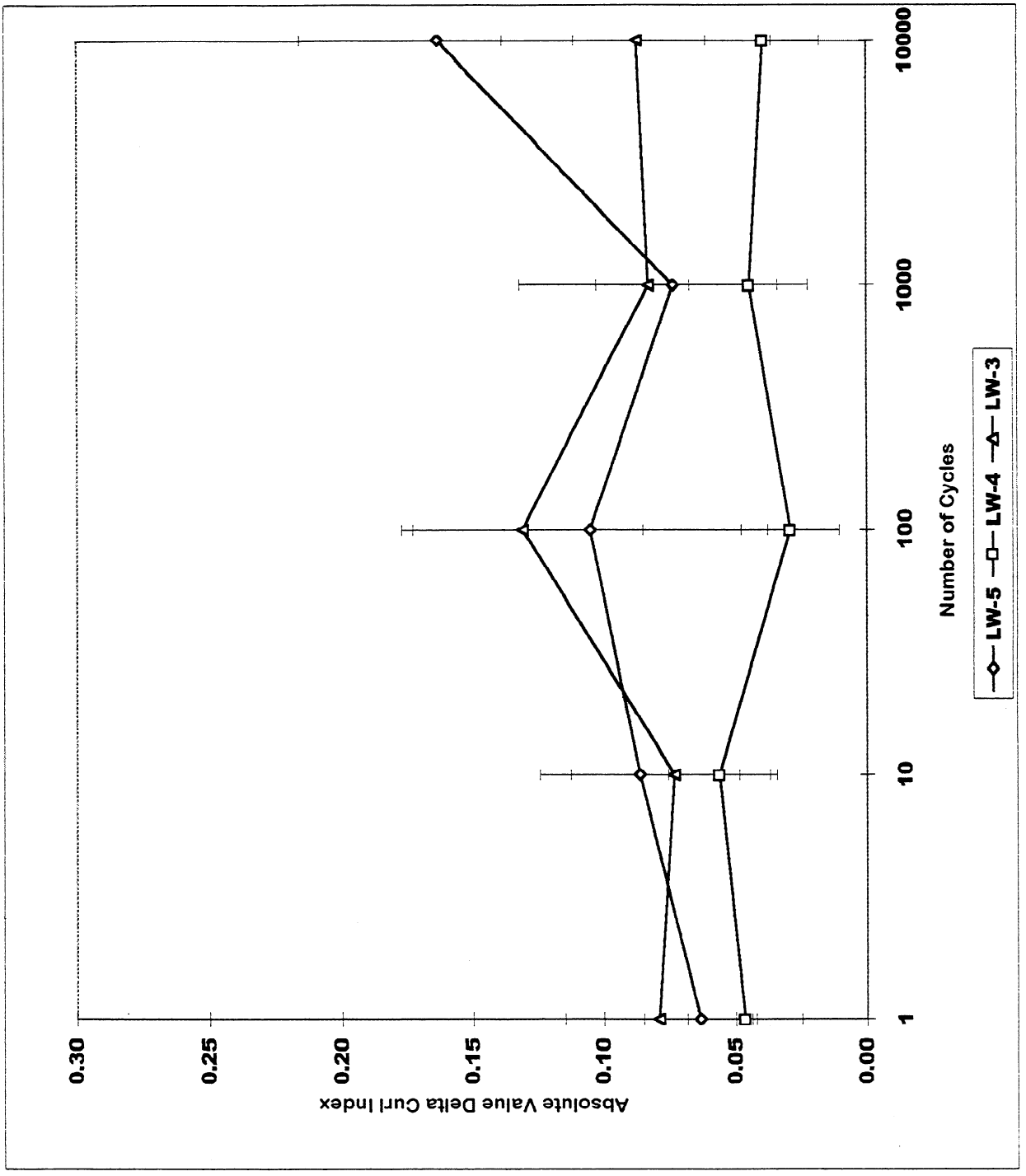

Figure 62. Change in curl index – 10 Hz, Latewood, MTS.

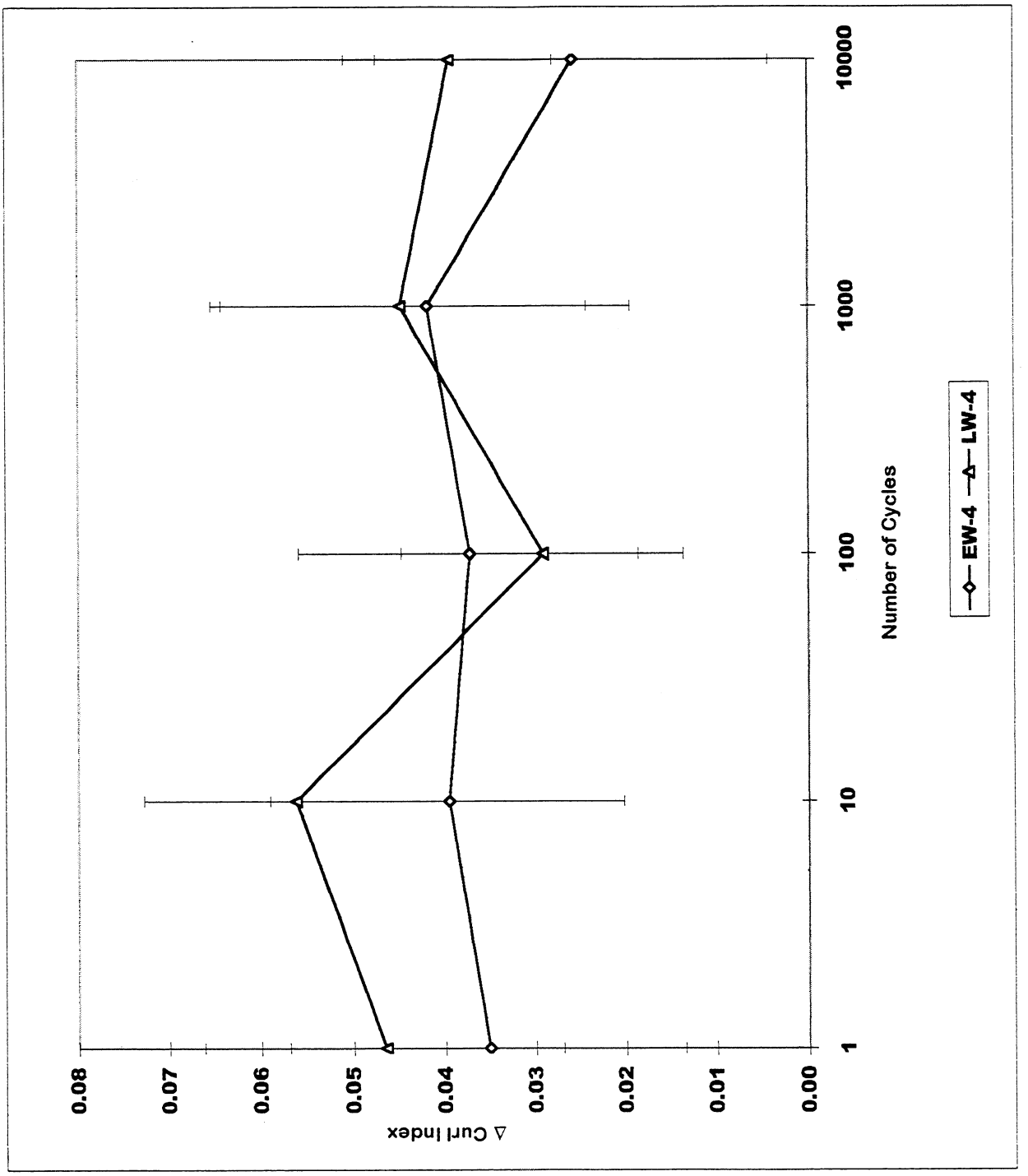

Figure 63. Change in curl index – 10 Hz, 4 mm, MTS.

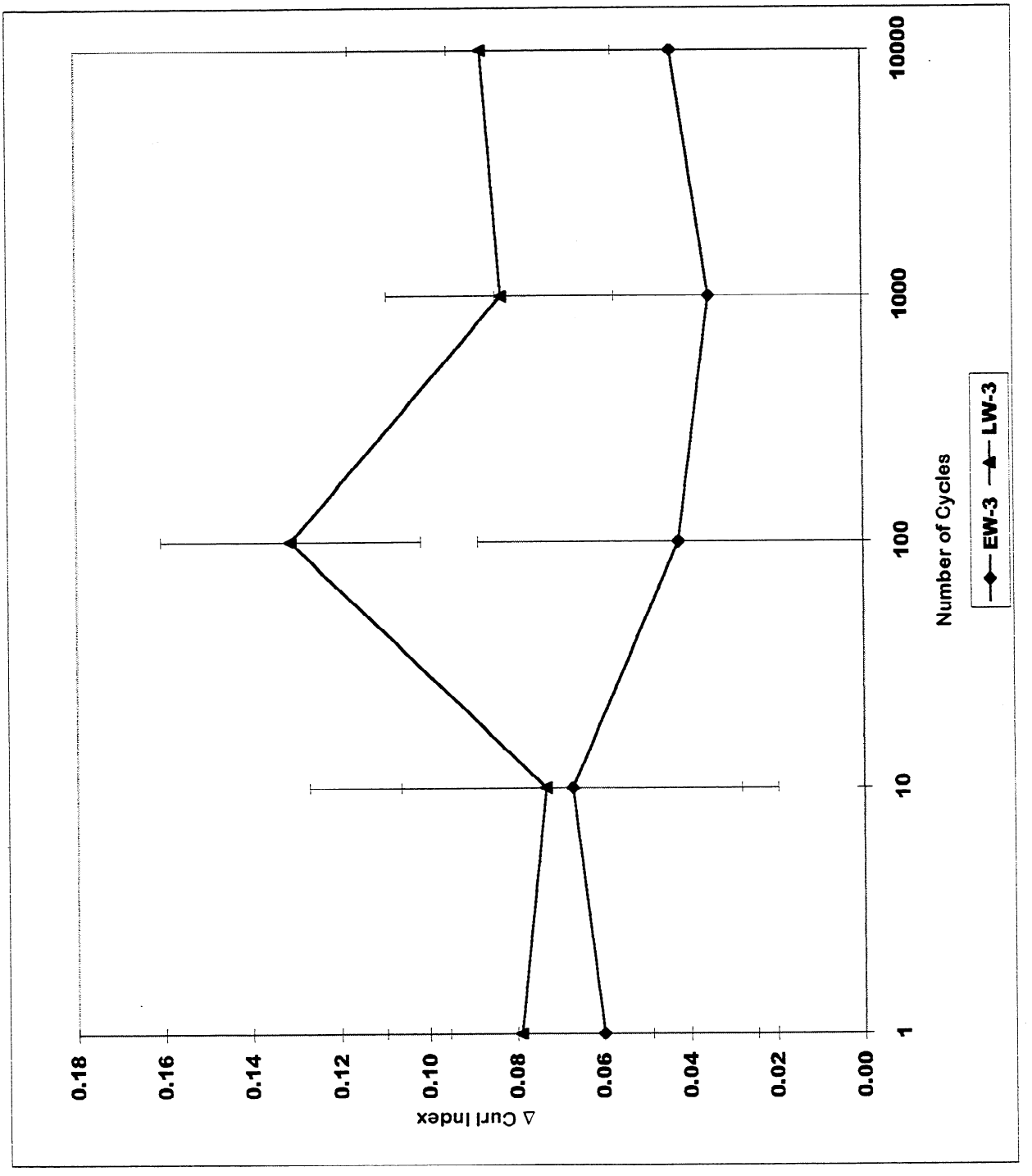

Figure 64. Change in curl index – 10 Hz, 3 mm, MTS.

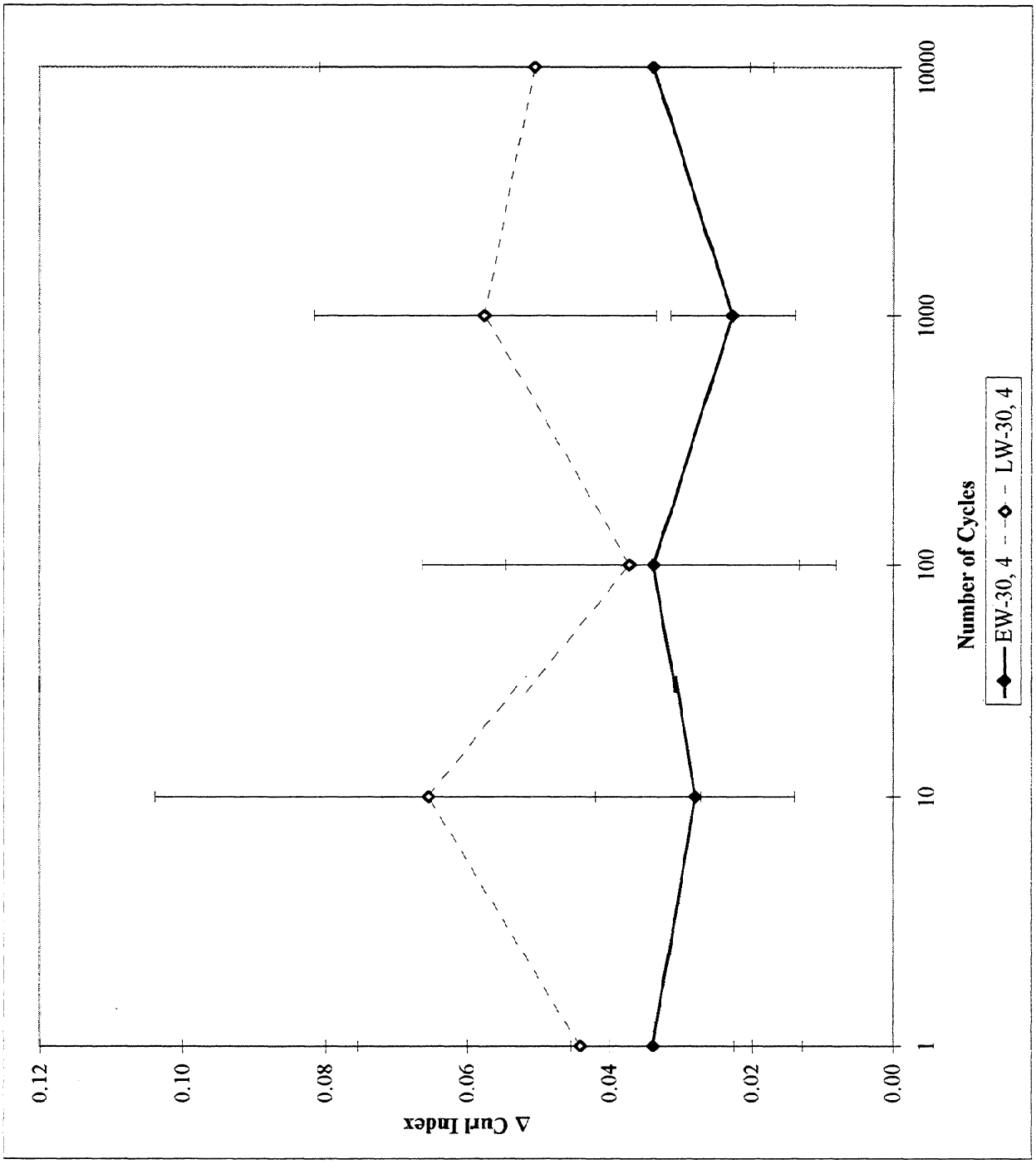

Figure 65. Change in curl index – 30 Hz, 4 mm, MTS.

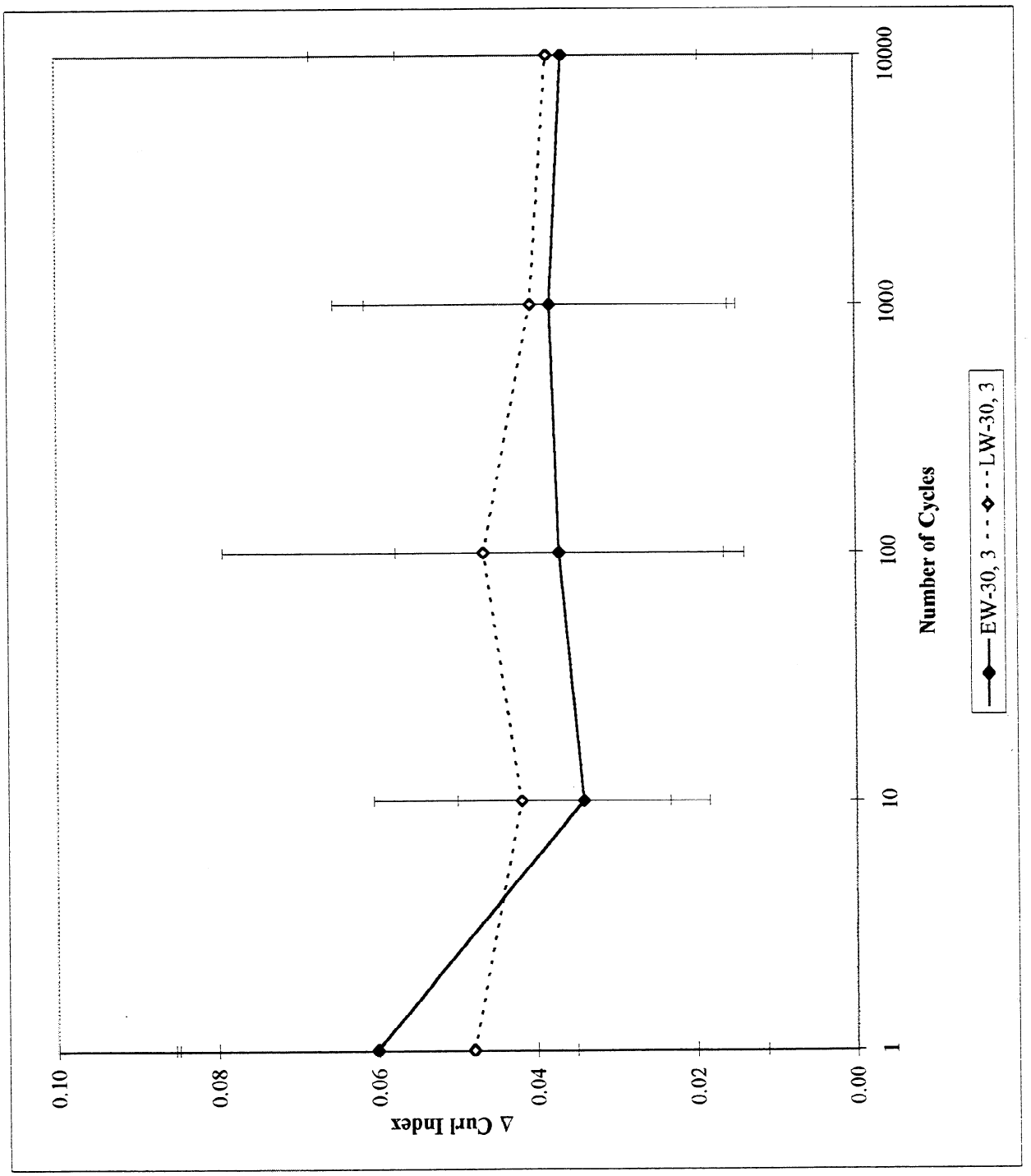

Figure 66. Change in curl index - 30 Hz, 5 mm, MTS.

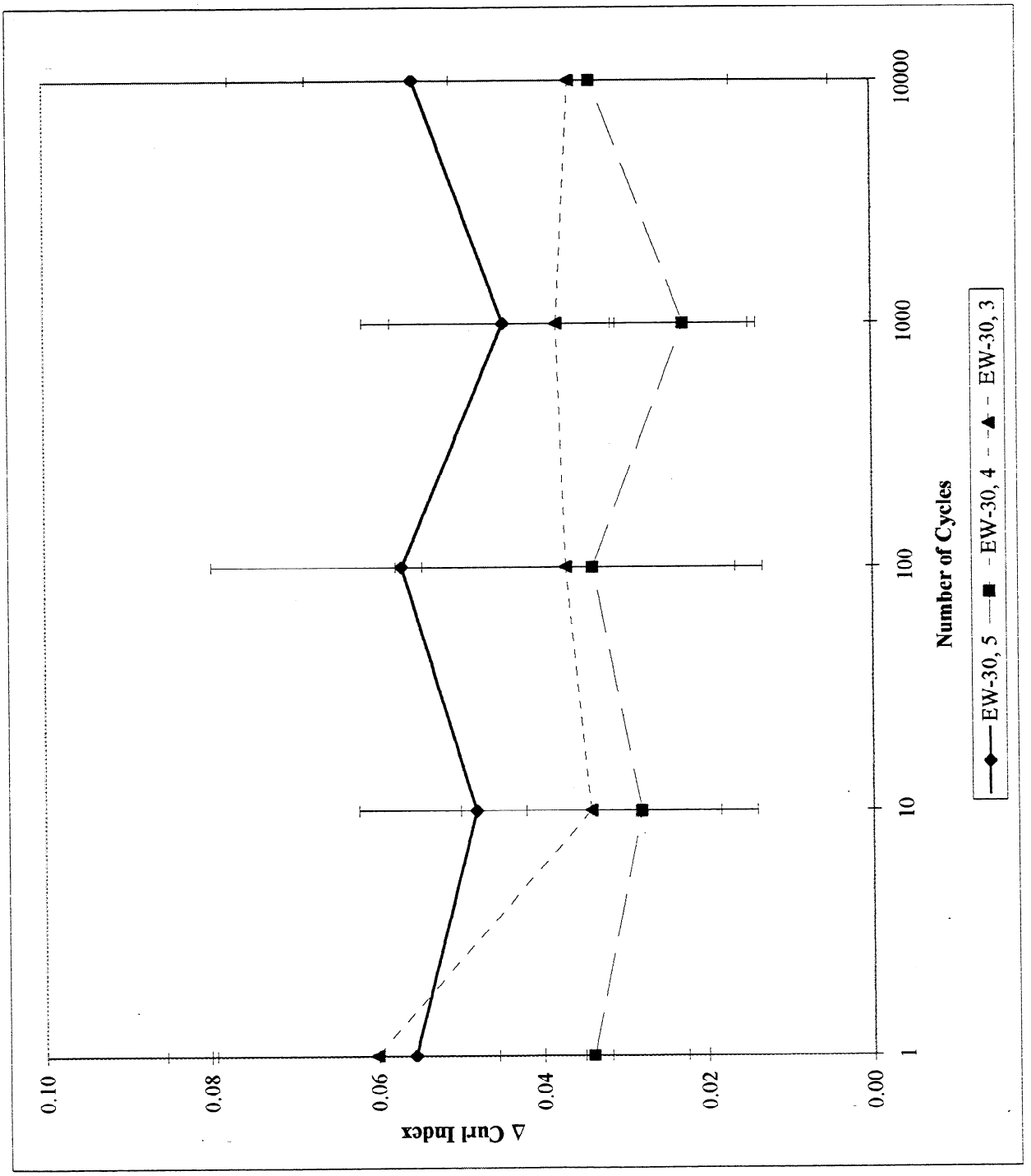

Figure 67. Change in curl index – 30 Hz, Earlywood, MTS.

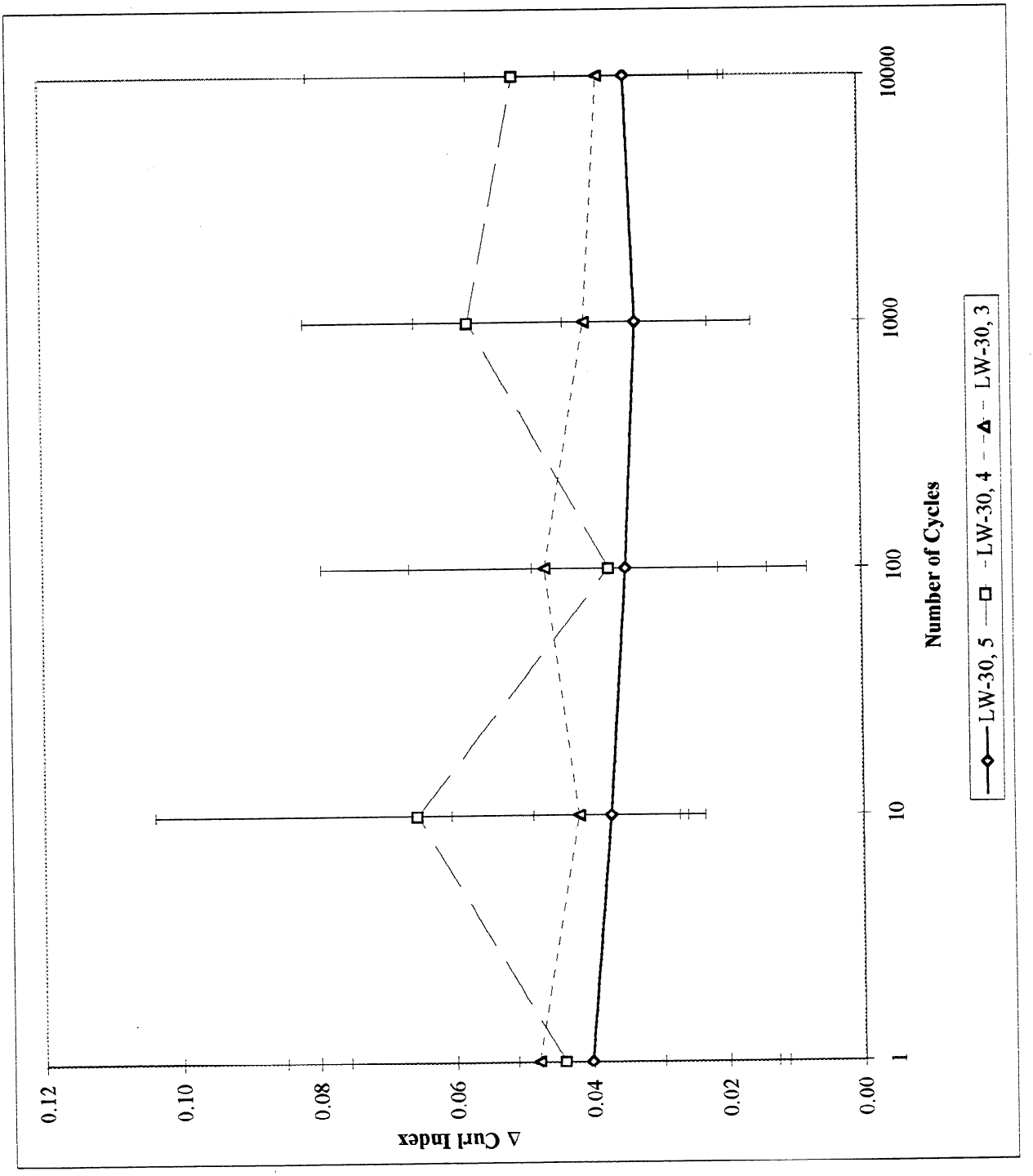

Figure 68. Change in curl index – 30 Hz, Latewood, MTS.

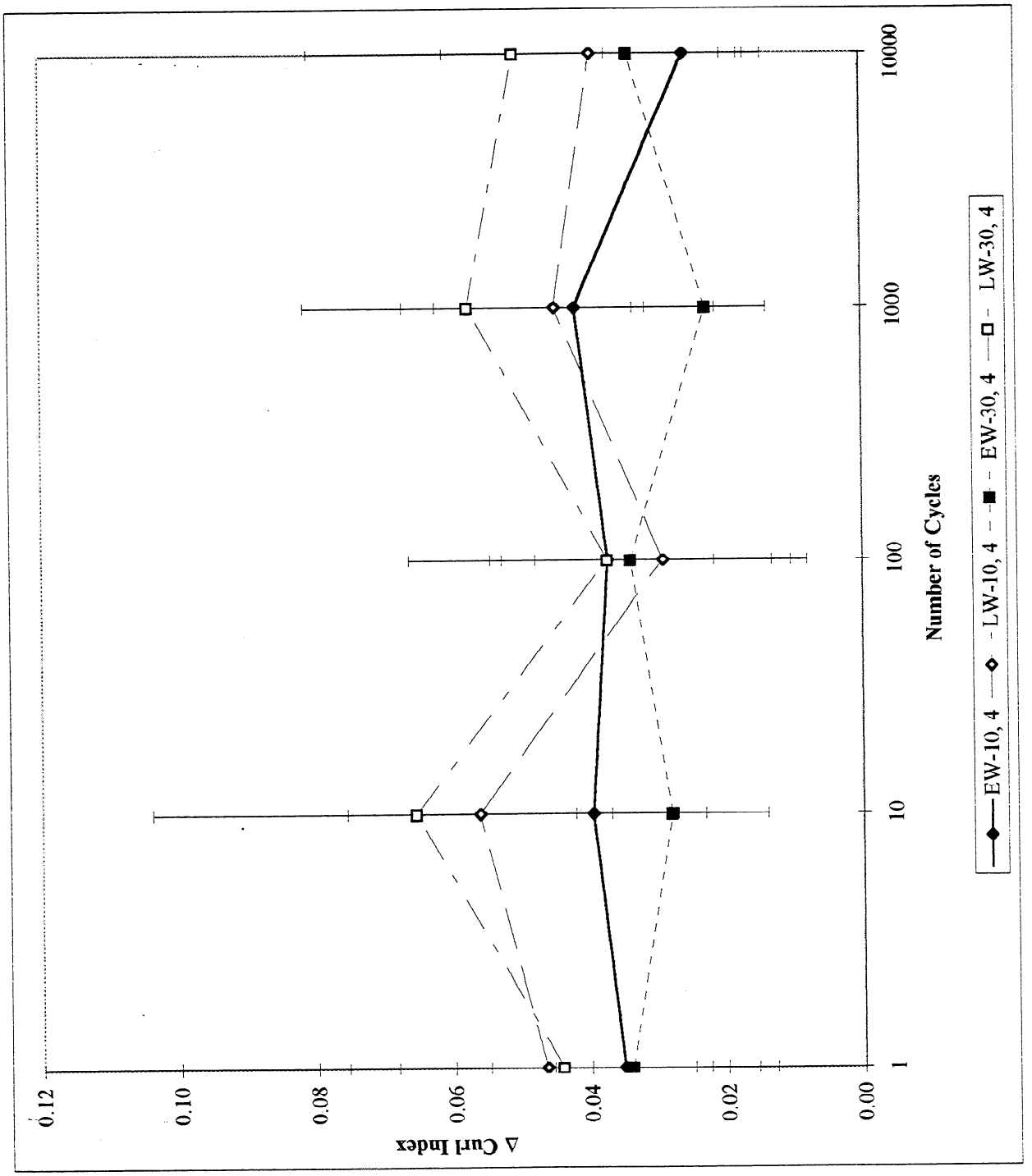

Figure 69. Change in curl index – 4 mm, 10 and 30 Hz, MTS.

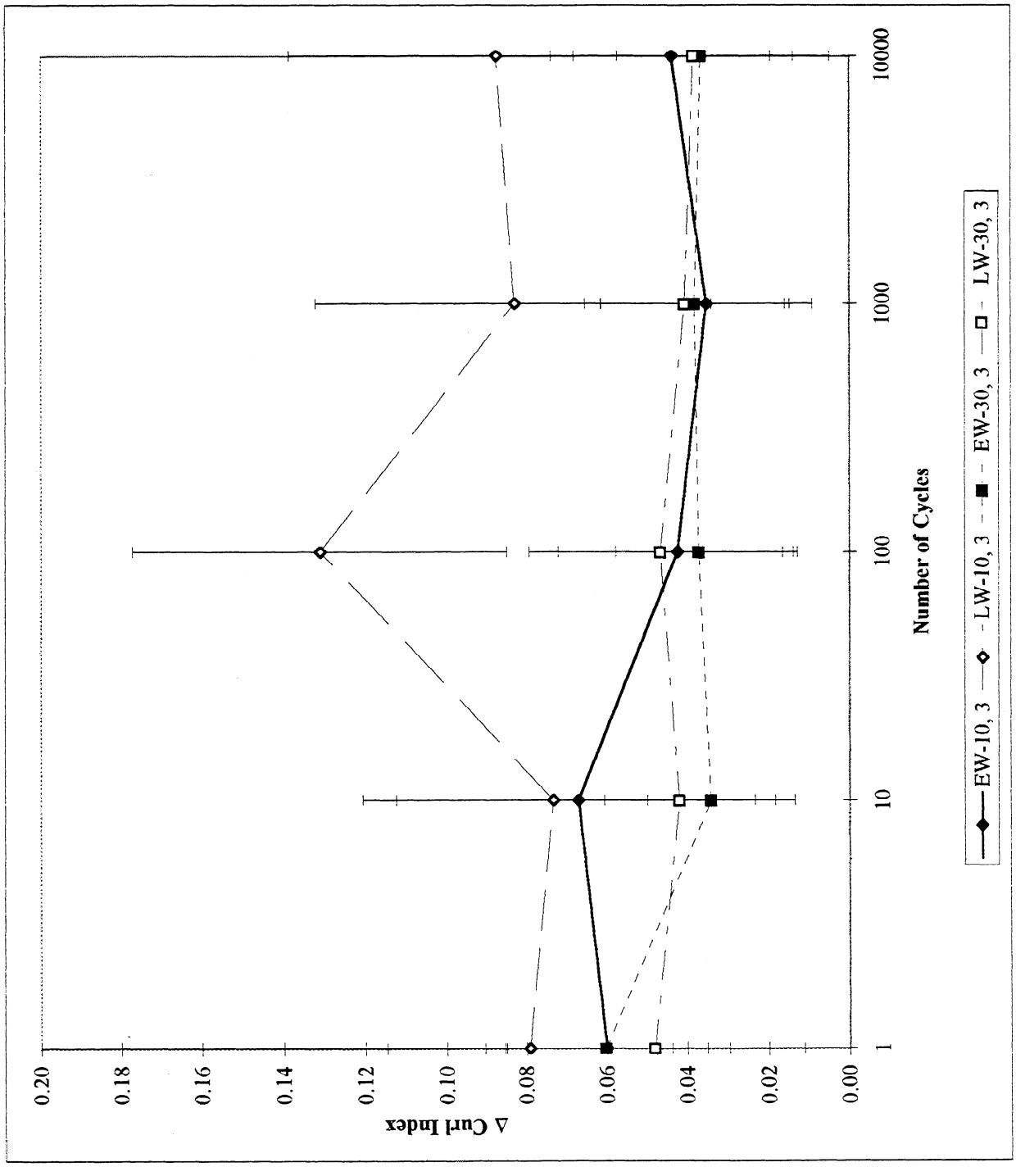

Figure 70. Change in curl index – 3 mm, 10 and 30 Hz, MTS.

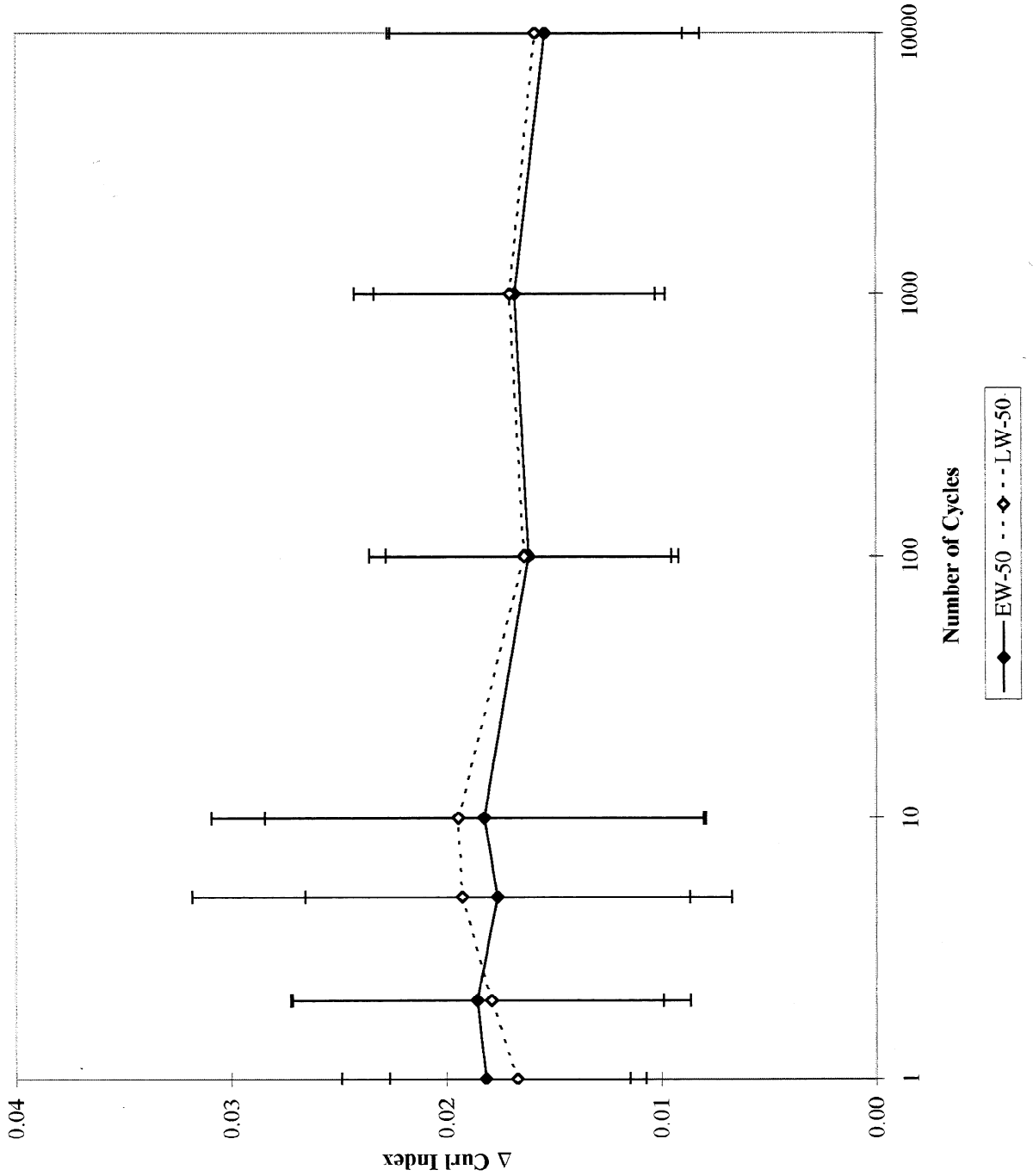

Figure 71. Change in curl index – 50 Hz, Shaker.

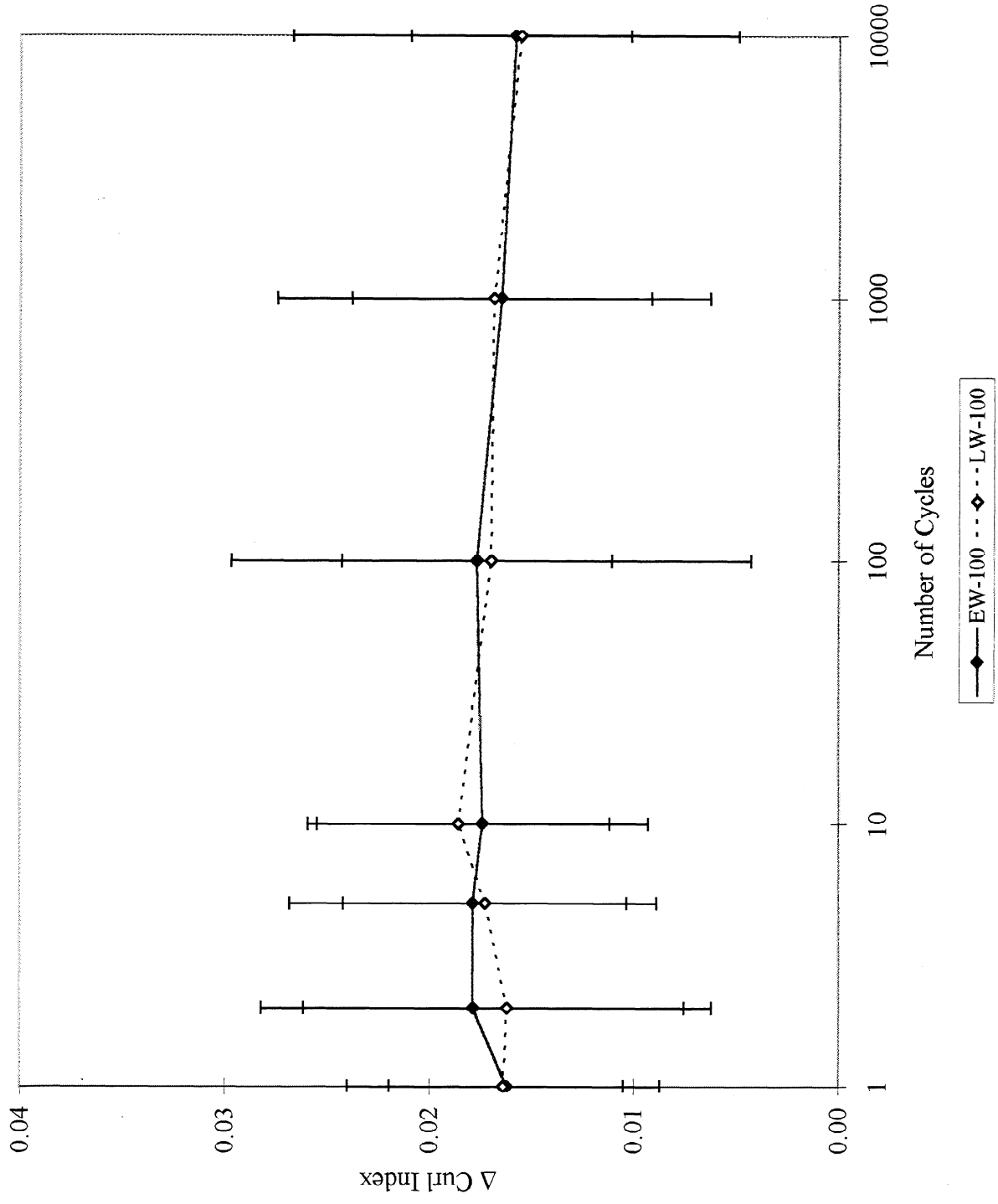

Figure 72. Change in curl index – 100 Hz, Shaker.

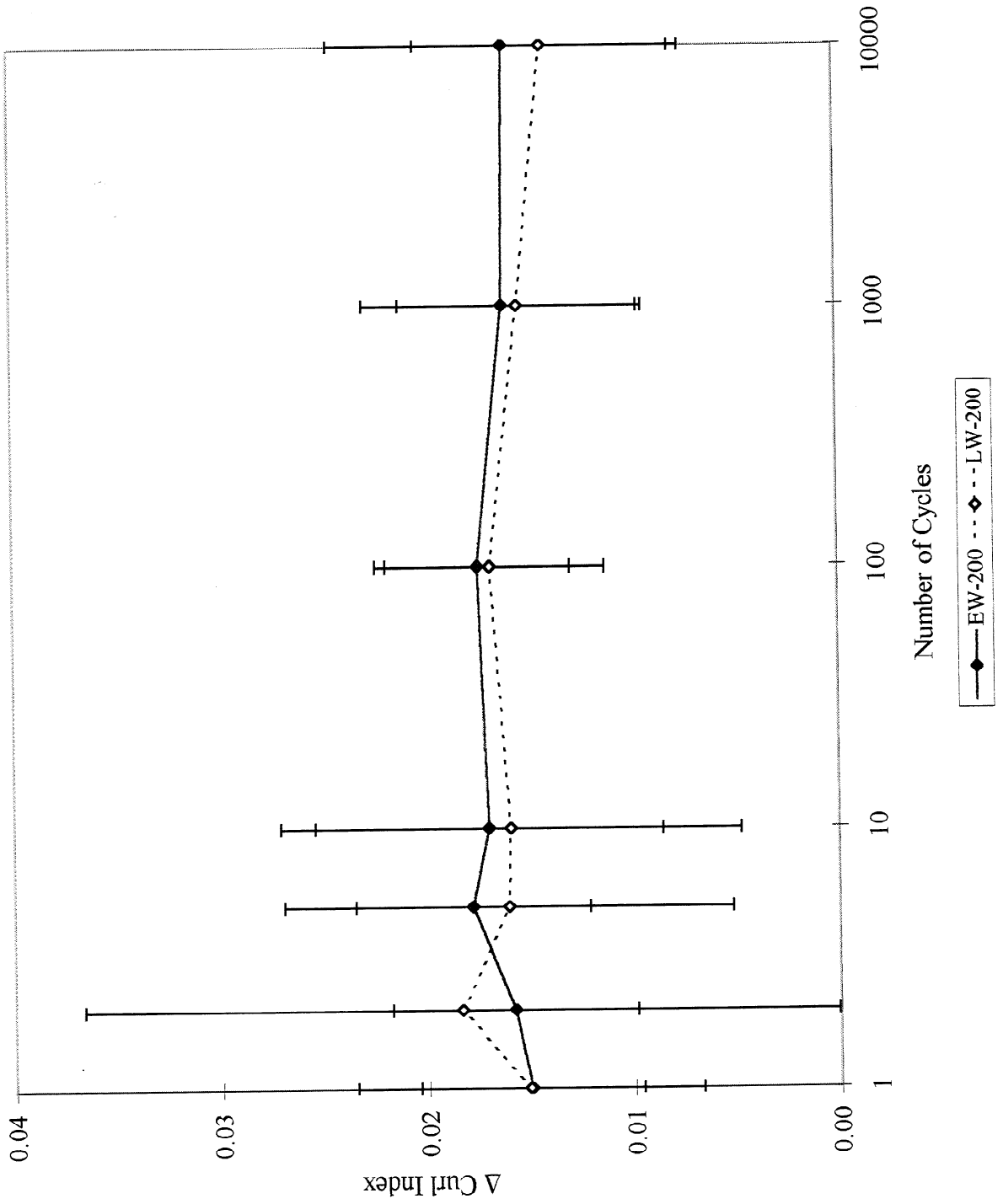

Figure 73. Change in curl index – 200 Hz, Shaker.

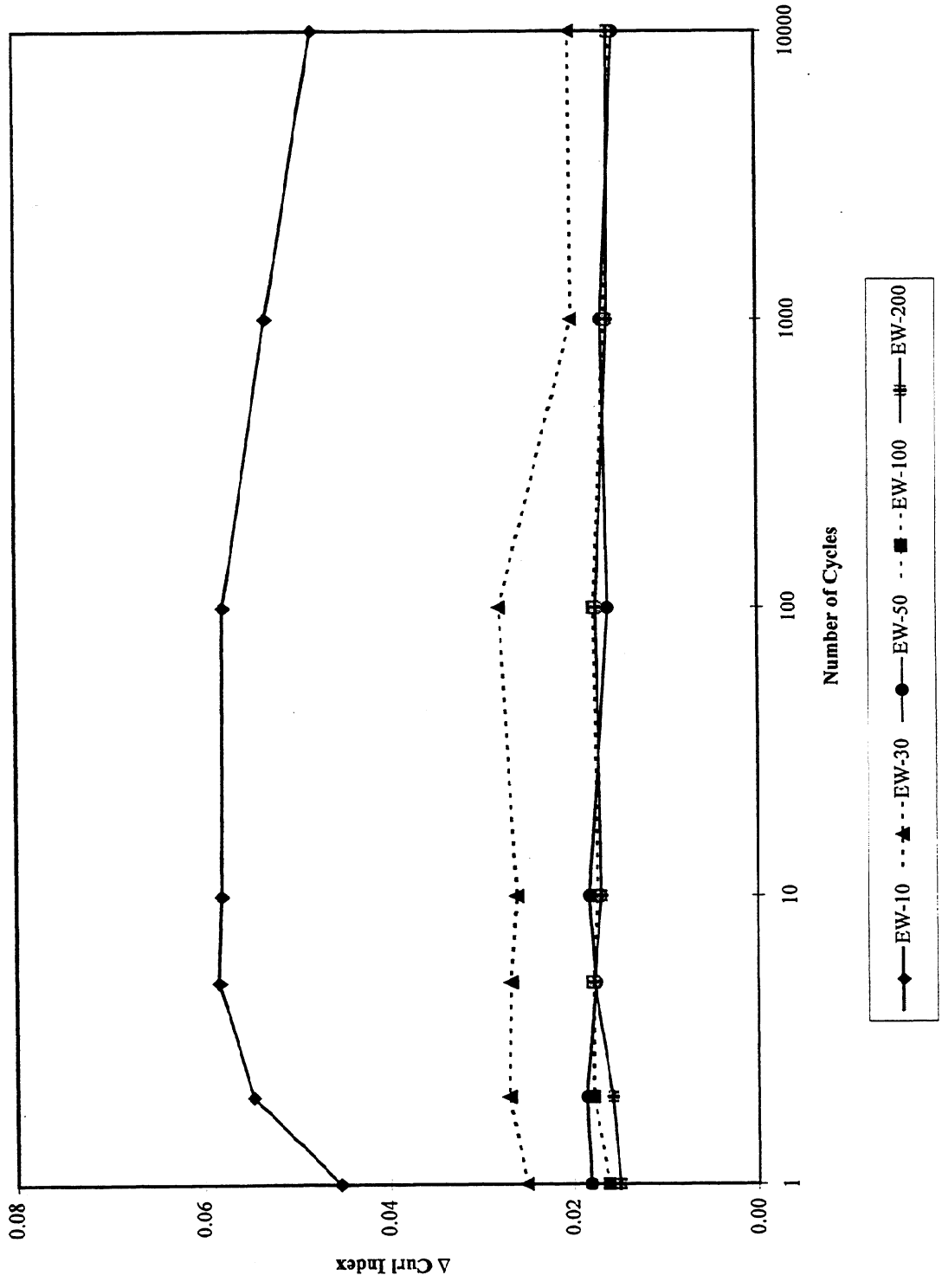

Figure 74. Change in curl index – Earlywood, Shaker.

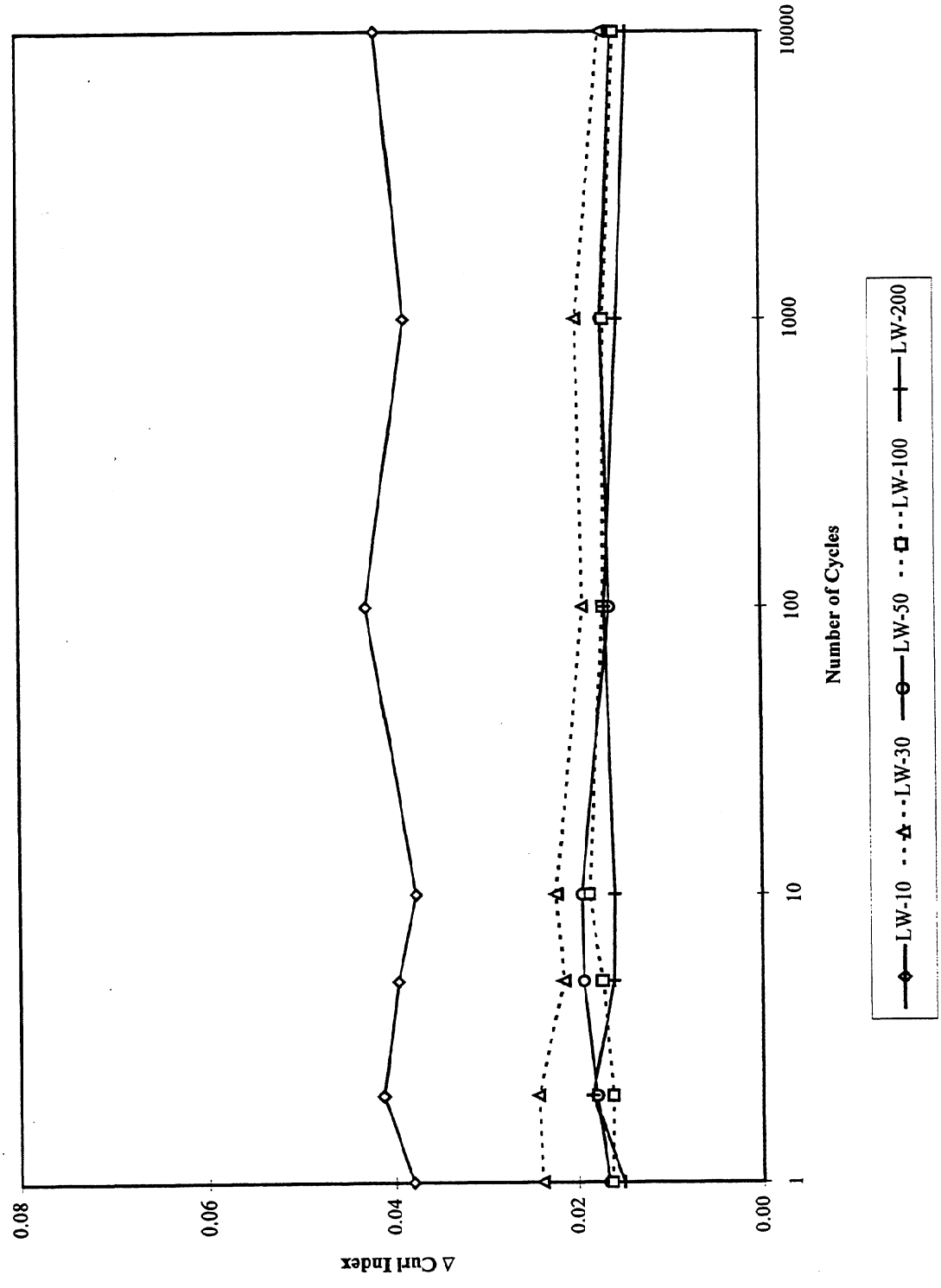

Figure 75. Change in curl index – Latewood, Shaker.

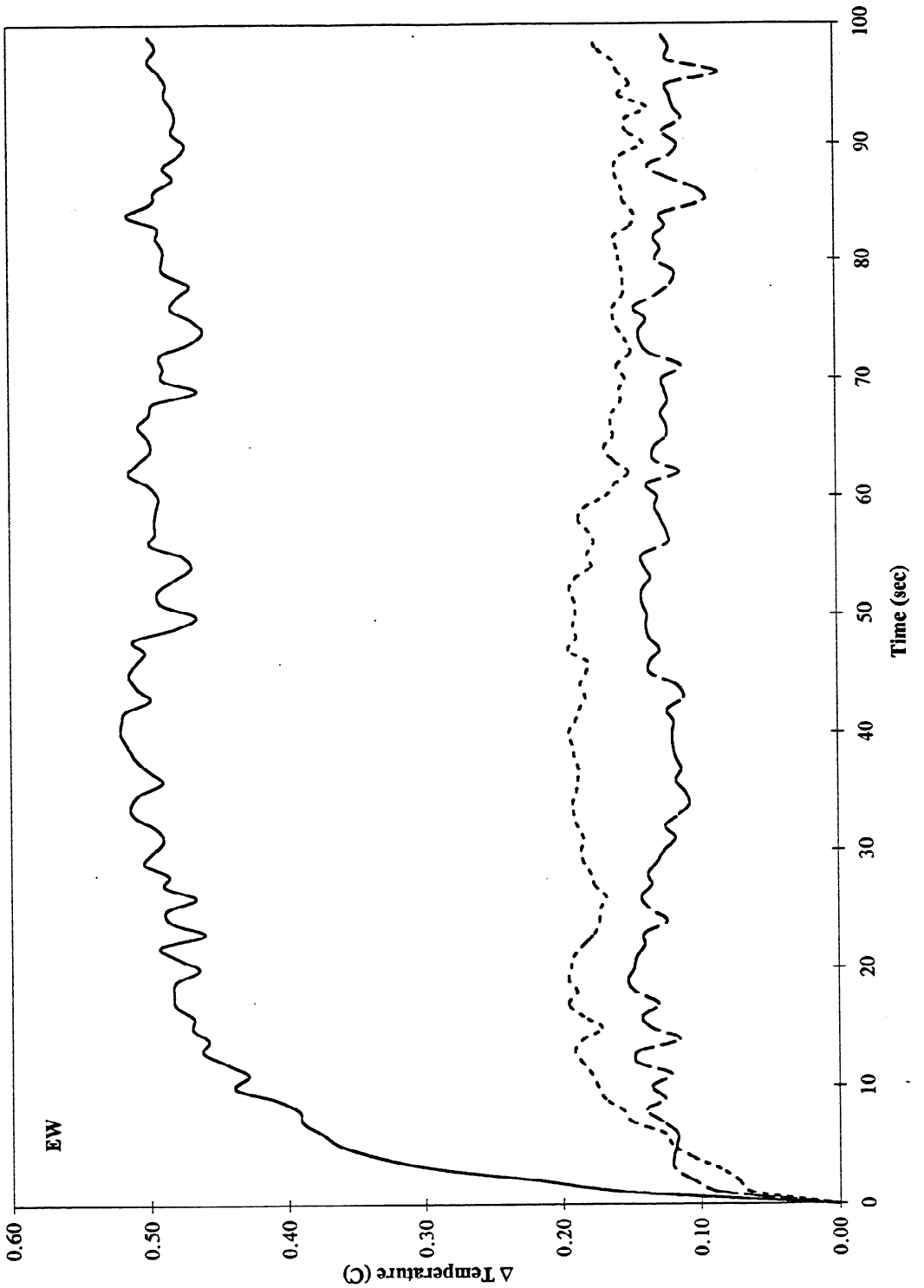

Figure 76. Change in temperature – Earlywood wood samples.

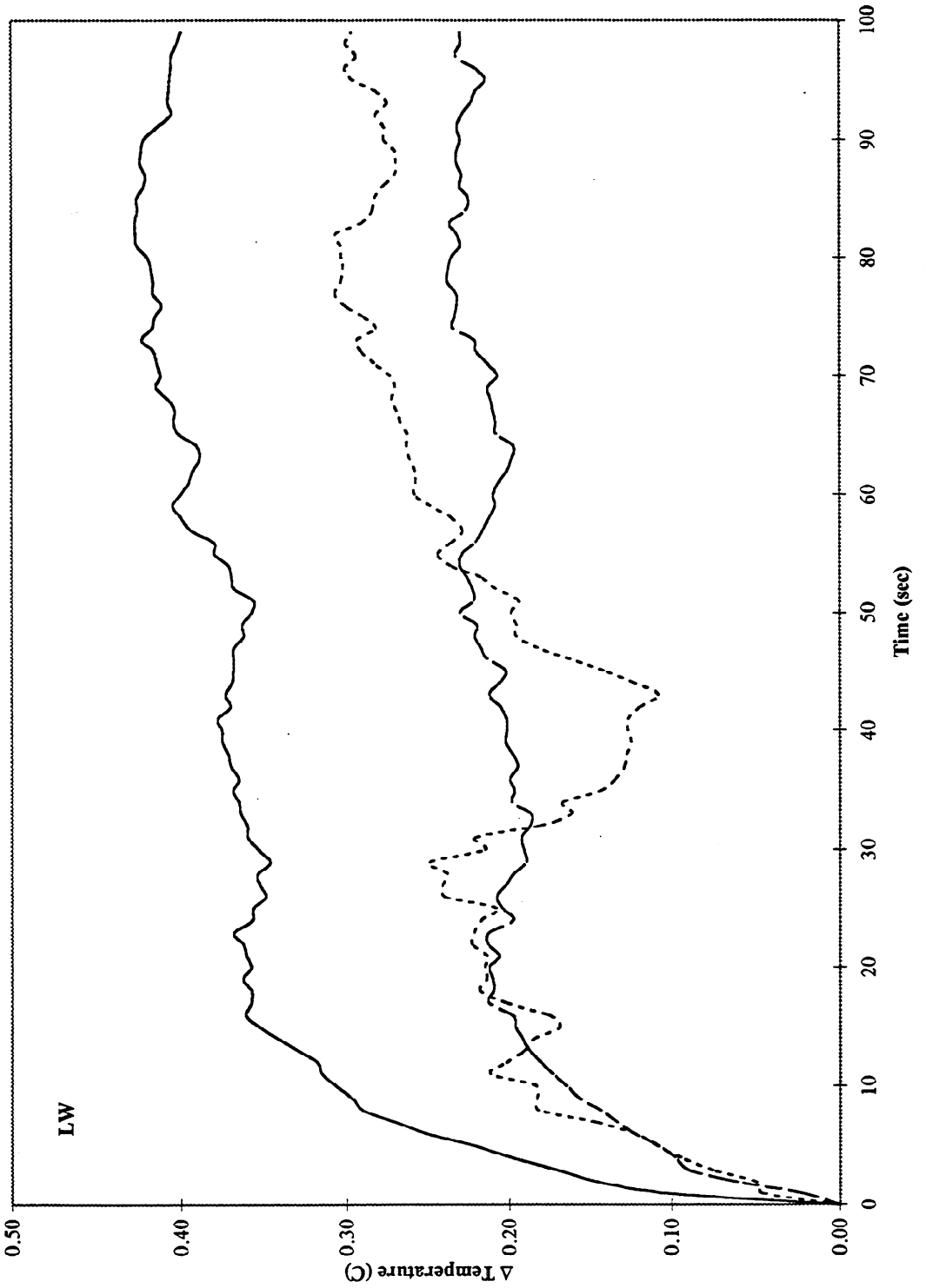

Figure 77. Change in temperature – Latewood wood samples.

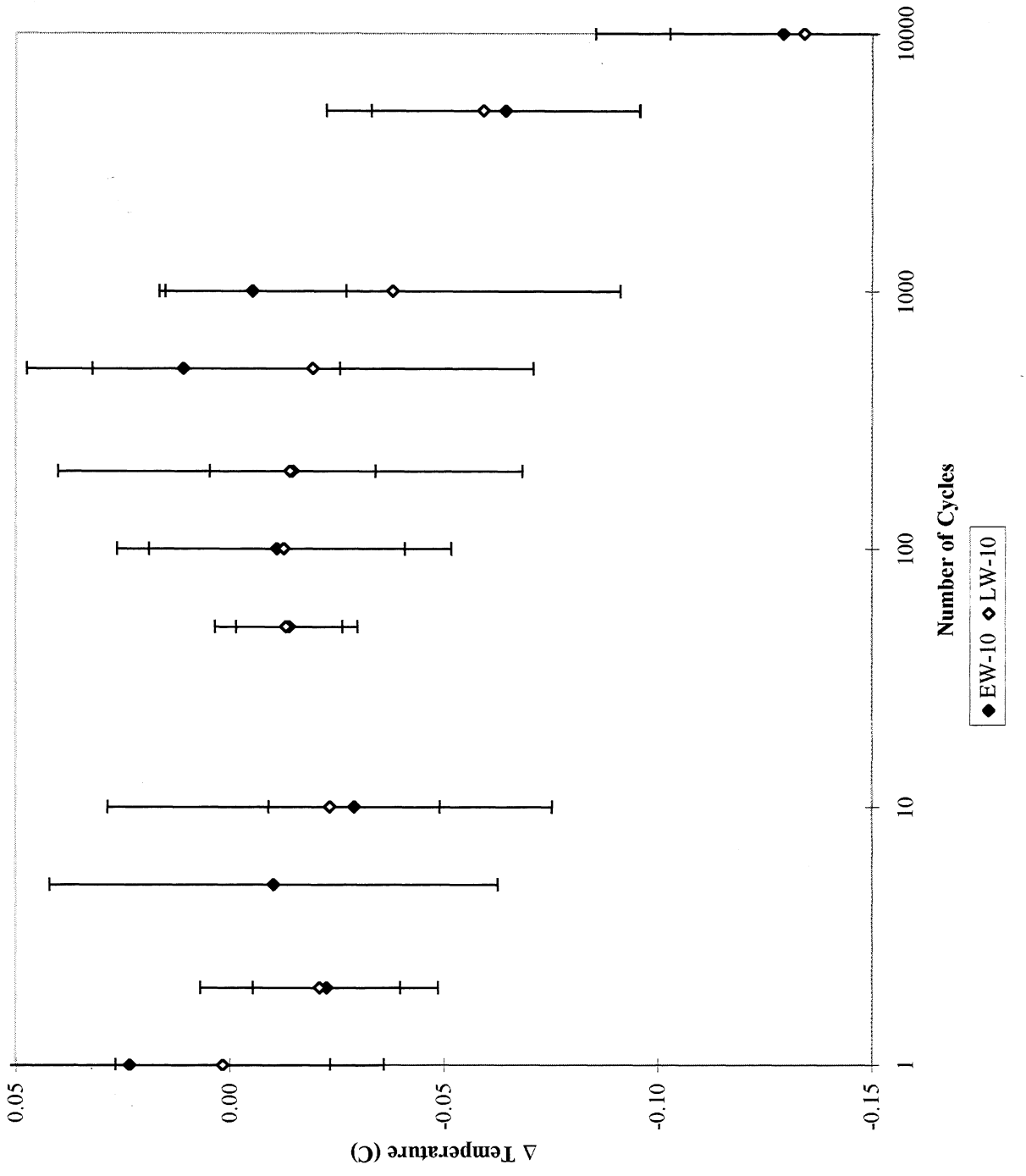

Figure 78. Change in temperature – pure aggregates, 10 Hz.

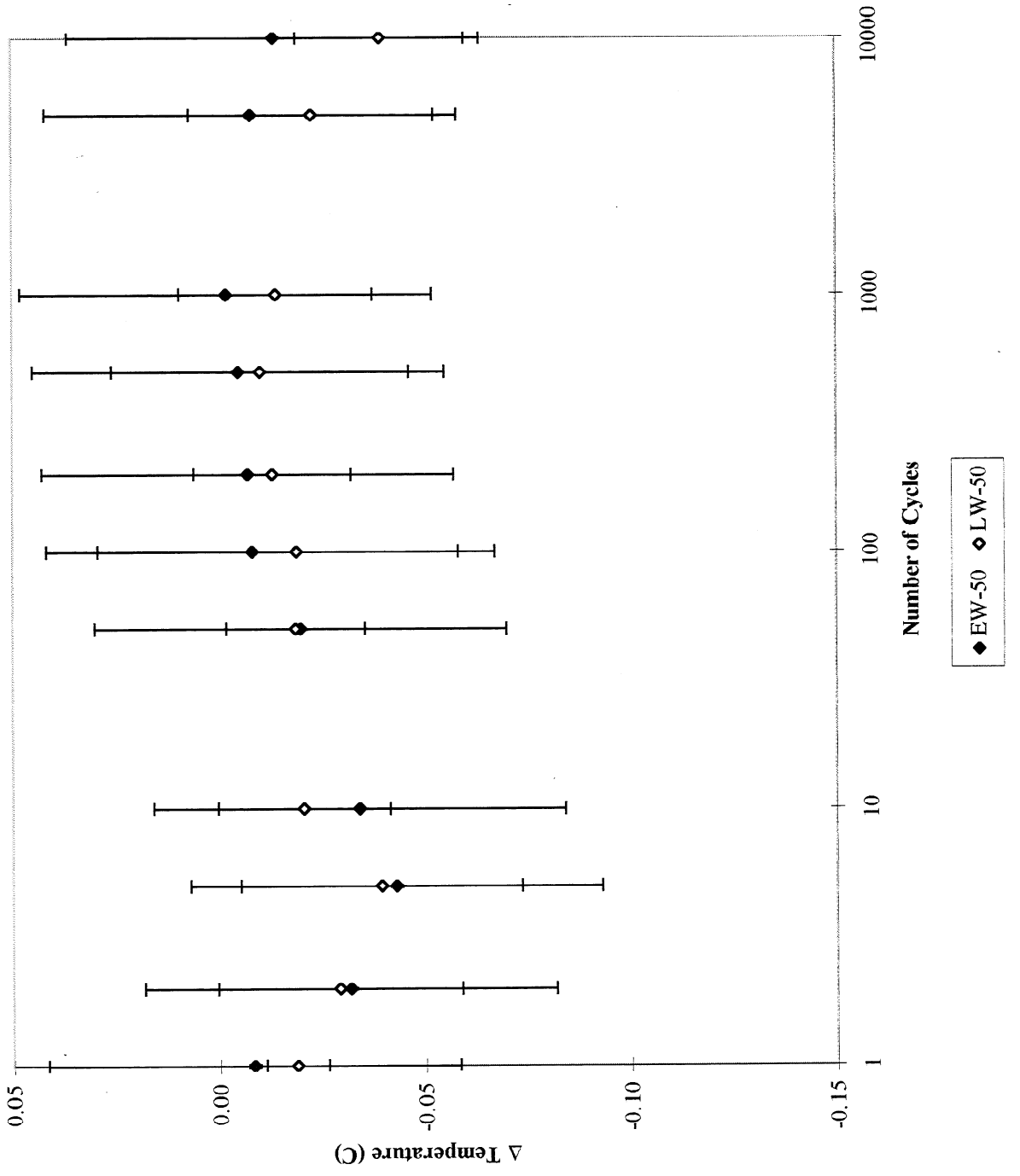

Figure 79. Change in temperature – pure aggregates, 50 Hz.

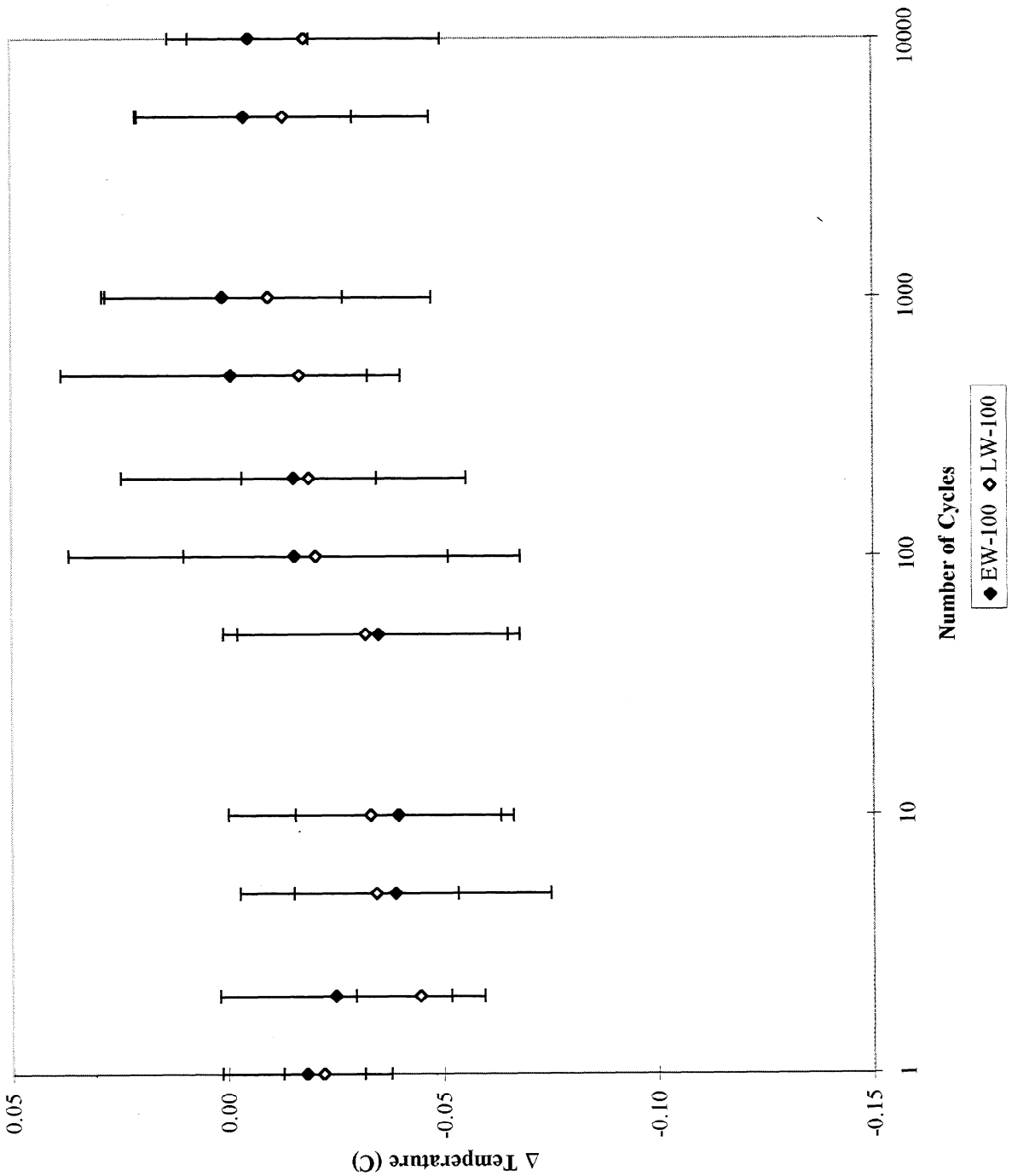

Figure 80. Change in temperature – pure aggregates, 100 Hz.

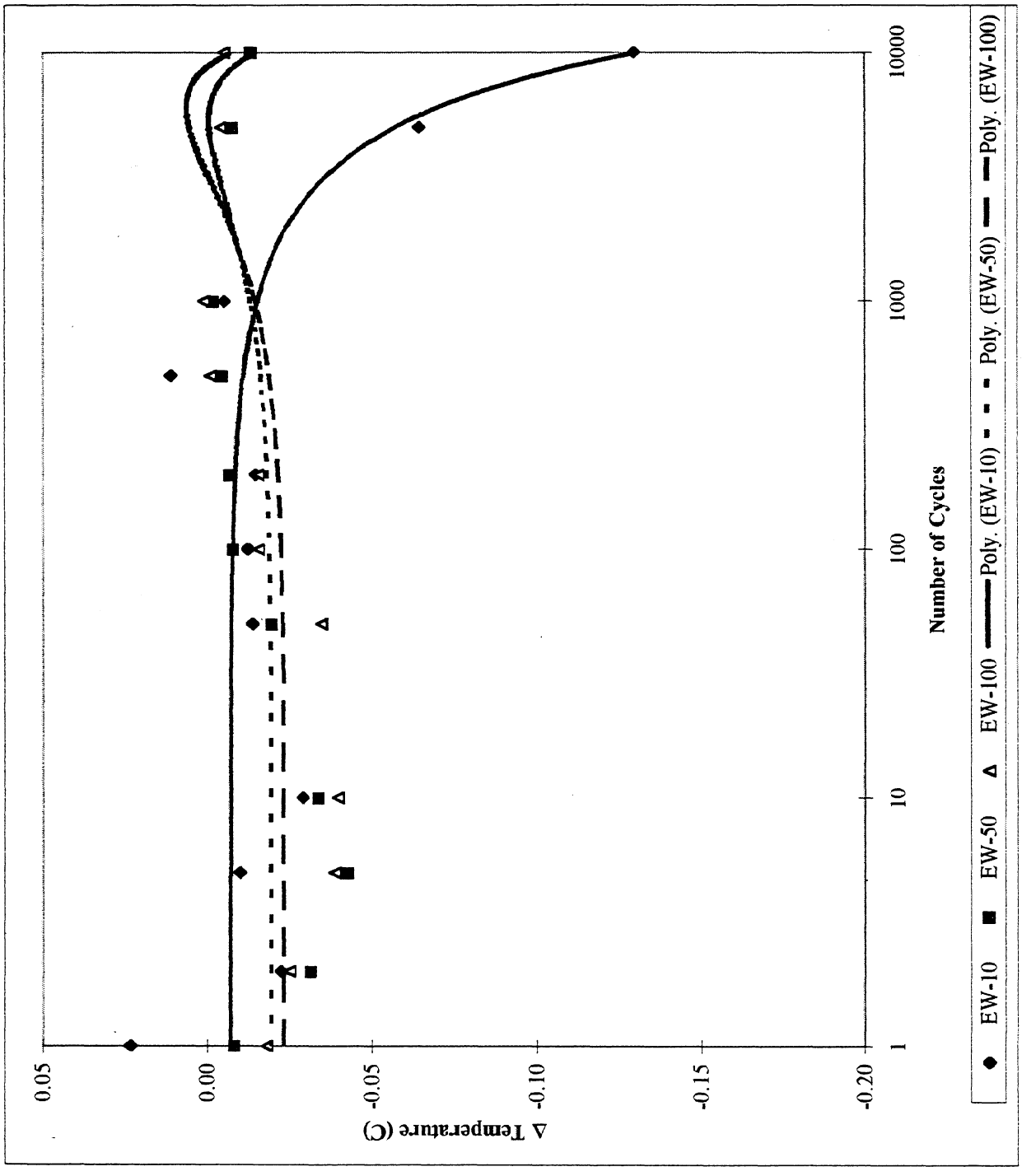

Figure 81. Change in temperature – pure aggregates, Earlywood.

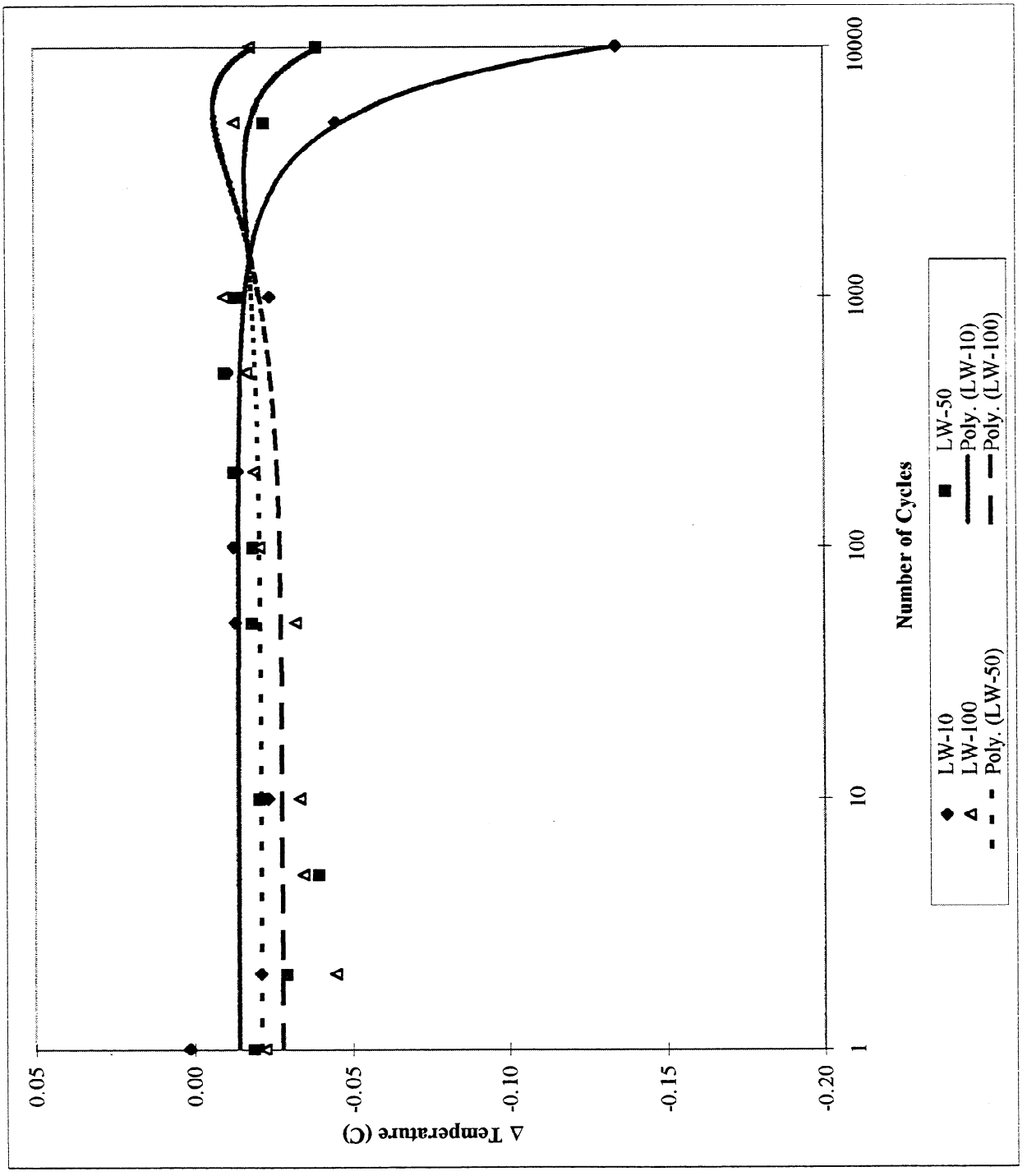

Figure 82. Change in temperature – pure aggregates, Latewood.

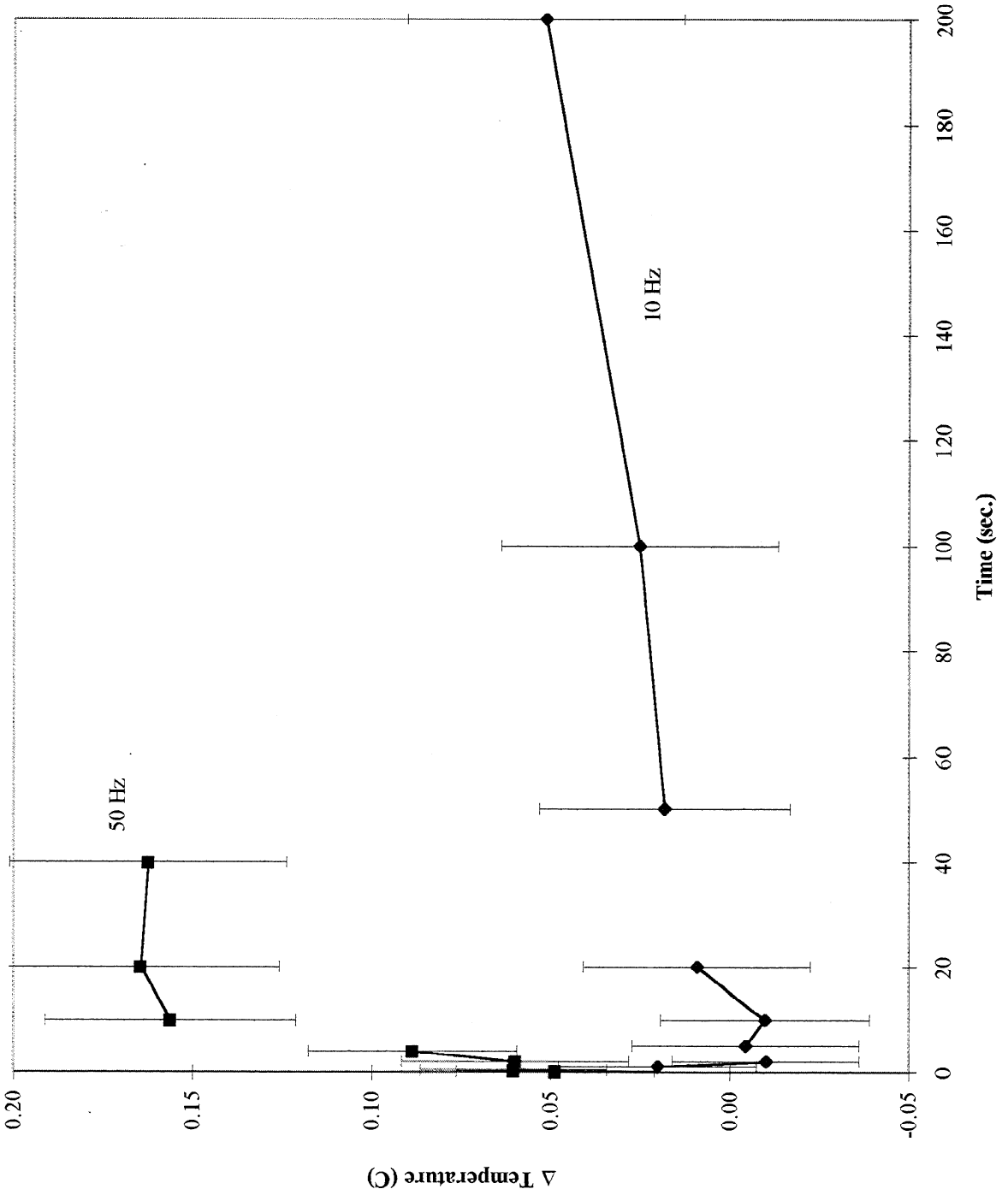

Figure 83. Change in temperature – pure, air-dried, time basis.

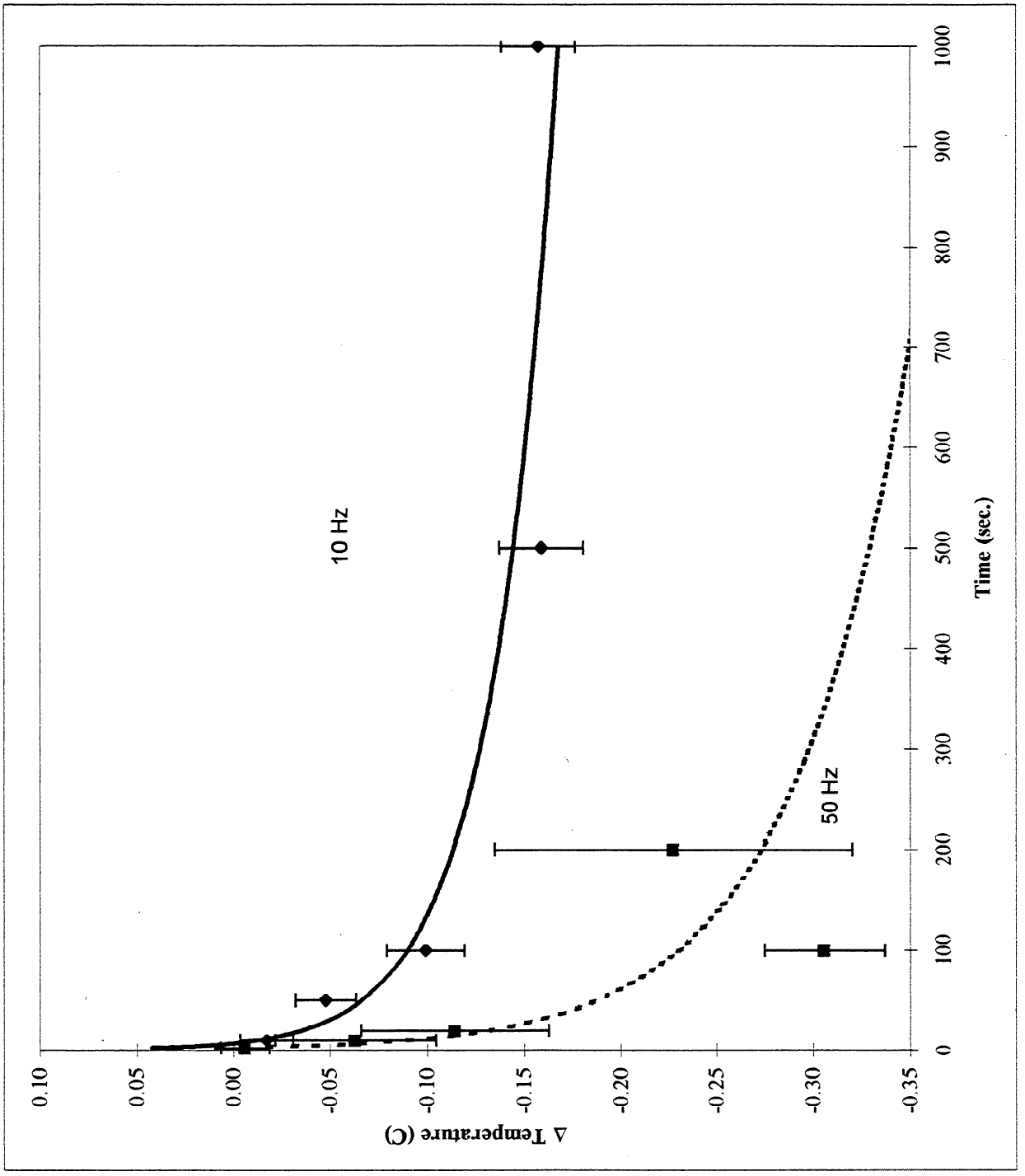

Figure 84. Change in temperature – pure, no fiber work, time basis.

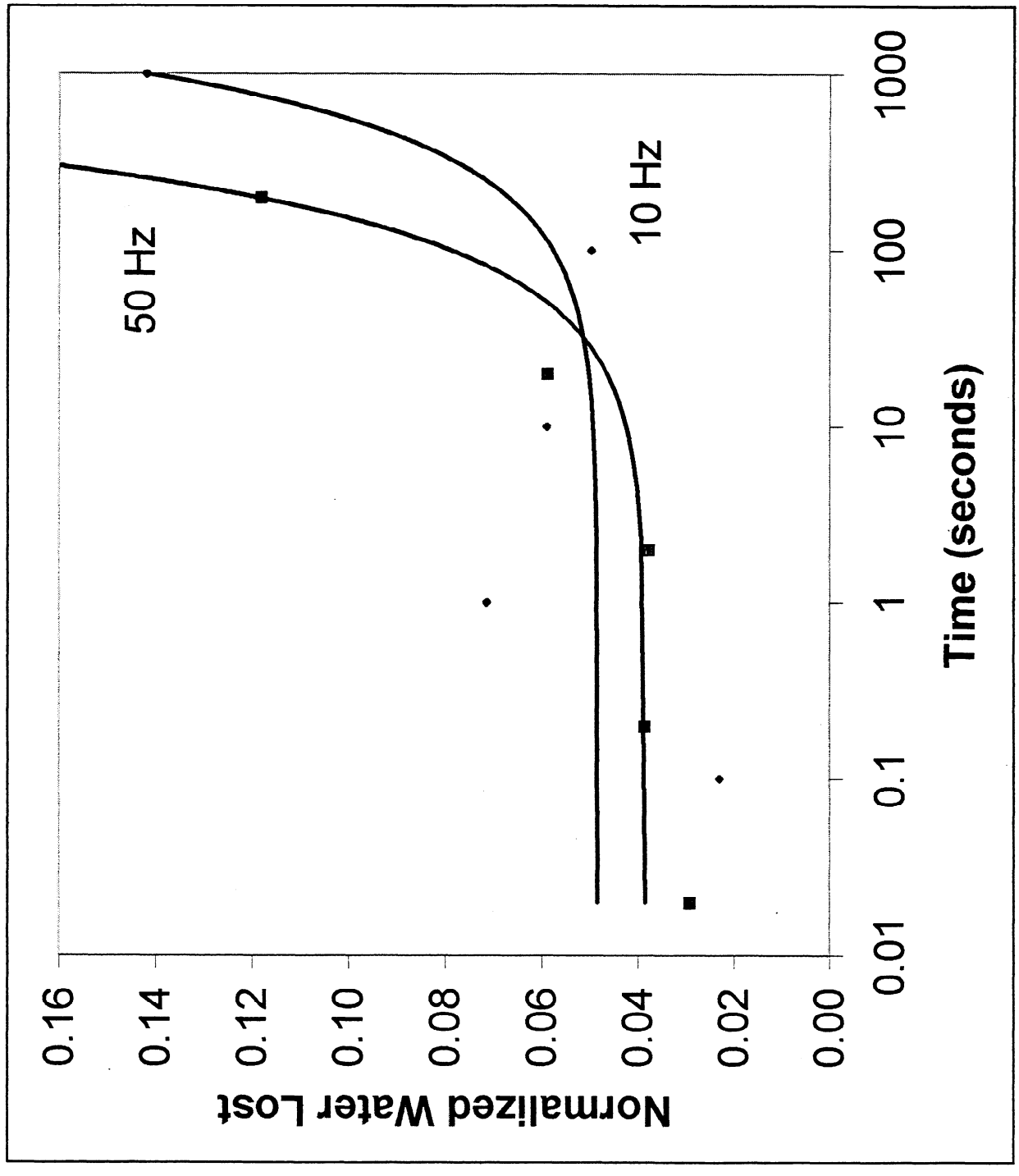

Figure 85. Evaporation study with cycling – normalized water lost. Normalized water lost is the water lost divided by the initial amount of water.

APPENDIX 8: DATA TABLES

Curl index reproducibility

Curl Index Reproducibility														
Fiber #	Curl Index										average	st dev	var	95%CI
1	0.054	0.025	0.068	0.074	0.068	0.102	0.061	0.058	0.051	0.072	0.063	0.020	0.000	0.014
2	0.005	0.002	0.000	0.003	0.012	0.009	0.010	0.004	0.006	0.004	0.005	0.004	0.000	0.003
3	0.016	0.007	0.005	0.010	0.004	0.011	0.005	0.010	0.018	0.022	0.011	0.006	0.000	0.004
4	0.591	0.576	0.583	0.688	0.744	0.682	0.634	0.589	0.683	0.635	0.640	0.057	0.003	0.041
5	0.051	0.045	0.033	0.018	0.026	0.056	0.053	0.040	0.045	0.051	0.042	0.012	0.000	0.009
6	0.087	0.024	0.063	0.071	0.058	0.068	0.069	0.047	0.041	0.060	0.059	0.018	0.000	0.013
7	0.032	0.023	0.015	0.018	0.037	0.020	0.012	0.028	0.030	0.031	0.024	0.008	0.000	0.006
8	0.014	0.006	0.009	0.085	0.008	0.025	0.010	0.014	0.005	0.011	0.019	0.024	0.001	0.017
9	0.057	0.037	0.061	0.011	0.057	0.057	0.062	0.066	0.078	0.056	0.054	0.018	0.000	0.013

IR reproducibility

IR Reproducibility (C)

	1	2	3	4	5	6	7	8	9	10	Ave
	20.45	20.57	20.48	20.61	20.59	20.58	20.55	20.52	20.56	20.53	
	20.50	20.61	20.55	20.59	20.62	20.57	20.56	20.51	20.58	20.52	
	20.49	20.59	20.50	20.60	20.63	20.59	20.53	20.50	20.56	20.51	
	20.46	20.61	20.56	20.61	20.58	20.58	20.56	20.51	20.58	20.54	
	20.51	20.58	20.51	20.62	20.63	20.62	20.57	20.50	20.56	20.47	
	20.50	20.62	20.54	20.62	20.63	20.59	20.55	20.51	20.57	20.51	
	20.46	20.62	20.47	20.63	20.64	20.61	20.55	20.51	20.60	20.49	
	20.46	20.57	20.53	20.62	20.61	20.60	20.58	20.51	20.59	20.50	
	20.47	20.59	20.53	20.61	20.60	20.61	20.55	20.51	20.58	20.48	
	20.43	20.56	20.55	20.61	20.62	20.57	20.53	20.51	20.58	20.50	
average	20.47	20.59	20.52	20.61	20.61	20.59	20.55	20.51	20.58	20.51	20.55
st dev	0.03	0.02	0.03	0.01	0.02	0.02	0.01	0.01	0.01	0.02	0.05
variance	0.00	0.00	0.00	0.00	0.00	0.00	0.00	0.00	0.00	0.00	0.00
95%Conf	0.02	0.02	0.02	0.01	0.01	0.01	0.01	0.00	0.01	0.02	0.04

Earlywood curl index - 10 Hz, 5mm

Earlywood Curl Index - 10 Hz, 5 mm												
Fiber Count	run #	fiber #	1	1.5	10	10.5	100	100.5	1000	1000.5	10000	10000.5
1	1	1	0.0353	0.0792	0.0618	0.3607	0.0529	0.3789	0.0636	0.2930	0.0767	0.1999
2	1	2	0.0484	0.0365	0.0536	0.0793	0.0322	0.0682	0.0575	0.0562	0.0720	0.0694
3	1	3	0.0437	0.0946	0.1267	0.0562	0.2334	0.0587	0.2807	0.0694	0.1130	0.0369
4	1	4	0.0191	0.0581	0.4524	0.0352	0.6738	0.0844	0.3557	0.0666	0.4123	0.0641
5	1	5	0.0085	0.0059	0.4023	0.0000	0.4267	0.0000	0.2626	0.0052	0.2010	0.0173
6	1	6	0.0407	0.0178	0.0037	0.0851	0.0815	0.0342	0.1354	0.0267	0.2231	0.0441
7	1	7	0.0233	0.0087	0.2642	0.0052	0.0682	0.0131	0.1041	0.0344	0.0551	0.0186
8	1	8	0.0334	0.0789	0.3206	0.0737	0.8004	0.0142	0.0213	0.0709	0.0000	0.0086
9	1	10	0.1021	0.1418	0.0071	0.1338	0.0230	0.0134	0.1123	0.0096	0.0637	0.0090
10	1	11	0.2889	0.2163	0.0071	0.1797	0.0110	0.1419	0.0195	0.2000	0.0230	0.1661
11	1	12	0.1922	0.1840	0.5834	0.0461	0.7459	0.2507	0.7011	0.2735	0.8030	0.1449
12	1	14	0.0254	0.0345	0.6203	0.0250	0.3728	0.0046	0.3533	0.0021	0.4065	0.0000
13	2	1	0.0153	0.0157	0.1154	0.1211	0.1792	0.2445	0.1528	0.2283	0.1537	0.0367
14	2	2	0.0141	0.0227	0.0970	0.0129	0.1341	0.0361	0.0850	0.0156	0.0930	0.1258
15	2	5	0.9437	0.8244	0.0452	0.9422	0.0633	1.3321	0.1038	0.7640	0.1014	0.6834
16	2	6	0.3017	0.3253	0.0105	0.2154	0.0167	0.1162	0.0254	0.1068	0.0147	0.0669
17	3	1	0.0376	0.1270	0.0645	0.3663	0.0732	0.0530	0.1330	0.2039	0.0651	0.2002
18	3	2	0.3015	0.3331	0.4333	0.3490	0.4108	0.3161	0.4048	0.4627	0.3625	0.5836
19	4	6	0.2730	0.2980	0.0083	0.1096	0.0452	0.3896	0.0014	0.5159	0.0000	0.6011
20	5	1	0.5469	0.3593	0.0749	0.2775	0.2062	0.4782	0.1067	0.9664	0.3825	0.3989
21	6	1	0.1278	0.1082	0.0095	0.1249	0.0219	0.0947	0.0699	0.1056	0.0647	0.1555
22	6	3	0.2076	0.2349	0.0384	0.6292	0.0461	0.4513	0.0897	0.6428	0.0725	0.8255
23	6	4	0.1829	0.1278	0.0746	0.3496	0.0747	0.1875	0.0469	0.0633	0.1129	0.0186
24	7	2	0.2098	0.2778	0.0000	0.0922	0.0000	0.0377	0.0101	0.0949	0.0082	0.0379
25	7	4	0.0022	0.0385	0.0120	0.1401	0.0068	0.0190	0.0144	0.0668	0.0556	0.0873
26	7	5	0.2733	0.4573	0.0338	0.4569	0.0177	0.5582	0.0466	0.5354	0.0244	0.5624
27	7	7	0.2347	0.0520	0.0124	0.1195	0.0339	0.1411	0.0170	0.0438	0.0299	0.0782
28	8	1	0.0308	0.0932	0.0058	0.0364	0.0003	0.0657	0.0043	0.0364	0.0988	0.0522
29	8	2	0.0482	0.1224	0.1627	0.0175	0.1607	0.0426	0.1597	0.0616	0.0931	0.0634
30	8	3	0.3155	0.0968	0.0565	0.1592	0.0520	0.3090	0.0664	0.2408	0.1955	0.3792
31	8	4	0.5867	0.8973	0.0017	0.6929	0.0051	0.5016	0.0057	0.4004	0.0000	0.5365
32	8	8	0.0592	0.0776	0.2086	0.0943	0.1652	0.0715	0.1896	0.0379	0.0371	0.0224
33	9	3	0.0830	0.0999	0.0492	0.1576	0.1110	0.1416	0.0549	0.0671	0.0286	0.1136
34	9	4	0.1937	0.2289	1.2085	0.3559	1.1283	0.6837	1.0765	0.0463	0.5169	0.0250
35	9	5	0.0124	0.0231	0.1961	0.0246	0.1496	0.0130	0.1832	0.0390	0.1943	0.0163
36	10	1	0.0177	0.0331	0.7008	0.0047	0.6119	0.0255	0.6271	0.0374	0.5679	0.0174
37	10	2	0.4542	0.7405	0.0947	0.7210	0.4318	0.6885	0.4649	0.8461	0.4596	0.5987
38	10	3	0.8317	0.6613	0.0940	0.4719	0.0411	0.3106	0.0095	0.3064	0.0163	0.4362
39	10	6	0.1267	0.1183	0.2148	0.0942	0.6015	0.0924	1.0562	0.1291	0.4518	0.1692
40	11	1	0.0749	0.0954	0.1195	0.1553	0.0604	0.1560	0.0492	0.1171	0.0572	0.1500
41	11	2	0.1535	0.2186	0.2841	0.2430	0.4704	0.0131	0.6433	0.0280	0.0000	0.0719
42	11	5	0.0695	0.0404	0.3602	0.1126	0.1419	0.0877	0.0388	0.0873	0.0398	0.0936
43	11	7	0.0175	0.0000	0.2125	0.0491	0.2209	0.0162	0.1644	0.0397	0.1644	0.0034
44	11	8	0.0508	0.1010	0.0167	0.1843	0.0278	0.0896	0.0083	0.0823	0.0083	0.0598
45	11	9	0.2463	0.1945	0.5016	0.6899	0.4692	0.2857	0.3763	0.3101	0.3763	0.3183
46	12	6	0.1719	0.1085	0.1489	0.0452	0.1493	0.0455	0.1104	0.0319	0.1104	0.0907

Change in curl index - earlywood, 10 Hz, 5mm

Change in Curl Index - Earlywood, 10 Hz - 5 mm							
Fiber Count	run #	fiber #	1	10	100	1000	10,000
1	1	1	0.0439	0.2989	0.3260	0.2294	0.1232
2	1	2	0.0119	0.0257	0.0360	0.0012	0.0026
3	1	3	0.0508	0.0705	0.1747	0.2113	0.0761
4	1	4	0.0389	0.4171	0.5894	0.2891	0.3482
5	1	5	0.0026	0.4023	0.4267	0.2574	0.1838
6	1	6	0.0228	0.0814	0.0473	0.1087	0.1791
7	1	7	0.0146	0.2590	0.0551	0.0698	0.0364
8	1	8	0.0455	0.2469	0.7862	0.0496	0.0086
9	1	10	0.0397	0.1267	0.0096	0.1027	0.0547
10	1	11	0.0727	0.1726	0.1309	0.1805	0.1430
11	1	12	0.0082	0.5373	0.4951	0.4276	0.6580
12	1	14	0.0091	0.5953	0.3682	0.3512	0.4065
13	2	1	0.0005	0.0058	0.0653	0.0756	0.1170
14	2	2	0.0085	0.0841	0.0980	0.0694	0.0328
15	2	5	0.1193	0.8970	1.2688	0.6602	0.5820
16	2	6	0.0236	0.2048	0.0995	0.0813	0.0521
17	3	1	0.0894	0.3018	0.0203	0.0709	0.1351
18	3	2	0.0316	0.0843	0.0947	0.0579	0.2211
19	4	6	0.0250	0.1013	0.3444	0.5145	0.6011
20	5	1	0.1876	0.2026	0.2720	0.8596	0.0164
21	6	1	0.0196	0.1155	0.0727	0.0357	0.0908
22	6	3	0.0272	0.5908	0.4052	0.5532	0.7530
23	6	4	0.0551	0.2750	0.1129	0.0163	0.0943
24	7	2	0.0680	0.0922	0.0377	0.0848	0.0297
25	7	4	0.0363	0.1281	0.0122	0.0523	0.0317
26	7	5	0.1840	0.4230	0.5405	0.4888	0.5380
27	7	7	0.1827	0.1071	0.1071	0.0268	0.0483
28	8	1	0.0624	0.0306	0.0655	0.0321	0.0466
29	8	2	0.0741	0.1452	0.1181	0.0981	0.0297
30	8	3	0.2187	0.1027	0.2569	0.1744	0.1837
31	8	4	0.3106	0.6912	0.4965	0.3947	0.5365
32	8	8	0.0184	0.1143	0.0938	0.1516	0.0148
33	9	3	0.0169	0.1085	0.0306	0.0122	0.0850
34	9	4	0.0353	0.8526	0.4446	1.0302	0.4919
35	9	5	0.0107	0.1715	0.1365	0.1442	0.1779
36	10	1	0.0153	0.6961	0.5863	0.5897	0.5505
37	10	2	0.2863	0.6263	0.2567	0.3812	0.1391
38	10	3	0.1705	0.3780	0.2695	0.2968	0.4199
39	10	6	0.0085	0.1206	0.5092	0.9271	0.2825
40	11	1	0.0205	0.0358	0.0956	0.0679	0.0929
41	11	2	0.0651	0.0411	0.4572	0.6153	0.0719
42	11	5	0.0291	0.2476	0.0542	0.0485	0.0538
43	11	7	0.0175	0.1635	0.2047	0.1247	0.1610
44	11	8	0.0502	0.1676	0.0617	0.0740	0.0515
45	11	9	0.0517	0.1882	0.1835	0.0662	0.0580
46	12	6	0.0634	0.1037	0.1038	0.0785	0.0197
		average:	0.0640	0.2572	0.2483	0.2442	0.1963
		st. deviation:	0.0740	0.2289	0.2488	0.2605	0.2084

Latewood curl index - 10 Hz, 5mm

Latewood Curl Index - 10 Hz, 5 mm												
Fiber Count	Run #	Fiber #	1	1.5	10	10.5	100	100.5	1000	1000.5	10000	10000.5
1	1	1	0.0415	0.0856	0.0641	0.0524	0.0413	0.0339	0.0355	0.0377	0.0451	0.0319
2	1	5	0.0198	0.0190	0.2687	0.0097	0.0668	0.0158	0.0338	0.0000	0.0329	0.0000
3	1	6	0.3460	0.3863	0.3097	0.1501	0.0769	0.1094	0.0918	0.1072	0.0134	0.0264
4	1	7	0.5239	0.4988	0.2739	0.3572	0.0848	0.1057	0.0741	0.0924	0.1321	0.1584
5	2	1	0.0532	0.0596	0.0000	0.0941	0.0096	0.0423	0.0128	0.0388	0.0115	0.0514
6	2	2	0.0355	0.0668	0.0317	0.0491	0.0279	0.0504	0.0556	0.0175	0.0711	0.0294
7	2	3	0.2917	0.2781	0.2227	0.2328	0.1807	0.1749	0.1512	0.1688	0.2139	0.1498
8	2	4	0.1194	0.1660	0.0344	0.0418	0.0406	0.0579	0.0424	0.0175	0.0189	0.0075
9	2	5	0.0000	0.0148	0.0351	0.0436	0.0451	0.0197	0.0809	0.0415	0.0361	0.0419
10	2	6	0.3601	0.2520	0.4657	0.1065	0.1353	0.0578	0.0219	0.0914	0.0254	0.0198
11	4	1	0.3081	0.1492	0.2112	0.1804	0.3543	0.2095	0.2235	0.1852	0.3355	0.4375
12	4	2	0.0245	0.0179	0.0000	0.0000	0.0166	0.0186	0.1385	0.0071	0.0532	0.0022
13	4	3	0.0302	0.0182	0.0218	0.0085	0.1664	0.0257	0.2477	0.0117	0.0922	0.0147
14	4	4	0.0814	0.0694	0.1555	0.4845	0.4035	0.3519	0.4674	0.6883	0.5687	0.9080
15	4	6	0.5688	0.9434	0.8144	0.8104	0.9687	0.9587	0.9843	0.9954	0.9228	0.9632
16	4	7	0.0285	0.0609	0.0295	0.0288	0.0291	0.0393	0.0266	0.0252	0.0279	0.0195
17	5	1	0.1871	0.3778	0.3852	0.3694	0.4732	0.3880	0.3518	0.3732	0.5111	0.2927
18	5	3	0.0131	0.0622	0.0203	0.0363	0.0338	0.0506	0.0444	0.0330	0.0186	0.0610
19	5	4	0.0316	0.1225	0.1316	0.1183	0.1275	0.1013	0.0834	0.1337	0.1807	0.3206
20	5	6	0.0439	0.0258	0.0748	0.0740	0.0454	0.0092	0.0431	0.0127	0.0989	0.0754
21	6	1	0.0453	0.0465	0.0185	0.0859	0.0156	0.0227	0.0190	0.0070	0.1013	0.1975
22	6	2	0.3469	0.2434	0.2162	0.2290	0.0177	0.1483	0.0203	0.0862	0.2224	0.0120
23	6	3	0.0155	0.0131	0.0218	0.0077	0.0005	0.0000	0.0000	0.0000	0.0000	0.0000
24	6	11	0.0483	0.0189	0.0465	0.0505	0.0561	0.0228	0.0489	0.0142	0.0511	0.2219
25	6	12	0.4450	0.7366	0.3692	1.0786	0.3379	0.1390	0.8172	0.1674	0.8268	0.0303
26	6	13	0.0316	0.0103	0.0187	0.0457	0.0360	0.0191	0.0622	0.1268	0.0187	0.3257
27	7	2	0.3067	0.2971	0.4561	0.3368	0.6555	0.3242	0.6152	0.3894	0.7535	0.3351
28	7	3	0.3507	0.4192	0.4725	0.3209	0.2868	0.3294	0.3086	0.3004	0.4059	0.6587
29	7	4	0.4119		0.3953	0.3548	0.5286	0.5098	0.3146	0.4596	0.5281	0.1447
30	7	5	0.9155	0.9685	0.5249	0.6503	0.6792	0.6631	0.5752	0.7502	0.1107	0.0316
31	8	1	0.1227	0.1147	0.0297	0.1083	0.0308	0.0726	0.0522	0.0305	0.0265	0.0610
32	8	2	0.1464	0.1315	0.1187	0.1135	0.1158	0.0943	0.0618	0.0860	0.0607	0.0295
33	8	3	0.0793	0.0937	0.0906	0.1145	0.0780	0.0892	0.0299	0.0435	0.0364	0.0000
34	8	6	0.0460	0.0222	0.0130	0.0862	0.0333	0.0000	0.0178	0.0000	0.0223	0.0140
35	9	1	0.0153	0.0295	0.0590	0.0210	0.0194	0.0057	0.0250	0.0211	0.0596	0.0373
36	9	2	0.1388	0.0906	0.0692	0.1021	0.2003	0.1501	0.0775	0.0611	0.1100	0.0067
37	9	3	0.0415	0.0196	0.0699	0.0606	0.0049	0.0191	0.0955	0.0218	0.3899	0.0000
38	9	5	0.0421	0.0248	0.0502	0.0584	0.0847	0.0187	0.0905	0.0116	0.0597	0.0000
39	9	7	0.9959	0.9204	0.7691	0.6632	0.7701	0.8189	0.9809	0.9620	1.0737	0.3312
40	10	2	0.1653	0.2512	0.3110	0.3371	0.3039	0.3275	0.2516	0.3287	0.3810	0.0353
41	10	3	0.0782	0.0960	0.2125	0.0905	0.0727	0.0945	0.1965	0.0787	0.4874	0.0194
42	10	4	0.0464	0.0403	0.0117	0.0238	0.0129	0.0225	0.0131	0.0243	0.0169	0.6484
43	11	1	0.8326	1.0753	0.9531	1.1390	0.9088	0.9819	0.5064	0.5666	0.6551	0.1870
44	11	2	0.1172	0.2030	0.0775	0.1289	0.0911	0.1345	0.1665	0.2359	0.1492	0.0906
45	11	3	0.0659	0.0915	0.0594	0.0975	0.0635	0.0663	0.0724	0.0669	0.1193	0.0000
46	12	2	0.4411	0.4210	0.7873	0.2243	0.6417	0.4662	0.3409	0.3096	0.3947	0.1989
47	12	3	0.3609	0.3203	0.3233	0.3054	0.4207	0.3355	0.3188	0.2983	0.3187	0.1436
48	13	2	1.1598	1.1787	0.0415	0.0243	0.1333	1.0061	0.0625	0.2530	0.0463	0.0982
49	13	3	0.0778	0.0660	1.2204	1.0918	1.6242	0.0597	0.2403	0.1060	0.2935	0.1390
50	13	4	0.9750	0.7551	0.0702	0.0854	0.0628	0.4147	0.0556	0.2753	0.0926	0.1794
51	13	6	0.0000	0.0000	0.5545	0.7771	0.3235	0.0000	0.1942	0.0000	0.1911	0.0000
52	13	7	0.0748	0.0555	0.0779	0.0614	0.2375	0.2224	0.2291	0.2439	0.2102	0.0955

Change in curl index - latewood, 10 Hz, 5mm

Change in Curl Index - Latewood, 10 Hz - 5 mm							
Fiber Count	Run #	Fiber #	1	10	100	1000	10,000
1	1	1	0.0441	0.0117	0.0074	0.0022	0.0132
2	1	5	0.0009	0.2590	0.0510	0.0338	0.0329
3	1	6	0.0403	0.1596	0.0325	0.0154	0.0130
4	1	7	0.0251	0.0833	0.0209	0.0183	0.0263
5	2	1	0.0064	0.0941	0.0327	0.0260	0.0399
6	2	2	0.0312	0.0174	0.0224	0.0381	0.0417
7	2	3	0.0136	0.0101	0.0058	0.0176	0.0641
8	2	4	0.0466	0.0074	0.0173	0.0249	0.0114
9	2	5	0.0148	0.0086	0.0253	0.0394	0.0058
10	2	6	0.1081	0.3593	0.0775	0.0695	0.0056
11	4	1	0.1588	0.0309	0.1448	0.0383	0.1019
12	4	2	0.0067	0.0000	0.0020	0.1314	0.0510
13	4	3	0.0120	0.0133	0.1407	0.2360	0.0775
14	4	4	0.0120	0.3290	0.0516	0.2209	0.3393
15	4	6	0.3745	0.0039	0.0100	0.0111	0.0403
16	4	7	0.0324	0.0006	0.0102	0.0013	0.0084
17	5	1	0.1906	0.0158	0.0851	0.0213	0.2184
18	5	3	0.0491	0.0160	0.0168	0.0114	0.0424
19	5	4	0.0908	0.0133	0.0263	0.0503	0.1399
20	5	6	0.0181	0.0008	0.0362	0.0304	0.0234
21	6	1	0.0012	0.0674	0.0072	0.0121	0.0961
22	6	2	0.1035	0.0128	0.1305	0.0659	0.2105
23	6	3	0.0024	0.0141	0.0005	0.0000	0.0000
24	6	11	0.0294	0.0040	0.0334	0.0347	0.1708
25	6	12	0.2916	0.7094	0.1989	0.6498	0.7966
26	6	13	0.0214	0.0270	0.0168	0.0646	0.3070
27	7	2	0.0096	0.1193	0.3312	0.2257	0.4183
28	7	3	0.0685	0.1516	0.0426	0.0083	0.2528
29	7	4	0.0000	0.0405	0.0188	0.1450	0.3834
30	7	5	0.0530	0.1254	0.0160	0.1750	0.0792
31	8	1	0.0080	0.0785	0.0417	0.0216	0.0345
32	8	2	0.0149	0.0053	0.0215	0.0242	0.0311
33	8	3	0.0144	0.0240	0.0111	0.0136	0.0364
34	8	6	0.0238	0.0732	0.0333	0.0178	0.0082
35	9	1	0.0142	0.0380	0.0137	0.0039	0.0223
36	9	2	0.0482	0.0330	0.0502	0.0165	0.1033
37	9	3	0.0219	0.0094	0.0141	0.0737	0.3899
38	9	5	0.0173	0.0083	0.0660	0.0789	0.0597
39	9	7	0.0754	0.1059	0.0488	0.0190	0.7425
40	10	2	0.0859	0.0262	0.0236	0.0771	0.3458
41	10	3	0.0178	0.1219	0.0218	0.1178	0.4680
42	10	4	0.0061	0.0121	0.0096	0.0112	0.6315
43	11	1	0.2428	0.1859	0.0731	0.0603	0.4682
44	11	2	0.0858	0.0514	0.0433	0.0694	0.0587
45	11	3	0.0256	0.0381	0.0028	0.0055	0.1193
46	12	2	0.0201	0.5630	0.1755	0.0313	0.1958
47	12	3	0.0405	0.0178	0.0852	0.0206	0.1751
48	13	2	0.0188	0.0172	0.8728	0.1905	0.0519
49	13	3	0.0118	0.1286	1.5645	0.1343	0.1545
50	13	4	0.2199	0.0152	0.3519	0.2197	0.0868
51	13	6	0.0000	0.2226	0.3235	0.1942	0.1911
52	13	7	0.0193	0.0165	0.0150	0.0148	0.1147
		average:	0.0556	0.0865	0.1053	0.0737	0.1635
		st. deviation:	0.0784	0.1391	0.2488	0.1062	0.1919

Earlywood curl index and change in curl index - 10 Hz, 4mm

Curl Index Earlywood - 10 Hz - 4mm

0	1	1.5	10	10.5	100	100.5	1000	1000.5	10000	10000.5
0.0107	0.0118	0.0146	0.0396	0.0601	0.0537	0.0293	0.0677	0.0232	0.0248	0.0169
0.0525	0.0269	0.0796	0.0446	0.0159	0.0571	0.0166	0.0364	0.0235	0.0258	0.0206
0.0208	0.0234	0.0223	0.0364	0.0579	0.0270	0.0561	0.0212	0.0098	0.0117	0.0269
0.0201	0.0146	0.0000	0.0029	0.0071	0.0049	0.0094	0.0128	0.0293	0.0144	0.0081
0.1965	0.4689	0.2373	0.3689	0.2052	0.4291	0.3267	0.3746	0.3116	0.2117	0.2508
0.0224	0.0357	0.0606	0.0446	0.0544	0.0568	0.0320	0.0570	0.0566	0.0545	0.0654
0.5440	0.5075	0.6387	0.3090	0.2262	0.4430	0.2763	0.3685	0.3634	0.3769	0.3749
0.2126	0.2005	0.1935	0.2184	0.2668	0.2278	0.2488	0.2757	0.2780	0.2263	0.2676
0.0661	0.0248	0.0828	0.0555	0.0131	0.0343	0.0392	0.0682	0.0000	0.0139	0.0064
0.0704	0.1138	0.1447	0.1877	0.1210	0.1101	0.1057	0.2479	0.1017	0.1694	0.1185
0.0210	0.0340	0.0413	0.0146	0.0557	0.0671	0.1184	0.1108	0.0526	0.0707	0.0505
0.0399	0.0545	0.0337	0.0376	0.0257	0.0273	0.0763	0.0513	0.0447	0.2034	0.1290
0.0178	0.0220	0.0233	0.0331	0.0225	0.0293	0.0232	0.0240	0.0590	0.0288	0.0397
0.1425	0.1126	0.1524	0.1084	0.1088	0.1909	0.2201	0.2499	0.1683	0.2809	0.1927
0.0852	0.1203	0.1003	0.1147	0.0321	0.1346	0.0813	0.1521	0.1155	0.1066	0.1077
0.0000	0.0015	0.0087	0.0024	0.0090	0.0205	0.0000	0.0041	0.0052	0.0000	0.0000
0.0000	0.0086	0.0329	0.0111	0.0102	0.0056	0.0069	0.0133	0.0277	0.0182	0.0134
0.0227	0.0539	0.0329	0.1708	0.0560	0.0821	0.0471	0.0808	0.0403	0.0854	0.0452
0.0286	0.0321	0.0422	0.0003	0.0193	0.0410	0.0470	0.0138	0.0233	0.0246	0.0097
0.1177	0.1956	0.2429	0.2773	0.2422	0.2087	0.1237	0.2963	0.2306	0.1479	0.2122
0.0119	0.0245	0.0284	0.0279	0.0241	0.0204	0.0205	0.0400	0.0316	0.0420	0.0647
0.0268	0.0342	0.0407	0.0310	0.0407	0.0439	0.0193	0.0043	0.0255	0.0187	0.0261
0.0297	0.0533	0.0359	0.0156	0.0389	0.0185	0.0299	0.0317	0.0392	0.0384	0.0285
0.1550	0.1104	0.0574	0.0571	0.0311	0.1199	0.0600	0.0236	0.0470	0.0766	0.0879
0.1788	0.2216	0.2681	0.1815	0.2891	0.3602	0.4502	0.4016	0.6258	0.5379	0.4369
0.1024	0.1181	0.0850	0.0515	0.0997	0.1096	0.0861	0.0379	0.1222	0.0372	0.0514

Δ Curl Index Earlywood - 10 Hz - 4mm

	1	10	100	1000	10000
	0.0028	0.0205	0.0244	0.0446	0.0079
	0.0527	0.0286	0.0406	0.0129	0.0052
	0.0011	0.0215	0.0291	0.0114	0.0152
	0.0146	0.0041	0.0045	0.0164	0.0063
	0.2316	0.1636	0.1023	0.0630	0.0391
	0.0249	0.0098	0.0249	0.0004	0.0109
	0.1312	0.0828	0.1667	0.0050	0.0020
	0.0070	0.0484	0.0209	0.0023	0.0413
	0.0580	0.0424	0.0049	0.0682	0.0075
	0.0310	0.0666	0.0044	0.1462	0.0509
	0.0072	0.0411	0.0513	0.0582	0.0202
	0.0208	0.0119	0.0489	0.0065	0.0743
	0.0013	0.0106	0.0061	0.0350	0.0109
	0.0398	0.0005	0.0291	0.0816	0.0883
	0.0200	0.0827	0.0534	0.0366	0.0011
	0.0073	0.0065	0.0205	0.0011	0.0000
	0.0244	0.0009	0.0012	0.0144	0.0049
	0.0210	0.1147	0.0351	0.0405	0.0402
	0.0101	0.0190	0.0060	0.0096	0.0149
	0.0473	0.0351	0.0850	0.0657	0.0643
	0.0039	0.0038	0.0001	0.0085	0.0227
	0.0065	0.0097	0.0246	0.0213	0.0074
	0.0174	0.0233	0.0114	0.0075	0.0100
	0.0529	0.0260	0.0599	0.0233	0.0113
	0.0465	0.1076	0.0900	0.2242	0.1009
	0.0331	0.0482	0.0234	0.0843	0.0141
average	0.0352	0.0396	0.0373	0.0419	0.0258

Latewood curl index and change in curl index - 10 Hz, 4mm

Curl Index Latewood - 10 Hz - 4mm

0	1	1.5	10	10.5	100	100.5	1000	1000.5	10000	10000.5
0.1075	0.1052	0.0926	0.1181	0.0682	0.2124	0.1852	0.1359	0.0773	0.1730	0.3531
0.1465	0.1715	0.1546	0.1598	0.2028	0.2139	0.2066	0.2049	0.1913	0.1833	0.1147
0.1207	0.0612	0.1662	0.1479	0.0661	0.0845	0.0695	0.0471	0.0785	0.0686	0.0559
0.0182	0.0250	0.0359	0.0298	0.0711	0.0550	0.0527	0.0403	0.0587	0.0600	0.0458
0.1431	0.1514	0.3588	0.1942	0.2818	0.2918	0.2800	0.2673	0.2377	0.2629	0.2772
0.0601	0.0785	0.0629	0.0416	0.1797	0.0751	0.0822	0.1592	0.1406	0.1194	0.1058
0.3373	0.3874	0.3023	0.2767	0.4447	0.4050	0.3191	0.3746	0.5887	0.4734	0.2772
0.1075	0.1834	0.1759	0.2642	0.1368	0.2047	0.1366	0.2331	0.2832	0.1093	0.1765
0.4090	0.2017	0.2563	0.1558	0.1597	0.2455	0.2268	0.2200	0.2707	0.3364	0.2648
0.0274	0.0160	0.0299	0.0229	0.0026	0.0184	0.0360	0.0253	0.0258	0.0304	0.0297
0.0845	0.0150	0.0679	0.0666	0.0541	0.0927	0.0448	0.0397	0.0550	0.0672	0.0191
0.0000	0.0050	0.0221	0.0103	0.0452	0.0137	0.0226	0.0178	0.0248	0.0156	0.0216
0.0000	0.0000	0.0113	0.0000	0.0210	0.0034	0.0025	0.0101	0.0046	0.0000	0.0011
0.0220	0.0234	0.0822	0.0324	0.0318	0.0357	0.0142	0.0479	0.0249	0.0468	0.0623
0.2000	0.1905	0.1390	0.1491	0.0635	0.0812	0.0944	0.0990	0.0865	0.0776	0.0650
0.0644	0.1334	0.0715	0.0696	0.1273	0.0680	0.0729	0.0868	0.0554	0.0575	0.0756
0.6109	0.5461	0.5305	0.5014	0.6466	0.6124	0.3911	0.3998	0.2817	0.2937	0.3991
0.0326	0.0223	0.0074	0.0471	0.0355	0.0020	0.0174	0.0189	0.0133	0.0144	0.0264
0.1346	0.0498	0.0509	0.1055	0.0927	0.0205	0.0690	0.0146	0.0683	0.0445	0.0389
0.0181	0.0056	0.0757	0.0274	0.0903	0.0452	0.0503	0.0239	0.0265	0.0300	0.0284
0.0616	0.0615	0.0565	0.0121	0.0639	0.0000	0.0323	0.0083	0.0196	0.0081	0.0333
0.1678	0.2845	0.1048	0.1243	0.1811	0.1671	0.1745	0.3517	0.5219	0.1559	0.1685
0.4757	0.1861	0.1385	0.2541	0.2212	0.2345	0.2488	0.2635	0.1704	0.2008	0.1509
0.0415	0.0188	0.0179	0.0147	0.0183	0.0061	0.0124	0.0126	0.0115	0.0214	0.0087
0.0884	0.0763	0.1223	0.0765	0.1307	0.0907	0.1111	0.0609	0.1459	0.0442	0.0651

Δ Curl Index Latewood - 10 Hz - 4mm

	1	10	100	1000	10000
	0.0126	0.0499	0.0272	0.0586	0.1800
	0.0169	0.0430	0.0073	0.0136	0.0686
	0.1049	0.0819	0.0150	0.0314	0.0127
	0.0110	0.0413	0.0023	0.0184	0.0142
	0.2074	0.0875	0.0118	0.0296	0.0143
	0.0157	0.1381	0.0071	0.0186	0.0136
	0.0851	0.1680	0.0859	0.2141	0.1962
	0.0075	0.1274	0.0681	0.0501	0.0672
	0.0546	0.0039	0.0187	0.0507	0.0715
	0.0139	0.0203	0.0176	0.0005	0.0007
	0.0529	0.0124	0.0479	0.0153	0.0480
	0.0170	0.0349	0.0089	0.0070	0.0060
	0.0113	0.0210	0.0009	0.0055	0.0011
	0.0588	0.0006	0.0215	0.0230	0.0155
	0.0515	0.0857	0.0132	0.0126	0.0126
	0.0619	0.0577	0.0049	0.0315	0.0181
	0.0157	0.1451	0.2213	0.1181	0.1055
	0.0149	0.0116	0.0154	0.0057	0.0120
	0.0011	0.0128	0.0485	0.0537	0.0056
	0.0701	0.0629	0.0051	0.0026	0.0016
	0.0050	0.0518	0.0323	0.0113	0.0251
	0.1797	0.0568	0.0074	0.1702	0.0127
	0.0476	0.0329	0.0142	0.0931	0.0499
	0.0009	0.0036	0.0063	0.0012	0.0127
	0.0460	0.0542	0.0204	0.0849	0.0209
average	0.0466	0.0562	0.0292	0.0448	0.0395

Earlywood curl index and change in curl index - 10 Hz, 3mm

Curl Index Earlywood - 10 Hz - 3mm

0	1	1.5	10	10.5	100	100.5	1000	1000.5	10000	10000.5
0.0995	0.0476	0.0943	0.0972	0.0482	0.0442	0.0519	0.1159	0.1234	0.0613	0.0622
0.0174	0.0323	0.0133	0.0093	0.0237	0.0110	0.0279	0.0225	0.0204	0.0535	0.0214
0.8542	0.9079	1.0338	1.0615	0.6921	0.6550	0.4654	0.5888	0.5525	0.6416	0.5317
0.0175	0.0274	0.0783	0.1012	0.0913	0.0732	0.0660	0.0713	0.0351	0.0666	0.0388
0.2927	0.0358	0.0928	0.0937	0.0891	0.2406	0.1158	0.0568	0.0611	0.3468	0.1852
1.1369	1.1002	1.3206	0.7933	0.7870	0.7846	0.7871	0.7207	0.8523	0.8433	0.7261
0.0313	0.0247	0.0571	0.2216	0.1231	0.0969	0.1470	0.0700	0.1411	0.0599	0.0789
0.0231	0.0367	0.0186	0.0279	0.0258	0.0642	0.0446	0.0364	0.0244	0.0223	0.0105
0.2677	0.3240	0.2781	0.2412	0.1448	0.2074	0.1952	0.3333	0.1841	0.1797	0.3010
0.0872	0.0289	0.0623	0.0106	0.0194	0.0309	0.0222	0.0440	0.0187	0.0533	0.0727
0.7636	0.9617	1.0327	0.8178	0.6760	0.3528	0.2797	0.1776	0.1715	0.0378	0.0360
0.1628	0.0375	0.0556	0.0764	0.0245	0.0498	0.0620	0.0343	0.0697	0.0215	0.0166
0.0297	0.0000	0.0172	0.0429	0.0493	0.0336	0.0316	0.0084	0.0090	0.0045	0.0078
0.4041	0.2081	0.0978	0.0556	0.1873	0.0477	0.0079	0.0280	0.0276	0.0189	0.0243
0.0608	0.0637	0.0295	0.0634	0.0481	0.0113	0.0819	0.0540	0.0428	0.0866	0.0651

Δ Curl Index Earlywood - 10 Hz - 3mm

	1	10	100	1000	10000
	0.0467	0.0490	0.0078	0.0075	0.0009
	0.0190	0.0144	0.0169	0.0022	0.0322
	0.1259	0.3693	0.1895	0.0363	0.1099
	0.0509	0.0099	0.0072	0.0362	0.0278
	0.0570	0.0046	0.1248	0.0042	0.1616
	0.2204	0.0063	0.0025	0.1317	0.1171
	0.0324	0.0985	0.0502	0.0712	0.0190
	0.0181	0.0021	0.0196	0.0120	0.0118
	0.0459	0.0964	0.0122	0.1493	0.1213
	0.0334	0.0088	0.0087	0.0252	0.0194
	0.0709	0.1418	0.0731	0.0061	0.0019
	0.0181	0.0519	0.0121	0.0354	0.0049
	0.0172	0.0064	0.0020	0.0006	0.0033
	0.1103	0.1316	0.0398	0.0004	0.0054
	0.0341	0.0153	0.0707	0.0112	0.0215
average	0.0600	0.0671	0.0425	0.0353	0.0439

Latewood curl index and change in curl index - 10 Hz, 3mm

Curl Index Latewood - 10 Hz - 3mm

0	1	1.5	10	10.5	100	100.5	1000	1000.5	10000	10000.5
0.1115	0.0982	0.1047	0.0636	0.0457	0.1458	0.0894	0.1335	0.1949	0.0625	0.0546
0.0726	0.0233	0.1086	0.0793	0.1156	0.0734	0.0357	0.1693	0.0833	0.0298	0.0232
0.2939	0.3026	0.3108	0.3068	0.2999	0.2448	0.4147	0.3256	0.4187	0.3634	0.3604
0.0261	0.0789	0.1102	0.0215	0.0779	0.0467	0.1095	0.0210	0.0547	0.0679	0.0422
0.4247	0.5675	0.4469	0.4523	0.3761	0.0722	0.4301	0.3353	0.3704	0.3106	0.5494
0.0142	0.0309	0.1549	0.2070	0.1693	0.3384	0.1583	0.1901	0.2149	0.2231	0.2517
0.0362	0.0297	0.0290	0.0248	0.0569	0.1937	0.0189	0.0205	0.0258	0.0170	0.0264
0.1232	0.0839	0.1603	0.0782	0.0924	0.1788	0.0565	0.1535	0.0613	0.1064	0.1246
0.2378	0.2939	0.3497	0.0876	0.2184	0.1068	0.2528	0.1416	0.1767	0.2814	0.1041
0.1065	0.0277	0.0537	0.0524	0.0531	0.0537	0.0666	0.1969	0.1896	0.0263	0.2059
0.4870	0.5861	0.7655	0.8413	0.8397	0.7519	0.7076	0.7843	0.7445	0.7899	0.6741
0.0491	0.0808	0.0821	0.0606	0.0949	0.0218	0.0311	0.0438	0.0343	0.0446	0.0366
0.3435	0.3160	0.4471	0.1817	0.2169	0.1988	0.2617	0.5257	0.1109	0.2038	0.3152
0.4483	0.7772	0.9849	0.9340	0.6637	0.7506	0.9459	0.2059	0.1080	0.7054	0.2039
0.2302	0.2992	0.2094	0.2663	0.4028	0.4726	0.3105	0.3004	0.2410	0.2512	0.1821
0.0677	0.0176	0.0240	0.0234	0.0081	0.0399	0.0200	0.0199	0.0156	0.0158	0.0117
0.4016	0.8688	0.8422	0.7835	0.5423	0.7138	0.8798	0.7192	0.8533	0.7126	0.7477
0.1182	0.1478	0.3003	0.1740	0.2049	0.1673	0.2785	0.1633	0.1713	0.0869	0.1531
0.0142	0.0172	0.0000	0.0000	0.0000	0.0358	0.0209	0.0806	0.0190	0.0201	0.0045
0.0065	0.0187	0.0340	0.0328	0.0295	0.0000	0.0000	0.0481	0.0000	0.0155	0.0174
0.1091	0.1165	0.4506	0.3906	0.7279	0.3107	0.7432	0.3669	0.8284	0.7060	0.4011
0.0261	0.0203	0.0091	0.0174	0.0118	0.0310	0.0387	0.0346	0.0233	0.0261	0.0315
0.0253	0.0302	0.0593	0.0665	0.1807	0.0609	0.1744	0.0982	0.1330	0.1041	0.0646
0.0939	0.1301	0.2943	0.2090	0.3331	0.2772	0.3130	0.2819	0.4156	0.3895	0.2632

Δ Curl Index Latewood - 10 Hz - 3mm

	1	10	100	1000	10000
	0.0065	0.0179	0.0564	0.0614	0.0079
	0.0853	0.0363	0.0376	0.0860	0.0066
	0.0082	0.0069	0.1698	0.0931	0.0030
	0.0314	0.0564	0.0628	0.0337	0.0257
	0.1206	0.0762	0.3580	0.0350	0.2389
	0.1241	0.0376	0.1801	0.0248	0.0286
	0.0007	0.0321	0.1748	0.0053	0.0094
	0.0764	0.0143	0.1224	0.0922	0.0182
	0.0558	0.1308	0.1460	0.0351	0.1773
	0.0260	0.0006	0.0129	0.0072	0.1796
	0.1794	0.0016	0.0443	0.0398	0.1158
	0.0013	0.0343	0.0093	0.0095	0.0080
	0.1311	0.0352	0.0629	0.4148	0.1114
	0.2077	0.2703	0.1954	0.0979	0.5015
	0.0899	0.1365	0.1621	0.0594	0.0691
	0.0064	0.0154	0.0199	0.0043	0.0040
	0.0266	0.2412	0.1659	0.1341	0.0351
	0.1525	0.0310	0.1112	0.0080	0.0662
	0.0172	0.0000	0.0148	0.0615	0.0156
	0.0154	0.0033	0.0000	0.0481	0.0019
	0.3341	0.3373	0.4325	0.4615	0.3050
	0.0112	0.0056	0.0077	0.0113	0.0054
	0.0291	0.1142	0.1136	0.0348	0.0394
	0.1642	0.1241	0.0358	0.1337	0.1263
average	0.0792	0.0733	0.1123	0.0830	0.0875

Earlywood curl index and change in curl index - 30 Hz, 5mm

Curl Index Earlywood - 30 Hz, 5mm										
0	1	1.5	10	10.5	100	100.5	1000	1000.5	10000	10000.5
0.2691	0.2475	0.2295	0.2292	0.2421	0.2331	0.1991	0.2265	0.1868	0.2249	0.2256
0.0106	0.0203	0.0306	0.0330	0.0092	0.0144	0.0209	0.0301	0.0183	0.0245	0.0154
0.1705	0.2167	0.2173	0.2278	0.1947	0.2683	0.2453	0.2238	0.1969	0.2201	0.2556
0.0920	0.0593	0.0324	0.0891	0.0371	0.0714	0.0616	0.0450	0.0616	0.0626	0.0648
0.0618	0.0508	0.0977	0.1064	0.0654	0.1071	0.1041	0.1138	0.0859	0.1033	0.1009
0.0404	0.0791	0.0190	0.0161	0.0308	0.0153	0.0337	0.0235	0.0087	0.0288	0.0178
0.3971	0.5187	0.5009	0.5887	0.6094	0.6209	0.6121	0.4908	0.7020	0.8284	0.7020
0.2245	0.2797	0.3176	0.3201	0.2819	0.3109	0.3913	0.3266	0.3154	0.5216	0.4204
0.5358	0.5534	0.4058	0.5454	0.5226	0.5324	0.5209	0.5039	0.4747	0.5952	0.5269
0.0327	0.0383	0.0174	0.0280	0.0553	0.0343	0.1369	0.0453	0.0323	0.0608	0.0312
0.0454	0.0294	0.0302	0.0258	0.0103	0.0199	0.0075	0.0379	0.0077	0.0120	0.0238
0.3362	0.2060	0.2705	0.2183	0.2620	0.2306	0.2420	0.2374	0.2444	0.2706	0.2735
0.0128	0.0290	0.0392	0.0427	0.0524	0.0456	0.0661	0.1124	0.0197	0.0259	0.0000
0.3957	0.4487	0.2447	0.2706	0.2982	0.2137	0.3036	0.3645	0.3859	0.0000	0.0000
0.6242	0.6621	0.4266	0.5681	0.7961	0.6261	0.6507	0.7227	0.6853	0.3950	0.4917
0.2210	0.1912	0.1993	0.3562	0.3250	0.2264	0.3162	0.3064	0.3894	0.3077	0.2776
0.0915	0.0888	0.1203	0.1281	0.1384	0.1098	0.2117	0.0872	0.0584	0.0765	0.0604
0.1645	0.2962	0.3333	0.3993	0.2540	0.5306	0.5221	0.4617	0.5817	0.5708	0.5275
0.6184	0.5644	0.8593	0.9250	0.8972	0.8087	0.8523	0.8267	0.8105	0.7362	0.7965
0.6601	0.8530	1.0858	0.9557	1.0108	1.2451	0.9982	1.0023	1.0541	1.0879	1.0396
0.0010	0.0000	0.0000	0.0125	0.0222	0.0165	0.0012	0.0000	0.0089	0.0156	0.0130
0.3762	0.2983	0.2528	0.1820	0.1603	0.2013	0.2152	0.2011	0.2847	0.2195	0.2760
0.1535	0.0813	0.0991	0.0503	0.0686	0.0514	0.0855	0.1291	0.1390	0.3045	0.0906
0.3698	0.3165	0.3098	0.3832	0.3085	0.3381	0.3982	0.3483	0.4149	0.0655	0.3144
0.0481	0.0634	0.0479	0.1404	0.2901	0.3623	0.0965	0.2493	0.2760	0.3286	0.6166
0.0598	0.0205	0.0380	0.0225	0.1156	0.1905	0.0911	0.0506	0.1380	0.0592	0.1010
0.0255	0.0165	0.0372	0.1273	0.0149	0.1266	0.0479	0.0181	0.0759	0.0329	0.2054
0.1147	0.1170	0.0785	0.1147	0.0608	0.1543	0.0531	0.0495	0.1310	0.0446	0.0788
0.1592	0.2708	0.1109	0.2063	0.2267	0.1583	0.1671	0.1436	0.1377	0.1394	0.1314
0.0061	0.0211	0.0135	0.0329	0.0734	0.0092	0.0083	0.0251	0.0127	0.0065	0.0053
0.0510	0.1316	0.0954	0.0980	0.1315	0.1106	0.1647	0.0617	0.1585	0.1266	0.1257
0.0825	0.1537	0.1744	0.1139	0.1590	0.1757	0.1313	0.0928	0.1853	0.1173	0.0927
0.0368	0.0320	0.0303	0.0264	0.0734	0.0563	0.0470	0.0390	0.0448	0.0712	0.0606
0.0273	0.0450	0.0566	0.0474	0.0958	0.0455	0.0795	0.0621	0.0509	0.0653	0.1021
0.0036	0.0452	0.2129	0.1234	0.1966	0.1464	0.4683	0.0700	0.0689	0.1195	0.1133
0.0605	0.1365	0.1176	0.1786	0.2100	0.1295	0.1934	0.1818	0.0775	0.1304	0.2092
0.1184	0.1485	0.1166	0.1270	0.0900	0.1279	0.1530	0.1194	0.1683	0.0958	0.2234
0.0898	0.1898	0.1836	0.2013	0.1304	0.0636	0.0958	0.0675	0.1062	0.0982	0.0637
0.0314	0.0077	0.0442	0.0299	0.0464	0.0499	0.0392	0.0288	0.0377	0.0169	0.0692

	Δ Curl Index Earlywood - 30 Hz, 5mm				
	1	10	100	1000	10000
	0.0180	0.0129	0.0340	0.0397	0.0007
	0.0104	0.0238	0.0064	0.0118	0.0091
	0.0006	0.0331	0.0230	0.0269	0.0355
	0.0269	0.0519	0.0098	0.0166	0.0022
	0.0469	0.0410	0.0030	0.0279	0.0025
	0.0601	0.0148	0.0185	0.0149	0.0110
	0.0178	0.0207	0.0088	0.2111	0.1263
	0.0380	0.0382	0.0804	0.0112	0.1012
	0.1476	0.0228	0.0115	0.0293	0.0682
	0.0209	0.0274	0.1026	0.0130	0.0296
	0.0008	0.0156	0.0125	0.0302	0.0117
	0.0645	0.0437	0.0114	0.0070	0.0029
	0.0102	0.0096	0.0206	0.0926	0.0259
	0.2040	0.0275	0.0898	0.0214	0.0000
	0.2355	0.2280	0.0246	0.0374	0.0967
	0.0081	0.0313	0.0898	0.0830	0.0301
	0.0315	0.0103	0.1019	0.0289	0.0161
	0.0372	0.1453	0.0085	0.1200	0.0433
	0.2950	0.0278	0.0436	0.0162	0.0603
	0.2329	0.0551	0.2469	0.0518	0.0482
	0.0000	0.0097	0.0153	0.0089	0.0026
	0.0455	0.0217	0.0139	0.0836	0.0565
	0.0178	0.0182	0.0341	0.0099	0.2139
	0.0068	0.0746	0.0601	0.0666	0.2489
	0.0155	0.1497	0.2658	0.0266	0.2880
	0.0176	0.0931	0.0994	0.0875	0.0418
	0.0208	0.1123	0.0787	0.0578	0.1725
	0.0385	0.0539	0.1012	0.0815	0.0341
	0.1599	0.0203	0.0088	0.0059	0.0080
	0.0076	0.0404	0.0009	0.0124	0.0012
	0.0362	0.0334	0.0540	0.0969	0.0009
	0.0207	0.0451	0.0443	0.0924	0.0246
	0.0017	0.0469	0.0093	0.0058	0.0106
	0.0117	0.0483	0.0340	0.0112	0.0369
	0.1677	0.0732	0.3219	0.0011	0.0061
	0.0189	0.0314	0.0639	0.1043	0.0788
	0.0319	0.0371	0.0251	0.0489	0.1276
	0.0061	0.0709	0.0323	0.0386	0.0346
	0.0364	0.0165	0.0107	0.0089	0.0523
average:	0.0556	0.0481	0.0570	0.0446	0.0554

Latewood curl index and change in curl index - 30 Hz, 5mm

Curl Index Latewood - 30 Hz, 5mm										
0	1	1.5	10	10.5	100	100.5	1000	1000.5	10000	10000.5
0.2523	0.2338	0.2937	0.3105	0.2684	0.3317	0.2799	0.3403	0.4166	0.3582	0.4836
0.0648	0.0218	0.0171	0.0431	0.0242	0.0285	0.0212	0.0568	0.0439	0.0545	0.0551
0.0097	0.0022	0.0270	0.0392	0.0114	0.0135	0.0110	0.0113	0.0176	0.0216	0.0137
0.0411	0.0126	0.0112	0.0417	0.0015	0.0247	0.0260	0.0607	0.0424	0.0725	0.0796
0.0806	0.1389	0.2497	0.3209	0.1750	0.1831	0.1807	0.1685	0.1654	0.2288	0.1946
0.2061	0.2013	0.3154	0.2091	0.3376	0.3325	0.3071	0.4281	0.3422	0.2624	0.4151
0.1764	0.2672	0.3453	0.3306	0.4043	0.1453	0.2064	0.3259	0.3425	0.1843	0.2205
0.4585	0.2479	0.2000	0.2390	0.3064	0.2800	0.3251	0.2694	0.2884	0.1845	0.2293
0.2445	0.3979	0.3071	0.3274	0.3371	0.3578	0.3461	0.3450	0.3803	0.3140	0.3952
0.0062	0.0066	0.0121	0.0032	0.0046	0.0165	0.0147	0.0104	0.0176	0.0148	0.0628
0.1354	0.1072	0.1257	0.1442	0.1493	0.1525	0.1343	0.1351	0.1041	0.1115	0.1038
0.0253	0.0473	0.0582	0.0421	0.0607	0.0474	0.0147	0.0558	0.0420	0.0269	0.0502
0.0000	0.0200	0.0703	0.0295	0.0273	0.0957	0.0494	0.0645	0.0727	0.0659	0.0258
0.0244	0.0582	0.0476	0.0441	0.0406	0.0355	0.0304	0.0223	0.0451	0.0415	0.0309
0.1937	0.1337	0.1203	0.1482	0.1840	0.1371	0.1840	0.1739	0.2347	0.1115	0.1908
0.1009	0.1137	0.1839	0.1064	0.1019	0.1301	0.0856	0.0938	0.0832	0.1138	0.1319
0.0238	0.0251	0.0182	0.0353	0.0227	0.0160	0.0393	0.0217	0.0412	0.0212	0.0427
0.1582	0.1643	0.0506	0.0931	0.1460	0.1812	0.0000	0.1900	0.1455	0.1448	0.1616
0.0474	0.0701	0.0850	0.0401	0.0405	0.0463	0.0662	0.0423	0.0578	0.0295	0.0237
0.0059	0.0918	0.0894	0.0381	0.0679	0.0324	0.0386	0.0126	0.0484	0.0116	0.0308
0.1351	0.1576	0.1359	0.1772	0.1561	0.1999	0.1799	0.2001	0.1646	0.1720	0.2387
0.0737	0.0513	0.0845	0.0761	0.0297	0.0938	0.1104	0.0364	0.0818	0.0694	0.0750
0.0301	0.0289	0.0371	0.0454	0.0491	0.0482	0.0530	0.0630	0.0434	0.0819	0.0612
0.0400	0.0309	0.0402	0.0493	0.0339	0.0473	0.0614	0.0532	0.0611	0.0543	0.0758
0.0321	0.0680	0.0836	0.0731	0.0559	0.0598	0.0653	0.0966	0.0636	0.0619	0.0769
0.1182	0.1276	0.1578	0.1198	0.0948	0.1127	0.1837	0.1684	0.1416	0.1514	0.1773
0.2078	0.2789	0.3476	0.3912	0.3911	0.4645	0.4747	0.5480	0.4999	0.4920	0.5231
0.0244	0.0213	0.0199	0.0419	0.0129	0.0211	0.0250	0.0484	0.0270	0.0367	0.0200
0.0292	0.0769	0.0743	0.0354	0.0589	0.0212	0.0333	0.0457	0.0479	0.0222	0.0467
0.6912	0.6523	0.7228	0.6127	0.5953	0.5948	0.6503	0.7741	0.6344	0.8285	0.7354
0.3802	0.3175	0.3546	0.3435	0.2981	0.3461	0.3152	0.3361	0.4168	0.3263	0.3298
0.0235	0.0714	0.1265	0.0463	0.0681	0.0989	0.0857	0.0923	0.0908	0.0755	0.0750
0.7800	0.4957	0.6283	0.5361	0.6826	0.5858	0.6730	0.6462	0.6428	0.5155	0.5540
0.0521	0.0648	0.1350	0.0459	0.0852	0.0786	0.0942	0.0988	0.1000	0.0840	0.0649
0.0918	0.0963	0.0790	0.0894	0.0492	0.0483	0.0571	0.0675	0.0772	0.0505	0.0334
0.1630	0.1633	0.2285	0.1620	0.1805	0.1364	0.1182	0.1580	0.1189	0.1320	0.0882
0.3473	0.4589	0.3438	0.4503	0.4512	0.5629	0.5971	0.4675	0.3647	0.4202	0.5137
0.1428	0.2419	0.1827	0.1542	0.2332	0.2093	0.2099	0.2902	0.2224	0.0440	0.1122
0.2124	0.1893	0.1669	0.1019	0.1504	0.0630	0.0690	0.0745	0.0591	0.0086	0.0071
0.0377	0.0401	0.0210	0.0192	0.0300	0.0093	0.1901	0.0095	0.0106	0.1685	0.1991
0.1815	0.3474	0.2985	0.2699	0.2254	0.2078	0.0405	0.1620	0.1645	0.0217	0.0327
0.0883	0.0317	0.0557	0.0452	0.0337	0.0421	0.0340	0.0204	0.0202	0.0403	0.0283
0.4537	0.4818	0.4556	0.4715	0.3226	0.3184	0.3215	0.4390	0.2830	0.3589	0.3043
0.0879	0.0577	0.0635	0.2188	0.1615	0.0153	0.1536	0.0935	0.1765	0.1415	0.1885
0.0742	0.0747	0.0675	0.1471	0.1019	0.0642	0.0731	0.1020	0.1036	0.1010	0.0909

Δ Curl Index Latewood - 30 Hz, 5mm				
1	10	100	1000	10000
0.0599	0.0421	0.0518	0.0763	0.1255
0.0048	0.0190	0.0074	0.0128	0.0006
0.0248	0.0278	0.0025	0.0063	0.0079
0.0014	0.0402	0.0013	0.0183	0.0071
0.1107	0.1458	0.0024	0.0031	0.0342
0.1140	0.1286	0.0254	0.0859	0.1528
0.0781	0.0738	0.0611	0.0166	0.0361
0.0479	0.0674	0.0451	0.0190	0.0449
0.0908	0.0097	0.0117	0.0353	0.0812
0.0054	0.0014	0.0019	0.0072	0.0480
0.0185	0.0051	0.0182	0.0310	0.0077
0.0109	0.0186	0.0327	0.0138	0.0234
0.0503	0.0023	0.0463	0.0082	0.0402
0.0106	0.0034	0.0050	0.0228	0.0106
0.0134	0.0358	0.0469	0.0608	0.0793
0.0702	0.0045	0.0445	0.0106	0.0181
0.0069	0.0126	0.0232	0.0195	0.0215
0.1137	0.0528	0.1812	0.0445	0.0168
0.0150	0.0004	0.0199	0.0155	0.0059
0.0023	0.0298	0.0062	0.0358	0.0193
0.0217	0.0211	0.0200	0.0355	0.0667
0.0332	0.0464	0.0166	0.0454	0.0057
0.0081	0.0037	0.0048	0.0196	0.0207
0.0093	0.0153	0.0142	0.0078	0.0216
0.0156	0.0172	0.0055	0.0330	0.0150
0.0302	0.0250	0.0710	0.0268	0.0259
0.0687	0.0001	0.0102	0.0481	0.0311
0.0014	0.0291	0.0039	0.0214	0.0167
0.0026	0.0235	0.0121	0.0022	0.0245
0.0704	0.0175	0.0555	0.1397	0.0930
0.0371	0.0454	0.0308	0.0806	0.0035
0.0551	0.0218	0.0133	0.0015	0.0005
0.1326	0.1465	0.0872	0.0035	0.0385
0.0701	0.0393	0.0156	0.0012	0.0191
0.0173	0.0401	0.0088	0.0097	0.0171
0.0652	0.0184	0.0182	0.0391	0.0437
0.1151	0.0009	0.0342	0.1028	0.0935
0.0591	0.0790	0.0006	0.0677	0.0682
0.0223	0.0485	0.0060	0.0154	0.0015
0.0191	0.0108	0.1808	0.0012	0.0306
0.0489	0.0445	0.1674	0.0025	0.0110
0.0239	0.0114	0.0081	0.0002	0.0120
0.0262	0.1489	0.0031	0.1560	0.0546
0.0058	0.0573	0.1383	0.0830	0.0470
0.0072	0.0452	0.0089	0.0016	0.0101
average:	0.0404	0.0373	0.0349	0.0331	0.0345

Earlywood curl index and change in curl index - 30 hz, 4mm

Curl Index Earlywood - 30 Hz, 4mm												Δ Curl Index Earlywood - 30 Hz, 4mm				
0	1	1.5	10	10.5	100	100.5	1000	1000.5	10,000	10,000.5		1	10	100	1000	10000
0.0370	0.0714	0.1265	0.1595	0.1389	0.1534	0.1497	0.1474	0.2047	0.2078	0.1627		0.0551	0.0206	0.0037	0.0574	0.0451
0.0635	0.0219	0.0537	0.0837	0.1009	0.0373	0.0280	0.0357	0.0228	0.0226	0.0275		0.0318	0.0172	0.0093	0.0129	0.0049
0.0542	0.0800	0.0599	0.0980	0.0515	0.0637	0.0356	0.0590	0.0780	0.0903	0.0892		0.0201	0.0465	0.0281	0.0190	0.0011
0.6769	0.6754	0.7246	0.6591	0.6507	0.6239	0.6631	0.6378	0.6693	0.7663	0.6711		0.0493	0.0083	0.0392	0.0315	0.0951
0.0219	0.0279	0.0444	0.0335	0.0437	0.0246	0.0237	0.0168	0.0109	0.0230	0.0159		0.0165	0.0102	0.0009	0.0060	0.0071
0.4992	0.5729	0.5261	0.4435	0.3496	0.5645	0.3610	0.4207	0.4914	0.5036	0.3881		0.0467	0.0939	0.2035	0.0707	0.1155
0.2659	0.2213	0.3158	0.3822	0.3719	0.2137	0.2948	0.2562	0.2523	0.2075	0.2394		0.0946	0.0104	0.0811	0.0039	0.0319
0.0247	0.0280	0.0375	0.0300	0.0313	0.0284	0.0325	0.0263	0.0483	0.0328	0.0448		0.0095	0.0013	0.0041	0.0220	0.0120
0.1743	0.1670	0.1193	0.1502	0.1832	0.2095	0.1390	0.1441	0.1893	0.1623	0.1967		0.0477	0.0330	0.0705	0.0452	0.0343
0.1143	0.1350	0.1107	0.1021	0.1786	0.0613	0.0284	0.0224	0.0514	0.1165	0.1295		0.0243	0.0765	0.0329	0.0290	0.0129
0.0083	0.0412	0.0206	0.0139	0.0063	0.0326	0.0667	0.0181	0.0521	0.0363	0.0262		0.0207	0.0076	0.0341	0.0340	0.0101
0.0830	0.1038	0.0829	0.0879	0.0862	0.0714	0.0762	0.0725	0.0751	0.0797	0.0791		0.0210	0.0017	0.0048	0.0026	0.0007
0.4811	0.4721	0.4588	0.3734	0.4763	0.4886	0.5012	0.5584	0.6000	0.5177	0.6452		0.0133	0.1029	0.0127	0.0415	0.1275
0.0558	0.0677	0.0913	0.0374	0.0850	0.0628	0.0584	0.0686	0.0633	0.0447	0.0395		0.0236	0.0476	0.0044	0.0054	0.0051
0.0959	0.1221	0.1434	0.1158	0.1344	0.0274	0.0721	0.3225	0.3206	0.3173	0.2809		0.0213	0.0185	0.0447	0.0019	0.0364
0.0205	0.0247	0.0093	0.0144	0.0185	0.0325	0.0128	0.0178	0.0070	0.0159	0.0355		0.0153	0.0041	0.0198	0.0107	0.0196
0.0178	0.0305	0.0081	0.0200	0.0243	0.0371	0.0435	0.0199	0.0242	0.0383	0.0246		0.0224	0.0043	0.0065	0.0043	0.0137
0.3209	0.2823	0.1911	0.2914	0.2954	0.2554	0.2995	0.2428	0.2702	0.4144	0.3691		0.0912	0.0040	0.0441	0.0275	0.0453
0.0260	0.0520	0.0567	0.0210	0.0644	0.0701	0.0651	0.0576	0.0308	0.0547	0.1035		0.0048	0.0433	0.0050	0.0268	0.0488
0.0503	0.0758	0.0254	0.0598	0.0519	0.0585	0.0298	0.0380	0.0407	0.0431	0.0551		0.0504	0.0080	0.0287	0.0027	0.0120
											average	0.0340	0.0280	0.0339	0.0227	0.0340

Latewood curl index and change in curl index - 30 Hz, 4mm

Curl Index Latewood - 30 Hz, 4mm												D Curl Index - 30 Hz, 4mm				
0	1	1.5	10	10.5	100	100.5	1000	1000.5	10,000	10,000.5		1	10	100	1000	10000
0.1557	0.1031	0.0000	0.0000	0.0000	0.0000	0.0000	0.1129	0.0237	0.0650	0.0442		0.1031	0.0000	0.0000	0.0892	0.0208
0.1284	0.0769	0.0585	0.0291	0.0174	0.0178	0.0180	0.0238	0.0065	0.0311	0.0123		0.0184	0.0117	0.0002	0.0173	0.0188
0.0725	0.0225	0.0551	0.0000	0.0390	0.0427	0.0479	0.1344	0.0700	0.1046	0.1069		0.0326	0.0390	0.0052	0.0644	0.0023
0.0570	0.0342	0.0235	0.0889	0.1194	0.1110	0.1255	0.0000	0.0000	0.0000	0.0000		0.0107	0.0305	0.0145	0.0000	0.0000
0.0148	0.0094	0.0088	0.0142	0.0088	0.0110	0.0076	0.0174	0.0161	0.0340	0.0270		0.0006	0.0054	0.0034	0.0012	0.0070
0.1004	0.0184	0.0222	0.0118	0.0237	0.0264	0.0000	0.0719	0.0261	0.2312	0.0935		0.0038	0.0119	0.0264	0.0458	0.1377
0.1819	0.1971	0.1986	0.1737	0.4512	0.1984	0.2274	0.2348	0.1809	0.2557	0.1939		0.0014	0.2775	0.0290	0.0539	0.0618
0.0419	0.0525	0.0220	0.0321	0.0408	0.0539	0.0284	0.0706	0.0259	0.0797	0.0528		0.0305	0.0087	0.0255	0.0447	0.0269
0.0563	0.1481	0.1085	0.1386	0.1101	0.0751	0.1067	0.0635	0.2015	0.0991	0.1009		0.0397	0.0285	0.0316	0.1380	0.0018
0.4214	0.3169	0.3229	0.3862	0.2463	0.2636	0.2844	0.3181	0.4808	0.3121	0.5158		0.0060	0.1399	0.0208	0.1627	0.2037
0.1650	0.1762	0.1826	0.2409	0.1771	0.1152	0.1478	0.2567	0.2888	0.2621	0.1251		0.0064	0.0637	0.0326	0.0321	0.1370
0.1928	0.2908	0.3783	0.5298	0.3943	0.2471	0.1917	0.1870	0.2336	0.2457	0.3042		0.0874	0.1355	0.0554	0.0466	0.0585
0.2540	0.4669	0.2274	0.4079	0.4668	0.3331	0.2502	0.4817	0.3731	0.4307	0.3812		0.2395	0.0588	0.0829	0.1086	0.0496
0.0217	0.0120	0.0078	0.0088	0.0332	0.0207	0.0353	0.0143	0.0051	0.0072	0.0080		0.0041	0.0245	0.0146	0.0091	0.0008
0.2784	0.1266	0.1521	0.1093	0.2655	0.2995	0.0596	0.1087	0.0567	0.0676	0.0457		0.0255	0.1563	0.2399	0.0520	0.0218
0.4623	0.6500	0.5532	0.6157	0.5592	0.5345	0.5487	0.4900	0.4350	0.6773	0.6164		0.0968	0.0565	0.0142	0.0550	0.0609
											average	0.0442	0.0655	0.0373	0.0575	0.0506

Earlywood curl index and change in curl index - 30 Hz, 3mm

Curl Index Earlywood - 30 Hz, 3mm												D Curl Index Earlywood - 30 Hz, 3mm				
0	1	1.5	10	10.5	100	100.5	1000	1000.5	10000	10000.5		1	10	100	1000	10000
0.2766	0.5749	0.4061	0.2654	0.3140	0.5261	0.5603	0.4309	0.3702	0.3125	0.3128		0.1688	0.0486	0.0342	0.0607	0.0002
0.0145	0.2423	0.1016	0.2270	0.0799	0.0446	0.0304	0.0453	0.0419	0.0324	0.0709		0.1407	0.1471	0.0142	0.0035	0.0385
0.0205	0.0603	0.0390	0.0371	0.0411	0.0205	0.0308	0.0231	0.0175	0.0329	0.0267		0.0212	0.0040	0.0103	0.0056	0.0063
0.0719	0.1201	0.0867	0.1628	0.1332	0.1085	0.0634	0.0979	0.0848	0.0917	0.1491		0.0335	0.0296	0.0451	0.0132	0.0574
0.1113	0.1045	0.1869	0.2106	0.2118	0.2938	0.1895	0.1347	0.3536	0.3442	0.2725		0.0824	0.0012	0.1042	0.2189	0.0718
0.0106	0.0122	0.0114	0.0071	0.0040	0.0076	0.0000	0.0105	0.0038	0.0028	0.0094		0.0007	0.0031	0.0076	0.0067	0.0066
0.2511	0.1967	0.2225	0.2082	0.1501	0.1268	0.0980	0.1309	0.1423	0.1901	0.1720		0.0258	0.0581	0.0288	0.0113	0.0181
0.1262	0.1421	0.1301	0.1353	0.1593	0.1682	0.1786	0.1850	0.2258	0.1334	0.1091		0.0120	0.0241	0.0103	0.0408	0.0243
0.0318	0.0687	0.1403	0.0652	0.0518	0.0416	0.0532	0.0531	0.0614	0.0462	0.0321		0.0717	0.0134	0.0116	0.0083	0.0141
0.7216	0.8766	1.0203	1.0768	1.1015	0.9902	0.9315	1.0531	1.0852	0.7944	1.1639		0.1437	0.0246	0.0587	0.0321	0.3694
0.2365	0.3402	0.1700	0.1378	0.1610	0.1292	0.1345	0.1038	0.0641	0.0812	0.0614		0.1702	0.0232	0.0052	0.0397	0.0198
0.1058	0.0901	0.1138	0.0673	0.1097	0.0763	0.1025	0.0823	0.0782	0.0850	0.0875		0.0237	0.0424	0.0262	0.0040	0.0025
0.2539	0.2122	0.2906	0.1995	0.1896	0.1070	0.0699	0.0481	0.0290	0.0144	0.0305		0.0784	0.0099	0.0371	0.0191	0.0160
0.0138	0.0145	0.0148	0.0254	0.0233	0.0195	0.0299	0.0209	0.0176	0.0319	0.0242		0.0003	0.0021	0.0104	0.0033	0.0077
0.0298	0.0501	0.0411	0.0554	0.0373	0.0411	0.0563	0.0485	0.0619	0.0591	0.0479		0.0090	0.0181	0.0152	0.0133	0.0112
0.1050	0.1195	0.1639	0.0918	0.2195	0.1382	0.1453	0.1284	0.3034	0.1846	0.1582		0.0445	0.1276	0.0072	0.1750	0.0263
0.1015	0.0421	0.0756	0.1061	0.0624	0.0968	0.3161	0.1316	0.0294	0.2994	0.3869		0.0335	0.0437	0.2193	0.1022	0.0876
0.0748	0.1081	0.0673	0.0510	0.0539	0.0683	0.0629	0.0655	0.0522	0.0683	0.0633		0.0408	0.0028	0.0054	0.0133	0.0050
0.0000	0.0000	0.0085	0.0127	0.0045	0.0044	0.0107	0.0052	0.0038	0.0016	0.0033		0.0085	0.0082	0.0063	0.0014	0.0018
0.0146	0.0100	0.0200	0.0354	0.0130	0.0576	0.1279	0.0765	0.0546	0.0393	0.0505		0.0100	0.0224	0.0703	0.0219	0.0112
0.0097	0.0000	0.0072	0.0000	0.0043	0.0000	0.0097	0.0055	0.0000	0.0000	0.0051		0.0072	0.0043	0.0097	0.0055	0.0051
0.3251	0.3591	0.2882	0.3556	0.4165	0.4082	0.3760	0.3782	0.3999	0.3970	0.3976		0.0710	0.0609	0.0322	0.0218	0.0006
0.3412	0.4338	0.4894	0.3990	0.4572	0.4118	0.3990	0.3920	0.4666	0.4547	0.3949		0.0556	0.0582	0.0128	0.0747	0.0598
0.6113	0.8792	0.6875	0.7733	0.8161	0.6549	0.7636	0.7923	0.7720	0.5931	0.5763		0.1918	0.0428	0.1087	0.0203	0.0168
											average:	0.0602	0.0342	0.0371	0.0382	0.0366

Latewood curl index and change in curl index - 30 Hz, 3mm

Curl Index Latewood - 30 Hz, 3mm													
0	1	1.5	10	10.5	100	100.5	1000	1000.5	10000	10000.5			
0.0612	0.0387	0.0315	0.0411	0.0390	0.0678	0.0460	0.0313	0.0351	0.0431	0.0462			
0.2662	0.2347	0.2511	0.3087	0.2408	0.2325	0.2575	0.2474	0.1910	0.1247	0.1453			
0.0780	0.1025	0.1148	0.0619	0.0801	0.0614	0.0931	0.0370	0.0596	0.0483	0.0449			
0.0746	0.1281	0.1145	0.1104	0.1099	0.1813	0.1363	0.2416	0.1984	0.1489	0.2016			
1.0003	1.3202	0.9161	0.9620	0.9291	0.8632	0.9449	0.7252	0.9499	0.9024	0.9649			
0.2208	0.0582	0.0444	0.1077	0.0560	0.1866	0.0853	0.2405	0.2286	0.1195	0.0785			
0.0387	0.0635	0.0427	0.0761	0.0730	0.0194	0.0368	0.0400	0.0425	0.0080	0.0270			
0.2965	0.2446	0.4565	0.3756	0.4964	0.6222	0.6025	0.6251	0.6429	0.6822	0.5843			
0.1342	0.1982	0.1909	0.1627	0.1248	0.2188	0.1204	0.0762	0.0870	0.0856	0.0942			
0.0161	0.0130	0.0180	0.0207	0.0302	0.0315	0.0412	0.0448	0.0248	0.0030	0.1029			
0.0806	0.1087	0.2167	0.1181	0.1506	0.0972	0.0870	0.0643	0.0481	0.0397	0.0506			
0.0596	0.0802	0.0301	0.0639	0.0479	0.0453	0.0197	0.0982	0.1422	0.1181	0.0951			
0.0887	0.0693	0.0767	0.0482	0.0187	0.0791	0.0410	0.0563	0.0380	0.0734	0.0515			
0.1435	0.1544	0.0942	0.1528	0.1647	0.1779	0.1692	0.1740	0.2308	0.2191	0.1775			
0.0615	0.0492	0.0450	0.0478	0.0629	0.0406	0.0606	0.0383	0.0335	0.0646	0.0361			
0.0145	0.0116	0.0216	0.0186	0.0138	0.0150	0.0189	0.0156	0.0499	0.0133	0.0182			
0.1774	0.0878	0.0807	0.0641	0.0597	0.0627	0.0542	0.0579	0.0416	0.0279	0.0329			
1.3409	1.4023	1.3547	1.2544	1.2739	1.3881	1.2709	1.2600	1.4216	1.2736	1.4672			
0.3214	0.2786	0.2468	0.3491	0.3866	0.3801	0.4224	0.3741	0.3739	0.3423	0.3515			
0.0960	0.1027	0.1052	0.1188	0.1206	0.1183	0.1056	0.1311	0.1284	0.1113	0.1202			
0.0188	0.0339	0.0334	0.0290	0.0337	0.0370	0.0366	0.0365	0.0525	0.0150	0.0230			
0.0783	0.0890	0.0859	0.0597	0.0803	0.0630	0.0607	0.0735	0.0593	0.0767	0.0694			
0.0321	0.0503	0.0504	0.0840	0.0730	0.0670	0.0628	0.0924	0.1037	0.1820	0.1080			
0.0740	0.0765	0.1655	0.3742	0.0467	0.0419	0.0489	average:						
0.0384	0.0407	0.0003	0.0092	0.0423	0.0375	0.0318							
0.1936	0.1615	0.1172	0.0195	0.0476	0.0114	0.0071							
0.0050	0.0163	0.0086	0.0038	0.0182	0.0133	0.0100							
0.0049	0.0343	0.0038	0.0200	0.0285	0.0151	0.0042							
0.0416	0.0568	0.0087	0.0319	0.0601									
0.0219	0.0182	0.0180	0.0295	0.0074									
0.0231	0.0440	0.0256	0.0259	0.0501									
0.0109	0.0163	0.0103	0.0325	0.1080									
0.0086	0.0108	0.0984	0.0678	0.0073									
0.0979	0.0178	0.0197	0.1208	0.2119									
0.0190	0.0025	0.0174	0.0180	0.0209									
0.0410	0.0119	0.1013	0.0517	0.0139									
0.0625	0.2247	0.0817	0.1529	0.3842									
0.0528	0.0432	0.0450	0.0405	0.0335									
0.0034	0.0226	0.0317	0.0232	0.0123									
0.0206	0.0564	0.0250	0.0679	0.0164									
0.0031	0.0038	0.0218	0.0121	0.0073									
10000	1000	100	10	1									
D Curl Index Latewood - 30 Hz, 3mm													

Earlywood and latewood curl index - 10 Hz, shaker

Curl Index - 10 Hz, Shaker															
Earlywood															
0	1	1.5	2	2.5	5	5.5	10	10	0	100	100.5	1000	1000.5	10000	10000.5
0.0117	0.0591	0.0095	0.0747	0.0070	0.0612	0.0198	0.0185	0.0604		0.2223	0.1495	0.1743	0.2097	0.1539	0.1763
0.0116	0.0183	0.0856	0.0752	0.0254	0.0523	0.0111	0.0128	0.0652		0.0045	0.0492	0.0353	0.0000	0.0198	0.0741
0.0239	0.0470	0.1021	0.0508	0.1277	0.0277	0.0826	0.2198	0.0925		0.0791	0.0026	0.0033	0.0667	0.0963	0.0024
0.0384	0.1256	0.0790	0.1351	0.0773	0.1384	0.0561	0.1201	0.0733		0.0400	0.0567	0.0633	0.0185	0.0098	0.0201
0.0189	0.0579	0.0262	0.0287	0.0750	0.0690	0.0285	0.0187	0.0657	0.0103	0.0103	0.0538	0.0682	0.0142	0.0111	0.0273
0.0075	0.0000	0.0371	0.0716	0.0053	0.0717	0.0022	0.0466	0.0040	0.0151	0.0566	0.0129	0.0209	0.0464	0.0339	0.0096
0.0042	0.0039	0.0340	0.0523	0.0038	0.0573	0.0032	0.0564	0.0034	0.0449	0.0462	0.1425	0.0819	0.0315	0.0000	0.0358
0.0032	0.1171	0.0274	0.0156	0.0682	0.1476	0.0303	0.0284	0.0997	0.0228	0.0641	0.0156	0.0463	0.0185	0.0183	0.0311
0.0000	0.0542	0.0233	0.0078	0.0492	0.0912	0.0194	0.0085	0.0814	0.0127	0.0036	0.0482	0.0431	0.0150	0.0068	0.0417
0.0092	0.0156	0.0542	0.0540	0.0012	0.0017	0.0448	0.0029	0.0507	0.0469	0.0934	0.0408	0.0402	0.0715	0.0655	0.0450
0.0087	0.0425	0.0824	0.0265	0.0789	0.0242	0.0770	0.0185	0.0601	0.0187	0.0135	0.0663	0.0341	0.0056	0.0556	0.0153
0.0171	0.0460	0.0133	0.0646	0.0105	0.0116	0.0545	0.0191	0.0702	0.0628	0.1351	0.1809	0.2919	0.1167	0.2096	0.0631
0.0602	0.0412	0.0060	0.0078	0.0503	0.0066	0.0502	0.0477	0.0066	0.0510	0.1763	0.2640	0.2930	0.2010	0.1908	0.3049
0.0244	0.0431	0.0108	0.0026	0.0448	0.0100	0.0000	0.0540	0.0128							
0.0288	0.0925	0.0283	0.0650	0.1349	0.0268	0.1076	0.1311	0.0371							
Latewood															
0	1	1.5	2	2.5	5	5.5	10	10	0	100	100.5	1000	1000.5	10000	10000.5
0.20503	0.0942	0.0602	0.0728	0.1046	0.0909	0.1109	0.1265	0.0986	0.2834	0.0283	0.0506	0.0158	0.0437	0.0536	0.0252
0.01948	0.0104	0.0054	0.0147	0.0000	0.0023	0.0132	0.0080	0.0280	0.0309	0.0200	0.0000	0.0274	0.0073	0.0333	0.0000
0.03364	0.0368	0.0238	0.0360	0.0281	0.0416	0.0092	0.0243	0.0175	0.0595	0.0245	0.0667	0.1063	0.0547	0.0602	0.1055
0.07567	0.0268	0.0327	0.0327	0.0539	0.1057	0.0873	0.0818	0.0916	0.0061	0.1416	0.0669	0.0470	0.0189	0.0182	0.0540
0.05882	0.0596	0.0821	0.0562	0.0846	0.1083	0.1748	0.0971	0.1040	0.2877	0.0248	0.0849	0.0687	0.0441	0.1495	0.0277
0.03862	0.0052	0.0230	0.0474	0.0337	0.0678	0.0220	0.0485	0.1073	0.0324	0.0141	0.0345	0.0048	0.0353	0.0448	0.0106
0.2264	0.4614	0.4102	0.4720	0.6250	0.6118	0.5080	0.6168	0.6118	0.0000	0.0039	0.0287	0.0337	0.0000	0.0322	0.0109
	0.0389	0.1168	0.0785	0.1117	0.1119	0.1524	0.0540	0.0391	0.0647	0.0653	0.0313	0.1423	0.1772	0.1312	0.1762
	0.0090	0.0394	0.0135	0.0330	0.0551	0.0388	0.0643	0.0589	0.0696	0.0000	0.0279	0.0200	0.0000	0.0200	0.0000
	0.1149	0.0768	0.1255	0.1033	0.1162	0.1542	0.1048	0.0785	0.0076	0.0055	0.0402	0.0403	0.0096	0.0307	0.0052
	0.0495	0.0269	0.0262	0.0370	0.0295	0.0500	0.0421	0.0697	0.1073	0.0558	0.0238	0.1023	0.0387	0.0791	0.0348
	0.0306	0.0224	0.0218	0.0098	0.0267	0.0100	0.0319	0.0215	0.0338	0.0265	0.0536	0.1437	0.0690	0.0939	0.0662
0.05023	0.0154	0.0227	0.0113	0.0325	0.0436	0.0155	0.0287	0.0223	0.0284	0.0825	0.0470	0.0485	0.0212	0.0206	0.0483
0.06922	0.0468	0.0404	0.0220	0.0129	0.0505	0.0285	0.0232	0.0367	0.1549	0.2127	0.2802	0.3464	0.2788	0.4563	0.5076
0.02233	0.0096	0.0000	0.0105	0.0052	0.0072	0.0175	0.0160	0.0068	0.6753	0.9384	0.8181	0.7440	0.7011	0.8123	0.7504
0.0138	0.0568	0.0879	0.1138	0.1738	0.1671	0.1571	0.1795	0.1435							
0.0266	0.0387	0.0000	0.0118	0.0235	0.0228	0.0160	0.0542	0.0765							

Earlywood and latewood change in curl index - 10 Hz, shaker

Δ Curl Index - 10 Hz, Shaker							
Earlywood							
	1	2	5	10	100	1000	10000
	0.0496	0.0677	0.0415	0.0419	0.0728	0.0354	0.0224
	0.0674	0.0498	0.0412	0.0524	0.0447	0.0353	0.0544
	0.0552	0.0769	0.0548	0.1273	0.0766	0.0634	0.0939
	0.0466	0.0577	0.0823	0.0467	0.0433	0.0448	0.0103
	0.0317	0.0463	0.0405	0.0471	0.0435	0.0541	0.0162
	0.0371	0.0663	0.0695	0.0426	0.0437	0.0255	0.0243
	0.0301	0.0485	0.0541	0.0529	0.0963	0.0504	0.0358
	0.0897	0.0525	0.1173	0.0713	0.0484	0.0278	0.0129
	0.0309	0.0414	0.0718	0.0729	0.0446	0.0281	0.0349
	0.0386	0.0529	0.0430	0.0477	0.0526	0.0313	0.0206
	0.0399	0.0524	0.0528	0.0417	0.0528	0.0285	0.0403
	0.0328	0.0540	0.0429	0.0510	0.0459	0.1752	0.1465
	0.0353	0.0425	0.0436	0.0412	0.0877	0.0920	0.1141
	0.0324	0.0422	0.0400	0.0411			
	0.0642	0.0699	0.0809	0.0940			
average	0.04542	0.05473	0.05842	0.05812	0.05792	0.05322	0.0482
st dev	0.01716	0.0109	0.02211	0.02433	0.0187	0.04119	0.04304
Latewood							
	1	2	5	10	100	1000	10000
	0.0490	0.0468	0.0310	0.0498	0.0223	0.0279	0.0284
	0.0201	0.0297	0.0220	0.0419	0.0200	0.0201	0.0333
	0.0279	0.0228	0.0434	0.0288	0.0421	0.0516	0.0453
	0.0209	0.0362	0.0294	0.0318	0.0746	0.0281	0.0358
	0.0375	0.0434	0.0776	0.0289	0.0601	0.0247	0.1218
	0.0328	0.0287	0.0568	0.0808	0.0204	0.0305	0.0342
	0.0662	0.1681	0.1148	0.0270	0.0248	0.0337	0.0213
	0.0929	0.0482	0.0515	0.0368	0.0340	0.0349	0.0450
	0.0454	0.0345	0.0273	0.0274	0.0279	0.0200	0.0200
	0.0531	0.0372	0.0490	0.0483	0.0347	0.0307	0.0255
	0.0376	0.0258	0.0315	0.0496	0.0320	0.0636	0.0442
	0.0232	0.0270	0.0276	0.0324	0.0272	0.0748	0.0277
	0.0223	0.0362	0.0391	0.0283	0.0356	0.0273	0.0277
	0.0215	0.0241	0.0329	0.0355	0.0675	0.0676	0.0513
	0.0246	0.0204	0.0213	0.0312	0.1203	0.0429	0.0618
	0.0310	0.0601	0.0101	0.0360			
	0.0387	0.0116	0.0068	0.0223			
average	0.0379	0.0412	0.0395	0.0375	0.0429	0.03856	0.04155
st dev	0.01923	0.03475	0.026	0.0139	0.02735	0.01766	0.02509

Earlywood and latewood curl index - 30 Hz, shaker

Curl Index - 30 Hz, 5mm, Shaker															
Earlywood															
0	1	1.5	2	2.5	5	5.5	10	10	0	100	100.5	1000	1000.5	10000	10000.5
0.07309	0.02503	0.03211	0.01602	0.03679	0.02059	0.04157	0.03600	0.05720	0.03583	0.05847	0.07472	0.03860	0.01632	0.03181	0.03182
0.03561	0.02676	0.03478	0.06046	0.04196	0.04105	0.08267	0.09790	0.17724	0.02207	0.03600	0.07456	0.06537	0.00751	0.01022	0.02547
0.01075	0.03646	0.03068	0.01695	0.04659	0.06514	0.08691	0.07042	0.04667	0.03727	0.15081	0.05342	0.05589	0.00411	0.04825	0.05724
0.02166	0.02623	0.03108	0.01185	0.09751	0.16646	0.16808	0.17187	0.11997	0.09998			0.52654	0.56032	0.24613	0.20417
0.09607	0.09356	0.08141	0.10857	0.09102	0.09252	0.09167	0.09811	0.10667	0.04572	0.12082	0.10381	0.12332	0.12508	0.13776	0.13776
0.02971	0.03029	0.01907	0.03280	0.04528	0.02074	0.03612	0.02120	0.03868		0.11967	0.10217	0.12678	0.15848	0.16589	0.12812
0.00712	0.03472	0.06623	0.01069	0.05013	0.03316	0.06776	0.04657	0.03381		0.02445	0.01897	0.03907	0.03897	0.06580	0.05951
0.05214	0.03396	0.03872	0.01767	0.03441	0.01042	0.07115	0.01959	0.05583		0.02506	0.05447	0.01192	0.02379	0.11451	0.07526
0.00517	0.04461	0.02422	0.05004	0.01361	0.02627	0.00757	0.04369	0.05961		0.01504	0.01911	0.00965	0.02660	0.04303	0.03744
0.02892	0.02058	0.00184	0.04050	0.01006	0.01278	0.01119	0.01366	0.04510	0.01888	0.00441	0.00792	0.04171	0.06947	0.01696	0.01044
0.07058	0.08135	0.07220	0.10094	0.05580	0.07223	0.08251	0.04433	0.09484	0.37063	0.30189	0.27925	0.25366	0.26212	0.17331	0.19132
0.06893	0.30796	0.42336	0.43889	0.42639	0.41038	0.24469	0.38347	0.34957	0.02834	0.01915	0.00000	0.04569	0.06093	0.56338	0.51475
0.04955	0.03204	0.06073	0.01637	0.05118	0.01744	0.07698	0.01632	0.03216	0.00962	0.33107	0.26044	0.28160	0.29579	0.45321	0.29825
0.01012	0.02012	0.02930	0.02157	0.04156	0.01617	0.01524	0.02312	0.01070	0.01254	0.00692	0.02613	0.01651	0.01185	0.00850	0.00850
0.01055	0.00085	0.00840	0.00000	0.01490	0.00000	0.00622	0.01636	0.00000							
0.00616	0.02815	0.01813	0.00950	0.02280	0.01409	0.00574	0.02392	0.00695							
0.05125	0.13580	0.00000	0.00880	0.03123	0.05627	0.01942	0.01582	0.02854							
0.01755	0.01928	0.03963	0.06535	0.03396	0.01567	0.00385	0.06388	0.04707							
0.00450	0.03930	0.00727	0.04543	0.02713	0.01553	0.01580	0.03831	0.00866							
0.01528	0.04590	0.05448	0.02091	0.03751	0.01471	0.03004	0.02166	0.00538							
Latewood															
0	1	1.5	2	2.5	5	5.5	10	10	0	100	100.5	1000	1000.5	10000	10000.5
0.66353	0.40283	0.41179	0.55598	0.56229	0.53343	0.51057	0.55002	0.50839	0.15329	0.31634	0.26264	0.20053	0.19756		
0.01634	0.09501	0.05806	0.07258	0.07203	0.06601	0.10082	0.09017	0.07876	0.00000	0.02464	0.08086	0.05964	0.04766		
0.30139	0.01834	0.00000	0.00100	0.00545	0.00000	0.00000	0.00000	0.00000	0.03190	0.05921	0.04080	0.04506	0.05646		
0.42786	0.02388	0.05347	0.05715	0.08043	0.08047	0.04334	0.06536	0.05550	0.16262	0.04121	0.01791	0.32890	0.38166		
0.47786	0.60414	0.54621	0.58349	0.50988	0.65102	0.61074	0.63081	0.68422	0.02703	0.39764	0.43758	0.55191	0.49075		
0.03296	0.00000	0.00000	0.00100	0.01198	0.00000	0.00000	0.00000	0.00000	0.06350	0.05216	0.08290	0.04457	0.09764		
0.64531	0.58522	0.55013	0.41533	0.43119	0.58134	0.60253	0.68253	0.71507	0.04069	0.04832	0.03178	0.03042	0.01644	0.00385	0.02959
0.06365	0.62712	0.71556	1.08187	1.02172	0.86322	0.81594	0.97578	0.92790	0.01295	0.00044	0.00044	0.00614	0.01760	0.00239	0.01448
0.15684	0.02637	0.00872	0.01109	0.02787	0.02214	0.01118	0.01877	0.00906	0.11275	0.00665	0.01109	0.00000	0.01424	0.00254	0.01958
0.02529	0.00291	0.00000	0.00100	0.01242	0.00472	0.00550	0.00827	0.00648	0.01046	0.01434	0.01434	0.01810	0.00929	0.03332	0.01678
0.02879	0.02019	0.02397	0.04663	0.02868	0.02906	0.02854	0.03265	0.02773	0.01563	0.00200	0.01078	0.01217	0.00117	0.00000	0.02123
0.02820	0.01955	0.01736	0.03963	0.04772	0.08996	0.04913	0.00987	0.02191	0.00322	0.03879	0.05749	0.04407	0.05623	0.05991	0.08299
0.05874	0.03304	0.03036	0.04109	0.02582	0.03059	0.02279	0.02198	0.04282	0.03111	0.02432	0.02553	0.01556	0.03359	0.02498	0.03265
0.03782	0.05818	0.08905	0.11569	0.05430	0.13182	0.09441	0.14743	0.11128	0.07887	0.07545	0.05859	0.06965	0.07152	0.03801	0.05729
0.06568	0.15722	0.17945	0.18973	0.15254	0.12477	0.10432	0.11497	0.06281	0.08362	0.03027	0.01579	0.03919	0.01987	0.03367	0.02405
									0.00000	0.02747	0.01778	0.05326	0.03865	0.03495	0.02103
									0.08043	0.16314	0.17720	0.10058	0.08116	0.06270	0.04126

Earlywood and latewood change in curl index - 30 hz, shaker

Δ Curl Index - 30 Hz, Shaker							
Earlywood							
	1	2	5	10	100	1000	10000
	0.00708	0.02077	0.02098	0.02120	0.01626	0.02228	0.00000
	0.00802	0.01850	0.04162	0.07935	0.03856	0.03985	0.01524
	0.00578	0.02964	0.02177	0.02375	0.09739	0.05178	0.00899
	0.00485	0.08566	0.00162	0.05189		0.03378	0.04197
	0.01216	0.01755	0.00085	0.00856	0.01701	0.00177	0.00000
	0.01122	0.01247	0.01538	0.01748	0.01750	0.03170	0.03777
	0.03151	0.03944	0.03460	0.01276	0.00548	0.00010	0.00629
	0.00477	0.01673	0.06072	0.03624	0.02941	0.01187	0.03925
	0.02038	0.03643	0.01870	0.01592	0.00407	0.01696	0.00559
	0.01874	0.03044	0.00159	0.03144	0.00350	0.02776	0.00652
	0.00914	0.04514	0.01028	0.05051	0.02264	0.00845	0.01802
	0.11540	0.01250	0.16570	0.03390	0.01915	0.01524	0.04863
	0.02869	0.03481	0.05953	0.01585	0.07064	0.01419	0.05496
	0.00918	0.01998	0.00093	0.01242	0.01920	0.00466	0.00000
	0.00755	0.01490	0.00622	0.01636			
	0.01001	0.01330	0.00835	0.01697			
	0.13580	0.02242	0.03685	0.01272			
	0.02035	0.03139	0.01182	0.01682			
	0.03203	0.01829	0.00027	0.02964			
	0.00857	0.01660	0.01534	0.01628			
average	0.02506	0.02685	0.02666	0.02600	0.02775	0.02003	0.02023
st dev	0.03560	0.01690	0.03760	0.01751	0.02735	0.01525	0.01988
Latewood							
	1	2	5	10	100	1000	10000
	0.00897	0.00631	0.02286	0.04164	0.05570	0.01097	
	0.03695	0.00055	0.03481	0.01141	0.05622	0.01198	
	0.01834	0.00445	0.00000	0.00000	0.01841	0.01140	
	0.02959	0.02328	0.03713	0.00986	0.02330	0.06876	
	0.05794	0.07361	0.04028	0.05341	0.03994	0.02501	
	0.00000	0.01098	0.00000	0.00000	0.02874	0.05307	
	0.03509	0.01585	0.02119	0.03253	0.01654	0.01398	0.02574
	0.08844	0.06014	0.04728	0.04788	0.00000	0.01147	0.01208
	0.01765	0.01677	0.01096	0.00970	0.00443	0.01424	0.01704
	0.00291	0.01142	0.00079	0.00179	0.00000	0.00881	0.01654
	0.00378	0.01794	0.00052	0.00492	0.00878	0.01100	0.02123
	0.00219	0.00809	0.04082	0.01204	0.01870	0.01216	0.02309
	0.00268	0.01527	0.00780	0.02083	0.00122	0.01803	0.00767
	0.03086	0.06139	0.03741	0.03615	0.01686	0.01413	0.01928
	0.02223	0.03719	0.02044	0.05217	0.01448	0.01932	0.00962
					0.00969	0.01461	0.01392
					0.01405	0.01941	0.02144
average	0.02384	0.02422	0.02149	0.02229	0.01924	0.01990	0.01706
st dev	0.02440	0.02299	0.01724	0.01971	0.01729	0.01619	0.00576

Earlywood and latewood curl index - 50 Hz, shaker

Curl Index - 50 Hz, 5mm, Shaker															
Earlywood															
0	1	1.5	2	2.5	5	5.5	10	10	0	100	100.5	1000	1000.5	10000	10000.5
0.0000	0.0094	0.0657	0.1121	0.1345	0.0533	0.0706	0.0438	0.0618	0.1996	0.0386	0.0474	0.0207	0.0524	0.0533	0.0752
0.0378	0.0015	0.0081	0.0107	0.0117	0.0086	0.0086	0.0056	0.0071	0.0281	0.0530	0.0631	0.0740	0.0595	0.0778	0.0774
0.0046	0.0000	0.0443	0.0447	0.0890	0.0378	0.0299	0.0514	0.0541	0.0453	0.2183	0.2515	0.2611	0.2355	0.3227	0.3024
0.1078	0.1568	0.1852	0.1739	0.2215	0.1922	0.2039	0.2355	0.2250	0.1524	0.1415	0.1388	0.5715	0.5764		
0.0023	0.0315	0.0133	0.0208	0.0501	0.0150	0.0599	0.0539	0.0560	0.0915	0.3521	0.3801	0.3372	0.3092	0.4234	0.3859
0.0355	0.0237	0.0124	0.0180	0.0341	0.0209	0.0157	0.0350	0.0262	0.0503	0.1527	0.1815	0.1819	0.1593	0.1365	0.1543
0.1185	0.0397	0.0652	0.0725	0.0882	0.1196	0.1001	0.0702	0.0596	0.0000	0.0104	0.0096	0.0198	0.0121	0.0252	0.0244
0.0162	0.0481	0.0107	0.0070	0.0239	0.0185	0.0224	0.0403	0.0364	0.0171	0.0106	0.0187	0.0269	0.0288	0.0309	0.0110
0.2119	0.0569	0.0498	0.0612	0.0502	0.0555	0.0324	0.0732	0.0284	0.0043	0.0074	0.0015	0.0000	0.0000	0.0244	0.0039
0.1827	0.1595	0.0972	0.0764	0.0937	0.1157	0.1157	0.2229	0.1768	0.3445	0.4356	0.4614	0.5486	0.5214	0.2321	0.2321
0.0031	0.0196	0.0240	0.0293	0.0315	0.0379	0.0653	0.0130	0.0354	0.0265	0.0517	0.0682	0.0600	0.0338	0.0236	0.0527
0.0257	0.1760	0.2584	0.2169	0.2475	0.2665	0.2930	0.4053	0.4338	0.0156	0.0164	0.0421	0.0356	0.0241	0.0823	0.0989
0.0116	0.0668	0.0194	0.0926	0.0959	0.0557	0.1053	0.1521	0.1011							
0.0165	0.0925	0.0373	0.0395	0.0371	0.0596	0.0695	0.0572	0.0527							
Latewood															
0	1	1.5	2	2.5	5	5.5	10	10	0	100	100.5	1000	1000.5	10000	10000.5
0.0104	0.0401	0.0407	0.0093	0.0197	0.0682	0.0899	0.0703	0.1306	0.0120	0.0037	0.0134	0.0061	0.0412	0.0566	0.0475
0.0062	0.0249	0.0386	0.0467	0.0279	0.0511	0.0445	0.0400	0.0323	0.0711	0.0230	0.0235	0.0359	0.0360	0.0175	0.0256
0.6676	0.5529	0.5820	0.6214	0.6379	0.6265	0.6529	0.6423	0.6791	0.0131	0.0591	0.0754	0.0256	0.0353	0.0511	0.0483
0.4245	0.9412	0.9591	0.9902	0.9610	0.6880	0.7495	0.8414	0.8340		0.0207	0.0481	0.0526	0.0273	0.0249	0.0282
0.0144	0.0279	0.0066	0.0344	0.0206	0.0185	0.0230	0.0121	0.0486		0.0771	0.0452	0.0405	0.0242	0.0456	0.0329
0.0099	0.0129	0.0000	0.0000	0.0080	0.0000	0.0015	0.0000	0.0020		0.1533	0.1690	0.0750	0.0708	0.2113	0.2321
0.0100	0.0078	0.0280	0.0258	0.0123	0.0133	0.0161	0.0269	0.0181		0.0206	0.0227	0.0878	0.0799	0.0473	0.0624
0.0417	0.0068	0.0057	0.0235	0.0074	0.0039	0.0085	0.0088	0.0028	0.1022	0.0511	0.0666	0.1177	0.1008	0.0659	0.0821
0.0382	0.0475	0.0270	0.0161	0.0270	0.0333	0.0298	0.0246	0.0287	0.0819	0.1353	0.0957	0.0829	0.0750	0.1748	0.1968
0.6309	0.5361	0.5639	-0.0994	0.7155	0.8627	0.8149	0.7190	0.7588	0.0214	0.0330	0.0374	0.0550	0.0827	0.0722	0.0535
0.1626	0.0980	0.0791	0.0690	0.0858	0.0974	0.0663	0.1027	0.0923	0.5180	0.0953	0.1126	0.3948	0.4314	0.6144	0.6333
0.1048	0.0000	0.0000	0.0000	0.0000	0.0000	0.0000	0.0000	0.0000							
0.0068	0.0129	0.0304	0.0234	0.0317	0.0125	0.0095	0.0582	0.0531							
0.0578	0.2268	0.2593	0.2139	0.2824	0.3647	0.3096	0.2366	0.2839							

Earlywood and latewood change in curl index - 50 Hz, shaker

Δ Curl Index - 50 Hz, Shaker							
Earlywood							
	1	2	5	10	100	1000	10000
	0.03331	0.02244	0.01724	0.01799	0.00872	0.03173	0.02191
	0.00356	0.00101	0.00000	0.00150	0.01006	0.01450	0.00040
	0.04125	0.04428	0.00786	0.00267	0.03320	0.02561	0.02033
	0.02542	0.04763	0.01171	0.01048	0.00272	0.00488	0.00000
	0.01518	0.02927	0.04489	0.00214	0.02800	0.02799	0.03756
	0.00823	0.01612	0.00517	0.00874	0.02882	0.02265	0.01779
	0.02253	0.01568	0.01947	0.01067	0.00077	0.00775	0.00073
	0.02445	0.01691	0.00394	0.00395	0.00805	0.00193	0.01989
	0.00402	0.01098	0.02309	0.04479	0.00594	0.00000	0.02045
	0.01936	0.01731	0.00000	0.04617	0.02581	0.02716	0.00000
	0.00141	0.00217	0.02743	0.02243	0.01649	0.02618	0.02911
	0.01934	0.03067	0.02656	0.02851	0.02563	0.01149	0.01663
	0.02441	0.00329	0.04962	0.05101			
	0.01218	0.00239	0.00997	0.00457			
average	0.01819	0.01858	0.01764	0.01826	0.01618	0.01682	0.01540
st dev	0.01161	0.01501	0.01551	0.01768	0.01150	0.01135	0.01248
Latewood							
	1	2	5	10	100	1000	10000
	0.00059	0.01037	0.02166	0.06032	0.00967	0.03513	0.00911
	0.01369	0.01880	0.00656	0.00764	0.00042	0.00001	0.00807
	0.02908	0.01650	0.02642	0.03686	0.01630	0.00970	0.00280
	0.01785	0.02918	0.06152	0.00744	0.02743	0.02531	0.00337
	0.02124	0.01375	0.00452	0.03652	0.03191	0.01633	0.01268
	0.01294	0.00800	0.00150	0.00200	0.01576	0.00415	0.02083
	0.02020	0.01351	0.00280	0.00884	0.00206	0.00785	0.01505
	0.00112	0.01614	0.00456	0.00598	0.01545	0.01696	0.01616
	0.02047	0.01089	0.00348	0.00408	0.03959	0.00797	0.02195
	0.02788	0.02023	0.04779	0.03983	0.00440	0.02773	0.01866
	0.01894	0.01683	0.03104	0.01041	0.01730	0.03656	0.04594
	0.00000	0.00000	0.00000	0.00200			
	0.01745	0.00829	0.00300	0.00513			
	0.03247	0.06843	0.05513	0.04726			
average	0.01671	0.01792	0.01929	0.01959	0.01639	0.01706	0.01587
st dev	0.01032	0.01604	0.02175	0.01993	0.01246	0.01252	0.01191

Earlywood and latewood curl index - 100 Hz, shaker

Curl Index - 100 Hz, 5mm, Shaker															
Earlywood															
0	1	1.5	2	2.5	5	5.5	10	10	0	100	100.5	1000	1000.5	10000	10000.5
0.03275	0.0576	0.0630	0.0456	0.0282	0.2923	0.3231	0.1227	0.1628	0.1174	0.0547	0.0180	0.0508	0.0284	0.0094	0.0187
0.00578	0.0340	0.0600	0.0280	0.0706	0.0829	0.0846	0.0593	0.0852	0.0365	0.0276	0.0194	0.0693	0.0350	0.0340	0.0309
0.08727	0.0741	0.1057	0.1099	0.0560	0.1280	0.1520	0.1298	0.1223	0.0125	0.0070	0.0054	0.0281	0.0127	0.0280	0.0293
0.1191	0.0000	0.0088	0.0295	0.0221	0.0148	0.0160	0.0092	0.0183	0.1320	0.2353	0.2105	0.2566	0.2916	0.2829	0.2504
0.03916	0.3307	0.3472	0.3681	0.3577	0.2278	0.2648	0.4290	0.4577	0.0589	0.0183	0.0129	0.0061	0.0181	0.0127	0.0082
0.12867	0.0531	0.0660	0.0857	0.0899	0.0968	0.0565	0.1167	0.1422	0.0297	0.0367	0.0119	0.0265	0.0138	0.0179	0.0227
	0.0189	0.0115	0.0055	0.0139	0.0079	0.0101	0.0072	0.0088	0.0248	0.0757	0.0979	0.0732	0.0893	0.0708	0.0745
	0.1195	0.1371	0.1567	0.1356	0.2014	0.2195	0.1749	0.1417	1.0314	1.1673	1.1420	1.2057	1.2336	1.0411	0.9917
	0.0040	0.0221	0.0470	0.0460	0.0143	0.0164	0.0468	0.0626	0.0398	0.0336	0.0485	0.0441	0.0549	0.0679	0.0372
	0.0000	0.0249	0.0247	0.0106	0.0307	0.0042	0.0162	0.0121	0.4497	0.3646	0.3763	0.3549	0.3534	0.1923	0.1908
	0.0207	0.0237	0.0000	0.0060	0.0061	0.0214	0.0088	0.0147	0.0037	0.0045	0.0063	0.0141	0.0099	0.0066	0.0016
	0.0388	0.0161	0.0325	0.0041	0.0352	0.0200	0.0030	0.0147	0.0412	0.0913	0.0673	0.2206	0.2498	0.1108	0.0838
									0.3259	0.6537	0.6686	0.8288	0.8074	0.4214	0.3728
									0.0463	0.0521	0.0240	0.0288	0.0298	0.0185	0.0308
									0.0285	0.0250	0.0036	0.0154	0.0118	0.0245	0.0337
Latewood															
0	1	1.5	2	2.5	5	5.5	10	10	0	100	100.5	1000	1000.5	10000	10000.5
	0.1653	0.1930	0.1183	0.1415	0.1740	0.1834	0.1911	0.2013	0.0551	0.0125	0.0116	0.0066	0.0154	0.0346	0.0467
	0.7280	0.6984	0.6921	0.7328	0.9226	0.8980	0.7661	0.7997	0.0325	0.0079	0.0000	0.0094	0.0094	0.0275	0.0144
0.0333	0.0062	0.0261	0.0114	0.0291	0.0131	0.0362	0.0312	0.0076	0.1258	0.0857	0.1433	0.1309	0.0937	0.0505	0.0444
0.0155	0.0066	0.0094	0.0022	0.0004	0.0130	0.0020	0.0081	0.0100	0.0119	0.0000	0.0165	0.0088	0.0097	0.0382	0.0175
0.0462	0.0252	0.0214	0.0257	0.0167	0.0324	0.0218	0.0419	0.0577	0.0084	0.0079	0.0090	0.0000	0.0080	0.0133	0.0285
0.0398	0.0372	0.0183	0.0162	0.0170	0.0374	0.0284	0.0071	0.0302	0.0018	0.0091	0.0085	0.0005	0.0314	0.0162	0.0381
0.0476	0.3989	0.4110	0.3505	0.3708	0.4481	0.4815	0.2675	0.2454	0.0116	0.0073	0.0198	0.0038	0.0088	0.0303	0.0077
									0.0399	0.0892	0.0629	0.0208	0.0075	0.0892	0.0616
									0.1217	0.1140	0.1456	0.5676	0.6049	0.6744	0.6620
									0.0107	0.0188	0.0338	0.0411	0.0138	0.0172	0.0213

Earlywood and latewood change in curl index - 100 Hz, shaker

Δ Curl Index - 100 Hz, 5mm, Shaker							
Earlywood							
	1	2	5	10	100	1000	10000
	0.00533	0.01737	0.03081	0.04011	0.03668	0.02239	0.00926
	0.02600	0.04256	0.00170	0.02581	0.00816	0.03430	0.00311
	0.03158	0.05394	0.02407	0.00748	0.00153	0.01534	0.00121
	0.00876	0.00741	0.00122	0.00909	0.02482	0.03501	0.0325
	0.01652	0.01040	0.03696	0.02872	0.00542	0.01199	0.00457
	0.01289	0.00422	0.04034	0.02548	0.02482	0.01269	0.0048
	0.00745	0.00840	0.00227	0.00169	0.02224	0.01607	0.00367
	0.01767	0.02109	0.01811	0.03317	0.02528	0.02793	0.04944
	0.01812	0.00096	0.00215	0.01585	0.01487	0.01085	0.03063
	0.02487	0.01410	0.02653	0.00418	0.01175	0.00150	0.00152
	0.00297	0.00602	0.01529	0.00590	0.00173	0.00418	0.00501
	0.02277	0.02838	0.01513	0.01169	0.02403	0.02923	0.02699
					0.01485	0.02132	0.04856
					0.02803	0.00105	0.01234
					0.02133	0.00360	0.0036
average	0.01624	0.01790	0.01788	0.01743	0.01770	0.01650	0.01581
st dev	0.00901	0.01628	0.01412	0.01274	0.01038	0.01153	0.01716
Latewood							
	1	2	5	10	100	1000	10000
	0.02624	0.02319	0.00942	0.01019	0.00088	0.00879	0.01213
	0.02823	0.04068	0.02455	0.03356	0.00789	2.8E-05	0.01317
	0.01847	0.01772	0.02314	0.0236	0.05763	0.03721	0.00613
	0.00135	0.00178	0.01100	0.0019	0.01653	0.00097	0.02073
	0.00234	0.00899	0.01054	0.01574	0.00112	0.00796	0.01514
	0.01742	0.00076	0.00899	0.0231	0.00063	0.03091	0.02185
	0.02069	0.0203	0.03342	0.02202	0.01252	0.00496	0.02259
					0.02629	0.01338	0.02755
					0.0316	0.03727	0.01234
					0.01496	0.02731	0.00407
average	0.01639	0.01620	0.01729	0.01859	0.01700	0.01688	0.01557
st dev	0.01068	0.01394	0.00969	0.01031	0.01776	0.0148	0.00752

Earlywood and latewood curl index - 200 Hz, shaker

Curl Index - 200 Hz, 5mm, Shaker															
Earlywood															
0	1	1.5	2	2.5	5	5.5	10	10	0	100	100.5	1000	1000.5	10000	10000.5
0.0638	0.0635	0.0528	0.0603	0.0647					0.0243	0.0864	0.0675	0.0760	0.0743	0.0786	0.0996
0.0868	0.0043	0.0006	0.0125	0.0079					0.0119	0.0062	0.0055	0.0064	0.0000	0.0009	0.0000
0.0586	0.1038	0.0722	0.0597	0.0221					0.0282	0.0637	0.0909	0.0669	0.0500	0.0000	0.0004
0.0864	0.0217	0.0203	0.0209	0.0062					0.0426	0.0928	0.0641	0.0172	0.0000	0.0052	0.0000
0.0083	0.0046	0.0302	0.0151	0.0232					0.0118	0.0339	0.0272	0.0319	0.0235	0.0312	0.0210
0.0688	0.0139	0.0125	0.0150	0.0073	0.0118	0.0197	0.0196	0.0262	0.0067	0.1262	0.1421	0.0984	0.0995	0.0741	0.1231
0.1980	0.0319	0.0166	0.0528	0.0494	0.1562	0.1254	0.1125	0.1334	0.1038	0.3166	0.2893	0.4854	0.5083	0.4341	0.3969
0.0350	0.0799	0.0622	0.0890	0.0824	0.0761	0.0559	0.0613	0.0576	0.0301	0.0000	0.0214	0.1125	0.0741	0.0952	0.1254
0.0865	0.0481	0.0358	0.0656	0.0869	0.0698	0.0618	0.0998	0.1624	0.0080	0.0728	0.0867	0.0779	0.0648	0.0803	0.0767
0.0165	0.1245	0.1035	0.0468	0.0251	0.0641	0.0340	0.0638	0.0913	0.0013	0.0389	0.0555	0.0211	0.0612	0.0371	0.0542
0.0105	0.0006	0.0151	0.0076	0.0271	0.0155	0.0060	0.0202	0.0342	0.0070	0.0770	0.0618	0.1629	0.1511	0.0467	0.0485
0.0392	0.1399	0.1237	0.0252	0.0167	0.0230	0.0101	0.0559	0.0561							
0.0000	0.0035	0.0035	0.0013	0.0095	0.0232	0.0046	0.0159	0.0069							
0.1648	0.1052	0.1268	0.1414	0.1688	0.1993	0.1604	0.1873	0.1999							
0.0865	0.0890	0.1065	0.0768	0.1193			0.1402	0.1231							
0.0780	0.1232	0.1603	0.1786	0.1932	0.1036	0.1169	0.1654	0.1441							
0.0298	0.0213	0.0141	0.0135	0.0314	0.0058	0.0000	0.0089	0.0000							
Latewood															
0	1	1.5	2	2.5	5	5.5	10	10	0	100	100.5	1000	1000.5	10000	10000.5
0.0090	0.0988	0.1168	0.0733	0.0423	0.1318	0.1149	0.1183	0.1044	0.0063	0.0041	0.0112	0.0041	0.0115	0.0036	0.0147
0.0092	0.0243	0.0356	0.0370	0.0339	0.0316	0.0090	0.0083	0.0309	0.0423	0.0228	0.0465	0.0288	0.0430	0.0106	0.0081
0.0000	0.0161	0.0261	0.0372	0.0179	0.0075	0.0140	0.0109	0.0165	0.1683	0.1529	0.1719	0.4220	0.4426	0.0505	0.0784
0.3410	0.9154	0.9365	0.8518	0.8318	0.8656	0.8474	0.8802	0.9018	0.0086	0.0284	0.0246	0.1584	0.1744	0.0810	0.0625
									0.0163	0.0501	0.0422	0.1208	0.1483	0.2217	0.2065
									0.0841	0.2102	0.1926	0.1823	0.2110	0.1596	0.1802
									0.0846	0.6551	0.6279	0.3938	0.4074	0.3131	0.3010
									0.0165	0.0709	0.0532	0.0287	0.0316	0.0071	0.0081
									0.0073	0.1836	0.1610	0.0804	0.0955	0.0735	0.0833
									0.0117	0.0489	0.0236	0.0145	0.0322	0.0709	0.0814
									0.0353	0.0511	0.0376	0.0301	0.0241	0.0381	0.0650

Earlywood and latewood change in curl index - 200 Hz, shaker

Δ Curl Index - 200 Hz, 5mm, Shaker							
Earlywood							
	1	2	5	10	100	1000	10000
	0.01072	0.00440			0.02894	0.00174	0.02097
	0.00374	0.00462			0.00072	0.00636	0.00086
	0.03158	0.03758			0.02716	0.01690	0.00037
	0.00149	0.01464			0.01876	0.01721	0.00520
	0.02553	0.00804			0.00661	0.00847	0.01017
	0.00147	0.00773	0.00792	0.00658	0.01583	0.00110	0.04902
	0.01529	0.00350	0.03082	0.02098	0.02727	0.02285	0.03720
	0.01770	0.00667	0.02017	0.00365	0.02138	0.03840	0.03020
	0.01238	0.02132	0.00803	0.06264	0.01388	0.01307	0.00354
	0.02105	0.02168	0.03005	0.02754	0.01651	0.04012	0.01712
	0.01448	0.01957	0.00953	0.01393	0.01518	0.01179	0.00176
	0.01624	0.00848	0.01291	0.00017			
	0.00005	0.00825	0.01860	0.00896			
	0.02168	0.02739	0.03892	0.01260			
	0.01750	0.04245		0.01701			
	0.03714	0.01462	0.01333	0.02129			
	0.00726	0.01789	0.00583	0.00895			
average	0.01502	0.01581	0.01783	0.01703	0.01748	0.01618	0.01604
st dev	0.01053	0.01154	0.01105	0.01639	0.00871	0.01317	0.01658
Latewood							
	1	2	5	10	100	1000	10000
	0.01792	0.03103	0.01697	0.01643	0.00717	0.00739	0.01118
	0.01138	0.00314	0.02262	0.02510	0.02378	0.01420	0.00247
	0.01001	0.01933	0.00650	0.00817	0.01903	0.02064	0.02786
	0.02107	0.02003	0.01823	0.01412	0.00380	0.01601	0.01843
					0.00796	0.02748	0.01516
					0.01765	0.02871	0.02060
					0.02727	0.01358	0.01213
					0.01768	0.00291	0.00103
					0.02267	0.01510	0.00977
					0.02530	0.01773	0.01051
					0.01354	0.00602	0.02690
average	0.01509	0.01838	0.01608	0.01596	0.01690	0.01543	0.01418
st dev	0.00527	0.01149	0.00683	0.00702	0.00789	0.00818	0.00875

IR mixed aggregates at 45% consistency change in temperature - 10 Hz

Initial IR Study - 10 Hz																										
Latewood - Δ Temperature (C)																										
1	-0.001	0.009	0.019	-0.007	0.038	-0.049	-0.003	-0.033	-0.007	-0.026	0.064	0.021	-0.029	0.111	0.046	-0.025	-0.040	-0.021	-0.003							
2	-0.029	0.014	0.083	-0.118	-0.004	-0.094	-0.029	0.015	-0.046	-0.131	-0.136	-0.009	-0.122	-0.103	-0.012	-0.081	-0.052	0.018	-0.031							
5	0.004	0.029	0.013	-0.069	-0.007	-0.066	-0.009	0.029	0.025	-0.032	-0.042	-0.043	-0.099	-0.019	-0.031	-0.078	-0.019	0.032	0.026							
10	-0.016	-0.047	0.028	-0.158	-0.012	-0.078	-0.003	-0.007	0.010	0.006	-0.129	0.037	-0.147	0.056	0.057	-0.029	-0.054	0.032	0.023							
50	-0.029	-0.011	-0.003	-0.151	-0.017	-0.072	0.003	0.029	-0.019	0.011	-0.141	-0.006	-0.118	-0.057	-0.019	-0.012	-0.046	-0.008	-0.048							
100	-0.014	0.019	0.013	-0.066	-0.036	-0.118	0.011	0.071	-0.069	-0.041	-0.123	-0.068	-0.154	-0.116	-0.011	0.024	-0.046	0.005	-0.034	-0.079	0.019	0.031	0.002	-0.068		
200	-0.007	0.008	0.032	-0.083	-0.036	-0.040	0.016	0.017	-0.037	-0.016	-0.139	-0.131	-0.219	-0.056	-0.139	0.044	-0.036	0.052	-0.041	0.032	-0.042	-0.062	-0.008	-0.108		
500	-0.048	-0.031	-0.032	-0.054	-0.128	0.105	-0.009	0.017	0.031	-0.065	-0.148	0.008	0.061	-0.009	-0.205	-0.016	0.001	0.087	0.006	-0.177	-0.034	-0.041	-0.036	-0.146		
1000	-0.093	0.027	-0.043	-0.051	-0.175	-0.010	-0.117	0.009	0.007	-0.089	-0.218	-0.102	-0.008	-0.045	-0.189	-0.031	-0.019	0.077	0.009	-0.097	-0.095	-0.043	-0.113	-0.105		
5000	-0.161	-0.182	-0.159	-0.194	-0.141	-0.163	-0.141	-0.035	0.018	-0.207	-0.321	-0.104	-0.121	-0.201	-0.339	-0.133	-0.093	-0.150	0.031	-0.116	-0.047	-0.081	-0.182	-0.212		
10000	-0.283	-0.236	-0.263	-0.267	-0.366	-0.224	-0.275	-0.048	0.034	-0.259	-0.348	-0.171	-0.374	-0.304	-0.266	-0.117	-0.080	-0.033	-0.118	-0.235	-0.222	-0.194	-0.276	-0.278		
	LW cont.		1																						average	
			2																						0.003	
			5																						-0.046	
			10																						-0.019	
			50																						-0.023	
			100	0.073	-0.077	0.058	0.039	-0.079	-0.105	0.041	0.101	-0.007	-0.162	-0.079	0.031	0.096	0.103	-0.051	0.050	-0.001	-0.048	-0.076	-0.041	-0.016	-0.038	
			200	0.034	-0.065	0.039	0.031	-0.051	-0.139	-0.017	0.098	0.015	-0.167	-0.011	-0.007	0.102	0.052	-0.116	0.004	-0.006	-0.066	-0.121	0.042	-0.027	-0.022	
			500	-0.076																					-0.031	
			1000	-0.085																					-0.038	
			5000	-0.096																					-0.064	
			10000	-0.342																					-0.141	
																									-0.222	
Earlywood - Δ Temperature (C)																										
1	0.004	-0.043	0.052	0.033	-0.009	0.042	0.004	0.023	0.068	0.114	0.043	0.037														
2	0.064	-0.111	-0.091	-0.080	0.032	0.004	-0.022	-0.049	-0.061	-0.121	-0.156	-0.014														
5	0.036	-0.107	-0.085	-0.024	0.051	-0.037	0.017	-0.001	-0.047	-0.017	-0.177	0.064														
10	0.031	-0.113	-0.076	-0.106	0.039	-0.116	0.072	-0.090	-0.012	-0.142	0.003	-0.002														
50	0.073	-0.126	-0.115	-0.013	0.042	-0.136	0.066	-0.043	-0.036	-0.040	-0.045	-0.022														
100	0.008	-0.092	-0.135	-0.034	0.058	-0.121	0.011	-0.098	-0.044	-0.124	-0.093	-0.057	0.059	0.153	0.061											
200	0.014	-0.112	-0.106	-0.049	0.014	-0.100	-0.045	-0.127	-0.061	-0.088	-0.123	-0.084	0.018	0.026	-0.074											
500	0.083	0.112	-0.063	0.093	-0.154	0.061	-0.221	0.011	-0.014	0.026	-0.080	0.077	0.197	-0.169	0.289											
1000	-0.031	0.047	-0.080	0.089	-0.166	-0.109	-0.143	-0.009	0.003	-0.008	-0.108	-0.024	0.183	-0.144	0.251											
5000	-0.114	0.004	-0.159	-0.074	-0.266	-0.238	-0.304	-0.117	-0.151	-0.120	-0.213	-0.137	0.027	-0.311	0.096											
10000	-0.162	-0.105	-0.251	-0.116	-0.286	-0.288	-0.357	-0.151	-0.156	-0.226	-0.310	-0.283	-0.053	-0.250	0.065											
	EW cont.		1														average									
			2														0.031									
			5														-0.050									
			10														-0.027									
			50														-0.043									
			100	0.052	-0.032	0.092	-0.112	-0.002	-0.078	-0.057	0.112	0.066	-0.037	-0.007	0.229	-0.179	-0.033									
			200	0.100	-0.111	-0.091	-0.177	0.005	0.029	-0.016	-0.058	0.003	0.192	-0.219	0.229	-0.104	-0.030									
			500	-0.037													-0.060									
			1000	-0.103													0.017									
			5000	-0.247													-0.016									
			10000	-0.370													-0.138									
																	-0.195									

IR mixed aggregates at 45% consistency change in temperature - 30 Hz

Initial IR Study - 30 Hz

Latewood - Δ Temperature (C)

1	0.018	0.031	0.033	-0.026	-0.023	0.044	0.086	-0.002	0.006	-0.070	-0.099	-0.061	-0.074	0.055										
2	0.038	0.004	0.032	-0.053	-0.047	-0.071	-0.132	-0.073	-0.067	-0.128	-0.134	-0.010	-0.072	-0.111										
5	0.058	-0.013	0.021	-0.032	-0.034	-0.042	-0.139	0.022	-0.039	-0.046	-0.123	-0.058	-0.051	-0.053										
10	0.058	-0.033	0.047	-0.023	-0.040	-0.020	-0.143	-0.033	-0.057	-0.044	-0.131	-0.055	-0.101	-0.156										
50	0.064	-0.029	0.021	-0.039	0.000	-0.105	-0.178	0.022	-0.007	-0.046	-0.100	-0.050	-0.006	-0.060										
100	0.050	-0.041	0.031	-0.048	-0.029	-0.122	-0.198	-0.026	-0.041	-0.030	0.018	0.083	0.007	0.108	-0.036	-0.113	-0.042	0.181	0.055	0.012	-0.113	-0.143	0.093	-0.114	-0.066
200	0.042	0.005	0.047	-0.010	-0.001	-0.094	-0.097	-0.032	-0.068	-0.102	-0.013	-0.040	0.009	0.087	-0.047	-0.058	-0.056	0.043	0.060	-0.008	-0.134	-0.095	0.103	-0.069	-0.073
500	-0.023	0.004	0.023	0.092	-0.064	-0.045	-0.111	0.017	0.065	0.035	-0.078	-0.077	0.028	0.004	0.076	-0.033	-0.059	0.007	0.076	-0.038	0.026	0.046	-0.107	-0.219	-0.249
1000	-0.017	0.005	-0.013	0.081	-0.018	0.021	-0.069	0.044	0.081	0.011	-0.086	-0.076	0.093	0.018	-0.019	-0.018	-0.069	-0.007	0.029	-0.084	0.045	-0.007	-0.097	-0.204	-0.263
5000	-0.017	-0.074	-0.034	0.054	-0.006	-0.019	-0.114	0.032	0.098	-0.004	-0.126	-0.117	0.106	-0.071	-0.023	-0.033	-0.099	-0.036	-0.040	-0.134	-0.071	-0.033	-0.207	-0.286	-0.328
10000	-0.051	-0.082	-0.005	0.051	-0.094	-0.036	-0.098	0.064	0.083	0.055	-0.114	-0.084	0.052	0.209	0.000	0.000	0.000	-0.103	-0.156	-0.159	-0.142	-0.118	-0.229	-0.278	-0.386

LW (cont.)

	average
1	-0.006
2	-0.059
5	-0.038
10	-0.052
50	-0.039
100	-0.035
200	-0.033
500	-0.027
1000	-0.030
5000	-0.068
10000	-0.082

Earlywood - Δ Temperature (C)

1	0.023	-0.018	0.037	-0.010	0.019	-0.032	0.014	-0.037	-0.004															
2	-0.019	-0.029	0.053	0.021	-0.108	-0.147	-0.004	-0.176	0.012															
5	-0.042	-0.033	0.053	0.034	0.003	-0.116	-0.040	-0.146	0.028															
10	-0.054	-0.078	0.051	0.016	-0.046	-0.134	-0.032	-0.173	0.025															
50	-0.019	-0.038	0.066	0.064	-0.078	-0.111	-0.002	-0.138	-0.056															
100	-0.050	-0.008	0.074	0.007	-0.080	-0.122	-0.078	-0.050	0.040	0.003	-0.009	-0.064	-0.060	0.058	0.074	0.069	-0.123	-0.047	0.196	0.018	-0.138	-0.050	0.068	-0.056	
200	-0.038	0.002	0.072	-0.044	-0.044	-0.243	-0.066	-0.089	0.054	0.019	0.029	-0.104	-0.057	0.104	0.105	-0.001	-0.086	-0.036	0.099	0.045	-0.165	-0.022	0.078	-0.057	
500	-0.084	-0.024	0.065	0.021	0.006	-0.082	-0.051	-0.013	0.118	-0.002	-0.109	-0.029	0.051	0.187	-0.101	-0.050	0.036	0.101	-0.016	0.028	-0.133	-0.139	-0.032	-0.212	
1000	-0.073	-0.029	0.065	0.029	0.031	-0.084	-0.019	0.092	0.061	0.036	-0.116	-0.021	0.069	0.194	0.054	0.061	-0.004	0.091	0.063	-0.021	0.019	-0.100	-0.026	-0.182	
5000	-0.061	-0.011	0.064	0.023	0.006	-0.094	-0.060	0.022	0.091	0.043	-0.148	-0.066	0.059	-0.018	-0.053	-0.116	0.048	-0.039	-0.020	0.014	-0.021	-0.124	-0.128	-0.188	
10000	-0.091	-0.056	0.021	0.019	-0.018	-0.074	-0.071	-0.016	0.089	0.000	-0.139	-0.026	0.054	0.000	0.000	0.000	-0.122	0.002	-0.087	-0.047	-0.123	-0.235	-0.220	-0.350	

EW (cont.)

	average
1	-0.001
2	-0.044
5	-0.029
10	-0.047
50	-0.035
100	-0.014
200	-0.019
500	-0.019
1000	0.008
5000	-0.032
10000	-0.062

IR mixed aggregates at 45% consistency change in temperature - 50 Hz

Initial IR Study - 50 Hz																															
Latewood - Δ Temperature (C)																													average		
1	-0.023	-0.026	0.017	0.013	-0.028	0.022	0.056	-0.037	-0.072	-0.106																			-0.018		
2	-0.085	-0.022	0.029	0.113	-0.152	0.020	0.039	-0.071	-0.103	-0.189																			-0.042		
5	-0.033	0.017	0.068	0.072	-0.142	-0.089	0.029	-0.096	-0.137	-0.141																			-0.045		
10	-0.041	0.029	-0.006	0.107	0.017	-0.017	0.003	-0.023	-0.057	-0.186																			-0.017		
50	-0.059	0.014	-0.008	0.129	0.009	0.009	0.062	-0.074	-0.045	-0.143																			-0.010		
100	-0.083	0.029	-0.013	0.117	0.031	0.049	0.066	-0.061	-0.102	-0.073	-0.079	-0.029	0.026	-0.003	0.023	-0.222	-0.061	0.001	-0.169	0.006	0.106	-0.003	0.011	-0.140	-0.103	-0.203	-0.063	-0.034		
200	-0.100	0.041	0.118	0.080	0.013	0.052	0.112	-0.093	-0.127	-0.102	-0.067	0.033	0.081	0.032	0.023	-0.164	-0.073	0.030	-0.117	0.018	0.159	0.122	-0.024	-0.108	-0.176	-0.113	-0.018	-0.014		
500	-0.062	-0.108	-0.044	-0.034	0.016	0.064	-0.039	-0.106	-0.112	0.119	0.134	0.071	-0.014	-0.174	-0.156	-0.164	-0.022											-0.037		
1000	-0.028	-0.129	-0.049	-0.004	-0.006	0.024	0.023	-0.189	-0.078	-0.024	0.152	0.154	-0.006	-0.152	-0.153	-0.172	0.011											-0.037		
5000	-0.026	-0.101	-0.078	-0.009	0.078	0.027	-0.064	0.014	-0.079	-0.256	0.025	-0.043	-0.033	-0.142	-0.158	-0.168	-0.025											-0.061		
10000	-0.031	-0.073	-0.099	0.030	0.077	0.039	-0.133	0.016	-0.099	-0.283	0.018	-0.072	-0.101	-0.153	-0.252	-0.232	-0.033											-0.081		
Earlywood - Δ Temperature (C)																															average
1	0.042	-0.014	0.040	0.073	-0.001	-0.016	-0.053	0.024	0.019	0.006	-0.137	-0.079	-0.088																		-0.014
2	0.039	-0.109	0.072	0.104	-0.011	-0.075	-0.067	-0.006	-0.133	-0.094	-0.117	-0.082	-0.230																		-0.054
5	-0.033	-0.028	0.070	0.010	-0.119	-0.078	-0.115	-0.022	-0.077	-0.067	-0.104	-0.037	-0.192																		-0.061
10	-0.026	-0.055	0.055	0.036	-0.089	-0.091	-0.079	-0.032	-0.091	-0.053	-0.133	-0.023	-0.193																		-0.060
50	-0.073	-0.059	0.038	0.086	-0.030	0.014	-0.108	-0.038	-0.060	-0.060	-0.101	0.050	-0.213																		-0.043
100	-0.154	-0.049	0.106	0.082	-0.043	-0.062	-0.102	-0.002	-0.029	-0.148	-0.039	0.071	-0.041	-0.081	-0.008	-0.015	-0.024	-0.014	-0.043	-0.093	0.037	-0.252	0.049	0.007	-0.004	-0.068	-0.078	-0.053	0.050	-0.035
200	-0.032	-0.118	-0.126	0.113	0.012	0.037	0.018	0.013	-0.003	-0.099	-0.076	0.028	-0.025	-0.120	-0.012	0.068	-0.001	-0.115	-0.054	-0.081	0.017	-0.192	0.141	0.062	-0.007	-0.056	-0.110	-0.103	0.030	-0.027
500	0.034	-0.045	-0.072	-0.020	0.052	0.110	-0.104	0.013	0.084	0.070	0.098	-0.058	-0.071	-0.099	-0.066	0.019															-0.003
1000	0.095	-0.007	-0.072	-0.011	-0.021	0.077	-0.077	0.025	0.015	0.134	0.137	0.033	-0.076	-0.058	-0.076	0.003															0.008
5000	0.093	-0.007	-0.101	-0.032	0.027	0.011	-0.082	0.027	0.119	-0.061	-0.071	-0.032	-0.098	-0.038	-0.072	0.027															-0.018
10000	0.097	0.000	0.002	0.012	-0.002	-0.116	-0.067	0.019	0.057	-0.157	0.021	-0.158	-0.136	-0.071	-0.080	0.000															-0.036

IR mixed aggregates at 45% consistency change in temperature - 100 Hz

Initial IR Study - 100 Hz																												
Latewood - Δ Temperature (C)																												average
1	-0.021	0.022	0.009	-0.033	0.027	0.009	-0.019	-0.008	-0.022	-0.127	0.011	0.000	0.014	0.025														-0.008
2	-0.053	-0.059	-0.107	-0.147	0.069	-0.026	-0.064	-0.002	0.017	-0.084	-0.105	-0.085	-0.024	-0.021														-0.049
5	-0.078	0.100	-0.071								-0.043	-0.127	-0.044	-0.017														-0.040
10	-0.013	0.057	-0.065	-0.021	-0.108	-0.067	-0.056	0.026	0.004	-0.075	-0.038	-0.069	-0.056	-0.048														-0.038
50	-0.074	0.006	0.015	0.011	-0.045	0.002	-0.040	-0.014	0.020	-0.109	-0.076	-0.109	-0.060	-0.120														-0.042
100	-0.125	-0.084	-0.014	0.007	-0.019	0.031	-0.098	0.049	-0.007	-0.058	-0.058	-0.084	-0.019	0.066	-0.113	0.006	-0.129	-0.029	0.054	0.084	-0.066	-0.058	0.000	0.018	-0.070	-0.347	-0.041
200	-0.088	-0.068	0.077	0.041	0.054	0.063	-0.053	0.054	-0.004	-0.081	-0.051	-0.076	-0.014	0.055	-0.089	-0.004	0.012	0.001	0.047	0.078	0.029	-0.118	-0.047	-0.044	-0.110	-0.205	-0.021
500	-0.049	0.020	-0.077	-0.012	0.026	0.066	-0.012	-0.141	0.034	-0.007	-0.059																-0.019
1000	-0.014	0.034	-0.022	-0.097	0.116	0.086	-0.054	-0.046	0.007	0.006	-0.229	-0.156															-0.031
5000	0.002	0.038	0.060	-0.132	0.109	0.044	-0.071	-0.160	-0.010	0.032	-0.098	-0.175															-0.030
10000	0.010	0.013	0.101	-0.081		0.026	-0.046	-0.176	-0.032	0.042	-0.120	-0.064															-0.030
Earlywood - Δ Temperature (C)																							average				
1	-0.003	0.0128	-0.056	-0.005	-0.042	-0.002	0.0144	-6E-04	-0.029														-0.012				
2	-0.024	0.0639	-0.017	-0.02	-0.047	-0.124	-0.095	-0.198	-0.047														-0.056				
5	0.0117						-0.077	-0.248	-0.023														-0.084				
10	-0.052	0.0006	-0.051	-0.005	-0.001	-0.182	-0.042	-0.119	-0.028														-0.053				
50	-0.048	-0.028	-0.06	0.0283	-0.049	-0.095	-0.057	-0.14	-0.013														-0.051				
100	-0.084	-0.039	-0.045	0.04	0.0133	-0.125	-0.064	-0.103	0.0144	-0.012		-0.129	0.0478	-0.012	0.0661	-0.018	-0.019	-0.021	-0.044	-0.006	-0.003	-0.334	-0.042				
200	-0.042	-0.009	-0.023	0.0461	-0.014	-0.103	-0.075	-0.071	0.0228	0.0428		-0.068	0.0617	0.0428	0.0744	-0.046	-0.019	0.0122	-0.056	-0.041	-0.091	-0.141	-0.024				
500	0.0933		0.0072	0.1544	0.0933	-0.116	-0.059	-0.016	-0.053	-0.031	-0.038	-0.06											-0.002				
1000	0.0544		0.0733	0.0928	0.0544	0.0411	-0.096	0.0083	0.0272	0.0228	0.0494	-0.075	-0.184										0.0057				
5000	0.0839		0.1289	0.1489	0.0839	-0.104	-0.114	-0.159	0.0378	0.0494	0.0394	-0.012	-0.208										-0.002				
10000	0.0711		0.0506	0.1439	0.0711	-0.137	-0.111	-0.026	0.0089	-0.008	0.0717	-0.014	-0.152										-0.003				

IR pure aggregates at 45% consistency change in temperature - 10 Hz

Experiment 1 - 10 Hz																
Latewood - Δ Temperature (C)											average					
1	0.029	0.008	0.003	-0.005	-0.027						0.002					
2	-0.006	-0.058	-0.021	-0.017	-0.002						-0.021					
5	0.000	0.000	0.000	0.000	0.000						0.000					
10	0.038	-0.064	-0.061	-0.011	-0.019						-0.023					
50	0.009	-0.011	-0.019	-0.024	-0.021						-0.013					
100	0.001	-0.066	0.012	0.003	0.000						-0.013					
200	0.028	-0.026	-0.026	-0.001	-0.047	-0.002	-0.099	0.066	-0.018	0.000	-0.014					
500	0.002	-0.080	0.012	-0.011							-0.019					
1000	-0.007	-0.101	-0.026	-0.018							-0.038					
5000	-0.053	-0.101	-0.032	-0.049							-0.059					
10000	-0.128	-0.168	-0.107	-0.133							-0.134					
Earlywood - Δ Temperature (C)																average
1	0.022	-0.024	0.012	0.145	0.011	-0.029	-0.062	0.113								0.024
2	-0.018	-0.018	-0.013	0.008	-0.015	-0.050	-0.056	-0.019								-0.022
5	-0.019	-0.047	0.005	0.077	-0.011	-0.077	-0.087	0.078								-0.010
10	-0.058	-0.002	-0.027	-0.003	-0.033	-0.028	-0.067	-0.013								-0.029
50	-0.006	-0.023	-0.024	0.012	-0.006	-0.019	-0.036	-0.007								-0.014
100	0.004	0.027	0.026	0.008	-0.064	-0.028	-0.059	0.000								-0.011
200	-0.016	-0.034	-0.027	0.016	0.003	-0.023	-0.019	-0.009	0.013	0.001	-0.035	0.029	-0.057	-0.029	-0.029	-0.014
500	0.041	-0.027	0.029	0.046	-0.072	0.037	0.023									0.011
1000	-0.001	-0.019	0.001	0.034	-0.052	0.006	-0.004									-0.005
5000	-0.019	-0.114	-0.050	-0.070	-0.091	-0.016	-0.089									-0.064
10000	-0.073	-0.215	-0.162	-0.130	-0.154	-0.074	-0.095									-0.129

IR pure aggregates at 45% consistency change in temperature - 50 Hz

Experiment 1 - 50 Hz																		
Latewood - Δ Temperature (C)																	average	
1	-0.007	-0.016	-0.022	-0.012	-0.012	-0.037	-0.021	-0.022									-0.019	
2	-0.059	-0.077	-0.026	0.011	0.007	-0.043	0.012	-0.057									-0.029	
5	-0.036	-0.085	-0.053	0.012	0.007	-0.051	-0.009	-0.099									-0.039	
10	-0.014	-0.049	-0.054	-0.005	0.007	-0.015	0.008	-0.042									-0.020	
50	-0.046	-0.027	-0.028	0.008	0.004	-0.024	0.001	-0.035									-0.018	
100	-0.086	0.031	0.009	0.065	-0.084	0.011	-0.019	-0.077									-0.019	
200	-0.030	-0.015	-0.020	0.011	0.006	-0.017	0.006	-0.031	-0.067	0.020	0.008	0.040	-0.086	0.039	-0.009	-0.060	-0.013	
500	-0.089	0.022	0.024	0.037	-0.046	-0.001	0.008	-0.036									-0.010	
1000	-0.073	0.009	0.011	0.009	-0.027	-0.010	-0.005	-0.025									-0.014	
5000	-0.091	0.001	0.010	0.009	-0.032	-0.012	-0.009	-0.056									-0.023	
10000	-0.083	-0.027	-0.015	-0.024	-0.033	-0.020	-0.043	-0.068									-0.039	
Earlywood - Δ Temperature (C)																		average
1	0.019	-0.027	-0.008	-0.030	0.008	-0.006	-0.016											-0.008
2	-0.018	-0.047	-0.019	-0.056	-0.009	-0.029	-0.044											-0.032
5	-0.023	-0.046	-0.026	-0.094	-0.017	-0.062	-0.033											-0.043
10	-0.007	-0.046	-0.042	-0.031	-0.018	-0.031	-0.065											-0.034
50	0.021	-0.052	-0.039	-0.031	-0.006	-0.014	-0.017											-0.020
100	-0.031	-0.023	-0.014	0.004	-0.053	0.050	0.029	-0.029	0.012	-0.024								-0.008
200	0.039	-0.042	-0.017	-0.031	0.024	0.022	-0.043	0.016	0.027	-0.009	0.021	-0.031	-0.020	0.010	-0.033	-0.019	-0.032	-0.007
500	0.020	0.008	0.026	-0.018	-0.054	0.029	0.016	-0.041	0.004	-0.038								-0.005
1000	0.002	0.017	-0.002	0.011	-0.078	0.051	-0.005	-0.022	0.024	-0.014								-0.002
5000	-0.005	0.008	0.011	-0.018	-0.039	0.033	0.009	-0.030	-0.028	-0.019								-0.008
10000	0.000	-0.021	-0.018	0.001	-0.047	-0.002	-0.019	-0.017	-0.024	0.012								-0.013

IR pure aggregates at 45% consistency change in temperature - 100 Hz

Experiment 1 - 100 Hz																	
Latewood - Δ Temperature (C)																	average
1	-0.029	-0.011	-0.014	-0.039	-0.016	-0.009	-0.024	-0.034									-0.022
2	-0.045	-0.027	-0.046	-0.066	-0.018	-0.036	-0.046	-0.071									-0.044
5	-0.059	-0.007	-0.025	-0.020	-0.009	-0.038	-0.048	-0.068									-0.034
10	-0.064	0.023	-0.032	0.003	0.009	-0.058	-0.066	-0.079									-0.033
50	-0.067	0.019	-0.031	0.003	0.017	-0.057	-0.066	-0.073									-0.032
100	0.012	-0.026	0.029	-0.025	-0.008	-0.072	-0.002	-0.073									-0.020
200	-0.055	0.024	-0.017	0.009	0.024	-0.038	-0.046	-0.056	0.008	-0.046	0.007	-0.024	-0.003	-0.056	0.004	-0.039	-0.019
500	-0.013	-0.028	-0.021	0.020	0.001	-0.034	-0.035	-0.024									-0.017
1000	-0.007	-0.035	0.012	0.037	0.067	-0.062	-0.052	-0.036									-0.010
5000	-0.013	-0.037	0.001	0.020	0.064	-0.059	-0.047	-0.032									-0.013
10000	-0.018	-0.023	-0.006	0.013	0.051	-0.062	-0.061	-0.038									-0.018
Earlywood - Δ Temperature (C)														average			
1	-0.006	0.001	-0.030	-0.036	-0.020									-0.018			
2	-0.012	-0.048	0.003	-0.021	-0.045									-0.025			
5	-0.059	-0.033	-0.078	-0.014	-0.011									-0.039			
10	-0.026	-0.026	-0.042	-0.072	-0.031									-0.039			
50	-0.019	-0.011	-0.057	-0.018	-0.069									-0.035			
100	0.009	0.007	-0.031	-0.016	0.023	-0.103	-0.037	0.024						-0.015			
200	-0.033	0.022	-0.003	-0.046	-0.018	0.028	0.007	-0.033	-0.031	0.011	-0.083	-0.038	0.016	-0.015			
500	0.022	0.030	-0.010	-0.012	0.034	-0.059	-0.024	0.012						-0.001			
1000	0.003	0.008	-0.036	0.001	0.031	-0.022	-0.003	0.028						0.001			
5000	-0.013	0.019	-0.016	0.016	0.024	-0.028	-0.020	-0.014						-0.004			
10000	-0.019	-0.008	-0.016	-0.003	0.015	-0.014	0.002	0.002						-0.005			

IR pure aggregates (air dried) change in temperature - 10 and 50 Hz

Experiment 4																	
50 Hz - Δ Temperature (C)																	average
10	0.073	-0.016	0.060	0.042	0.006	0.005	0.016	0.077	0.093	0.012	-0.001	0.029	0.024	-0.064	-0.012	0.078	0.026
20	0.118	0.001	0.072	0.016	0.001	0.012	0.078	0.089	0.092	0.005	0.031	0.022	-0.016	-0.038	-0.021	0.063	0.033
50	0.092	0.003	0.009	0.029	0.029	-0.021	0.006	0.037	0.086	-0.029	-0.016	-0.016	0.017	-0.063	0.021	0.045	0.014
100	0.063	0.046	0.028	0.035	0.029	0.043	0.061	0.100									0.051
500	0.149	0.041	0.127	0.084	0.077	0.138	0.101	0.223	0.182	0.076	0.161	0.086	0.050	0.079	0.059	0.111	0.109
1000	0.164	0.048	0.086	0.112	0.133	0.149	0.101	0.223									0.127
2000	0.158	0.064	0.069	0.078	0.098	0.161	0.129	0.238	0.200	0.098	0.142	0.119	0.112	0.117	0.086	0.151	0.126
10 Hz - Δ Temperature (C)															average		
10	0.064	0.041	0.097	0.041	0.001	0.034	0.078	0.127	0.047	0.025	0.016	0.078	0.111	0.011	0.055		
20	0.068	0.049	0.074	0.063	0.037	0.028	0.073	0.110	0.023	-0.019	0.046	0.089	0.070	0.037	0.054		
50	0.113	0.042	0.021	0.058	0.007	0.022	0.078	0.106	0.041	-0.031	0.051	0.033	0.048	0.043	0.045		
100	0.092	0.038	0.064	0.076	0.005	0.048	0.061	0.042	0.063	0.062	0.042	0.022	0.022	0.016	0.047		
500	0.055	-0.036	0.047	0.082	0.012	0.028	0.089	0.122	0.034	-0.030	0.034	0.064	0.032	0.061	0.042		
1000	0.059	0.006	0.059	0.116	0.017	0.073	0.104	0.132	0.096	-0.034	0.067	0.091	0.098	0.051	0.067		
2000	0.148	0.042	0.113	0.109	0.052	0.119	0.087	0.158	0.077	0.003	0.043	0.116	0.051	0.096	0.087		

IR pure aggregates at 45% consistency without fiber work change in temperature - 10 and 50 Hz

Experiment 6																		
10 Hz - Δ Temperature (C)																		average
100	-0.028	-0.007	0.000	0.021	-0.013	-0.061	-0.041	0.029	-0.009	-0.004	-0.015	-0.008	-0.010	-0.035	-0.072	-0.042	0.005	-0.017
500	-0.043	-0.056	-0.029	-0.004	-0.017	-0.057	-0.083	0.005	-0.021	-0.042	-0.093	-0.029	-0.042	-0.096	-0.077	-0.078	-0.046	-0.048
1000	-0.081	-0.105	-0.078	-0.049	-0.037	-0.111	-0.117	-0.029	-0.066	-0.075	-0.127	-0.132	-0.117	-0.148	-0.154	-0.149	-0.105	-0.099
5000	-0.119	-0.178	-0.131	-0.082	-0.118	-0.190	-0.160	-0.105	-0.124	-0.149	-0.185	-0.217	-0.174	-0.193	-0.227	-0.210	-0.135	-0.159
10000	-0.206	-0.194	-0.163	-0.071	-0.175	-0.192	-0.189	-0.108	-0.101	-0.141	-0.149	-0.186	-0.164	-0.172	-0.171	-0.167	-0.122	-0.157
50 Hz - Δ Temperature (C)															average			
100	-0.031	0.009	-0.023	0.009	-0.024	-0.007	-0.038	0.014	-0.006	0.015	0.021	-0.043	0.010	0.012	-0.006			
500	-0.012	0.042	-0.035	-0.009	-0.003	0.006	-0.012	-0.197	-0.108	-0.079	-0.058	-0.119	-0.127	-0.169	-0.063			
1000	-0.069	-0.061	-0.064	-0.019	-0.022	-0.027	-0.039	-0.262	-0.202	-0.149	-0.101	-0.154	-0.196	-0.234	-0.114			
5000	0.000	0.000	0.000	0.000	0.000	0.000	0.000	-0.329	-0.357	-0.269	-0.214	-0.354	-0.275	-0.340	-0.153			
10000	-0.139	-0.098	-0.074	-0.077	-0.022	-0.078	-0.089	-0.263	-0.369	-0.413	-0.363	-0.505	-0.308	-0.379	-0.227			

Evaporation study without cycling

Cuvet + Piston

mass

time	E1	E2	E3	L1	L2	L3	PE1
CPi	14.6337	14.6337	14.6336	14.6333	14.6334	14.6333	14.6330
Bottle + sample	12.3518	12.3579	12.3809	12.3768	12.2200	12.2214	
Bottle w/o sample	12.2402	12.2994	12.2930	12.2728	12.0932	12.1328	
0	14.7511	14.6905	14.7198	14.7345	14.7584	14.7203	14.6559
1	14.7509	14.6903	14.7197	14.7344	14.7584	14.7204	14.6559
2	14.7509	14.6903	14.7197	14.7343	14.7583	14.7203	14.6559
3	14.7508	14.6903	14.7193	14.7343	14.7583	14.7201	14.6559
5	14.7508	14.6904	14.7192	14.7342	14.7583	14.7200	14.6559
10	14.7507	14.6904	14.7192	14.7340	14.7581	14.7200	14.6559
15	14.7506	14.6898	14.7192	14.7338	14.7580	14.7200	14.6559
20	14.7505	14.6898	14.7190	14.7337	14.7579	14.7200	14.6558
Botle + sample	12.3540	12.3547	12.3741	12.3694	12.2129	12.2153	
CPa	14.6343	14.6339	14.6336	14.6336	14.6339	14.6335	14.6330
dry bottle + dry sample	12.2888	12.3511	12.3287	12.3110	12.1229	12.1632	
dry bottle	12.2352	12.2984	12.2871	12.2689	12.0847	12.1265	
consistency	45.97	88.57	44.35	39.02	28.23	38.67	

Fiber

	E13	E14	E6	L4	L5	L6	PE3	PE4
0	0.5573	0.5664	0.5603	0.5535	0.5485	0.5757	0.5070	0.4945
1	0.5561	0.5651	0.5591	0.5526	0.5476	0.5748	0.5066	0.4941
2	0.5549	0.5637	0.5577	0.5516	0.5466	0.5740	0.5059	0.4937
3	0.5537	0.5623	0.5557	0.5506	0.5453	0.5726	0.5056	0.4934
5	0.5517	0.5605	0.5545	0.5487	0.5432	0.5706	0.5051	0.4929
10	0.5462	0.559	0.5485	0.5443	0.5380	0.5657	0.5039	0.4917
15	0.5413	0.554	0.5431	0.5403	0.5332	0.5610	0.5026	0.4914
20	0.5373	0.5493	0.5385	0.5361	0.5290	0.5566	0.5020	0.4910
wet sample + bottle	12.284	12.4348	12.255	12.4054	12.3996	12.4215		
wet bottle	12.1803	12.321	12.1467	12.3043	12.3051	12.2992		
after replace	12.2568	12.4045	12.2255	12.3806	12.3740	12.3960		
weigh dish after	0.4569	0.4564	0.4564	0.4559	0.4561	0.4560		
dry bottle + sample	12.2213	12.3703	12.1924	12.3302	12.3288	12.3254		
bottle	12.1702	12.3164	12.1418	12.3003	12.2980	12.2934		
Consistency	44.90	45.52	44.70	28.45	30.31	24.98		
wet fiber	0.1138	0.1184	0.1132	0.1051	0.1016	0.1281		
diff=(0-WD)-wetfiber	-0.0124	-0.0079	-0.0088	-0.0075	-0.0090	-0.0083		
wet fiber in wet bottle	0.0101	0.0046	0.0049	0.004	0.0071	0.0058		
water evap in transfer	-0.0023	-0.0033	-0.0039	-0.0035	-0.0019	-0.0025		

Block

2 min

	E7	E8	E9	L7	L8	L9
before	12.3523	12.2275	12.3871	12.3974	12.2356	12.3741
after	12.3474	12.2240	12.3836	12.3942	12.2328	12.3715
bottle w/o sample	12.2677	12.1329	12.2600	12.3017	12.1356	12.2933
dry bottle + sample	12.3129	12.1797	12.3081	12.3236	12.1452	12.3074
dry bottle	12.2620	12.1276	12.2556	12.2929	12.1241	12.2804
Consistency	56.37	52.15	39.92	29.38	18.92	28.82

Consistency before

	E10	E15	E12	L10	L13	L12
wet + bottle	12.4070	12.2156	12.2809	12.3965	12.2475	12.3044
dry + bottle	12.3653	12.1661	12.2088	12.3216	12.1685	12.2680
bottle	12.3151	12.1126	12.1552	12.2869	12.1316	12.2321
consistency	54.62	51.94	42.64	31.66	31.84	49.65

Evaporation study with cycling

Drying Study				
Frequency	Number of Cycles	Time (sec)	Ave Water Lost	Ave Δ Consistency
10	10000	1000	0.00790	3.743
10	1000	100	0.00383	1.066
10	100	10	0.00403	1.351
10	10	1	0.00340	1.814
10	0	0	0.00197	0.678
Frequency	Number of Cycles	Time (sec)	Ave Water Lost	Ave Δ Consistency
50	10000	200	0.00693	2.748
50	1000	20	0.00380	1.814
50	100	2	0.00293	0.825
50	10	0.2	0.00253	0.908
50	0	0	0.00197	0.678

IR pure aggregates (oven-dried) change in temperature - 10 and 50 Hz

Experiment 3																
50 Hz - Δ Temperature (C)																average
10	0.183	0.107	0.184	0.078	0.159	-0.026	0.042	0.036	-0.057	-0.008	0.021	0.019	-0.046	0.024	0.015	0.049
20	0.192	0.146	0.218	0.075	0.157	-0.017	0.036	0.006	0.024	-0.003	0.020	0.022	-0.017	0.023	0.025	0.060
50																
100	0.188	0.119	0.217	0.079	0.155	-0.028	0.049	0.056	0.026	-0.019	0.068	0.019	-0.079	0.018	0.032	0.060
200	0.209	0.181	0.197	0.119	0.179	0.017	0.009	0.054	0.038	0.022	0.112	0.052	0.028	0.045	0.066	0.089
500	0.260	0.357	0.474	0.258	0.309	0.053	0.045	0.037	0.009	0.049	0.153	0.078	0.062	0.077	0.121	0.156
1000	0.294	0.396	0.518	0.283	0.313	0.019	0.029	0.068	0.032	0.061	0.059	0.174	0.035	0.082	0.103	0.165
2000	0.340	0.369	0.432	0.124	0.281	0.040	0.047	0.106	0.041	0.071	0.186	0.101	0.062	0.121	0.116	0.163
10 Hz - Δ Temperature (C)										average						
10	-0.001	-0.024	0.014	0.004	0.043	0.013	0.009	0.104	0.020	0.020						
20	-0.021	-0.031	-0.053	-0.031	0.049	-0.044	0.012	0.019	0.010	-0.010						
50	-0.002	-0.029	-0.073	-0.031	0.052	-0.039	0.022	0.031	0.032	-0.004						
100	-0.013	-0.024	-0.080	-0.013	0.052	-0.037	0.031	-0.003	0.000	-0.010						
200	0.024	-0.002	-0.043	-0.042	0.067	-0.027	0.063	0.018	0.024	0.009						
500	0.031	-0.026	-0.052	0.006	0.074	-0.031	0.066	0.044	0.052	0.018						
1000	0.024	0.003	-0.075	0.018	0.099	-0.009	0.070	0.046	0.051	0.025						
2000	0.058	0.054	-0.028	0.040	0.136	-0.006	0.109	0.052	0.049	0.052						

IR pure aggregates (wet and dry) moisture desorption/adsorption

Experiment 5																						
																						average
Wet - Δ Temperature (C)																						
1	0.127	0.004	0.057	0.019	0.035	-0.012	0.036	-0.046	-0.044	0.004	-0.027	-0.052	-0.024	-0.039	0.013	-0.002	-0.044	-0.009	0.006	-0.030	-0.002	
3	0.035	0.000	0.001	0.029	0.046	0.020	0.033	-0.022	-0.014	0.003	-0.002	-0.088	-0.007	-0.044	-0.006	-0.035	-0.032	-0.054	0.000	-0.004	-0.007	
5	0.077	0.042	0.046	0.044	0.072	0.026	0.061	-0.016	-0.031	-0.001	-0.021	-0.069	-0.020	-0.035	-0.012	-0.127	-0.092	0.003	-0.030	0.010	-0.004	
10	0.054	0.002	0.016	0.036	0.047	0.022	0.041	-0.007	-0.012	-0.003	-0.020	-0.098	-0.005	-0.039	-0.064	-0.127	-0.092	0.003	-0.030	0.010	-0.013	
15	0.003	-0.018	-0.024	0.017	0.013	-0.039	-0.019	-0.091	-0.075	-0.048	-0.061	-0.140	-0.071	-0.070	-0.034	-0.084	-0.009	-0.050	-0.035	-0.064	-0.045	
20	-0.030	-0.026	-0.064	-0.002	0.029	-0.041	-0.004	-0.114	-0.095	-0.001	0.002	-0.034	-0.035	-0.046	-0.016	-0.047	-0.022	-0.015	-0.017	-0.039	-0.031	
																				average		
Dry - Δ Temperature (C)																						
1	0.065	0.008	0.112	0.022	0.042	-0.006	0.028	-0.009	0.015	0.023	0.011	0.038	-0.003	0.032	0.028	0.012	0.057	0.034	0.008	0.027		
3	-0.008	-0.005	0.034	-0.030	-0.007	0.012	0.001	-0.063	-0.022	-0.017	0.119	0.103	0.073	0.091	0.093	0.108	0.111	0.106	0.075	0.041		
5	-0.001	0.002	0.048	-0.008	0.031	0.020	0.046	-0.041	-0.023	0.022	0.209	0.172	0.152	0.196	0.190	0.183	0.219	0.191	0.171	0.094		
10	0.044	0.029	0.094	-0.008	0.034	0.084	0.005	-0.016	0.020	0.022	0.209	0.172	0.152	0.196	0.190	0.183	0.219	0.191	0.171	0.105		
15	-0.097	-0.085	-0.048	-0.083	-0.045	0.011	-0.027	-0.119	-0.069	-0.092	0.273	0.313	0.269	0.291	0.258	0.265	0.312	0.263	0.258	0.097		
20	0.020	0.017	0.054	0.027	0.045	0.103	0.042	0.004	0.043	-0.034	0.223	0.233	0.214	0.258	0.221	0.216	0.278	0.262	0.262	0.131		

APPENDIX 9: FORMULAS FOR THE T-TEST STATISTIC AND DEGREES OF FREEDOM

$$t = \frac{X/N - Y/M - \Delta_0}{(S_1^2/M + S_2^2/N)^{1/2}}$$

$$df = \frac{(S_1^2/M + S_2^2/N)^2}{(S_1^2/M)^2/M-1 \; + \; (s_2^2/N)^2/N-1}$$

where:

X/N = average x value

Y/M = average y value

S^2 = variance

M = number of data points of M

N = number of data points of N

Δ_0 = theorized difference between data sets

APPENIDIX 10: CALIBRATION CURVE FOR IR IMAGING SYSTEM.